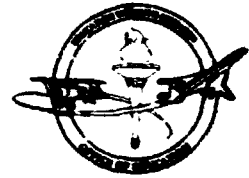


This microfiche was produced according to ANSI/AIIM Standards and meets the quality specifications contained therein. A poor blowback image is the result of the characteristics of the original document.

TECHNICAL REPORTS



LANGLEY

AEROSPACE

RESEARCH

SUMMER

SCHOLARS

PART 2

JUNE 5, 1995 - AUGUST 11, 1995
NASA LANGLEY RESEARCH CENTER OFFICE OF EDUCATION
HAMPTON UNIVERSITY

DISCLAIMER

This document was prepared as an account of the work sponsored by NASA Langley Research Center. Neither Langley Research Center, Hampton University, nor any of their employees makes any warranty, implied, or assumes any legal liability or responsibility for the accuracy, completeness of any information. The Langley Aerospace Research Summer Scholars (LARSS) Technical Reports are the original Technical Reports submitted by the LARSS participants. No changes have been made by the Office of Education, or Hampton University.

Work performed under the auspices of NASA Langley Research Center.

The use of trade names of manufacturers in this report does not constitute an official endorsement of such products or manufacturers, either expressed or implied, by the National Aeronautics and Space Administration.

FOREWORD

The Langley Aerospace Research Summer Scholars (LARSS) Program was established by Dr. Samuel E. Massenberg in 1986. The program has increased from 20 participants in 1986 to 114 participants in 1995. The program is LaRC-unique and is administered by Hampton University.

The program was established for the benefit of undergraduate juniors and seniors and first-year graduate students who are pursuing degrees in aeronautical engineering, mechanical engineering, electrical engineering, material science, computer science, atmospheric science, astrophysics, physics, and chemistry.

Two primary elements of the LARSS Program are: (1) a research project to be completed by each participant under the supervision of a researcher who will assume the role of a mentor for the summer, and (2) technical lectures by prominent engineers and scientists. Additional elements of this program include tours of LaRC wind tunnels, computational facilities, and laboratories. Library and computer facilities will be available for use by the participants.

The LARSS Program is intended to encourage high-caliber college students to both pursue and earn graduate degrees and to enhance their interest in aerospace research by exposing them to the professional research resources, people, and facilities of Langley Research Center.

CONTENTS

Foreword	iii
Introduction	xv
Listing of Langley Aerospace Research Summer Scholars	xix

Part 1

Clouds and the Earth's Radiant Energy System (CERES) Visualization Single Satellite Footprint (SSF) Plot Generator	1
Julia A. Barsi, Rochester Institute of Technology	
Oshkosh Logistics Management and Public Relations Responsibilities at NASA Langley	11
Danielle L. Beck, University of Utah	
Development of a 3-Phase CCD Timing Generator	21
Kory L. Bennett, North Carolina A&T State University	
Structural Analysis of Composite Test Panels	25
Sean Berhan, University of Virginia	
Geographic Information System Data Analysis	35
Chad J. Billings, University of Utah	
Polarization and Characterization of Piezoelectric Polymers	45
Hollie N. Bodiford, Hampton University	
Technology Transfer	57
Kimberly R. Bullock, North Carolina A&T State University	
A Numerical Study of Hypersonic Fuel Injectors	63
Jason G. Bush, Old Dominion University	
Stress Tuning of Laser Crystals	69
Atherton A. Carty, Syracuse University	
Geographic Information System Data Analysis	(35)†
Christopher C. Casad, Old Dominion University	
Emergency Operations Center	79
Anoushka Z. Chinae, University of Puerto Rico	
NASA Langley Teacher Resource Center (TRC): Brochure and Home Page Design	87
Monet L. Cogbill, Hampton University	

†Group report page numbers are in parentheses.

Precollege Science Education: Development of Distant Learning Laboratory and Creation of Educational Materials	91
Michelle Considine, Old Dominion University	
The Office of Equal Opportunity Programs Duties of Reasonable Accommodation	103
Angela R. Coppedge, Radford University	
Validation of Global Climatologies of Trace Gases Using NASA Global Tropospheric Experiment (GTE) Data	107
Brian D. Courchaine, University of Washington	
User Interface on the World Wide Web: How to Implement a Multi-Level Program Online	133
Jonathan W. Cranford, Brigham Young University	
Office of Education Guide to Graphic Arts Software	137
Angela M. Davis, Meredith College	
The Development and Use of a Flight Optimization System Model of a C-130E Transport Aircraft	145
Jeremy D. Desch, University of Kansas	
Curation of Federally Owned Archeological Collections at NASA Langley Research Center	155
John Arnold Eastman, College of William and Mary	
NASA LaRC Hazardous Material Pharmacy	163
Remy S. Esquenet, Old Dominion University	
Assessment of Electromagnetic Fields at NASA Langley Research Center	171
Carter B. Ficklen, Old Dominion University	
Geographic Information System Data Analysis	(35)†
Luis G. Floriano, University of Texas at El Paso	
Marketing NASA Langley Polymeric Materials	185
Diane M. Flynn, London Business School	
Controlling Air Traffic (Simulated) in the Presence of Automation	195
Jennifer R. French, Clemson University	
LaRC Patent Process and Patent Counsel Team Article	205
Christy E. Gall, Norfolk State University	
Finance	209
Kevin H. Garrido, University of Florida	

Active Flow Control	213
Norman W. Gimbert, Virginia Polytechnic Institute and State University	
Dynamic Acoustic Detection of Boundary Layer Transition	219
Jonathan R. Grohs, University of Missouri - Rolla	
Figures of Merit for Aeronautics Programs and Addition to LaRC Fire Station	227
Belinda M. Harper, Virginia Polytechnic Institute and State University	
Royalty Sharing for Private Employees Under the Stevenson-Wydler Act	237
M. Bruce Harper, College of William and Mary	
The Patent Prosecution Program	259
George W. Hartnell, College of William and Mary	
Drawing the Reverberation Chambers Lab Using AutoCad	263
Jonathan M. Harucki, Rochester Institute of Technology	
NASA Langley Exchange Investment Portfolio	267
Marcus A. Hathaway, Hampton University	
Comparisons of the Maxwell and Cercignani-Lampis-Lord Gas/ Surface Interaction Models Using Direct Simulation Monte Carlo	285
Marc O. Hedahl, University of Notre Dame	
Various Embodiments of the Non-Invasive Endoscopic Feedback for Learning of Voluntary Control of Physiological Functioning	295
Mina D. Henriksen, College of William and Mary	
Implementation of a Remote Acquisition and Storage System	299
Jason R. Hess, Virginia Polytechnic Institute and State University	
Geographic Information System Data Analysis	(35)†
Tracie Hill, Norfolk State University	
A Comparison of Three Determinants of an Engagement Index for use in a Simulated Flight Environment	307
James M. Hitt, Old Dominion University	
Improvement of Subsonic Basic Research Tunnel Flow Quality as Applied to Wall Mounted Testing	315
Brian M. Howerton, George Washington University	
Mode I and Mode II Analysis of Graphite/Epoxy Composites Using Double Cantilever Beam and End-Notched Flexure Tests	325
Kathleen P. Hufnagel, Rutgers University	

An Examination of NASA LaRC Travel Reimbursement Procedures	335
Esta M. Jarrett, University of Virginia	
The Value of NASA Form 533 and the Related Activities That Aid in Obtaining Reliable NASA Contractors	345
Angela N. Jenkins, Virginia Polytechnic Institute and State University	
17-4 PH & 15-5 PH	355
Howard T. Johnson, Gallaudet University	
The Effect of Different Materials on the Accuracy of the HYDRA Optical-Fiber-Coupled Coherent Range/Pressure Measurement System and The Development of the Health Care Database System at Old Dominion University.....	359
Kimberly D. Johnson, Old Dominion University	
Geographic Information System Data Analysis	(35)†
Rashunda K. Johnson, University of Arkansas at Pine Bluff	
Payload Planning for the International Space Station	365
Tamcka J. Johnson, Virginia Union University	
Free-Flight Evaluation of Forebody Blowing for Yaw Control at High Angles of Attack.	373
Jason S. Kiddy, University of Maryland at College Park	
Conversion of the Aerodynamic Preliminary Analysis System (APAS) to an IBM PC-Compatible Format	379
John M. Kruep, Virginia Polytechnic Institute and State University	
Modeling of the Expected Lidar Return Signal for Wake Vortex Experiments	389
Craig A. Kruschwitz, College of William and Mary	
Langley Sign Language Home Page	393
Susanna Lai, Rochester Institute of Technology	
A Variational Formulation for the Finite Element Analysis of Sound Wave Propagation in a Spherical Shell	397
Catherine G. Lebiedzki, University of Virginia	
Synthesis and Characterization of Poly (Arylene Ether Benzimidazole) Oligomers	407
Michael J. Leonard, Roanoke College	
Importance of the Office of Inspector General to the Efficient Operation of Langley Research Center	417
Anthony L. Linton, Florida A&M University	

Part 2*

Effects of Nose Strakes On Transport Aircraft421 - /
Calvin T. Locklear, Pembroke State University

Geographic Information System Data Analysis(35)†
John M. Locklear, Pembroke State University

**Home Page: The Mode of Transport Through The Information
Superhighway**425
Michelle R. Lujan, University of Texas at El Paso

Design Considerations For The Next Generation of General Aviation Designs431
Brian D. Marchesseault, Embry-Riddle Aeronautical University

Creating a Database443
Brian C. Mays, Hampton University

**Materials For The General Aviation Industry: Effect of Environment on
Mechanical Properties of Glass Fabric/Rubber Toughened Vinyl Ester
Laminates**.....449 /
Timothy M. McBride, Boston University

**Using The World-Wide Web to Facilitate Communications of Non-Destructive
Evaluation**459 - /
Sean M. McBurney, Rochester Institute of Technology

Technology Applications Group Multimedia CD-ROM Project467 /
Kristi D. McRacken, Christopher Newport University

Development of a Small Area Sniffer473 /
Laurie A. Meade, Tufts University

**Terminal Area Productivity/Airport Surface Traffic Automation Flight Demo
Data Analysis**483 /
Eric O. Mejdrich, St. Cloud State University

Multimedia Information Kiosk505 /
Golnar G. Miamee, Old Dominion University

Introducing Current Technologies513 /
Tiffany N. Mitchell, University of Virginia

Product Assurance For Spaceflight Hardware517 /
Michael J. Monroe, Virginia Polytechnic Institute and State University

Finite Element Analysis of an Energy Absorbing Sub-floor Structure533 /
Scott C. Moore, North Carolina State University

**Part 2 is presented under separate cover.*

Reusable Software Technology	545	12
Timothy E. Morgan, Norfolk State University		
Eliminating Flow Separation and Reducing Viscous Drag Through Boundary Layer Analysis and Manipulation	555	13
Matthew D. Oser, University of Illinois		
Electronic Photography	565	14
Meredith L. Payne, Rochester Institute of Technology		
Technology Transfer: A Contact Sport	571	15
Nina P. Paynter, Swarthmore College		
Fabrication of Fabry-Perot Interferometer Sensors and Characterization of their Performances for Aircraft Inspection	579	16
LeRuth Q. Pendergrass, Hampton University		
Geographic Information System Data Analysis	(35)	†
Stephen A. Penn, Hampton University		
Performance Comparison of a Matrix Solver on a Heterogeneous Network Using Two Implementations of MPI: MPICH and LAM	589	17
Jennifer K. Phillips, University of Illinois		
A Study of How Stitch Placement Affects the Open Hole Tension Strength of Stitched Textile Composite Materials	599	16
Kathleen A. Pierucci, Illinois Institute of Technology		
A Summer in Public Affairs	609	
India Pinkney, University of Virginia		
Geographic Information System Data Analysis	(35)	†
Tori D. Rnoulac, Howard University		
1995 Summer Intern NASA Langley Research Center, Office of Education	621	
Nature A. Richard, Hampton University		
TAC CD-ROM	62	
Myrna S. Rivera, Christopher Newport University		
Correlations of Difference Surfaces Tests, Tire Behavior Math Model for the High Speed Civil Transport (HSCT) and Michelin Tire Properties Tests for Boeing 777	629	
Ivan Roman, University of Puerto Rico		
The Use of the Internet to Support General Aviation Research.	637	
James H. Rowbottom, Norfolk State University		

Aviation Research and the Internet	641-22 ✓
Antoinette M. Scott, Norfolk State University	
Geographic Information System Data Analysis	(35)†
Adam H. Shay, University of Virginia	
Development of a Pressure Sensitive Paint System With Correction for Temperature Variation	643
Kantis A. Simmons, Norfolk State University	
Technology Transfer	655-14
Nanette R. Smith, College of William and Mary	
Langley Learning Laboratory	663
Kenneth R. Smith, Hampton University	
Characteristics of Three-node Smoothing Element Under Penalty Constraints	667
Seth S. Sobel, James Madison University	
Office of Public Affairs	677
Mary M. Spracher, Virginia Polytechnic Institute and State University	
Langley Research Center - Soluble Imide (LaRC-SI)	685
David Stang, Old Dominion University	
Congressional Affairs	695
Ronald E. Stephenson, Virginia Polytechnic Institute and State University	
The Calibrations of Space Shuttle Main Engines High Pressure Transducers	697-17
Christopher S. Steward, Norfolk State University	
The Dependence of the Change in the Coefficient of Thermal Expansion of Graphite Fiber Reinforced Polyimide IM7-K3B on Microcracking Due to Thermal Cycling	707-1
Melissa C. Stewart, Rensselaer Polytechnic Institute	
Analog Processing Assembly for the Wake Vortex Lidar Experiment	717-27
Edwood G. Stowe, Washington University	
Parallel Processing with Digital Signal Processing Hardware and Software	725-1
Corey V. Swenson, St. Cloud State University	
Geographic Information System Data Analysis	(35)†
Antone L. Taylor, Hampton University	
Technology Transfer - Marketing Tomorrow's Technology	735
Erene Tcheng, University of Virginia	

Open Loop Simulation	743
Camera L. Thomas, Hampton University	
Geographic Information System Data Analysis	(35)†
Karina M. Thorpe, University of Utah	
Entrepreneurship Within General Aviation	747
Brian M. Ullmann, University of Kansas	
Determination of Stress-Corrosion Cracking in Aluminum-Lithium Alloy ML377.....	759
Bryan C. Valck, Georgia Institute of Technology	
A MATLAB/Simulink Based GUI For The CERES Simulator	769
Luis H. Valencia, University of Puerto Rico	
Oxidation Behavior of Carbon Fiber Reinforced Silicon Carbide Composites	781
Victor M. Valentin, University of Puerto Rico	
Validation of Global Climatologies of Trace Gases Using NASA Global Tropospheric Experiment (GTE) Data	(107)†
Jessica Venable, Princeton University	
Homepage for the Global Tropospheric Experiment	791
Eugene L. Ward, Norfolk State University	
System Construction for the Measurement of Bragg Grating Characteristics in Optical Fibers	799
Douglas P. West, Eastern New Mexico University	
Analysis Of a High-Lift Multi-Element Airfoil Using a Navier-Stokes Code	807
Mark E. Whitlock, University of Illinois	
Wake Vortex Encounter Research	817
Jeffrey M. Wilson, University of Kansas	
Langley Aerospace Research Summer Scholars (LARSS) Program Coordination.....	825
Terri L. Wilson, Virginia Polytechnic Institute and State University	
Converting The Active Digital Controller For Use in Two Tests	833
Robert G. Wright, University of Missouri	
My Networking and Interpersonal Skills Developed At NASA Langley Research Center	837
Sara J. Yancey, College of William and Mary	
Very Light Aircraft: Revitalization Through Certification.	845
Michael K. Zyskowski, University of Kansas	

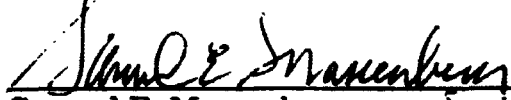
1995 Langley Aerospace Research Summer Scholars Program (LARSS) Technical Reports

**The 1995 LARSS program was sponsored by NASA Langley Research Center
and Hampton University.**

**Compiled by:
Rafaela Schwan
Hampton University
Hampton, Virginia 23668**

1995 Langley Aerospace Research Summer Scholars Program (LARSS) Technical Reports

**NASA Langley Research Center
Office of Education**



**Samuel E. Massenberg
Director, Office of Education**

Hampton University



**Calvin W. Lowe
Vice President for Research
and Dean of the Graduate College**



**Roger A. Hathaway
University Affairs Officer**



**Rafaela Schwan
LARSS Program Coordinator**

INTRODUCTION

The LARSS Technical Reports are a summary of the research project developed by the students during the summary of 1995.

The following is a list of the areas where students were placed for the 10-week period.

OFFICE OF EDUCATION

The Office of Education serves as the primary focal point for most educational opportunities through research. The Office of Education also serves as the focal point for internal customers who require information on institutions of higher education and provides selected funding support for research scholarships, fellowships, and post-doctoral research associateships.

OFFICE OF HUMAN RESOURCES

The goal of the Office of Human Resources (OHR) is to maximize the performance potential of the employees of NASA Langley Research Center through planning, policy formulation, and administration of human resource programs and procedures. The areas of emphasis include: position classification, recruitment, career development, labor relations, performance management and awards, training and education, employee benefits, organizational development, occupational health, and retirement. Research opportunities exist in the following categories of effort: personnel information systems, human performance technologies, learning support and transfer techniques, organization design, and change dynamics.

OFFICE OF EXTERNAL AFFAIRS

The Office of External Affairs manages a broad range of programs designed to communicate with and monitor the external environment. These programs involve public affairs, congressional affairs, public services, freedom of information (FOI), technical conference management, research, writing and editing, exhibit design and fabrication, speech writing, and a variety of other staff support for the Center. The office includes the Office of Public Affairs (OPA) and the Office of Public Services (OPS). OPA serves as a communications facilitator between center management and news media and the public about research programs and other subjects of interest. OPA issues news releases, etc., and publishes the center newspaper. OPS communicates the Langley and NASA's story through special events, exhibits, Center tours, community services, trade shows, speaking engagements, special publications, and public mail.

OFFICE OF COMPTROLLER

The Office of Comptroller is responsible for the centralized planning and analysis of all Center resources and financial management activities. The office is the focal point for the development and execution of financial and resource decisions. The Comptroller has two divisions: Financial Management Division and Programs and Resources Division.

AERONAUTICS PROGRAM GROUP

The Aeronautics Program Group (APG) is responsible for planning and guiding aeronautics programs for the Center. The Group leads the Center's aeronautics strategic planning and is the single point of contact for committing the Center to aeronautics programs. APG interacts with customers and performs aircraft vehicle studies to obtain an integrated set of research objectives. APG also provides program management for focused programs when implementation is distributed across several Langley organizations. APG vehicle class leaders work with external customers and other Langley groups to define specific programs to accomplish the objectives. The group is responsible for resource allocation and reporting aeronautics program results. The APG contains the Aeronautics Systems Analysis Division, Systems Analysis Branch.

INTERNAL OPERATIONS GROUP

The Internal Operations Group (IOG) supports the Center's research programs and project activities, with special emphasis on formulating and implementing major policies and programs relating to resources management, acquisition and contracting activities, data systems management and technical support services. This support also includes the Center's Construction of Facilities program; all functions necessary to design, install, operate and maintain large mechanical and electrical systems, complex research facilities and equipment and test apparatus; all functions necessary to provide and maintain institutional buildings, structures, and grounds; all functions necessary to provide design, analysis, fabrication and operation of complex aerospace systems and research test articles; Center-wide electronic discipline for projects and programs; the operation and maintenance of the Center's central computer complex and simulation facilities; and all functions necessary to operate and maintain the Center's daily flight operations inclusive of aircraft and avionics maintenance, research pilot staff management, and direction of all related design, fabrication, testing, and certification of experimental flight control and display systems. The following items represent active research disciplines: Electronic and Information Systems, Advanced Sensor Systems, Measurement Science and Instrument Technology, Advanced Computational Capability, Engineering, Mechanical Systems Engineering, Facility Systems Engineering, Materials Characterization Technology, and Engineering Laboratory Unit.

RESEARCH AND TECHNOLOGY GROUP

The Research and Technology Group consists of approximately 800 scientists, engineers, technicians and support personnel who are responsible for performing basic research and technology development in a broad range of aeronautical and selected space disciplines. Through an interdisciplinary approach, the group produces proven and usable technology for aerospace and non-aerospace customers. The Research and Technology Group program includes research activities in: Aerodynamics, Flight Dynamics and Controls, Fluid Mechanics and Acoustics, Gas Dynamics, Competitiveness, Information and Electromagnetic Technology, Materials, and Structures.

SPACE AND ATMOSPHERIC SCIENCES PROGRAM GROUP

The Group conducts the Atmospheric Sciences Research Program; leads Space Project Management; provides management of the space-focused technology programs of Space Transportation, Spacecraft, and Remote Sensing; and conducts system analysis for technology planning, assessment, and prioritization. The program includes the following specific research activities: Stratospheric Aerosol and Gas Experiment (SAGE), Climate Research Program, Tropospheric Chemistry Research Program, Upper Atmosphere Research Program, Earth Radiation Budget Experiment (ERBE), Halogen Occultation Experiment (HALOE), Global Biogeochemical Cycling, Transportation Systems, Spacecraft and Sensor Systems Definition and Analysis Tools, Conceptual Designs for Small Spacecraft and Instruments, and In-Space Technology Experiments.

TECHNOLOGY APPLICATIONS GROUP

The Technology Applications Group (TAG) leads the Center's technology transfer and commercialization program. This includes the early identification of technologies of high commercial potential and promoting the expedient transfer of new technologies to the commercial sector focusing primarily on the nonaerospace community. This is accomplished by identifying potential technology applications and creating teams of nonaerospace customers and LaRC technologist to accomplish the transfer process. In addition, the TAG has the lead in determining and protecting the government's rights to patent inventions made by NASA and contractor employees and providing counsel with respect to NASA's rights in intellectual property matters. TAG also provides the overall leadership for planning and implementing the Center's Small Business Innovation Research Program (SBIR) and the Small Business Technology Transfer Program (STTR). The Agency conceives and matures innovative concepts and methodologies applicable to its focused research programs in aeronautics and space. Langley seeks synergistic partnerships with industries and universities in these mission programs. A dynamic, cooperative teaming with national laboratories, industry, and universities creates a win-win situation. Industry has access to state-of-the-science experts, facilities, and intellectual property; universities have access to enabling research topics and teams for student growth and faculty focus; and NASA benefits through the mission-related accomplishments. As students graduate, they have improved opportunity for jobs, and industry has in addition to a new product, a well-trained work force familiar with their products and initiatives. In practice, depending on the relationship of the work to our mission and technology thrust, industry funds a university faculty member and a

student to work on a technical problem related to one of their products, and LaRC signs a Space Act Agreement spelling out our respective responsibilities. The parties work together as a team, bringing their collective strength to bear on a specific problem. Colleges and universities complement NASA's basic research by introducing and formulating theoretical bases for new concepts and ideas for inclusion in NASA's mission and programs. In addition, academic institutions facilitate, promote, and support technology transfer and commercialization of advanced aeronautics, space, and related technologies to both technical and non-technical settings through creation or enhancement of courses and curricula to reflect knowledge transferred from NASA-conceived methodologies or technologies, direct student involvement in NASA-sponsored research projects and missions, and publication and presentation of research findings.

Listing of the 1995 Langley Aerospace Research Summer Scholars

<u>Name/University</u>	<u>Title</u>	<u>Group/Mentor</u>
Julia A. Barsi Rochester Institute of Technology	Clouds and the Earth's Radiant Energy System Visualization Single Satellite Footprint Plot Generator	Space and Atmospheric Sciences Program Group Jon C. Currey
Danielle L. Beck University of Utah	Oshkosh Logistics Management and Public Relations Responsibilities At NASA Langley	Office of External Affairs Margaret Hunt
Kory L. Bennett North Carolina A&T State University	Development of a 3-Phase CCD Timing Generator	Internal Operations Group Preston I. Carraway
Sean Berhan University of Virginia	Structural Analysis of Composite Test Panels	Research and Technology Group Marshall Rouse
Chad J. Billings University of Utah	Geographic Information System Data Analysis	Internal Operations Group William B. Ball
Hollie N. Bodiford Hampton University	Polarization and Characterization of Piezoelectric Polymers	Research and Technology Group Joycelyn O. Simpson
Kimberly R. Bullock North Carolina A&T State University	Technology Transfer	Technology Applications Group Rosemary Baize
Jason G. Bush Old Dominion University	A Numerical Study of Hypersonic Fuel Injectors	Research and Technology Group Griff Anderson
Atherton A. Carty Syracuse University	Stress Tuning of Laser Crystals	Internal Operations Group Norman Barnes
Christopher C. Casad Old Dominion University	Geographic Information System Data Analysis	Internal Operations Group William B. Ball
Anoushka Z. Chinae University of Puerto Rico	Emergency Operations Center	Office of Safety, Environment & Mission Assurance Alan H. Phillips

<u>Name/University</u>	<u>Title</u>	<u>Group/Mentor</u>
Monet L. Cogbill Hampton University	NASA Langley Teacher Resource Center (TRC): Brochure and Home Page Design	Office of Education Marchelle D. Canright
Michelle Considine Old Dominion University	Precollege Science Education: Development of Distant Learning Laboratory and Creation of Educational Materials	Office of Education Marchelle D. Canright
Angela R. Coppedge Radford University	The Office of Equal Opportunity Programs Duties of Reasonable Accommodation	Office of Equal Opportunity Programs Vivian Merritt
Brian D. Courchaine University of Washington	Validation of Global Climatologies of Trace Gases Using NASA Global Tropospheric Experiment (GTE) Data	Space and Atmospheric Sciences Program Group Joel S. Levine
Jonathan W. Cranford Brigham Young University	User Interface on the World Wide Web: How to Implement a Multi-Level Program Online	Internal Operations Group David B. Yeager
Angela M. Davis Meredith College	Office of Education Guide w Graphic Arts Software	Office of Education Samuel E. Massenberg
Jeremy D. Desch University of Kansas	The Development and Use of a Flight Optimization System Model of a C-130E Transport Aircraft	Aeronautics Program Group Michael J. Logan
John Eastman College of William and Mary	Curation of Federally Owned Archeological Collections at NASA Langley Research Center	Internal Operations Group John Mouring
Remy S. Esquenet Old Dominion University	NASA LaRC Hazardous Material Pharmacy	Office of Safety, Environment, and Mission Assurance Robert D. Brown
Carter B. Ficklen Old Dominion University	Assessment of Electromagnetic Fields at NASA Langley Research Center	Office of Safety, Environment, and Mission Assurance Alan H. Phillips

<u>Name/University</u>	<u>Title</u>	<u>Group/Mentor</u>
Luis G. Floriano University of Texas at El Paso	Geographic Information System Data Analysis	Internal Operations Group William B. Ball
Diane M. Flynn London Business School	Marketing NASA Langley Polymeric Materials	Technology Applications Group Barry V. Gibbens
Jennifer R. French Clemson University	Controlling Air Traffic (Simulated) in the Presence of Automation	Research and Technology Group Alan Pope
Christy E. Gall Norfolk State University	LaRC Patent Process and Patent Counsel Team Article	Technology Applications Group Barry V. Gibbens
Kevin H. Garrido University of Florida	Finance	Office of the Comptroller Debra E. Watson
Norman W. Gimbirt Virginia Polytechnic Institute and State University	Active Flow Control	Research and Technology Group Rich W. Wlezien
Jonathan R. Grohs University of Missouri - Rolla	Dynamic Acoustic Detection of Boundary Layer Transition	Research and Technology Group Guy T. Kemmerly
Belinda M. Harper Virginia Polytechnic Institute and State University	Figures of Merit for Aeronautics Programs	Office of Safety, Environment, and Mission Assurance Walter S. Green
M. Bruce Harper College of William and Mary	Royalty Sharing for Private Employees Under the Stevenson-Wydler Act	Technology Applications Group Kimberly A. Chasteen
George W. Hartnell College of William and Mary	The Patent Prosecution Program	Technology Applications Group Kimberly A. Chasteen
Jonathan M. Harucki Rochester Institute of Technology	Drawing the Reverberation Chambers Lab Using AutoCad	Research and Technology Group Richard Chase
Marcus A. Hathaway Hampton University	NASA Langley Exchange Investment Portfolio	Office of the Comptroller James Ogiba

<u>Name/University</u>	<u>Title</u>	<u>Group/Mentor</u>
Marc O. Hedahl	Comparisons of the Maxwell and Cercignani-Lampis-Lord Gas/Surface Interaction Models Using Direct Simulation Monte Carlo	Research and Technology Group Richard G. Wilmoth
Mina D. Henriksen College of William and Mary	Various Embodiments of the Non-Invasive Endoscopic Feedback for Learning of Voluntary Control of Physiological Functioning	Research and Technology Group Alan T. Pope
Jason R. Hess Virginia Polytechnic Institute and State University	Implementation of a Remote Acquisition and Storage System	Internal Operations Group Kenneth D. Wright
Tracie Hill Norfolk State University	Geographic Information System Data Analysis	Internal Operations Group William B. Ball
James M. Hitt Old Dominion University	A Comparison of Three Determinants of an Engagement Index for use in a Simulated Flight Environment	Research and Technology Group Alan T. Pope
Brian M. Howerton George Washington University	Improvement of Subsonic Basic Research Tunnel Flow Quality as Applied to Wall Mounted Testing	Research and Technology Group Greg Gatlin
Kathleen P. Hufnagel Rutgers University	Mode I and Mode II Analysis of Graphite/Epoxy Composites Using Double Cantilever Beam and End-Notched Flexure Tests	Research and Technology Group T. Kevin O'Brien
Esta M. Jarrett University of Virginia	An Examination of NASA LaRC Travel Reimbursement Procedures	Office of the Comptroller James Ogiba
Angela N. Jenkins Virginia Polytechnic Institute and State University	The Value of NASA Form 533 and the Related Activities That Aid in Obtaining Reliable NASA Contractors	Office of the Comptroller James Ogiba
Howard T. Johnson Gallaudet University	17-4 PH & 15-5 PH	Internal Operations Group Larry Cooper

<u>Name/University</u>	<u>Title</u>	<u>Group/Mentor</u>
Kimberly D. Johnson Old Dominion University	The Effect of Different Materials on the Accuracy of the HYDRA Optical - Fiber - Coupled Coherent Range/Pressure Measurement System and The Development of the Health Care Database System at Old Dominion University	Research and Technology Group Sixto Vazquez
Rashunda K. Johnson University of Arkansas at Pine Bluff	Geographic Information System Data Analysis	Internal Operations Group William B. Ball
Tameka J. Johnson Virginia Union University	Payload Planning for the International Space Station	Space and Atmospheric Sciences Program Group David T. Shannon, Jr.
Jason S. Kiddy University of Maryland at College Park	Free-Flight Evaluation of Forebody Blowing for Yaw Control at High Angles of Attack	Research and Technology Group Kay Brandon
John M. Kruep Virginia Polytechnic Institute and State University	Conversion of the Aerodynamic Preliminary Analysis System (APAS) to an IBM PC-Compatible Format	Space and Atmospheric Sciences Program Group Walter C. Engelund
Craig A. Kruschwitz College of William and Mary	Modeling of the Expected Lidar Return Signal for Wake Vortex Experiments	Space and Atmospheric Sciences Program Group Lamont R. Poole
Susanna Lai Rochester Institute of Technology	Langley Sign Language Home Page	Internal Operations Group Jerry Hoerger
Catherine G. Lebiedzik University of Virginia	A Variational Formulation for the Finite Element Analysis of Sound Wave Propagation in a Spherical Shell	Research and Technology Group Jay Robinson
Michael J. Leonard Roanoke College	Synthesis and Characterization of Poly (Arylene Ether Benzimidazole) Oligomers	Research and Technology Group Joseph G. Smith, Jr.

<u>Name/University</u>	<u>Title</u>	<u>Group/Mentor</u>
Anthony Linton Florida A&M University	Importance of the Office of Inspector General to the Efficient Operation of Langley Research Center	Office of Inspector General Lee Ball
Calvin T. Locklear Pembroke State University	Effects of Nose Strakes On Transport Aircraft	Research and Technology Group Gautam Shah
John M. Locklear Pembroke State University	Geographic Information System Data Analysis	Internal Operations Group William B. Ball
Michelle R. Lujan University of Texas at El Paso	Home Page: The Mode of Transport Through The Information Superhighway	Research and Technology Group Odilyn L. Santa Maria
Brian D. Marchesseault Embry-Riddle Aeronautical University	Design Considerations For The Next Generation of General Aviation Designs	Research and Technology Group H. Paul Stough
Brian C. Mays Hampton University	Creating a Database	Office of Human Resources Janet McKenzie
Timothy M. McBride Boston University	Materials For The General Aviation Industry: Effect of Environment on Mechanical Properties of Glass Fabric/Rubber Toughened Vinyl Ester Laminates	Research and Technology Group H. Benson Dexter
Sean M. McBurney Rochester Institute of Technology	Using The World-Wide Web to Facilitate Communications of Non-Destructive Evaluation	Internal Operations Group Lawrence Cooper
Kristi D. McRacken Christopher Newport University	Technology Applications Group Multimedia CD-ROM Project	Technology Applications Group Stuart Pendleton
Laurie A. Meade Tufts University	Development of a Small Area Sniffer	Research and Technology Group Jerome Kegelman

<u>Name/University</u>	<u>Title</u>	<u>Group/Mentor</u>
Eric O. Mejdrich St. Cloud State University	Terminal Area Productivity/Airport Surface Traffic Automation Flight Demo Data Analysis	Research and Technology Group Steve Young
Golnar G. Miamee Old Dominion University	Multimedia Information Kiosk	Internal Operations Group Lillian Ross
Tiffany N. Mitchell University of Virginia	Introducing Current Technologies	Technology Applications Group Barry Gilbert
Michael J. Monroe Virginia Polytechnic Institute and State University	Product Assurance For Spaceflight Hardware	Office of Safety , Environment and Mission Assurance John Greer
Scott C. Moore North Carolina State University	Finite Element Analysis of an Energy Absorbing Sub-floor Structure	Research and Technology Group Benson Dexter
Timothy F. Morgan Norfolk State University	Reusable Software Technology	Space and Atmospheric Sciences Program Group Calvin Mackey
Matthew D. Oser University of Illinois	Eliminating Flow Separation and Reducing Viscous Drag Through Boundary Layer Analysis and Manipulation	Research and Technology Group Richard L. Campbell
Meredith L. Payne Rochester Institute of Technology	Electronic Photography	Internal Operations Group Thomas E. Pinelli
Nina P. Paynter Swarthmore College	Technology Transfer: A Contact Sport	Technology Applications Group Marisol Romero
LeRuth Q. Pendergrass Hampton University	Fabrication of Fabry-Perot Interferometer Sensors and Characterization of their Performances for Aircraft Inspection	Research and Technology Group Robert S. Rogowski
Stephen A. Penn Hampton University	Geographic Information System Data Analysis	Internal Operations Group William B. Ball

Name/University	Title	Group/Mentor
Jennifer K. Phillips University of Illinois	Performance Comparison of a Matrix Solver on a Heterogeneous Network Using Two Implementations of MPI: MPICH and LAM	Research and Technology Group Jerrold M. Housner
Kathleen A. Pierucci Illinois Institute of Technology	A Study of How Stitch Placement Affects the Open Hole Tension Strength of Stitched Textile Composite Materials	Research and Technology Group Keith Furrow
India Pinkney University of Virginia	A Summer in Public Affairs	Office of External Affairs Keith Henry
Tori D. Rhoulac Howard University	Geographic Information System Data Analysis	Internal Operations Group William B. Ball
Nature A. Richard Hampton University	1995 Summer Intern NASA Langley Research Center Office of Education	Office of Education Roger A. Hathaway
Myrna S. Rivera Christopher Newport University	TAC CD-ROM	Technology Applications Group Stuart Pendelton
Ivan Roman University of Puerto Rico	Correlations of Difference Surfaces Tests, Tire Behavior Math Model for the High Speed Civil Transport (HSCT) and Michelin Tire Properties Tests for Boeing 777	Research and Technology Group Robert H. Daugherty
James H. Rowbottom Norfolk State University	The Use of the Internet to Support General Aviation Research	Internal Operations Group Gretchen L. Gottlich
Antoinette M. Scott Norfolk State University	Aviation Research and the Internet	Internal Operations Group Gretchen L. Gottlich
Adam H. Shay University of Virginia	Geographic Information System Data Analysis	Internal Operations Group William B. Ball
Kantis A. Simmons Norfolk State University	Development of a Pressure Sensitive Paint System With Correction For Temperature Variations	Internal Operations Group Billy T. Upchurch

<u>Name/University</u>	<u>Title</u>	<u>Group/Mentor</u>
Nanette R. Smith College of William and Mary	Technology Transfer	Technology Applications Group Robert L. Yang
Kenneth R. Smith Hampton University	Langley Learning Laboratory	Office of Education Marchelle Canright
Seth S. Sobel James Madison University	Characteristics of Three-node Smoothing Element Under Penalty Constraints	Research and Technology Group Alexander Tessler
Mary M. Spracher Virginia Polytechnic Institute and State University	Office of Public Affairs	Office of External Affairs Keith Henry
David Stang Old Dominion University	Langley Research Center - Soluble Imide (LaRC-SI)	Internal Operations Group Carl Voglewede
Ronald E. Stephenson Virginia Polytechnic Institute and State University	Congressional Affairs	Office of External Affairs Lee Rich
Christopher S. Steward Norfolk State University	The Calibrations of Space Shuttle Main Engines High Pressure Transducers	Internal Operations Group Allan J. Zuckerwar
Melissa C. Stewart Rensselaer Polytechnic Institute	The Dependence Of The Change In The Coefficient Of Thermal Expansion Of Graphite Fiber Reinforced Polyimide IM7-K3B on Microcracking Due To Thermal Cycling	Research and Technology Group Craig W. Ohlhorst
Edwood G. Stowe Washington University	Analog Processing Assembly For The Wake Vortex Lidar Experiment	Internal Operations Group Phil Brockman
Corey V. Swenson St. Cloud State University	Parallel Processing with Digital Signal Processing Hardware and Software	Research and Technology Group Robert L. Jones
Antone L. Taylor Hampton University	Geographic Information System Data Analysis	Internal Operations Group William B. Ball
Erene Tcheng University of Virginia	Technology Transfer - Marketing Tomorrow's Technology	Technology Applications Group Barry V. Gibbens

<u>Name/University</u>	<u>Title</u>	<u>Group/Mentor</u>
Tamera L. Thomas Hampton University	Open Loop Simulation	Internal Operations Group John White
Karina M. Thorpe University of Utah	Geographic Information System Data Analysis	Internal Operations Group William B. Ball
Wilmer B. M. Ullmann University of Kansas	Entrepreneurship Within General Aviation	Research and Technology Group Daniel J. DiCarlo
Bryan C. Valek Georgia Institute of Technology	Determination of Stress- Corrosion Cracking in Aluminum-Lithium Alloy ML377	Research and Technology Group Marcia S. Domack
Luis H. Valencia University of Puerto Rico	A MATLAB/Simulink Based GUI For The CERES Simulator	Space and Atmospheric Sciences Program Group Calvin Mackey and John Chapman
Victor M. Valentin University of Puerto Rico	Oxidation Behavior of Carbon Fiber Reinforced Silicon Carbide Composites	Research and Technology Group Wallace Vaughn
Jessica Venable Princeton University	Validation of Global Climatologies of Trace Gases Using NASA Global Tropospheric Experiment (GTE) Data	Space and Atmospheric Sciences Program Group Joel S. Levine
Eugene L. Ward Norfolk State University	Homepage For The Global Tropospheric Experiment	Space and Atmospheric Sciences Program Group Jim Hoeli
Douglas P. West Eastern New Mexico University	System Construction For The Measurement of Bragg Grating Characteristics In Optical Fibers	Research and Technology Group Robert S. Rogowski
Mark E. Whitlock University of Illinois	Analysis Of a High-Lift Multi- Element Airfoil Using a Navier- Stokes Code	Research and Technology Group Kenneth M. Jones
Jeffrey M. Wilson University of Kansas	Wake Vortex Encounter Research	Research and Technology Group Robert A. Stuever

<u>Name/University</u>	<u>Title</u>	<u>Group/Mentor</u>
Terri L. Wilson Virginia Polytechnic Institute and State University	Langley Aerospace Research Summer Scholars (LARSS) Program Coordination	Office of Education Roger A. Hathaway
Robert G. Wright University of Missouri	Converting The Active Digital Controller For Use in Two Tests	Research and Technology Group Sheri Hoadley
Sara J. Yancey College of William and Mary	My Networking and Interpersonal Skills Developed At NASA Langley Research Center	Office of Education Marchelle D. Canright
Michael K. Zyskowski University of Kansas	Very Light Aircraft: Revitalization Through Certification	Research and Technology Group Natale Strain

**NEXT
DOCUMENT**

Effects of Nose Strakes

On Transport Aircraft

Student: Calvin T. Locklear

Mentor: Mr. Gautam Shah

Research and Technology Group

Flight Dynamics and Control Division

Vehicle Dynamics Branch

August 9, 1995

Abstract

A low-speed wind tunnel investigation was conducted in the Langley 12-Foot Tunnel on a typical commercial transport configuration to determine the effect of adding nose strakes on the aerodynamic characteristics of the model. The fuselage and wings of the model were scaled versions of the McDonnell-Douglas DC-9 aircraft. A generic tail assembly was employed that was different from that of the DC-9. Three different strake configurations were tested at several inclination angles. One strake configuration was identical to that employed on the DC-9 aircraft. The model was tested through a range of angles of attack and sideslip angles. Tests were made both with and without strakes and also with the vertical tail removed.

Introduction

During this summer LARSS program, I worked with Mr. Gautam Shah on a research project involving strakes in use on transport aircraft. Strakes are small fins placed on the nose of an aircraft to aid in yaw stability and control (ability of an airplane to turn about its vertical axis). A low-speed tunnel investigation was undertaken to see if strakes placed on a transport model would provide any appreciable stability or control improvements. Information was also wanted on possible interaction between the strakes and the vertical tail.

Vertical tails and rudders of transport aircraft pose many problems for designers. Due to their large size, they add extra weight to an aircraft. In addition the vertical tail produces drag for the entire flight, therefore adding to the cost to operate the aircraft. Since transports fly at cruise most of the time, the rudder is inactive for a good portion of the flight time. Consequently there is a real desire to find a way to reduce vertical tail size without sacrificing either stability or yaw control. The use of nose strakes may provide a positive contribution in this area.

Nose strakes are currently employed on a number of McDonnell-Douglas commercial transports including their DC-9 aircraft. Since a scale model of a DC-9 fuselage and wing configuration was available for testing, this model was chosen for the research project. The DC-9 model tail assembly and engines were unavailable, however, a generic tail assembly was available and was substituted for these initial tests. Detailed drawings of the DC-9 aircraft and the strake configuration presently in use on the aircraft were supplied by McDonnell-Douglas so that a scale strake model could be constructed and mounted similarly on the wind tunnel model. The model with this strake served as the baseline for the present tests. Various strake sizes and inclination angles were employed during this investigation.

Background

Research on the use of nose strakes on fighter aircraft configurations has been conducted for over ten years. Currently, there are some fighter configurations which react well with strakes and research has shown that there is a benefit from their use. Strakes have been effective at high angles of attack (above 30 degrees) in providing yaw control power. Their use has been particularly appealing because conventional vertical tails and rudders lose their effectiveness from becoming immersed in the low energy wing wake at these high angles of attack. It is important to realize that strakes, while they have a tremendous effect at high angles of attack, produce almost no yaw control at low angles of attack. This is significant because fighter aircraft operate at wide ranges of angles of attack (up to 70 degrees), while transport aircraft operate over a much lower range (0 degrees to 30 degrees). If strakes as employed on fighter aircraft were as effective at low angles of attack as they are at high angles, then this technology could be utilized on transports as well as fighters with obvious gains to operators. The fact that strakes are used on transport aircraft indicates that the size, shape, placement, and effectiveness of these strakes influence the aircraft in a manner different than the strakes used on fighter aircraft. The use of such strakes is obviously beneficial since McDonnell-Douglas uses nose strakes in so many of their commercial transport designs.

Test Facility

The tests were conducted in the 12-foot Low-Speed Wind Tunnel. The 12-Foot Low-Speed Wind Tunnel is an atmospheric pressure tunnel completely enclosed in a 60-foot diameter sphere. The test section has a 12-foot diameter octagonal-shaped cross section and a length of 15 feet. The drive system consists of a single 15.8-foot diameter 6-blade drive fan with an adjustable fan speed up to a maximum of 750 RPM. Dynamic pressure up to a maximum of 7 psf is available

as the test conditions. A sting system can position a model at any pitch angle from -10 degrees to 90 degrees, and sideslip angles from -90 degrees to 90 degrees. Smoke generation equipment is available for use in the facility to permit visual observations of the flow field.

The Test

Only a limited number of tests were made during this wind tunnel entry, and data were obtained only for the model configured for the cruise configuration with leading and trailing edge flaps undeflected and the rudder and horizontal tails set to zero. Two different strake configurations in addition to the baseline were tested. One strake had the same span width as the baseline strake, but it had a 80% increase in the chord length. The other strake had the same chord length as the baseline strake, but a 50% increase in the span. All strakes were constructed from sheet metal in the technician's shop and mounted on the model such that the trailing edge of all three strakes was at the same location on the fuselage. Rotation of a strake about its trailing edge varied the strake inclination angle. Inclination angles of 0 degrees, +10 degrees, and +20 degrees were tested.

The model was placed in the 12-foot tunnel and installed on the proper force balance and sting as needed to ensure the model was properly placed for this test. Several stings and mounting brackets were tried before settling on the 20-in. sting with a 30-degree offset mounting block and a force balance rated for 120-lbs. Once the model was mounted and the equipment was checked out the tunnel was started and testing began.

The model was tested at a single dynamic pressure of 5 psf in two manners; alpha runs and beta runs. Alpha runs consist of placing the model at a certain beta angle, which is the angle between the direction of the airflow and the centerline of the aircraft on a horizontal plane, and sweeping through a series of pitch angles. Beta runs consist of placing the model at a certain pitch angle and sweeping through a series of sideslip angles.

The schedule of tests is as follows: first, the model was tested, as is, with no strakes. Then the baseline strake was added, then the larger span strake, and then the larger chord strake. After these tests were completed, the vertical tail was removed from the model, in order to test the model's characteristics without a vertical tail. We then proceeded to repeat the same sequence of strakes (strakes off, baseline, larger span, and larger chord). Once these tests were completed, the vertical tail was replaced and the baseline strake was pitched to +10 degrees from its original position. We also did this with the larger span strake. Once again the baseline strake was replaced and canted to +20 degrees. After obtaining this data, the left baseline strake was removed leaving just the right baseline strake, which was tested at +20 degrees, +10 degrees, and 0 degrees. The next test performed was to remove all the strakes and to deflect the rudder to -25 degrees. The last test performed was a smoke test, where smoke was blown past the model to determine the flow field around the model.

Results/Conclusions

Since my summer session at NASA Langley is ending and this particular test is not completed, results from the data collected thus far are inconclusive. The test did determine that the strakes do have an effect, but how much and how significant is still to be determined. We have ascertained that the strakes do interact with the vertical tail in actually yawing the aircraft, because with the vertical tail removed almost no yawing capability was observed. Obviously, more tests will need to be performed before more specific conclusions can be drawn that may result in an actual change in aircraft configurations of the future.

**NEXT
DOCUMENT**

[Handwritten signature]

**Home Page: The Mode of Transport
Through The Information Superhighway**

Michelle R. Lujan

Odilyn L. Santa Maria

**Research and Technology Group
Fluid Mechanics and Acoustics Division
Aeroacoustics Branch**

Abstract

The purpose of the project with the Aeroacoustics Branch was to create and submit a home page for the internet about branch information. In order to do this, one must also become familiar with the way that the internet operates. Learning Hypertext Markup Language (HTML), and the ability to create a document using this language was the final objective in order to place a home page on the internet (World Wide Web). A manual of instructions regarding maintenance of the home page, and how to keep it up to date was also necessary in order to provide branch members with the opportunity to make any pertinent changes.

Introduction

As the world becomes more automated with every passing moment, it is the responsibility of NASA to keep pace with the ever-changing society as it adapts to a world of technology. The information super highway, also known as the internet or World Wide Web, is only one of the new options available. The internet provides the user with access to international information, as it provides information from other cities, states, countries, and even continents. The internet consists of a system of links that connect one location to another. The user is enabled to follow these links by "clicking" the mouse on underlined or highlighted text that is displayed on the screen. Information is displayed on the monitor by home pages at these various locations. A home page is a document that displays information, and is the foundation of the internet. They are created by individuals who have a desire or necessity to make information accessible to the internet worldwide.

Hypertext Markup Language, known simply as HTML, is a code used to create documents to be displayed on the internet. HTML introduces a series of predefined commands that provide the user with the flexibility to design the appearance of the information displayed when accessed. This code has the capability to display different fonts and graphical images on the monitor. The primary advantage of HTML is its ability to link documents together, which is the major reason this code is used.

HTML is not a difficult programming language that only computer experts can master. It is instead, a straightforward way of communicating to the computer the desires of the user and how to display the information. All that is needed to write a document in HTML are a few basic commands. Using these commands, the user can create a very simple, yet professional-looking home page. For those who would prefer more distinctive and intricate home pages, HTML provides commands to include graphics within the document and the option to change the background of the page. HTML provides all computer users with a special interest they would like to share with others over the internet with an avenue to do so.

Summary of Project

Creating a home page with information that others will find informative and interesting may seem a simple process to many, yet in reality, it involves much research and time to determine exactly what type of document would be most beneficial to internet users. Following through this process results in a home page that best reflects what both the creator and internet user desire.

Comprehending how the internet works aids the home page creator, as they learn more about the types of information and may view various ways of displaying it on the internet. By doing this research first, the creator benefits from the home pages from everywhere in all shapes, colors, and designs as the creative options are endless. "Surfing the net" helps the creator get a better idea of what information is necessary and how to display it on the home page. Viewing a wide variety of graphics and various texts provides the creator with more of a basis of what appears best on the computer screen, and creates the greatest visual impact. Even the most experienced home page creator can benefit by getting reacquainted with the internet on occasion.

Learning HTML becomes an easier task to understand after getting acquainted with the internet. The internet offers many HTML manuals on-line to refer to, instead of a hard copy handbook. Another alternative is to use the "view source" option available on most internet servers. The HTML commands that create any particular home page can be retrieved by choosing this option. This option provides even the most inexperienced creator with the opportunity to create more complicated home pages. By finding a page that looks similar to what the creator wants, producing a home page is just a matter of viewing the source code and reproducing the same commands. Once the HTML commands are learned, the home page can be created.

Upon completion of the home page, it becomes necessary to provide instructions pertaining to revisions that will need to be made to the home page in order to keep the

information current. A manual seems to be the easiest way to instruct the branch members on how to make necessary revisions to the home page. By doing this, branch members can make all the necessary revisions themselves by consulting the manual. The manual must be specific to the branch home page to ensure that the same format is maintained. Any new developments or changes that may take place in the branch can be easily reflected on the home page.

To create a professional home page, it is necessary to use certain equipment. A Macintosh IIfx and Microsoft Word 5.0 aids in creating an HTML file. The home page, while under construction, could be viewed by using Netscape 1.1. Another feature, photographs in a home page, add a personal touch to any page. To do this, a Kodak DCS 420 digital camera can aid in producing a digital image that can easily be included in the home page. Retrieving the image from the camera is made possible through the use of the Adobe Photoshop software package. Another alternative for photographs is to use a laser scanner to scan a photo that has already been taken. The Apple LaserScanner can create a facsimile of any photograph and prepare it for use on a home page. Adobe Photoshop can also be used on these images to make them better quality images.

With the aid of the available technology and equipment, a home page can be created with greater ease.

Once the process has been completed and the equipment has been used, the final result is a home page. Now that the home page has been created, all that remains is to submit it to the internet. Once the home page joins the internet, it will be viewed by thousands of people on a day to day basis. Everyone will have access to general information concerning the function of the branch. By joining the internet, the Aeroacoustics branch keeps pace with the fast moving society of today.



DFC - Aeroacoustics Branch

The **Aeroacoustics Branch** is part of the Fluids Mechanics and Acoustics Division(DF) at Langley. The branch is under the largest division at LaRC due to the recent reorganization.

● **Location:**

Mail Stop 461
Building 1208a
2a North Dryden Street
Hampton, VA 23681-0001
Phone: (804) 864-5660
Fax: (804) 864-8290

● **Functional Statement**

Explains the area of acoustics that the branch conducts research in.

● **Management:**

John S. Preisser, Head
Joe W. Posey, Assistant Head
Peggy Sipes, Secretarial Co-op

● **Personnel**

A listing of the current personnel in the Aeroacoustics branch including civil employees and contractors.

● **Facilities**

A complete listing of the facilities that the Aeroacoustics Branch frequently uses to conduct research.

● **Publications**

A listing of publications that the branch has published over the years.

● Groups in the Branch

● TSD

 [LaRC Home Page](#)

 [NASA Home Page](#)

*This home page was created by
Michelle R. Lujan
LARSS student
University of Texas at El Paso*

*Responsible NASA official:
Odilyn Santa Maria
o.l.santamaria@larc.nasa.gov*

**NEXT
DOCUMENT**

**DESIGN CONSIDERATIONS FOR THE NEXT GENERATION OF
GENERAL AVIATION DESIGNS**

11-25

9.11

BY

BRIAN D. MARCHESSEAULT

GRADUATE STUDENT

AEROSPACE ENGINEERING DEPARTMENT

EMBRY-RIDDLE AERONAUTICAL UNIVERSITY

DAYTONA BEACH, FLORIDA

PRESENTED TO

THE LANGLEY RESEARCH SUMMER SCHOLARSHIP PROGRAM

AUGUST 8, 1995

HAMPTON, VIRGINIA

Abstract

This paper discusses the results of research conducted at NASA Langley Research Center during two summer programs during 1994 and 1995. These programs were the NASA Advanced Design Program and the Langley Research Summer Scholars program. The work was incorporated in a three phase project at Embry-Riddle Aeronautical University which focused on development of the next generation Primary Flight Trainer, as well as in ERAU's participation in the AGATE General Aviation Design Competition. The project was conducted as part of the ERAU/NASA/USRA Advanced Design Program in Aeronautics as well as the AGATE competition. A design study was completed which encompassed the incorporation of existing conventional technologies and advanced technologies into PFT designs and advanced GA aircraft designs. Multiple aircraft configurations were also examined throughout the ADP/AGATE. Evaluations of the various technologies and configurations studied will be made and recommendations will be included.

1. Introduction and Background

Embry-Riddle Aeronautical University has been involved with the NASA/USRA Advanced Design Program since 1992, when the university was invited to participate in the Aeronautics division of the program. At that time, the ERAU aerospace engineering department's design faculty recognized an important role that the Embry-Riddle could play in the program. Although General Aviation had been addressed at times in the first eight years of the program, the subject had been underemphasized. In particular, the topic of Primary Flight Trainer aircraft had been completely neglected. Due to Embry-Riddle's position as one of the leading aviation training schools in the world, the development of a contemporary PFT was of obvious importance to the school. This fact, coupled with the overall plight of the GA industry, prompted the decision to focus the ERAU/NASA/USRA ADP on the development of the next generation PFT.

As part of the ADP structure, each participating university is teamed with a NASA center that shares a focus common to the school's ADP topic. In Embry-Riddle's case, NASA Langley Research Center was chosen. Through this cooperative arrangement, a Graduate Teaching Assistant was sent to LaRC each summer to complete research on topics relevant to the university's ADP. The research gathered by each GTA was then incorporated into the next phase of the ADP design study. Support work from outside of the ADP, including LARSS participation, the AGATE General Aviation Design Competition, and other such programs, was integrated into the overall study. The AGATE program is being conducted by the General Aviation/Commuter Element of the NASA Advanced Subsonic Technology Program in an effort to create a new generation of GA aircraft. Through graduate student participation in the ADP and LARSS, ERAU was able to make it's first ties to the AGATE program. This affiliation has expanded into ERAU becoming a member of the AGATE government/industry/academia consortium on a higher level, and has also included student participation through the AGATE General Aviation design competitions. In this manner, the ADP study does not end with the completion of the ADP, but is to continue into future AGATE, LARSS, and other ERAU program participation.

Phase I of the ADP focused on incorporating existing "off the shelf" technologies and on integrating a true concurrent engineering environment into the ERAU design classroom. Phase II further developed some of the Phase I baseline configurations with more advanced technologies and created a high emphasis on occupant safety and crashworthiness. The goal of Phase III was to incorporate further advanced technologies (such as those still under development) and to summarize the efforts of the entire ERAU/NASA/USRA ADP. Through the overall efforts of the ADP, a design database of technologies (old and new) and configurations specific to GA was created. Throughout each phase of the projects, the utilization of cutting edge technologies as design tools was also a major goal. The manner in which the design classes were conducted and in which the group projects were assigned generated the most successful attempts at CE ever made at ERAU. The use of CAD and FEM at the Daytona Beach campus were highly stressed as design tools in the classroom, as well. Another of the major innovations in undergraduate design course work, due in part to the ADP, was the introduction of rapid prototyping at ERAU. Through a National Science Foundation grant, the university obtained a stereolithography (SL) capability at the same time the ADP was commenced. In Phase III, SL has been incorporated directly into the detailed design curriculum at Embry-Riddle as part of the ADP, AGATE competitions, and other programs.

2. The Need in GA

The GA industry has undergone a severe depression, nearly to the point of extinction. The boom in production of Single Engine Piston aircraft in the 1970's was followed by a major decrease in shipments in the years to follow. The fact that such a sharp dive in production has occurred in the GA industry has been of major concern to the aviation industry, in general. It is GA aircraft that supplies the training necessary in the production of pilots that go on to fly larger aircraft. A number of studies have been conducted to analyze the decline in GA and to try to create a means of revitalization of the industry. The results of the past studies have indicated that the average age of the SEP airplane is 28 years¹, which is a rather long lifetime. The obvious reason for such a high average age is the fact that newer aircraft simply have not been produced to replace the older fleets. However, a demand still exists for the aircraft. The major reason that new aircraft have not been produced in large numbers is primarily the influence of product liability.

Reference 2 states the product liability situation in 1987: "Product liability costs for manufacturers (of GA aircraft) have skyrocketed in the past three years (1985-1987). Huge awards or settlements have driven up costs." The reference states that in 1985 manufacturers and their insurers paid over \$200 million in judgments, settlements, and defense costs, up from \$47 and \$77 million in 1981 and 1983, respectively. "The manufacturers report in 1985 insurance cost averaged \$70,000 for each airplane delivered... This amount, if added to the price of small aircraft, would make the price astronomical." It is easy to see why the GA industry entered such a plummet.

The recent passage of the products liability reform bill, known as the "1994 General Aviation Revitalization Act (S.1458)," has created some aid to the problem. However, the bill is far from solving all liability problems, and still allows for many potential suits that could continue to

devastate the GA industry. The employees of companies such as Piper Aircraft Company still see a nightmare of liability problems to be solved before a true revitalization of the industry can take place.

One way to alleviate the liability problem is to look to the automotive industry. The last Cessna 152 produced in 1986 was essentially the same aircraft as the original model 150 designed in the 1950's¹. Yet, the automotive industry continues to make vast improvements in design and particularly in crashworthiness. With added design features such as airbags and 5 mile-an-hour bumpers, automotive insurance prices progressively decrease. A similar trend could be applied to the future of GA design.

During 1980-85, the National Transportation Safety Board conducted a study of GA aircraft occupant restraint and seat systems under the title of the "General Aviation Crash Worthiness Program."¹ The results of this study indicated the need for energy absorbing seats and the use of shoulder harnesses. As a result of the study, major changes were made to the airworthiness regulations for GA.

3. ERAU's Response to the Need

Due to the effect of product liability and its relation to occupant safety upon the GA industry, crashworthiness was a major focus throughout Phases II and III of the ADP, as well as in AGATE design efforts. In order to accomplish this, aspects of FAR Part 23 regarding occupant safety, crashworthiness and the Head Injury Criterion were incorporated into the ADP/AGATE designs. The HIC is an equation, integrated over the time duration of impact, which places a specific upper limit on the integral acceleration of the head's CG¹. The HIC and the other crashworthiness requirements of FAR 23 were then incorporated into the ERAU designs through the generation of Spatial Requirements Specification Documents.

The SRSDs were documents generated for individual aircraft configurations (for example, a two-seat high wing tractor versus another document for a three-seat low wing pusher). The SRSDs provided cabin volumes for each given configuration which adequately met the HIC and Part 23 requirements. Simultaneously, each provided room for adequate structural volume around the cabin, which was designed to accommodate up to the 95th percentile man. A brief explanation of the spatial requirements accompanying the cabin volume was also included in the SRSDs. These documents were then to be given to preliminary design students for incorporation into future designs. This was to allow for realistic cabin and surrounding structural volumes in the generation of future preliminary designs.

4. Results of the ERAU ADP and AGATE Programs

Throughout the process of generating crashworthy designs, a large database of information regarding a myriad of GA design parameters such as engines, airfoils, and many other topics was created at ERAU. This information was gathered throughout the ADP by the GTA's during their internships at LaRC (through the ADP and LARSS), as well as by the faculty and students at

Embry-Riddle. The following sections discuss some of the observations made and conclusions drawn from the ADP which were also integrated into ERAU AGATE participation.

4.1 Airfoil Selection and Wing Position

In Phase I of the ADP, conventional airfoils were employed in the designs. However, in Phase II it was decided to explore the possibility of incorporating Natural Laminar Flow (NLF) airfoils. The Phase I designs were refitted with NLF airfoils and the new designs generated in Phase II also included them. The study revealed that the NLF airfoils were effective in providing improved performance over traditional airfoils. However, the manufacturing of the NLF airfoils required high tolerances, perhaps even beyond the practicality of aluminum construction. Therefore, composite construction was considered for the NLF designs. Another potential problem with the NLF designs was the effect of debris, such as insects, collecting on the wings. However, NLF performance in this state was, at worst, equivalent to traditional NACA series airfoil performance. The final problem recognized with NLF airfoils was the low speed power requirements, which were potentially dangerous to student pilots. After considering all the advantages and disadvantages of the NLF airfoils, it was concluded that a NACA 6-series airfoil may be the best option for a low cost PFT with safe, desirable training characteristics. Conversely, for advanced GA designs, such as the ERAU AGATE design submittal, NLF airfoils were considered an effective choice.

Wing positions examined in the ADP and AGATE activities varied from low to mid to high wing. The driving force behind this parameter was primarily the general configuration of the aircraft. In other words, the engine and cabin area positions were of major concern to wing position. The structural weight and complexity of each wing configuration was another factor. The mid wing configuration appeared to be the least desirable due to complexities of wing structure at the cabin interface, while maintaining a desired cabin size.

4.2 Powerplant Selection and Position

Several powerplants were explored in the design studies. These included currently certified engines such as the Lycoming O-235 and non-certified engines such as the Zoche Diesel. The non-certified engines considered were engines with potential for near-term certification. Air cooled engines were the most common type of engine used, however, liquid cooled engines such as the Rotax 914 were also examined. For the pusher aircraft, it was determined that a liquid cooled engine may be most advantageous. This eliminated the problem of providing venting to the engine compartment, and thus reduced the associated drag as well. The tractor configuration aircraft would also benefit from the reduced cooling drag of a liquid cooled engine, however not as dramatically as the pusher.

In the course of the design activities, several configurations were considered for engine position. The first designs pursued were originally tractor and mid-engine configurations. Later in the study, a pusher configuration was added. The mid-engine concept was eventually phased out and modified to a tractor arrangement. This was due chiefly to the problem of the drive shaft required for such an aircraft. The drive shaft offered intriguing possibilities in acting as an aid in shock absorption upon impact. Examination was conducted of using the drive shaft to crumple in stages, thereby absorbing impact shock during a crash. However, the shaft added unnecessary

weight, cost, and maintenance complexity to the aircraft design and was therefore removed from the design.

The incorporation of a ducted fan into the designs was made towards the end of the ADP and continues into AGATE. In the early stages of the studies, it was decided to first examine designs with more conventional powerplant configurations, even in the pusher configuration. However, upon further assessment of desired performance, safety, and noise characteristics, the ducted fan was considered for the pusher design. The inclusion of a ducted fan for the tractor designs would have been impossible concerning the practicality of both mounting the fan shroud and providing proper pilot visibility. For these very reasons, the pusher design seemed to provide a perfect testbed for the fan concept.

Mounting of the fan shroud was considered in several different configurations including incorporation into the tail boom design, as the booms granted obvious mounting points for the shroud. However, this configuration was thought to possibly cause complications in the operation of the ducted fan. Because a very small tolerance must be included between the blade diameter and the inside of the fan shroud, it is necessary to minimize any possibility of the blades striking the shroud. The mounting of the shroud to the tail booms, with a rigid connection (via a drive shaft) to the engine, could potentially introduce vibrations from the booms. This would thereby creating interference between the shroud and the blades. Therefore, another shroud mounting configuration under scrutiny is to mount the shroud directly to the aft portion of the fuselage. Yet another design being studied incorporates the ducted fan as a self contained unit attached to the tail booms, but connected to the engine through a flexible coupling. This would also reduce the vibration problem at the prop-shroud interface, but may add undesired weight to the design (despite the possible increased maintenance accessibility). The only practicable alternative to the pusher configuration would be a high mounted tractor or pusher configuration, such as is typically designed in amphibious aircraft. However, this type of design would produce undesirable thrust line effects versus the direct thrust line of a more "conventional" pusher engine mounting.

The reasoning behind the inclusion of a ducted fan in the advanced designs was multifaceted. The initial consideration was to improve the noise characteristics of the aircraft. Noise abatement can be addressed by three basic issues: propeller blade number, blade contour, and inclusion of a ducted fan. In the tractor configurations, the only options were to increase the blade number and modify the blade contour until desired noise characteristics were achieved. However, with the pusher, the ducted fan could be used, as well. By including a higher number of blades, the prop cost will increase significantly. Yet, by using a fan concept, the blade number can be kept to a minimum while still attaining favorable noise characteristics.

Admittedly, the fan will also increase the price of the aircraft. However, the price increase is accompanied by more than just improvements in noise abatement. Ducted fans are known to increase thrust due to their effect of increasing prop efficiency. This factor could potentially offset the extra cost of including the ducted fan. Also, in a mass production market, particularly the one projected for AGATE, this and other advanced technologies will be highly reduced in acquisition price (due to supply and demand).

Apart from the increased cost of a ducted fan, Foreign Object Damage may prove a potential problem for such a design. This problem is being considered by examining the spray pattern of debris off the landing gear tires. Corrective action could then be taken, if necessary, but may not be required due to the smaller disk area of the fan versus a regular prop. Additionally, one of the concepts for the self contained ducted fan includes a stabilizing strut from the fan to the fuselage. This strut may aid in protecting the fan from FOD.

4.3 Landing Gear

In approaching the landing gear design, the original decision in each ADP design was to use fixed gear. This was chosen due to the reduced cost (for design, manufacturing and maintenance) and complexity. The drag penalty and resulting performance reduction were not considered a problem with the original design goal of approximately 120 knots (for the ADP). In order to achieve higher cruise speeds (if so desired for upgrades of the design outside the PFT market, or more specifically, as required to achieve AGATE requirements), partially or fully retractable gear become necessary. In the original case (lower speed requirement), the early pusher designs considered oleo struts for both the nose gear and the main gear. Later study considered changing to a damped spring nose gear. This would greatly reduce the cost and complexity associated with oleo type gear. Spring gear could also replace the oleo gear for the pusher main gear, as was originally conceived for the tractor designs. Similar, but somewhat more advanced, concepts were also employed in the AGATE retractable designs which, again, were tailored towards crashworthiness.

4.4 Seating Arrangement

In order to create higher performance in each of the concepts, it was decided to examine the effect of incorporating staggered seating. This was done in both the tractor and pusher designs. Initially, it appeared intuitively obvious that by incorporating staggered seating, the resulting reduction in fuselage cross-section would produce improvement in aircraft performance. In order to check this, a related study was conducted¹ to examine the actual effects of cabin width upon performance. From the study, it was determined that the reduced fuselage cross-section associated with staggered seating actually had very little effect upon aircraft performance. For fuselages with larger length-to-diameter ratios, the change in diameter did not change performance appreciably.

One benefit of staggered seating in the cockpit was more shoulder room for the student and instructor, while still allowing the instructor to view the student at the controls and vice versa. Another benefit of the staggered seating arrangement in the pusher was that it allowed for the reduction of parallax in viewing instruments from the instructor's seat. This arrangement could potentially require a separate set of instruments for the instructor. With an advanced cockpit system of the projected AGATE variety (i.e., a glass cockpit system which incorporates all instruments with an on-board central computer system, displayed on screens in front of the pilot), this would pose little problem. The same central computer and instrumentation would be used to drive both the student and instructor displays. This would also dispose of parallax problems associated with today's instruments as well as the problems of side viewing associated with CRT displays. Using the AGATE type display in conjunction with a fly-by-wire control system would

also eliminate problems with control system routing typically associated with staggered seating. However, an AGATE type system is not currently available and may not be for quite some time. The cost and complexities associated with staggered seating may not be worth the benefits in creating a low cost PFT in the immediate future. Therefore, these technologies are reserved for potential applications in the AGATE market to come.

The other major consideration in seating arrangement for the designs was the number of seats to be included. For the AGATE program, the design specifications called out a range of two, four, or six seat aircraft. A four seater was the choice for the 1995 AGATE design as middle ground, and due to the larger potential market (initially at least). However, in future AGATE design efforts at ERAU, it is anticipated that the designs will be expanded to an AGATE family of all seat configurations.

Since the primary mission of a PFT requires only a student pilot and an instructor on board, the obvious choice would be a two-seat configuration. However, ERAU utilizes a training program dubbed "Gemini" in which a second student pilot is to fly on training flights as an observer. This increases the seating requirement to a minimum of three seats. There are very few existing three-seat aircraft. The trend is to step from two seats to four seats. Yet, in order to keep the power and cost requirements to a minimum, it was decided to incorporate no more than three seats into the ADP designs. In the end, a two-seat configuration was seen to be the best for the general PFT market, excluding the "Gemini" program.

4.5 Crashworthiness and Occupant Safety

As stated previously, a primary focus of the ADP and AGATE was to address the issues of crashworthiness and occupant safety. The history of GA has shown little regard for these topics, which has made major contributions to the current nightmarish litigation situation. The goal of these projects was to create a revolution in the thinking associated with crashworthiness/occupant safety and GA. To accomplish this, the first problem to be addressed was to determine exactly how crash safety could be incorporated into all stages of the design process. This began with conceptual design, where students were informed of design attributes which could greatly enhance crash survivability (such as angling the bottom edge of firewalls/bulkheads directly in front of the crew to prevent scooping on impact). The problem was then expanded to include detail design. In this stage, crashworthiness was heavily addressed and fully developed. This was accomplished by determining design constraints that would ultimately conclude in a truly crashworthy design process.

The crashworthy design constraints originated from several sources. Although historically neglected in GA, crashworthiness and occupant safety have been widely researched and addressed by numerous sources such as the NTSB, NASA, the FAA, industry and academia. From the study of this broad database, general points for crashworthy design were selected. Precise design constraints were also determined from the FAR Part 23. From FAR 23.561, the loading conditions at impact were determined to be 9 or 18 g's, depending on the predicted impact scenario for a given component. From FAR 23.562, the conditions to be met were at both a 60 degree impact at 19 g's from the horizontal and at a 10 degree yawed frontal impact at 26 g's for occupant restraint systems and seats. These conditions were incorporated to address emergency

landing conditions within the cockpit. From these regulations, the requirements for proper cockpit volume could be determined and the integration of a seat that could withstand a 26 g impact was found necessary. These total loading conditions, from FAR 23.561 and .562 were then to be used as the design guidelines, as they were found to be the worst possible loading constraints for crashes (as determined in the development of the regulations).

The loading constraints were then to be applied to all detail designs. The particular loading conditions applied to a given component were selected from the constraints. This was based on the position of the component in the aircraft. For example, if the component was in the cockpit, it would need to withstand the constraints for items of mass in the cockpit per FAR 23.561. The integration of a seat that could withstand 26 g's played an integral part in this. It reduced the loading constraints in some cases due to the fact that the seat could absorb 26 g's, thereby requiring less severe loading constraints for a related structure. In addition to applying the loading constraints to detail design, multiple features were evaluated for integration into a complete aircraft design which provided the highest level of crashworthiness and occupant safety possible. These included items such as the incorporation of crashworthy seats, restraint systems, and many other items.

Each design for the ADP and AGATE was created with the intent of surviving the worst case impact scenarios determined from FAR Part 23. However, it was worth considering a means of returning the aircraft to the ground in an emergency situation with as little stress as possible placed upon the occupants. To do this, a ballistic parachute was considered for integration into the designs. The pusher design provided a perfect opportunity to explore this option. More than sufficient volume existed in the cabin area behind the occupants for mounting a ballistic parachute system. This location was also directly in the CG range of the aircraft, thus providing for the desired balance upon deployment of the parachute. The package offered by Ballistic Recovery Systems³ was used for comparison of volume and mounting requirements of a ballistic parachute for the ERAU designs. The particular package used for comparison was the Cessna 150/152 model. Although the incorporation of such a package was found to be possible, it was also determined to add considerable weight and cost to the overall aircraft design. Therefore, it was decided to include the BRS as a design parameter for both the PFT and AGATE designs, but to potentially offer it only as an option at the time of sales.

Crashworthy seats are becoming a reality slowly, but surely. In the development of the ERAU designs, a seat/restraint system developed by the Jungle Aviation and Radio Service was implemented. The seat, commonly referred to as the "JAARS seat," was the only seat available at the time that withstood dynamic testing requirements of FAR Part 23. Although the seat was never certified, it has been flown in a number of JAARS missionary aircraft. With the development of crashworthy seats under FAR 23.562 in the future, it will be possible to redesign the next generation GA aircraft around these alternate seats.

Another technology under investigation for occupant safety was the incorporation of airbags. This is one of many areas in which the automotive industry is far ahead of the GA industry. The integration of air bag into cars has saved numerous lives, prevented many injuries, and has even resulted in the reduction of insurance costs. Obviously, this is an area in which GA could use

improvement. Therefore, in Phase III of the ADP as well as in AGATE design efforts, students were challenged with incorporating airbags into their designs. The installation of such devices has proven thus far to be a challenge in GA aircraft. Yet, studies have been conducted by the FAA, NTSB, and NASA in the incorporation of airbags into both GA and other types of aircraft. The student investigations have so far resulted in preliminary suggestions for airbag integration. One configuration considered involved mounting the airbag installation in the top of the instrument panel, perhaps set behind the instruments (requiring slight repositioning of the instruments as a possibility). This configuration is similar to some automotive installations and may reduce obstruction of the instrument panel while preventing an oversized and complex yoke design. Another possible configuration involved airbags installed in the headrests, similar to a design considered in military aircraft. The method employed in the AGATE design was to have the airbag deploy from the passenger side of the instrument panel, instantaneously expanding to cover the pilot's side as well.

Some of the other advanced technologies considered in the studies have included fire hazard reduction schemes and smart structures. Items such as impact activated fuel cut-off switches and fuel bladders have already been integrated into the later ADP designs. Additionally, a workable in-situ fire extinguishing system was designed for installation into the AGATE design. This design has led to the concept of a water spray system in the cockpit, with a chemical extinguishing agent introduced in the contained engine compartment behind the cabin area. Yet, items such as smart structures are still in the early stages of design. This is due primarily to the highly experimental status of such technologies, as applicable to GA. Following future developments in these areas, it may be possible to integrate them into future advanced GA designs in a cost-effective and practical manner.

By enhancing the overall safety attributes of GA aircraft, benefits additional to product liability will be realized. If GA were to appear an even safer mode of transportation to the general public (beyond its already exemplary record as compared to automobiles), then wider interest in the industry could potentially be realized. This would expand the market and thereby truly allow for not only a revitalization of the GA industry, but indeed would create a renaissance within the industry (as is projected for AGATE). Admittedly, the initial production cost of this new breed of crashworthy PFT would be higher than that of existing designs, and would also most likely be higher for AGATE. However, the possible reductions in product liability problems may easily counter this cost increase. The increased fuselage size of a crashworthy aircraft is also of concern at first glance. However, a study conducted at ERAU proved that the increased fuselage size would only affect aircraft weight and performance very modestly (about a 2 pound increase per inch of fuselage width, and a maximum of 5-10 knot decrease in cruise speed versus existing aircraft)¹.

4.6 The Recommended Platform

Of all the designs generated by the ADP, the twin boom pusher configuration was found to be the most successful. Although there were benefits to the other configurations studied, this one provided the best overall platform for integration of the technologies studied. The ADP pusher design has attributes which lend directly to the concept of crashworthy design. Therefore, this configuration was applied to the AGATE design efforts. In many GA crashes, the aircraft is

subjected to belly-in landings where the underside of the aircraft sustains extensive damage and the props are destroyed. For fully or partially retractable gear designs (such as for AGATE), this issue is of prime concern. The ducted fan pusher configuration permits higher protection of the prop in such an impact scenario, in addition to the benefits discussed previously. Also, the possibility of a removable shock absorbing nose cone allows for easy replacement and/or removal and repair in the event of a relatively minor crash. The pusher concept was the most adaptable to the application of this and the other technologies discussed above.

5. Conclusion

This paper has discussed the study of the design of the next generation of general aviation aircraft as conducted through the ERAU/NASA/USRA ADP and AGATE design efforts. The various technologies and configurations studied throughout the ADP, AGATE and LARSS programs were discussed and recommendations were made regarding many of them. Certain areas of examination have not yet been completed, as the AGATE program continues, and with it further ERAU research through programs such as LARSS. From the efforts conducted thus far, a large database containing data on a myriad of GA technologies has been assembled at Embry-Riddle. The database consists of information on engines, airfoils, crashworthy related technologies and other items, as well as ERAU student and faculty reports, and external reports and articles. This database is offered as an item of interest for evaluation in the design of future GA aircraft, particularly PFT and AGATE designs.

6. Acknowledgments

The author would like to thank Dr. James G. Ladesic and Professor Charles N. Eastlake for their guidance and support throughout the duration of the ADP and AGATE design programs. Thanks also to Dr. Bruce J. Holmes and H. Paul Stough, III, of NASA LaRC for their support throughout the author's internships (as part of the ADP and LARSS programs). Special thanks goes to the students who participated in the ERAU/NASA/USRA ADP and AGATE design competition from 1992 to 1995.

7. References

1. Eastlake, Ladesic, The Effect of Occupant Crashworthiness Regulation Compliance on General Aviation Aircraft Size and Performance, AIAA Aircraft Design, Systems and Operations Meeting, Mississippi, May 1994.
2. Rubin, VanDuzee, The Demand for Single Engine Piston Aircraft, FAA-APO-87-18, Office of Policy and Plans, Federal Aviation Administration, Washington, DC, August, 1987.
3. FAA Certified Emergency Parachute System for Cessna 150/152, Ballistic Recovery Systems, Inc., Minnesota, 1994.

**NEXT
DOCUMENT**

**MATERIALS FOR THE GENERAL
AVIATION INDUSTRY: Effect of
Environment On Mechanical Properties
of Glass Fabric / Rubber Toughened
Vinyl Ester Laminates**

**Timothy M. McBride, LARSS
H. Benson Dexter, Mentor**

**NASA Langley Research Center
Research & Technology Group
Materials Division
Mechanics of Materials Branch**

Table of Contents

- I. Background- NASA's Role in GA Aircraft Manufacturing**
- II. Material Selection- Fabrics and Matrix Resins**
- III. Test Plan- Standards and Environmental Conditioning Description**
- IV. Results to Date and Discussion**
 - A. Effect of Fabric**
 - i. Tension Modulus**
 - ii. Tension Strength**
 - iii. Compression Strength**
 - B. Effect of Resin**
- V. Concluding Remarks**
- VI. NASA LaRC Facilities Utilized**
- VII. References**

Abstract

A screening evaluation is being conducted to determine the performance of several glass fabric/vinyl ester composite material systems for use in primary General Aviation aircraft structures. In efforts to revitalize the GA industry, the Integrated Design and Manufacturing Work Package for General Aviation Airframe and Propeller Structures is seeking to develop novel composite materials and low-cost manufacturing methods for lighter, safer and more affordable small aircraft. In support of this Work Package, this study is generating material properties for several glass fabric/rubber toughened vinyl ester composite systems and investigates the effect of environment on property retention. All laminates are made using the Seemann Composites Resin Infusion Molding Process (SCRIMP), a potential manufacturing method for the General Aviation industry.

I. Background

Lighter, safer and more affordable aircraft structural concepts are needed to revitalize the American General Aviation (GA) industry. Such goals are the focus of the Integrated Design and Manufacturing Work Package for General Aviation Airframe and Propeller Structures at NASA Langley Research Center (LaRC). As part of this Work Package, NASA LaRC researchers are currently developing novel composite materials and low-cost manufacturing methods to meet the specific needs of the GA industry.

In an effort to ultimately determine design guidelines for GA aircraft manufacturers, extensive testing is underway to generate material properties for the glass fabric/vinyl ester (VE) composites and to investigate the effect of humidity and temperature on these properties [1]. The primary glass fabric chosen for evaluation was an 8-harness satin composed of E-glass fibers (Style 7781). This fabric is known to have superior drape, a critical measure of manufacturability, but is more expensive than other glass fabrics and with a thickness of only 10 mils per ply, requires extensive layup time to build up to the designed laminate thickness. The primary vinyl ester chosen for evaluation was the Novolac based Dow Derakane 470-3. This resin has the highest glass transition temperature (T_g) of all available vinyl esters, and therefore, will have the highest operating temperature capabilities, but its low failure strain has generated concerns of possible reductions in fatigue life and adhesive properties, both key to successful aircraft composites.

To address these concerns, a 10-week material property screening evaluation of alternative glass fabric/vinyl ester composites was conducted. The study was sponsored by the Langley Aerospace Research Summer Scholars (LARSS) Program.

II. Material Selection

Because the GA industry is primarily driven by cost, reductions in part lay-up time is crucial. The high lay-up time associated with small ply thickness fabrics, like the woven yarns, is avoided when using knit rovings. These fabrics contain multiple layers of fiber, oriented at various angles and all knit together to form one ply. This feature allows for far more cost efficient part lay-up. For this reason, it was thought that a comparison of the mechanical properties of knit roving laminates with the existing data on woven yarns would be beneficial to the GA aircraft manufacturers. Table 1 summarizes some of the characteristics of the glass fabrics considered.

Further, because the questions surrounding the performance of the Novolac based VE chosen as the primary matrix resin were mainly raised due to its low failure strain, it was thought that a comparison of the mechanical properties of rubber toughened VE laminates with the existing Novolac based data would also be beneficial. Table 2 summarizes properties of the Novolac based and rubber toughened vinyl esters available as laminating resins.

<u>Woven Yarns</u>	<u>Knit Rovings</u>
* 10 oz./sq. yd.	* 12-72 oz./sq. yd.
* good drape characteristics	* low fiber waviness
* expensive	* multiple layers per ply
* small ply thickness	* low lay up time

Table 1: Comparison of Candidate Glass Fabrics

<u>Vinyl Ester Type</u>	<u>Tg (°F)</u>	<u>Failure Strain (%)</u>	<u>Viscosity (cps)</u>	<u>E (KSI)</u>	<u>Example</u>
Rubber Toughened	200	10	400	440	Derakane 8084
Novolac Based	280	2-3	350	500	Derakane 470

Table 2: Comparison of Candidate Matrix Resins

In considering alternative materials to supplement the current data for the woven glass yarn/Novolac based VE, it was decided that 5 different panels would be constructed using the Seemann Composites Resin Infusion Molding Process (SCRIMP). This process has been the focus of several studies of low-cost resin transfer forming [2,3,5,6]. Components of the five panels are as follows (glass fabric/resin):

- 1) 8-Harness Satin (Style 7781)/Dow Derakane 8084
- 2) 16 oz. Biaxial Knit (Style C16)/Dow Derakane 8084
- 3) 18 oz. Biaxial Knit (Style C18)/Dow Derakane 8084
- 4) 24 oz. Biaxial Knit (Style C24)/Dow Derakane 8084
- 5) 32 oz. Biaxial Knit (Style C32)/Dow Derakane 8084

III. Test Plan

The core questions to be answered in testing the five laminates follow:

- Are rubber toughened vinyl esters suitable laminating resins for General Aviation aircraft?
- What is the effect of biaxial knit fabric weight on laminate properties?
- How do glass biaxial knit/vinyl ester laminates compare to glass weave/vinyl ester laminates?
- Is the reduction in hot/wet data due to property degradation of resin? of fiber? and/or of interface?

Table 3 summarizes the testing planned to deliver answers to the above questions.

Test	Condition	7781/8084	c16/8084	c18/8084	c24/8084	c32/8084
Tension	RTD	5	5	5	5	5
Tension	ETD	5	5	5	5	5
Tension	RTW	5	5	5	5	5
Tension	ETW	5	5	5	5	5
Compress.	RTD	5	5	5	5	5
Compress.	ETD	5	5	5	5	5
Compress.	RTW	5	5	5	5	5
Compress.	ETW	5	5	5	5	5
Condition	RTD	No Conditioning/Tested @ 70°F				
Key:	ETD	No Conditioning/Tested @ 165°F				
	RTW	Conditioned @ 120°F, 85%RH, 3 months/Tested @ 70°F				
	ETW	Conditioned @ 120°F, 85%RH, 3 months/Tested @ 165°F				
Test	Tension	ASTM D638				
Key:	Compression	ASTM D695				
	Volume Fraction	ASTM D2584				
	Transition Temp.	DSC				

Table 3: Test Matrix

IV. Results to Date and Discussion

Due to time constraints, the samples (100 in all) that require 3 months of pre-test conditioning have not been tested at this point. All testing should be concluded in the near future at Boston University. The data for the 100 unconditioned test samples follows.

A) Effect of Fabric:

i) Tension Modulus

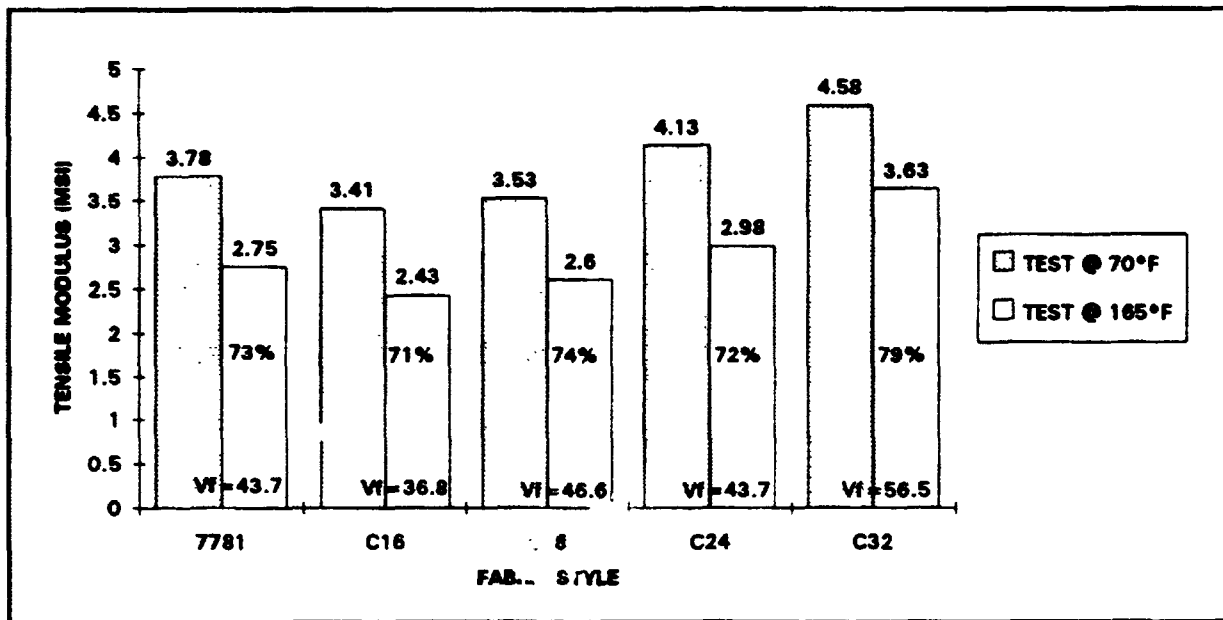


Figure 1: RTD and ETD Tension Modulus

As seen in Figure 1, with regard to the knit laminates, tension modulus increased as the fabric weight increased, not necessarily as fiber volume fraction increased as one typically expects of composites. This anomaly to the common trend is evident in the 17% higher tension modulus of the 24 oz. fabric than of the 18 oz. fabric despite a slightly lower fiber volume fraction. In general for the knit laminates and especially for the heavier ones, tension moduli were higher than for the weave. This is consistent with the idea that uncrimped (straight) fibers result in higher composite tension moduli. Moduli retention at 165°F was similar for all laminates (71-79%).

ii) Tension Strength

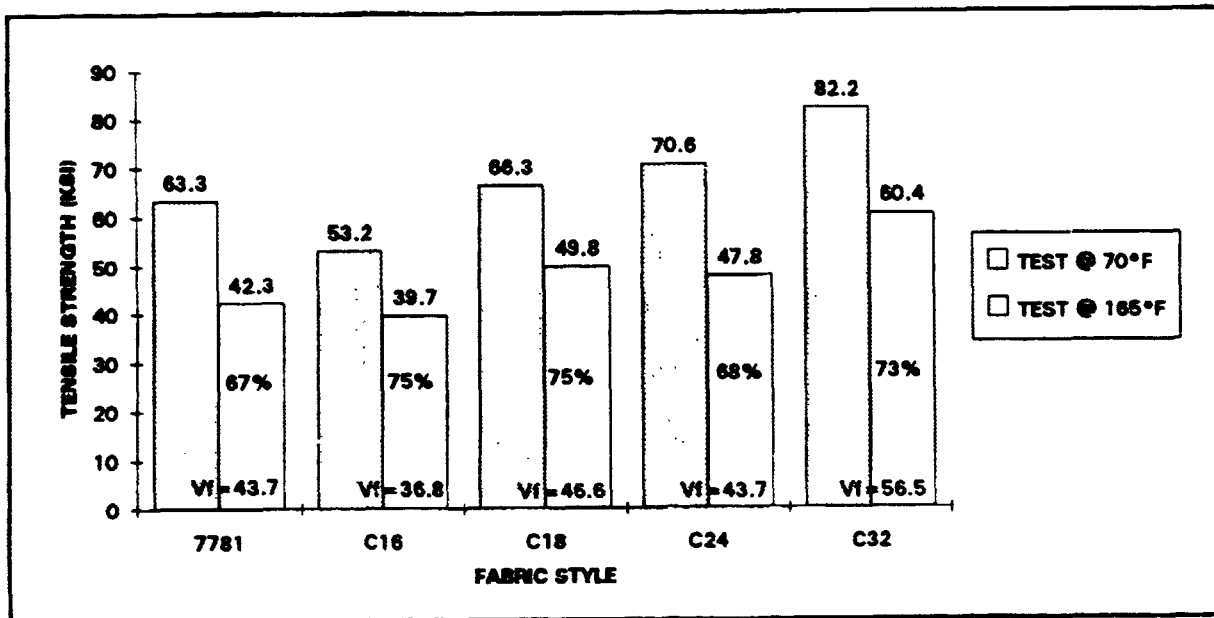


Figure 2: RTD and ETD Tension Strength

The trends of measured tension strength were similar to those of tension modulus as seen in Figure 2. With regard to the knit laminates, tension strength increased as fabric weight increased, not necessarily as fiber volume fraction increased. Similar findings for glass fabric/rubber toughened vinyl ester laminates have been reported elsewhere [2]. The knits were in general stronger than the weave. Again, this is attributed to the low crimp typically associated with knit fabrics. Tension strength retention at 165°F was similar for all laminates (67-75%). Because tension tests are fiber dominated, reduced matrix performance at the higher test temperature has minimal effect on tension properties. As will be seen following, this is certainly not the case for matrix dominated performance such as compression.

iii) Compression Strength

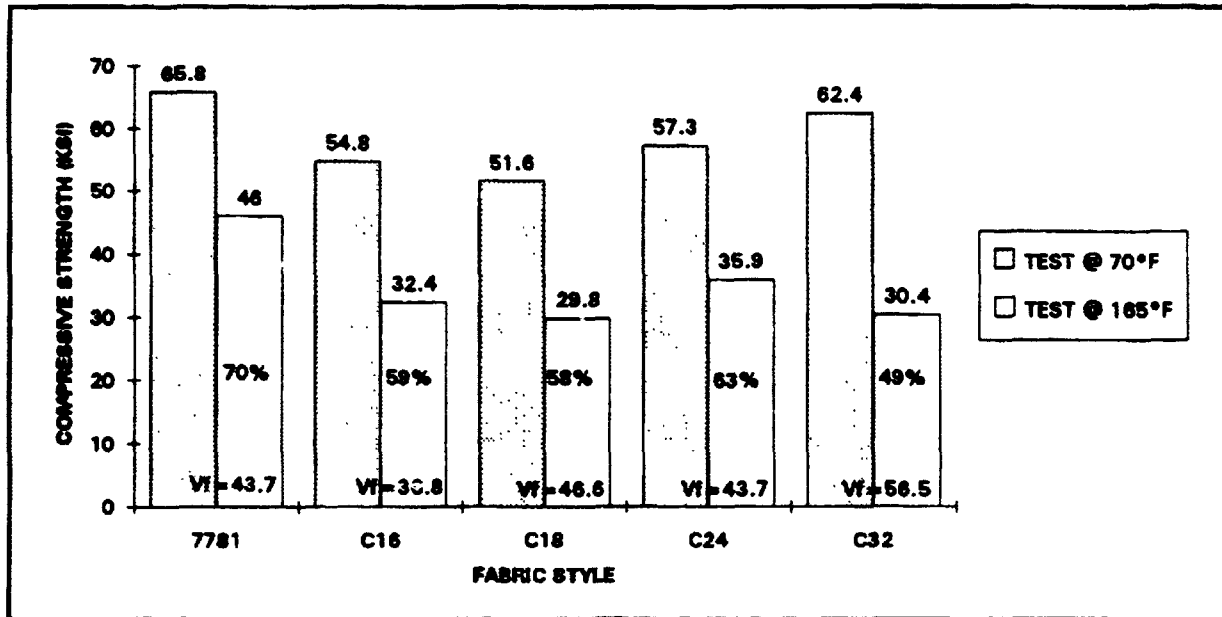


Figure 3: RTD and ETD Compression Strength

From Figure 3, it is seen that compression strength was 6% lower for the 18 oz. fabric than for the 16 oz. fabric despite a measured 26% increase in fiber volume fraction. Compression strength then increased for the two heavier knits. The lower than expected compression strength of the 18 oz. fabric may be attributed to the higher than expected crimp of that particular laminate. Initial visual observation of photomicrographs revealed more fiber waviness for the 18 oz. fabric than for the other knits.

The compression strength retention at 165°F of the knit laminates is alarmingly low, as up to 51% of compression strength was lost at the higher test temperature. Since compression tests are matrix dominated, this reduction of composite property is likely due to a reduction in the bearing ability of the resin. The large reduction of strength at 165°F indicates that additional matrix dominated testing (such as testing for bearing loads) should take place. Apparently, the lower T_g (200°F) of the rubber toughened VE used in this study is hindering the laminate's bearing ability at the higher test temperature when used in conjunction with the knit fabrics. It is anticipated that the knit laminate retention would be higher for the Novolac based VE chosen as the primary resin because of its high T_g.

The woven fabric laminate had a higher compression strength than all of the knit laminates. This was unexpected as higher crimp is typically associated with woven fabrics than with knit fabrics. Visual inspection of photomicrographs however, revealed lower than expected fiber waviness for the 8-harness satin being studied. Still, the measured difference between the weave and the knits is puzzling. It is obvious that parameters describing the form of the reinforcing fiber (fiber diameter, tow diameter, tow weight, etc) significantly affect compressive properties.

B) Effect of Resin

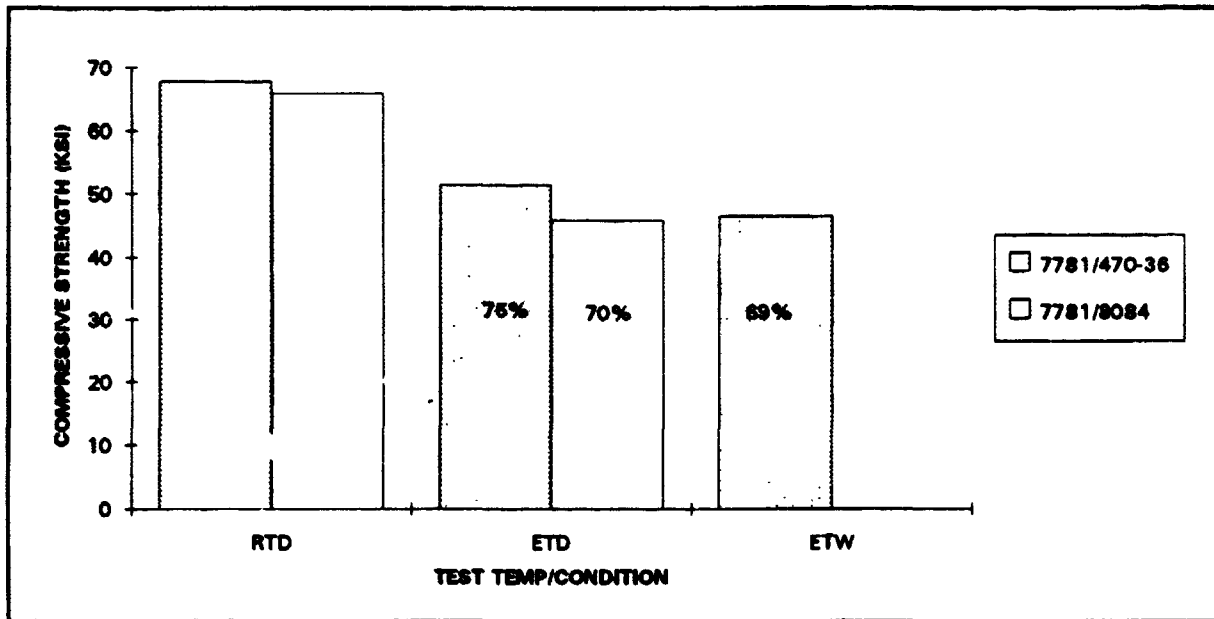


Figure 4: Compression Strength Retention, Rubber Toughened vs. Novolac Based VE

As can be seen in Figure 4 from the ETD and RTD data, the rubber toughened VE laminate had compression strength and retention similar to the Novolac based VE. Both laminates contained Style 7781 woven yarn. The conditioned samples are yet to be tested, but the ETW data point is anticipated to be the critical metric in determining the applicability of rubber toughened vinyl esters for certified use in the GA industry.

V. Concluding Remarks

From testing completed to date, the rubber toughened vinyl ester, Dow Derakane 8084 compares favorably to the higher temperature Novolac based vinyl ester Dow Derakane 470. The one exception to this statement occurs when the rubber toughened vinyl ester is reinforced with a knit glass fabric, as the compressive strength retention at 165°F was much lower than desired (only ≈50%).

It is apparent at this point in the screening evaluation that the rubber toughened VE may provide sufficient mechanical properties for GA aircraft when reinforced with 8-harness satin weave. Eventually, testing of fatigue life and adhesive properties should take place to validate the idea that this performance will be improved with the rubber toughened VE versus the Novolac based VE. Until the conditioned samples are tested later this year, no conclusion can be made about the ultimate use of rubber toughened vinyl esters in the General Aviation industry.

VI. NASA LaRC Facilities Utilized

Mechanics of Materials Laboratory, Building 1205

- Instron Series 8500 Mechanical Test Machine
- 56.2 kip Load Cell
- Linear Variable Displacement Transducer
- 386 PC w/ Instron Flaps Software Controller
- Measurement Group System 4000 Data Acquisition Tower
- Machine Shop
- Tennyson Temperature/Humidity Chamber

Polymer Physics Laboratory, Building 1293

- Sintech Mechanical Test Machine
- Test Oven, Thermocouple and Temperature Controller
- 486 PC w/ Test Works Software Controller and Data Acquisition

Light Alloy Metallography Laboratory, Building 1205

- Photomicograph Camera

Polymer Characterization Laboratory, Building 1293

- DuPont 9900 Digital Scanning Calorimeter

Model Shop, Building 1238B

- Seemann Composites Resin Infusion Molding Process (SCRIMP) [3]

NASA Technical Library

VII. References

- [1] Dexter, H.B. and Hasko, G., personal communication
- [2] Juska, T., Mayes, J.S. and Seemann III, W.H., "Mechanical Properties and Impact Damage Resistance of Composites Fabricated by Low Cost, Vacuum Assisted, Resin Transfer Molding," Naval Surface Warfare Center, Carderock Division, Survivability, Structures and Materials Directorate, Research and Development Report SSM-64-93/04, August 1993
- [3] Seemann III, W. H., US Patent # 4,902,215
- [4] Dow Chemical, Derakane Epoxy Vinyl Ester Resins Technical Product Information
- [5] Research Release, "Low Cost, High Quality Composite Ship Structures Technology Demonstrated," Naval Surface Warfare Center, Carderock Division, May 1993.
- [6] Nguyen, L.B. et al, "Design and Fabrication of a High-Quality GRP Advanced Materiel Transporter," unpublished

**NEXT
DOCUMENT**

Using the World-Wide Web to facilitate communications of
Non-Destructive Evaluation

Sean McBurney

Mentor:
Lawrence Cooper III

Internal Operations Group
Fabrication Division
Models and Materials Branch

August 8, 1995

1995 LARSS Program
NASA, Langley Research Center
Hampton, VA

Abstract

The high reliability required for Aeronautical components is a major reason for extensive Nondestructive Testing and Evaluation. Here at Langley Research Center (LaRC), there are highly trained and certified personal to conduct such testing to prevent hazards from occurring in the workplace and on the research projects for the National Aeronautics and Space Administration (NASA). The purpose of my studies was to develop a communication source to educate others of the services and equipment offered here. This was accomplished by creating documents that are accessible to all in the industry via the World Wide Web.

Introduction

Man has always been concerned with the quality and reliability of the things he fashions upon his immediate senses as instruments by which to test these products.

Nondestructive evaluation (NDE) is a serious business. The health and lives of people are at stake. Cracks in fuselages, combustion chambers of aircraft engines, steam pipes, wind tunnel turbine blades are just some of the bigger obstacles that have surfaced as potentially dangerous problems. Our space program suffered a serious setback with the loss of the seven young men and women. Although the shuttle disaster appears to have been caused by several factors, including weather, design, and failure to follow established procedures, the investigation committee has also recommended that additional inspection methods be instituted¹

NDE involves use of various non-invasive measurement techniques to determine the integrity of a structure, component, or material without destroying the usefulness of the item. The field of nondestructive evaluation is more alive today than ever before. Many of the major technical societies, such as the American Society for Nondestructive Testing (ASNT) and the American Society for Testing and Materials, are deeply involved in nondestructive evaluation and are leading the drive for better understanding through universal standardization and information disbursement.

With the recent addition of a Power Macintosh 6100/60AV and a World Wide Web server connection to the Models and Materials Technology Branch, it has given us the opportunity to publish information about NDE. It provides the means to make selected information (in the form of text, graphs, tables, and images) available to interested parties. During last years Langley Aerospace Research Summers Scholarship program (LARSS), I became familiar with the fundamentals of NDE. With the adequate background, equipment and some research, I was able to create information pages regarding NDE. General information about NDE services is now accessible to the whole world via the Internet.

The Internet and the World Wide Web

The Internet is a network of networks. You can use electronic mail to contact other people on the Internet. From your computer, you can logon to another computer, called a remote computer. The remote computer may be thousands of miles away, and you can run programs on it as if it were in the same room. You can search libraries of information around the world and transfer that information back to your own computer.

The World Wide Web (WWW) is a menu system. It gathers Internet resources from all over the world into a series of menu pages, or screens that appear on your computer. The

WWW is also a distributed system. A distributed system stores data of information on many computers. WWW servers maintain points or links to data that are spread out over the entire Internet, and can go out and get that data when you ask for it.

Hypermedia is the foundation of the WWW. Media refers to the type of data you find on the Internet. One can "click" on a section and visit other hypermedia. Media can be ASCII text, a PostScript file, an audio file, a graphic image, or any other sort of data that can be stored in a computer file.

A WWW browser like Mosaic, Netscape, or MacWeb allows you to "see and hear" the information on the Internet. A WWW browser uses data about links to accomplish this. The data is stored on a WWW server. WWW browsers all function in much the same manner. A WWW browser can link you to other Internet resources, not just text documents, graphics, or sound files. As you choose an item or resource, or move from one document to another, you may be jumping between computers on the Internet without knowing it. The WWW browser handles all the connections seamlessly.²

For this project, I solely used Netscape 1.1 which is the main browser licensed to LaRC. Netscape 1.1 is the "King" of all Web browsers at the moment. Documents, images or any sort of data are located by links and are displayed as pages. The objective of my research was to learn how to write these "pages".

You can write HTML (HyperText Markup Language) pages using any word processor or text editor. (To publish pages on the Internet, you need to submit your pages to a server computer.) HTML uses embedded codes (tags) to designate graphical elements and links. These codes can be produced simply from your keyboard using angled brackets and the slash character. For example, the tag <I> presents text in italic letters. An HTML source file containing the expression <I>This stands out </I> is displayed on screen in italic. Notice that the tag </I> is required to notate the end of the italic expression.

HTML consists of many such tags, including tags for big headlines, underlining, italics, bold, titles, and paragraph breaks. One feature you'll use is the HTML link. Here's an example HTML that creates a link for users to click on.

```
<A HREF="http://beginning.larc.nasa.gov/tct32home/ndes/NDES.html">Non-Destructive Evaluation Section TCT #32</A>
```

The part of the tag between quotation marks is the URL of the page that clicking on the link brings. The text following the URL contains the highlighted text (Non-Destructive Evaluation Section TCT #32) the user sees on screen. The tag coding and brackets are also a required part of the link. The above URL is a link to our home page.

To understand how a single page is kept distinct in a world of electronic pages, you ought to recognize its URL, short for Uniform Resource Locator. Every page has a unique URL just like every person has a unique palm print. A URL is text used for identifying and addressing an item in a computer network. In short, a URL provides location information and Netscape displays a URL in the location field. Most often you don't need to know a page's URL because the location information is built into a highlighted link; Netscape already has the URL available when you click on highlighted text, press an arrow button, or select a menu item. But sometimes you won't have an automatic link and instead have only the text of the URL (perhaps from a friend or a newspaper article).

Upon studying various "HTML Writing Guides" on Netscape, I was able to construct pages for our section. All it takes is a lot of time and some basic programming knowledge. The NDE Section Home Page is located at the previously mentioned URL address. The information gathered to create the page came from our section head and my previous LARSS experience. The following is a print out of the NDE Section home page on the World Wide Web. It was printed out using Netscape 1.1.

Non-Destructive Evaluation Section

Under Construction.... Images coming soon!

OPERATION OVERVIEW

The Nondestructive Evaluation Section is charged with supporting the NDE requirements for all of NASA/Langley's operations. To accomplish this task various inspection techniques are employed to test the integrity of research facilities and equipment, materials, space flight projects and ground support equipment.

LOCATION

The NDE Section is part of the Models and Materials Technology Branch of the Fabrication Division, Internal Operations Group. The Section is located in Building 1296 (8 East Reid Street). The Phone number is (804)864-4110 and the fax number (804)864-8854.

● Management:

- SECTION HEAD: HUGHES, JOHN T. III
- FACILITY COORDINATOR: BENNETT, RICHARD W

HISTORY

The NDE Section was established in the early 1960's and during this time has gathered both the equipment and experience necessary to perform inspections and consultations for a variety of applications. The Section currently consists of a staff of eleven engineering technicians with an engineering technician Head. Each technician has been trained and certified in accordance with The American Society for Non-Destructive Testing and is re-certified as necessary to maintain proper credentials.

Many inspection problems have been approached and solved by the NDE section, affording the opportunity to establish an extensive list of NDE accomplishments, capabilities and services. This list is not complete, but provides an overview of the services and capabilities the Section has provided in the past.

SERVICES AND CAPABILITIES

UNDER CONSTRUCTION

- Ultrasonic Inspection - UT
 - Magnetic Particle Inspection - MT
 - Dye Penetrant Inspection - PT
 - Eddy Current Inspection - ET
 - Radiographic Inspection - RT
 - Visual Inspection - VT
 - Hardness Testing
 - Special NDE Inspection Techniques
 - Other NDE Services
 - Other Section Services
-

[NDES Technician Team Page](#)



[LANTERN](#)



[LaRC Home Page](#)



[NASA Home Page](#)

Last Updated Mon August 7, 1995
[Sean M. McBurney \(smm4984@rtvax.usc.nit.edu\)](mailto:smm4984@rtvax.usc.nit.edu)

[TCT Home Page](#)

TCT Operator #32 - E.T.Hall@LaRC - 9/95

The underline text are highlighted links which take you automatically to another page when selected. There are images in the different "Services and Capabilities" categories. The pictures were provided by taking captured images off of a camcorder and downloading them into files using "Video Monitor for the Macintosh" software. These files are viewed as images when a page is loaded by the Web browser.

HTML Text Sample

The following is a sample of the HTML codes used to create the top half of the Home Page. Starting with the "Title" section up to the end of the "Management" section.

NDES.html

```
<title>NASA LaRC NDES Home Page</TITLE><center>
```

```
<center><table border=6><tr align=center><td align=center><h1>Non-Destructive  
Evaluation Section</h1></a></td></tr></table></center><br><h2>Under Constructic  
Images coming soon!</h2></center>
```

```
<hr><h3>OPERATION OVERVIEW</h3>
```

```
<p align=left><BODY> The Nondestructive Evaluation Section is charged with  
supporting the NDE requirements for all of NASA/Langley's operations. To accom  
this task various inspection techniques are employed to test the integrity of  
research facilities and equipment, materials, space flight projects and ground  
support equipment.</BODY><BR>
```

```
<hr><h3>LOCATION</h3>
```

```
<BODY>
```

```
The NDE Section is part of the Models and Materials Technology Branch of the  
Fabrication Division, Internal Operations Group. The Section is located in Buil  
1296 (8 East Reid Street). The phone number is (804)864-4110 and the fax number  
804)864-9854.</BODY><BR><hr>
```

```
<ul><li><h3>Management:</h3> <ul> <li>SECTION HEAD: <a href="http://  
pcny.larc.nasa.gov/cgi-bin/whois.pl?emp=3032AE">HUGHES, JOHN T, III</a><BR><LI>  
FACILITY COORDINATOR: <a href="http://pcny.larc.nasa.gov/cgi-bin/whois.pl?emp=  
3092AX">BFINETT, RICHARD W</a></li></ul></ul><p>
```

As you can see from the code sample, the HTML language is really just written in plain English with a few tags to identify the different characteristics and format of texts. Once HTML is understood, there are many advanced features available. From your basic background colors to large fancy borders and tables. A good beginner's guide to writing HTML documents can be reviewed in the World Wide Web by accessing the following URL: <http://www.ncsa.uiuc.edu:80/demoweb/html-primer.html>

Results

Nondestructive testing is a serious business and will always have a place in the world of progress and technology. NASA has set the standards and contributed greatly to the industry. With the information now available to all at the touch of a computer, it eases technology transfer as well as gets the most bang for the buck out of the taxpayers funds.

Although the primary objective of my project was to make the NDE Section Services available on the web, I also constructed the Polymer Technology Section(PTS) Home Page. This proved a little more difficult due to my insufficient knowledge of PTS background and the short length of the intern. This page may be viewed at the following URL: <http://beginning.larc.nasa.gov/tct32home/PTS/PTS.html>

References

1. John Wiley & Sons, Inc. 1987. Introduction to Nondestructive Testing; A Training Guide. Austin, TX p 5.
2. Gretchen L. Gottlich. May 31, 1995. WWW Reference Sheet. Netscape Document; <http://boardwalk.larc.nasa.gov/isd-www/cheatsheet.html>

**NEXT
DOCUMENT**

Technology Applications Group Multimedia CD-ROM Project

Kristi D. McRacken

Stuart Pendleton

Technology Applications Group, Data Systems Team

Abstract

To produce a multimedia CD-ROM for the Technology Applications Group which would present the Technology Opportunity Showcase (TOPS) exhibits and Small Business Innovative Research (SBIR) projects to interested companies. The CD-ROM format is being used and developed especially for those companies who do not have Internet access, and cannot directly visit Langley through the World Wide Web. The CD-ROM will include text, pictures, sound, and movies. The information for the CD-ROM will be stored in a database from which the users can query and browse the information, and future CD's can be maintained and updated.

The Project

The Technology Applications Group needed a way to transfer technological ideas to the private sector companies. A great way to transfer this technology is reaching millions of people through the Internet. However, another huge section of society does not have Internet access, and those are the people and the companies that we hope to target with this and future CD-ROM's.

The CD-ROM team consists of Myrna 'Sya' Rivera, a senior at Christopher Newport University majoring in Computer Information Science, Dr. Joshua Anyiwo, Associate Professor of Physics and Computer Science at Christopher Newport University, and myself, a recent graduate of Christopher Newport University with a degree in Computer Information Science. Sya and Dr. Anyiwo started work early, and at the end of a previous job, I joined them on the June 5th beginning of the 1995 LARSS program. Stuart Pendleton, our mentor, knew that this would be a very interesting, yet time-consuming project and suggested that they begin as soon as possible. There was a huge learning curve that was associated with this multimedia project. None of us had experience in multimedia, but Sya and I had worked together before in a team environment developing World Wide Web (WWW) pages for our senior project at CNU under direction of Dr. Anyiwo. This gave us a general knowledge of graphical user interface (GUI) development and the structure of information and ideas.

In the beginning, the team had considered developing the CD-ROM in the Hyper Text Markup Language which is used for development of World Wide Web pages on the Internet. However, due to limitations in time and the ability to acquire distribution rights of the WWW browser, the group decided to use a relational database format.

The purpose of producing the CD-ROM is to inform the different organizations of the TOPS exhibits and the SBIR projects at NASA. The CD-ROM will allow companies that cannot afford Internet capabilities or to send representatives to the TOPS exhibits, the opportunity to obtain the information available. The CD will also allow small businesses to quickly access information on TOPS or SBIR projects and determine if they could use the technology, or would like to participate in the development of a new technology. The primary function of the CD-ROM is to distribute information.

The TOPS portion will be composed of approximately 100 one pagers from the 1995 exhibit. The purpose of TOPS is to identify new multi-use technology opportunities and develop new partnerships with U.S. industry for commercialization of this technology. The purpose of SBIR is to seek innovative concepts that meet NASA mission needs, as well as have the potential for commercial applications.

The Design

Maintainability

The design of the CD-ROM is modular, meaning that maintaining and updating the CD will only require updating the necessary information contained in the database, such as video, audio, text and movies.

Usability

The GUI format of the CD will require that the users 'click' on the desired information or enter a keyword for topical searches of the TOPS technologies..

Reusability

Storing the CD information will keep future developers from having to start from scratch. Inputting the new information is all that will required.

Extendibility

Changes to the CD can be made through changes to the database and how the information can translated into Hyper Text Markup Language (HTML) for future LAPSS students.

LaRC Equipment and facilities

Software

Software used included Microsoft Power Point for graphics and presentation formats, Microsoft Excel for a few spreadsheet documents, Microsoft Word for lots of word processing. We also used Claris Impact and Color-It to produce the screen layouts including the clip art, gradient backgrounds and a variety of colored screens. Adobe Photoshop was used for scanning images and enhancing the images quality of color, brightness, etc. Adobe Premiere was used for editing the video and audio portions of movies and remaking the movies with the changes. Fusion Recorder was used to gather video clips from a VCR using an audio/video capture board. Movie Shop was used to process the Premiere movies and apply compression algorithms for play back off of a double speed CD-ROM drive. Netscape, a WWW browser was used to gather information. Fetch, a FTP software package was used to download needed files. Microsoft FoxPro was used to assemble all of the data sources in one program for ease of use and browsing.

Hardware

The team used huge amounts of hardware and computing power. The three of us each used a Power Macintosh. I had a 21" monitor that was absolutely fabulous. I also had an 540 Mb internal hard drive, as well as a 1 Gb external hard drive. This amount of space was essential since some of the movie files that were created exceed 350 Mb a piece. Some of the other equipment consisted of a ScanMaker II scanner, a Pinnacle CD-ROM writer, and a VCR.

Facilities

For the most part, we used the equipment in our office, and got information and files of the network and file servers. We did request some information and images from Graphics, as well as the Video Production Lab.

Conclusion

We hope to have the CD finished by the end of this week, or the very beginning of next week. We will probably present the CD to the Technology Applications Group on Monday, August 14th. We have learned a lot, and made long strides of progress. I have learned a great deal, and value the experience that I have gained.

**NEXT
DOCUMENT**

DEVELOPMENT OF A SMALL AREA SNIFFER

Laurie A. Meade

Dr. Jerome Kegelman

**Research and Technology Group
Fluid Mechanics and Acoustics Division
Flow Modeling and Control Branch**

Abstract:

The aim of this project is to develop and implement a sniffer that is capable of measuring the mass flow rate of air through a small area of pinholes whose diameters are on the magnitude of thousandths of an inch. The sniffer is used to scan a strip of a leading edge panel, which is being used in a hybrid laminar flow control experiment, in order to survey the variations in the amount of air that passes through the porous surface at different locations. Spanwise scans are taken at different chord locations by increasing the pressure in a control volume that is connected to the sniffer head, and recording the drop in pressure as the air is allowed to flow through the tiny holes. This information is used to obtain the mass flow through the structure. More importantly, the deviations from the mean flow rate are found and used to determine whether there are any significant variations in the flow rate from one area to the next. The preliminary results show little deviation in the spanwise direction. These results are important when dealing with the location and amount of suction that will be applied to the leading edge in the active laminar flow control experiment.

All information presented in this report is owned by industry and therefore no specific numerical results can be presented.

Introduction/ Background Information:

The intended application of this sniffer is to examine the variations in the flow rate through the tiny holes on the leading edge panel of a wing that is being used in a hybrid laminar flow control experiment. In hybrid laminar flow control, suction is applied to the leading edge. Thousands of minuscule electron-beam-drilled holes in the titanium skin of the leading edge act like tiny vacuum cleaners sucking away the turbulent air closest to the surface to create laminar flow. The size of the pinholes and the amount of suction applied through them are the keys to the success of the laminar flow control system. The location of the suction is also important and can be applied at different flutes. The flutes are the passage ways for the air to move through the structure. Each flute is one inch wide and contains thousands of holes.

Since the holes are drilled using a laser it is probable that there is some variation in the diameters of the holes and it is also possible that some holes may not be drilled all the way through to the flutes due to fluctuations in power. There is also the possibility that some holes may be clogged. Therefore, the suction that is thought to be applied may not be the actual suction that is taking place. This sniffer is able to determine the actual flow through different areas of each flute.

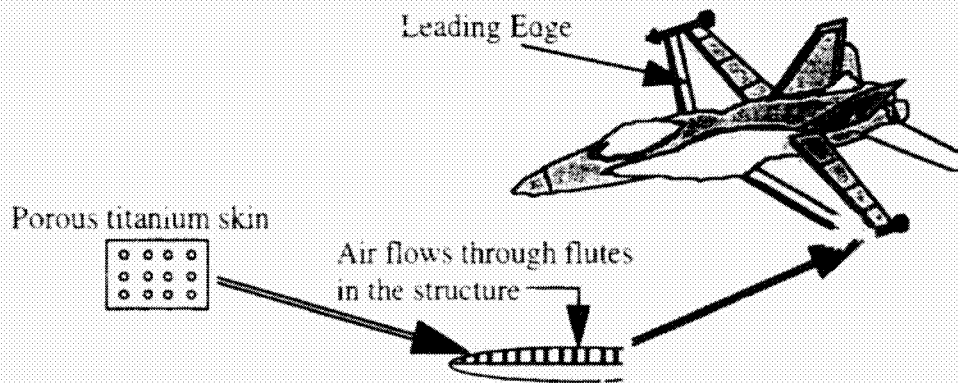


Figure 1

Apparatus and Procedure:

Figure 2 shows a schematic of the experimental setup. This setup is being used to survey a leading edge panel that was tested in the hybrid laminar flow control experiment that is currently taking place in the 8 ft Transonic Pressure Tunnel. The release valve is shut while air is allowed to flow through the fill valve until the pressure in the control volume has reached 5 psi. At this time, the fill valve is shut and the sniffer head is placed over the appropriate section of the leading edge. The release valve is then opened and the pressure drop is recorded. The pressure in the control volume is measured using a pressure tap and a digital pressure indicator. The analog voltage signal sent out by the pressure indicator passes through an analog-digital converter and the digital voltage is then read by the Macintosh computer and converted to psi. All data acquisition and analysis programs for this project were written using LabVIEW.

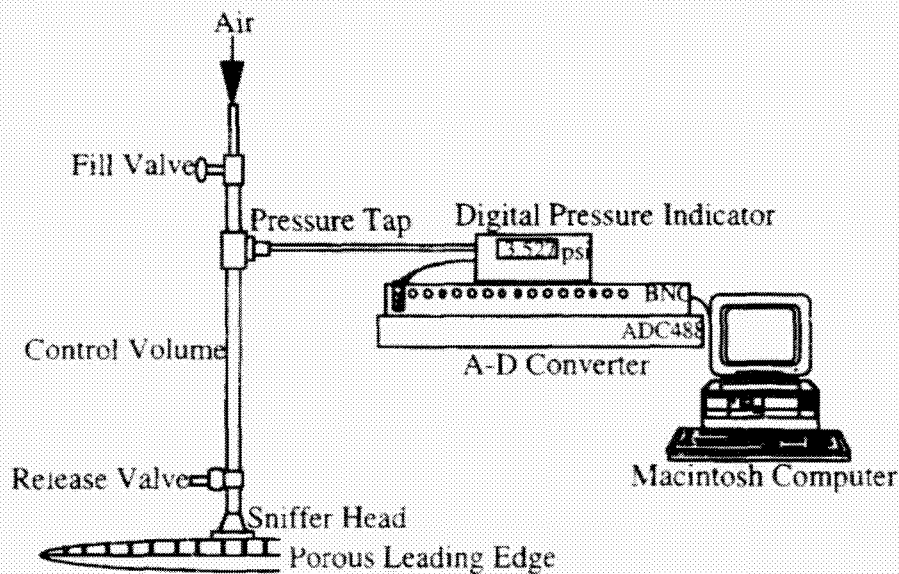


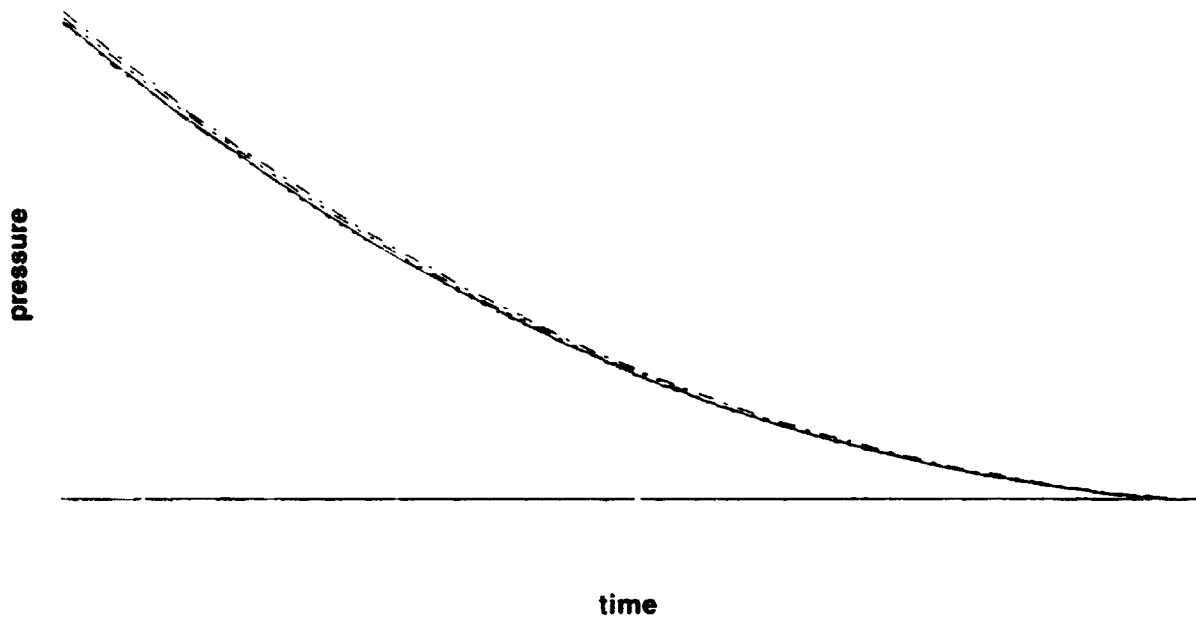
Figure 2

This procedure is repeated as the sniffer is moved along the flute that is being surveyed. The sniffer head was designed and constructed to cover an area of 1 inch x 1/8 inch in order to cover the width of a flute and only a small area in the spanwise direction. Each scan covers a distance of 2.0625 inches along a flute. The pressure drop of 32 areas is recorded by moving the sniffer by 1/16 inch each time, allowing for an overlap of 1/16 inch for each move. Once a scan is complete the derivative of the pressure versus time curve is computed for each location. This gives the corresponding mass flow at every pressure difference for each area. From here, the deviation in the flow rate at each area from the mean flow rate of the entire scanned area can be obtained for a single pressure difference.

Prior to surveying the actual leading edge of interest, experiments were done on a sample of the perforated titanium skin. It is evident by simple examination of this sample that several holes were not drilled completely through the surface. This gives reason to believe that the skin on the panel also has several holes that do not completely puncture the surface. All software was developed and tested on this sample before being used on the actual panel.

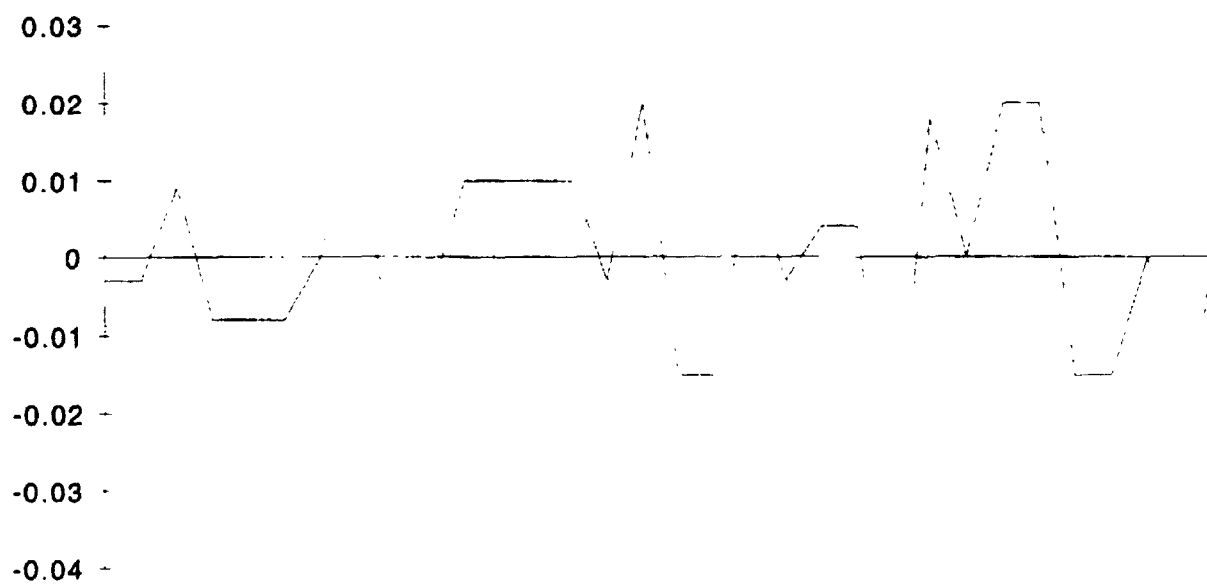
Results:

REPEATABILITY CHECK

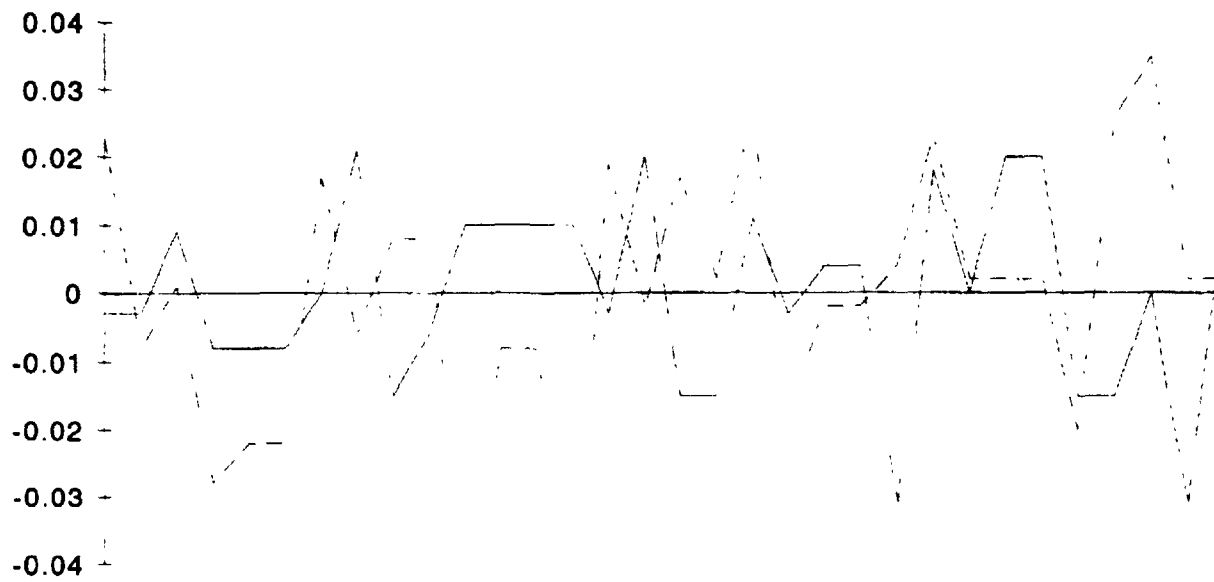


Figur. 3

**DEVIATION FROM THE MEAN FLOW RATE
scan taken on flute A**



**COMPARING THE DEVIATIONS OF FLUTES A AND B
OVER THE SAME SPANWISE SECTION**



Discussion of Results:

As stated earlier, specific numerical results cannot be given in this report. The presented results show a sample of data that has been acquired and used to examine the flow rate through the surface. Figure 3 shows the repeatability of the setup for acquiring the pressure drop for several surveys at the same location on the surface. Once the setup was found to be repeatable at the same location, the spanwise scans were taken and a set of the results can be seen in figures 4-6. Figures 4 and 5 show plots of the deviation from the mean flow rate across flutes A and B. In figure 4 it can be seen that the maximum deviation is 3% and in figure 5 the maximum deviation is 4%. The deviation was expected to be much greater than this. The average deviation from the mean is 1% for each flute. The mean flow rate through flute A was found to be approximately 9% percent greater than the flow rate through flute B. The section of the skin at flute A is known to have more perforations, so this was expected. Figure 6 shows the deviation from the mean of both flutes at the same spanwise location. This was done to check for any trends in the deviations that may run in the direction in which the holes were drilled. From this plot there doesn't appear to be any relationship between the slight variations in flow and the spanwise location.

Conclusion:

The sniffer developed in this project is able to record the pressure drop as air flows through the perforated titanium skin. The programs that were developed can then use this information to calculate the mass flow and the deviations from the mean flow rate. These results can then be used to examine any variations in the flow rate at different locations on the leading edge panel. The sections that have been tested with this sniffer have not produced the results that were expected. It was expected that deviations up to 100% would occur, but to this point no significant deviations have been found in the results. There was also some speculation that a relationship might occur between the spanwise location and the variation. No trend has been found by the sniffer to indicate that this is true.

**NEXT
DOCUMENT**

TAP / ASTA Flight Demo Data Analysis

Eric Mejdrich
Steve Young

***Research and Technology Group
Information and Electromagnetic Technology Division
Systems Integration Branch***

Data Analysis

Eric Mejdrich

1.0 Abstract

Recently the Low Visibility Landing and Surface Operations (LVLASO) project team of the Systems Integration Branch at the NASA Langley Research Center completed a flight demonstration of TAP / ASTA concepts at the Atlantic City airport. This paper is concerned with the analysis of the aircraft data that was recorded by the test vehicle during the duration of the flight demonstrations.

2.0 Introduction

The Airport Surface Traffic Automation (ASTA) program was started by the Federal Aviation Administration to increase the capacity of today's airports while maintaining high levels of safety. The NASA Terminal Area Productivity (TAP) program is concerned with the possibilities of clear weather capacities in Instrument Flight Rule (IFR) conditions. The test demonstration at the Atlantic City airport illustrated many aspects of the TAP and ASTA programs.

During a test, data was recorded by the test aircraft itself, and by NORDEN on the ground. This data consisted of positions, velocity, time, altitude, and a host of other variables.

3.0 Objective

This analysis is concerned with two main questions.

1. What was the accuracy of the various GPS and radar data that was recorded ?

In all cases the "true" position of the aircraft is the post processed GPS which is accurate to within three centimeters of the actual position. ASDE-3 radar, Raw GPS, and Differential GPS are all compared to the post processed GPS to determine their accuracy.

2. What was the availability of the data link that was used to transmit data to the test aircraft from the ground station ?

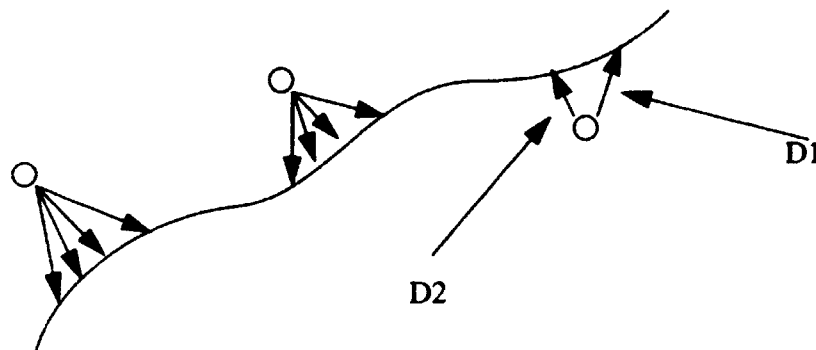
When looking at the ARINC message data, one finds that there are 'gaps' in the data stream where there is no data. These 'gaps' represent the time when the aircraft did not receive ASDE-3 radar data. By looking at these gaps, one can find the percentage of time that the radar data was not available.

4.0 Procedure

To analyze the GPS data, the collected data is first extracted from a file that contains all of the variables that were recorded by the test aircraft during the test. Then the latitude and longitude position data for the DGPS, and the Raw GPS are converted into an x,y position in a local plane coordinate system with the NGS Monument used as the reference position. Once the data is in the local plane coordinate system, plots are made. Next the error in the DGPS and Raw GPS position are calculated using the post processed GPS as a reference. The error is just the linear distance away from the post processed GPS at a given time.

Analysis of the radar data is a bit more complicated, as there is a time delay from when the radar echo was seen on the ground, to when the radar echo was received in the plane. The reason is that the radar uses a rho, theta coordinate system which must be converted to a local plane x,y coordinate system, which is then converted to a lat, lon. Then the data is transmitted to the plane on a wireless RF link. Once the data is received by the plane, it is converted back into a local plane coordinate system. So we have to make sure one knows what question they are asking when doing the analysis. If an error analysis is done using the positions based on a matching timestamp, then all of this delay is going into the error measurement. To do a strictly positional error analysis the time must be disregarded.

To do this, a Matlab(tm) routine was written to take a radar point, and the nearest 20 points in time, and compute the distance between them. The smallest distance must be the error that one desires to find. In the simple drawing below, the line represents the post processed track, and the small circles are the radar returns. D1 would represent the error, when comparing positions using timestamps. The strictly positional error would be D2. This kind of measurement is what is recorded in the table *Position Sensor Accuracy*.



To analyze the 'gaps' in the data, the file that contains the saved ARINC messages is manipulated into an ASCII format. Then the test aircraft's timestamps are extracted from the file for examination. 'Double' entries are removed, and analysis of the timestamps can occur.

Gaps in the timestamps were counted using a simple C program that lets the user specify the gap width to ignore, and the file to parse. If a user specified a gap width of two, gaps such as 15:08:25 - 15:08:27, and of course 15:05:12 - 15:05:13 are ignored. The program then parsed the time stamp file counting the time that elapsed in the gaps.

5.0 Data

The data used in this analysis was collected from the June 27th, 28th, and 29th demo flights of the test aircraft at the Atlantic City airport. The data is sampled at 20 times per second. For the purpose of this analysis, one took one sample of the 20 Hz data per second to match the post processed data which is one sample per second. Most of the test flight intervals were between 20 and 30 minutes long. The run number and the start and stop times are listed in the next table.

TABLE 1. Start and Stop Times

Demo Label	Start Time	Stop Time
June 27#1	14:40:42	15:07:20
June 27#2	15:15:11	15:32:19
June 27#3	15:35:50	15:49:27
June 27#4	18:20:17	18:33:44
June 27#5	19:05:52	19:14:43
June 27#6	19:33:19	19:46:30
June 27#7	19:52:17	20:05:21
June 28#1	14:28:36	14:44:44
June 28#2	18:41:44	18:55:00
June 28#3	19:52:31	20:06:33
June 28#4	20:07:28	20:18:30
June 29#1	15:08:26	15:18:40
June 29#2	16:08:30	16:19:30
June 29#3	16:43:00	16:51:00

The radar data came from two sources. The ARINC messages file contains the radar data that was received by the plane over the RF data link from the ground station. The ground station (NORDEN) also kept a file of the radar data that was uplinked from the ground station. By looking at what was sent, versus what was received gives one another view on the radar data availability.

The Norden radar data was in a hexadecimal format that must be manipulated to extract the data that one wants to look at, particularly the target positions. Once the target positions are extracted, they are sorted based on the identification number of the target.

Also, the June 27th radar data was off by a constant rho,theta factor which turned out to be approximately negative forty feet, and one one hundredth of a radian.

6.0 Results

The table entitled *Position Sensor Accuracy*, on the next page, shows the error in the DGPS, Raw GPS, and the ASDE data as received by the test aircraft, compared to the post processed GPS. The position plots are shown after this table, as is a plot showing the Atlantic City airport itself.

The *Norden Ground Tracks* plot and *TSRV Ground Tracks* plot show the radar data in a three dimensional perspective. The *Norden Ground Tracks* plot is a plot of the targets that were seen by the radar ground station. The *TSRV Ground Tracks* plot is a plot of the same radar data after it was uplinked to the plane on the RF data link. The z axis is time, and the x, and y axis are x and y position of the target. Also the targets are projected down onto the x, y plane. These plots show the gaps in the radar data vividly. Look at the long red target on the Norden Ground Tracks plot, and compare it to the same target on the TSRV Ground Tracks plot. Notice the breaks in the TSRV plot's target. These are gaps in the radar data.

The three dimensional availability charts that follow represent the percentage of time that radar data was NOT available.

Example: For an ignored gap of two on the June 27-1 test - gaps in the data of 1 (i.e. 15:08:25 - 15:08:26), and 2 (i.e. 15:08:25 - 15:08:27) are ignored - the radar data was unavailable for approximately 45% of the time.

There are three separate charts for *June 27th*, *28th*, and *29th* respectively.

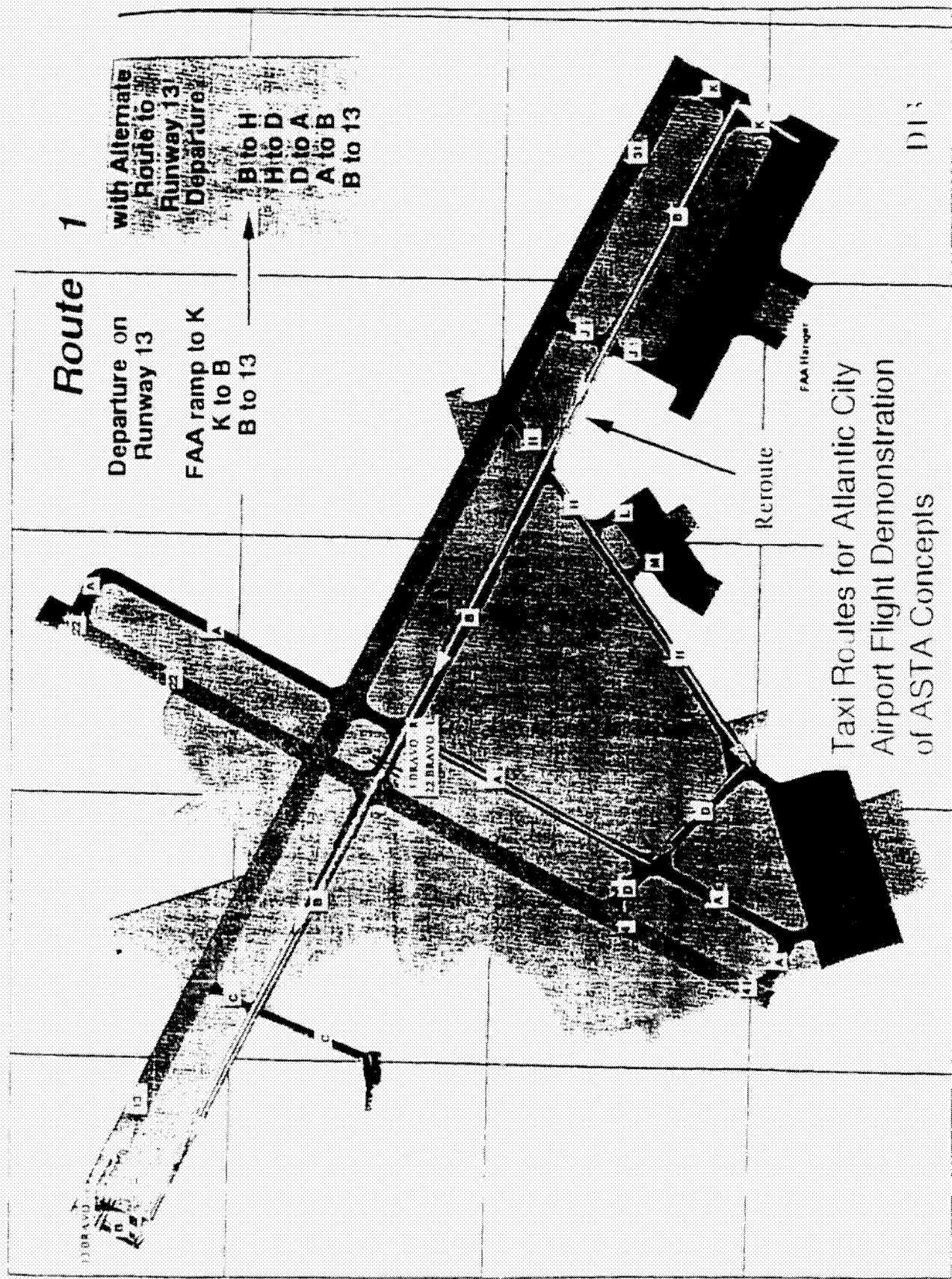
The *Maximum and Minimum Nonavailability* chart shows the maximum and minimum percentage for each gap count in the data.

The *Nonavailability* chart shows for ignored gaps of one, two, and three, the percent of time that radar data was NOT available.

Example: For the June 27-1 test with an ignored gap of three, the radar data is available approximately 77% of the time.

Table 1: Position Sensor Accuracy

Run	DGPS		Raw GPS		ASDE		Min	Ave	St Dev
	Ave	St Dev	Ave	St Dev	Max	Min			
June 27 #1	1.428	.872	2.2488	1.1891	131.1947	.3466	26.2402	12.7354	
June 27 #2	.981	.758	1.5082	.900	78.3067	.1291	21.1918	13.1129	
June 27 #3	1.071	.710	1.5469	.0854	101.1187	1.0096	21.2796	18.0285	
June 27 #4	2.124	1.06	2.5198	1.0918	80.0446	2.6318	25.2072	15.6991	
June 27 #5	1.853	.680	3.3280	1.434	143.1957	.7720	49.7544	33.033	
June 27 #6	2.468	1.018	4.0093	1.6173	129.419	1.8322	32.0267	24.4280	
June 27 #7	2.175	.860	4.2102	38.58	170.966	2.2097	25.9786	19.5341	
June 28 #1	2.32	3.175	3.5347	3.7858	201.4672	3.7559	55.0196	57.4167	
June 28 #2	2.122	1.175	2.44	1.0605	120.02	3.6650	36.6327	22.7458	
June 28 #3	2.40	1.03	3.1066	.9930	82.7639	.6285	21.7515	15.0172	
June 28 #4	1.88	1.07	2.482	1.11	521.0634	2.3769	42.4445	87.9175	
Average	1.8929		2.7934		159.9608	1.7552	32.5024		
St Dev	.517		.8919		125.8380	1.2860	11.9384		



Route 1

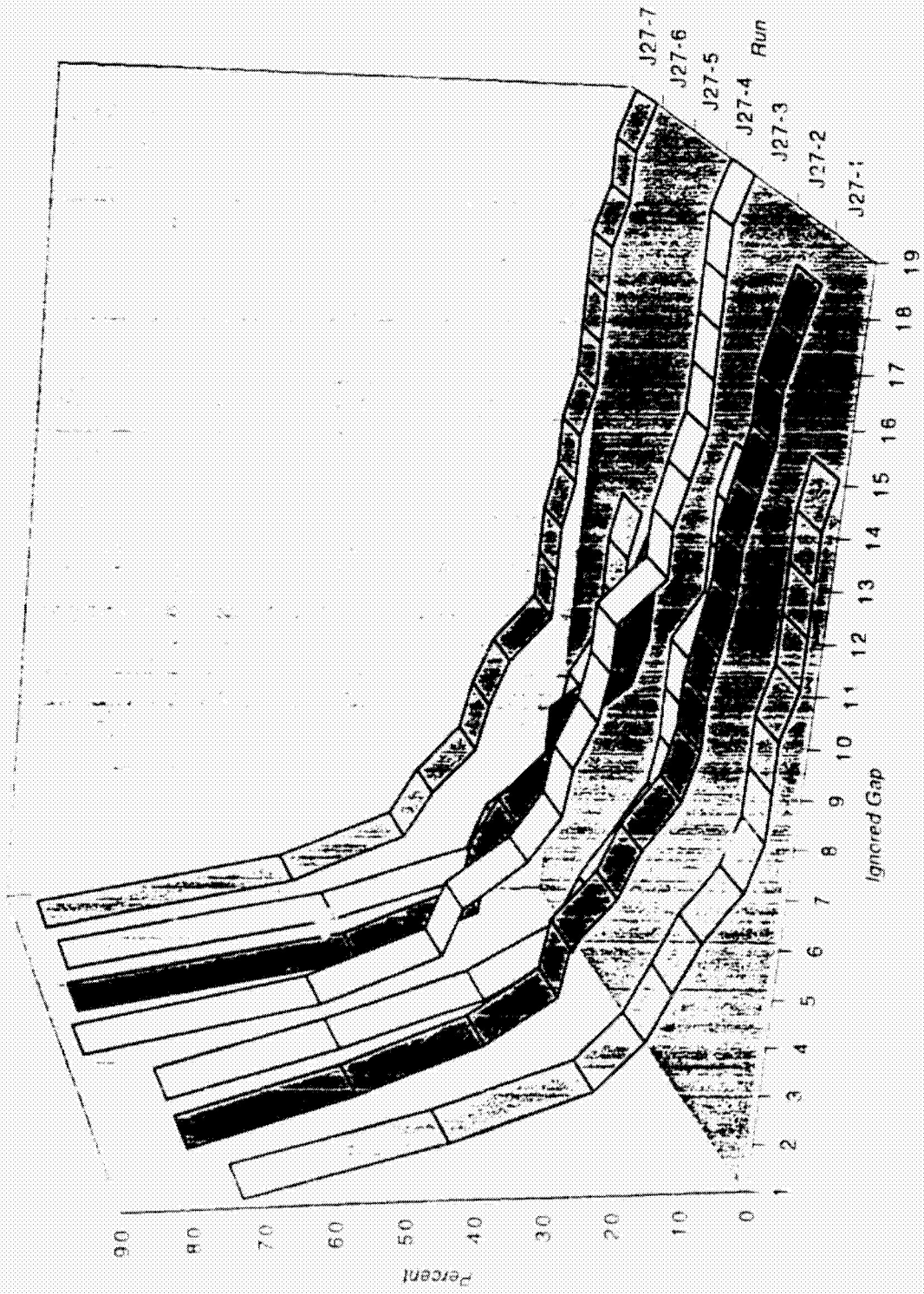
Departure on Runway 13
 FAA ramp to K
 K to B
 B to 13

With Alternate Route to Runway 13 Departure
 B to H
 H to D
 D to A
 A to B
 B to 13

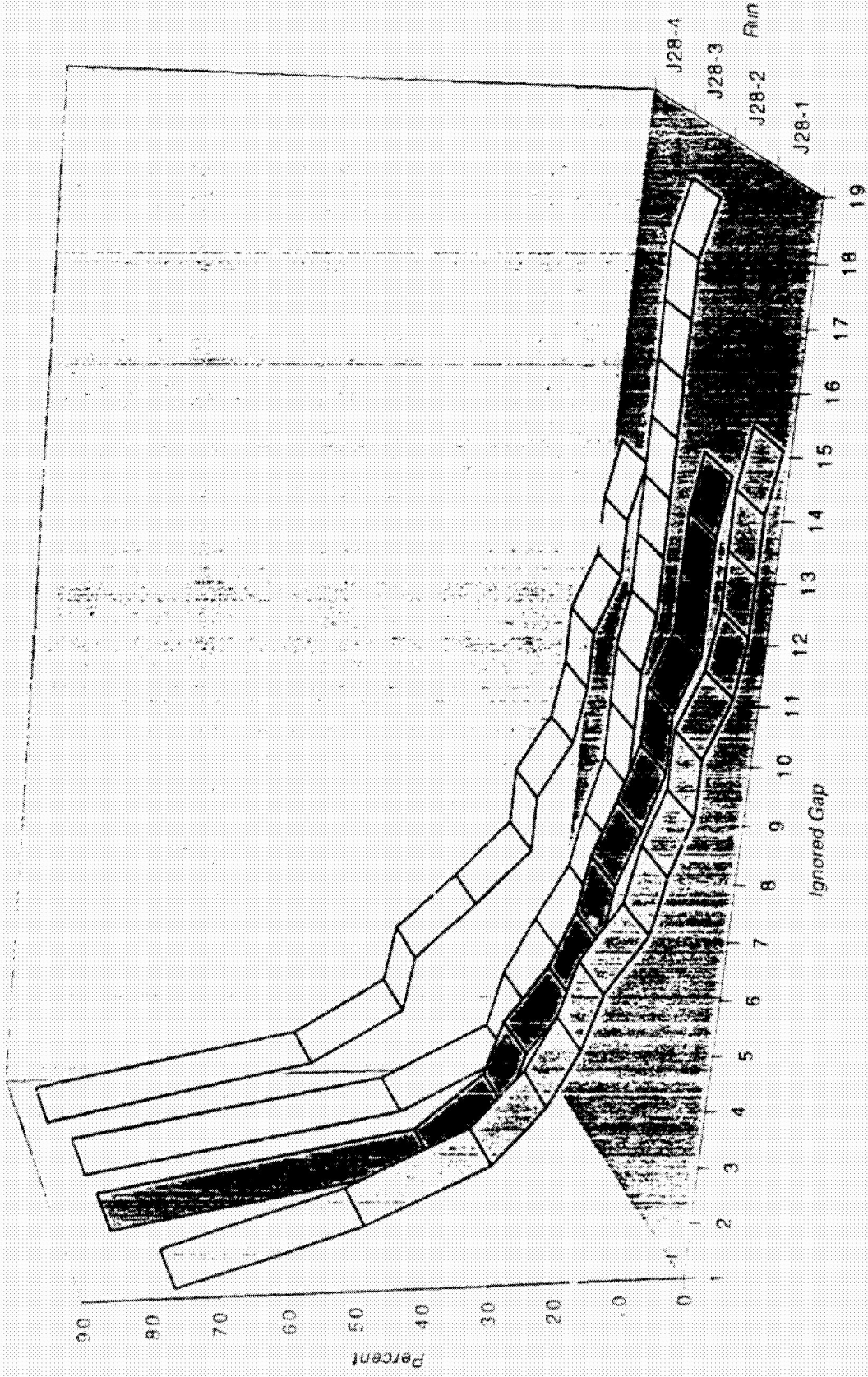
Taxi Routes for Atlantic City Airport Flight Demonstration of ASTA Concepts

DI 3

June 27



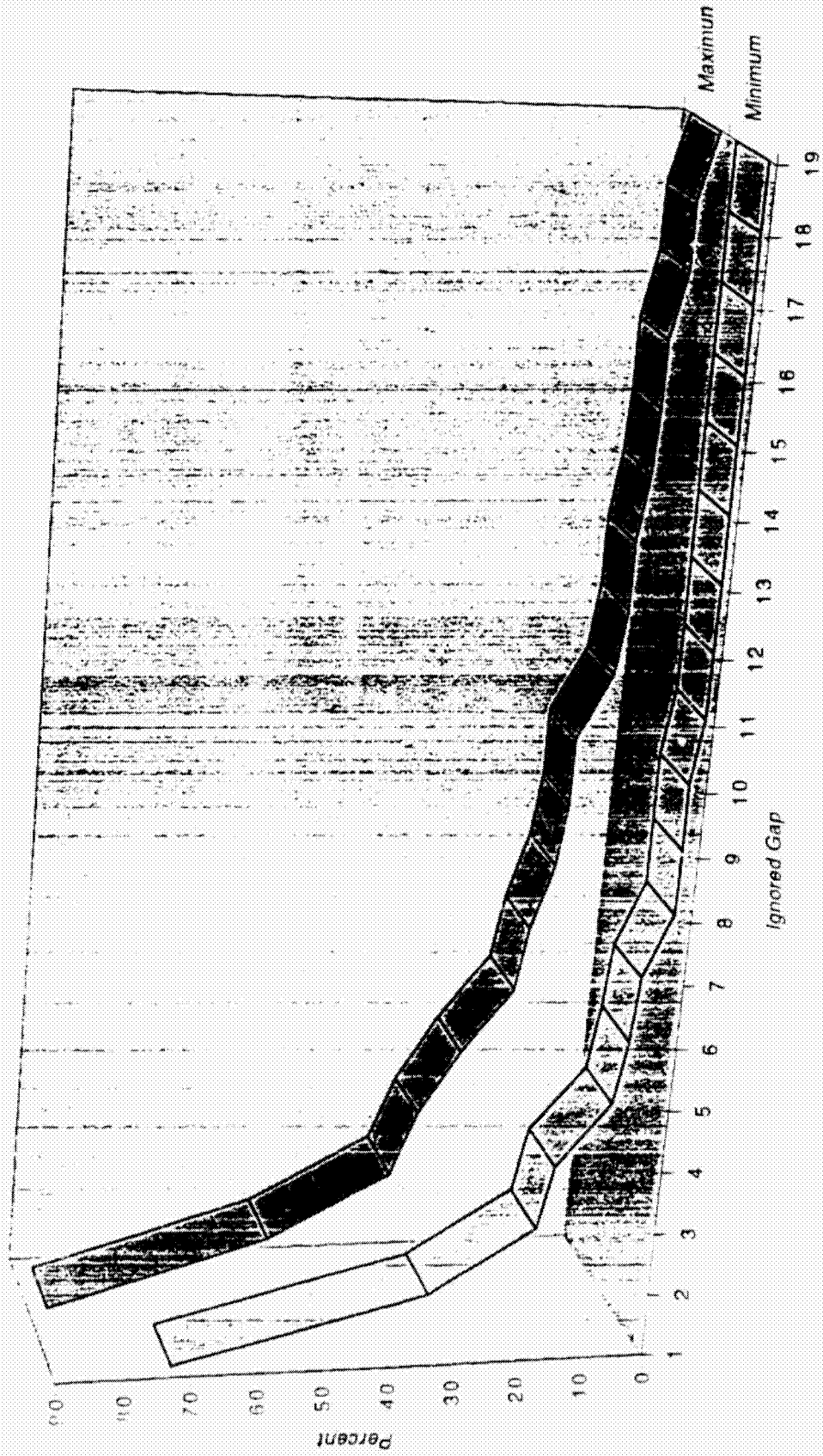
June 28



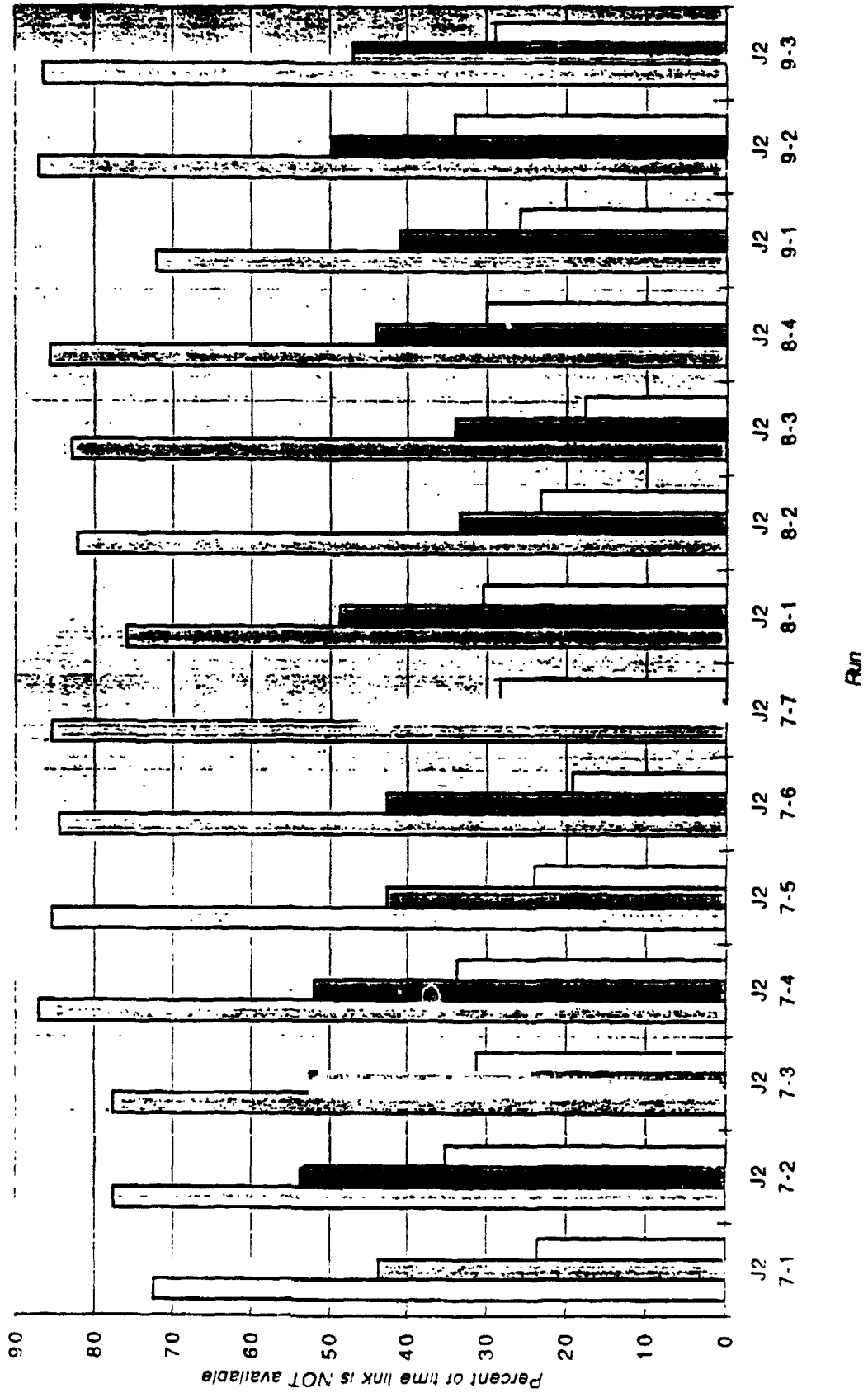
June 29



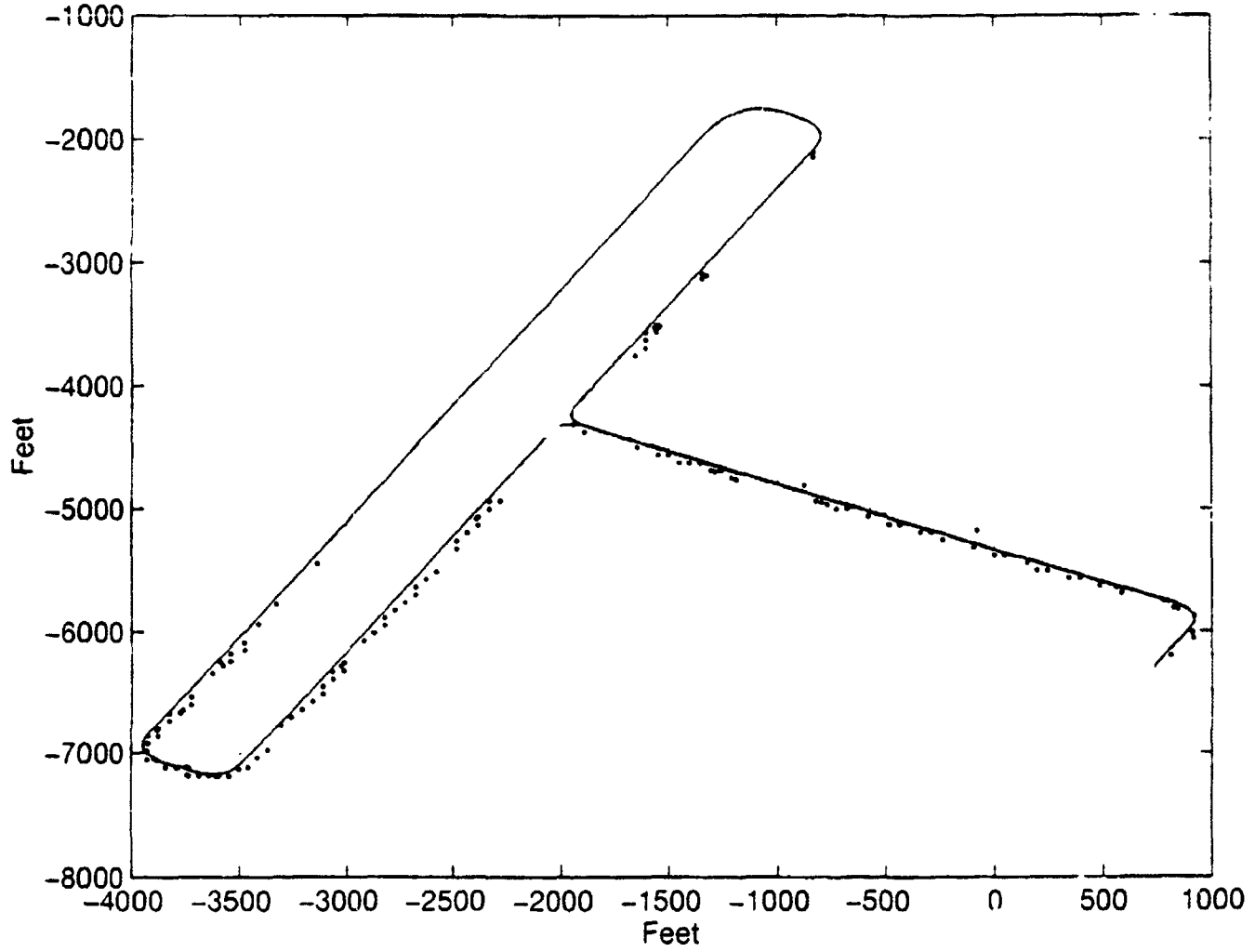
Maximum and Minimum Nonavailability



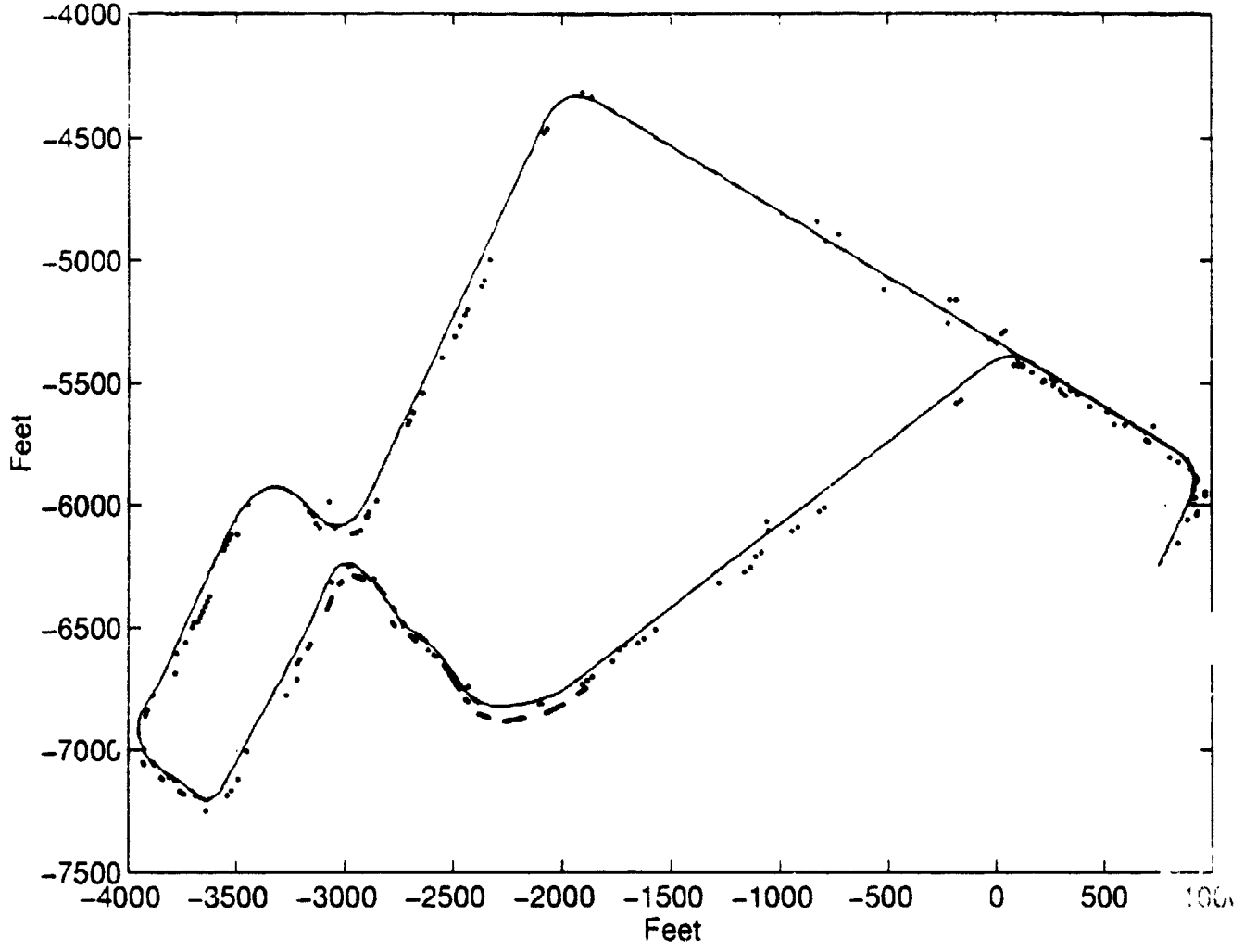
Nonavailability



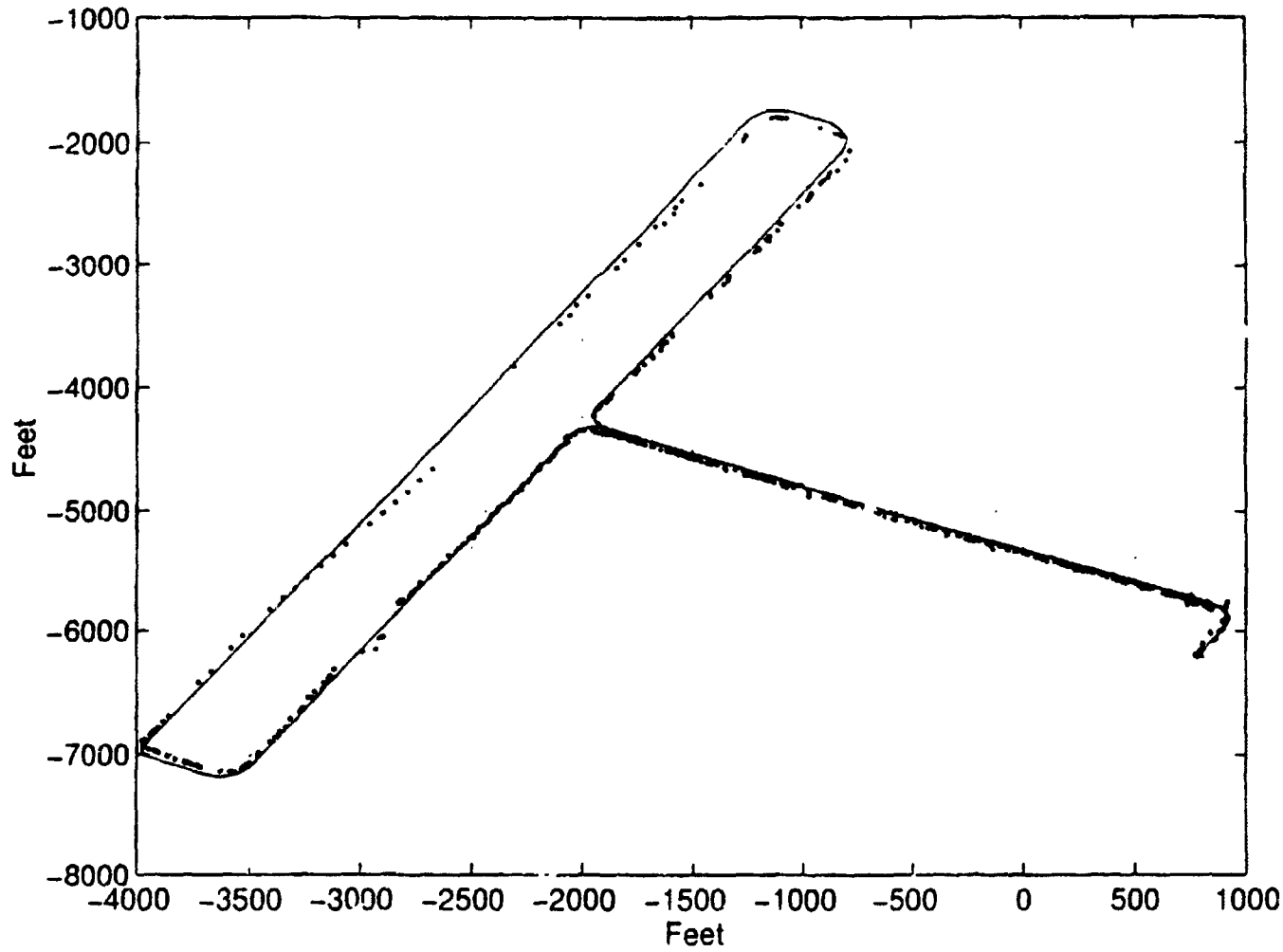
- DGPS -- Raw GPS . ASDE-3 Radar



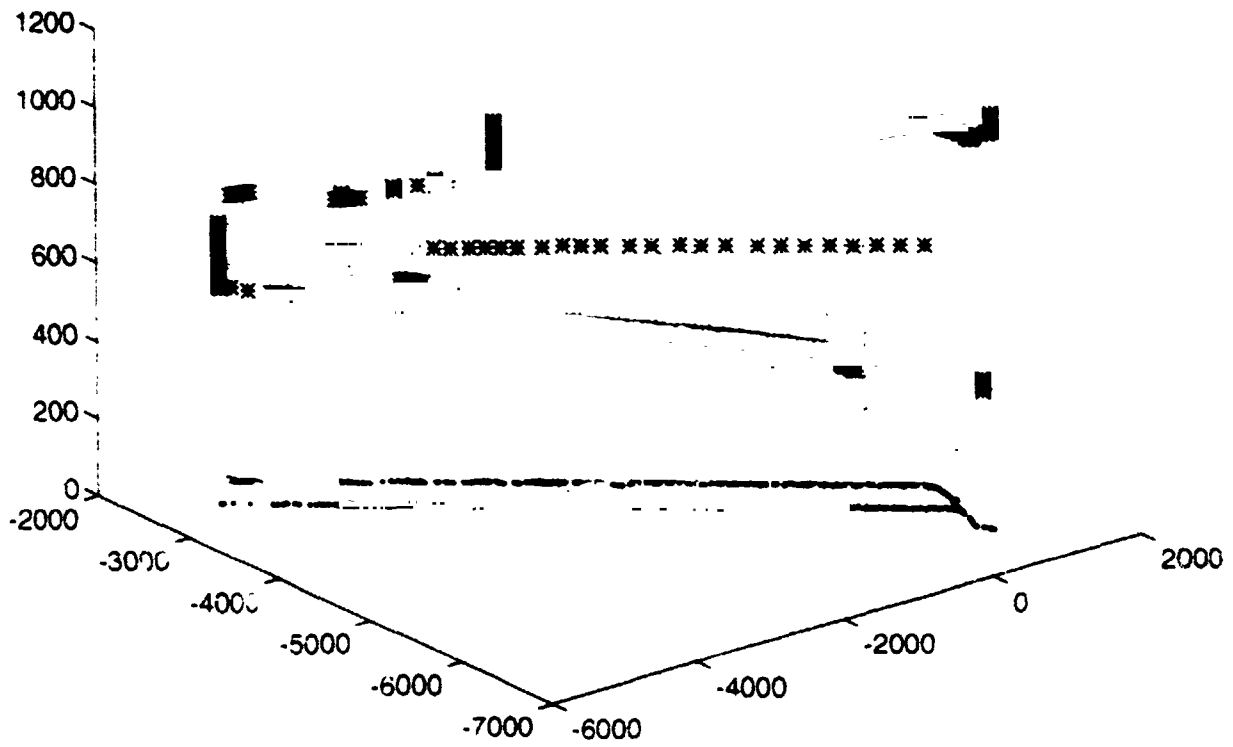
- DGPS -- Raw GPS . ASDE-3 Radar



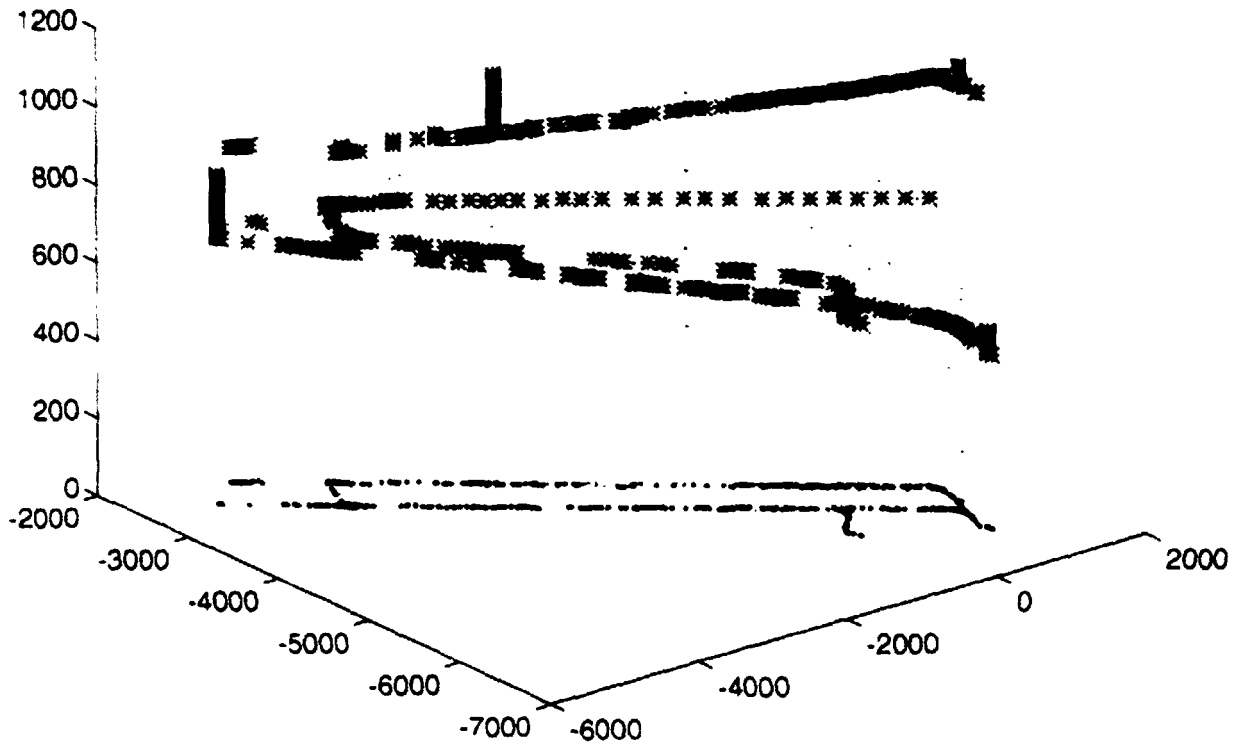
- DGPS -- Raw GPS . ASDE-3 Radar



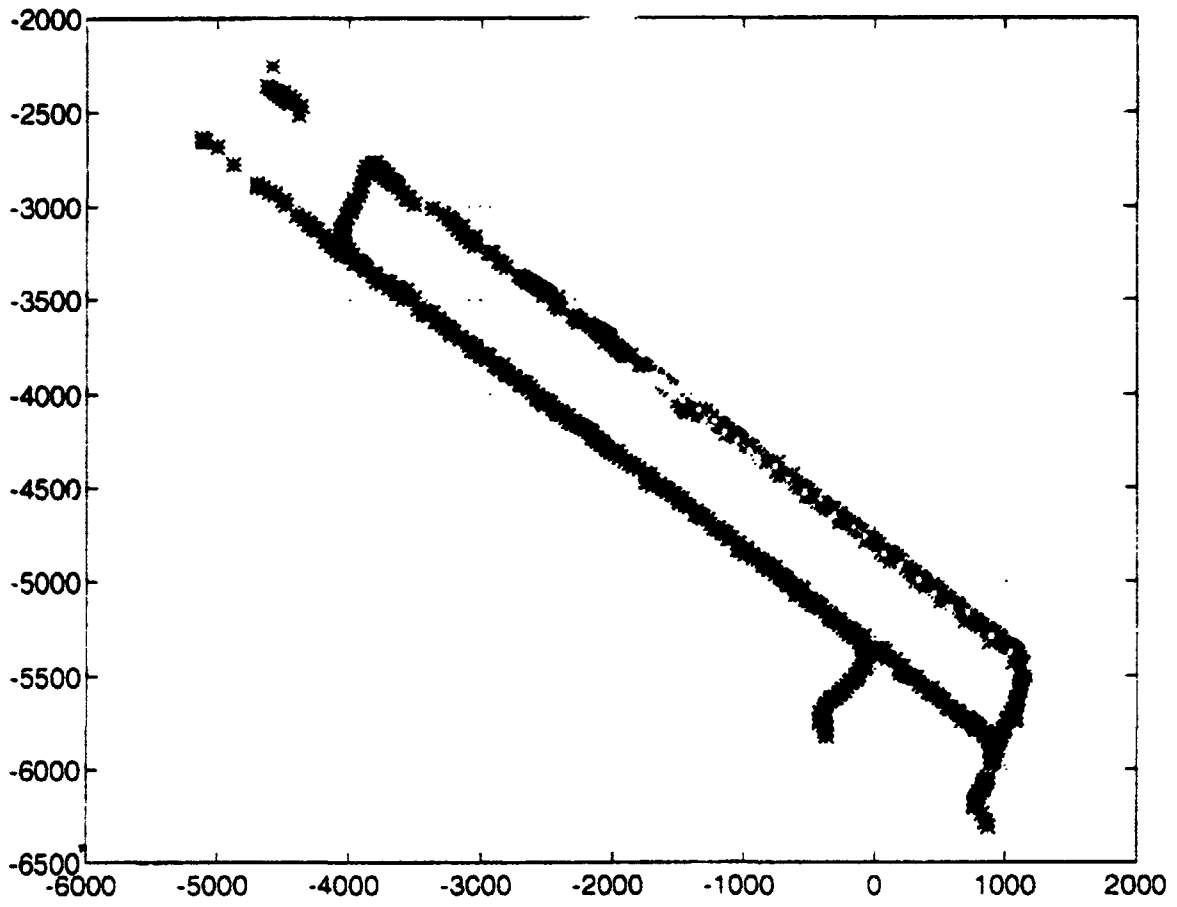
Norden Ground Tracks June 28 20:07z



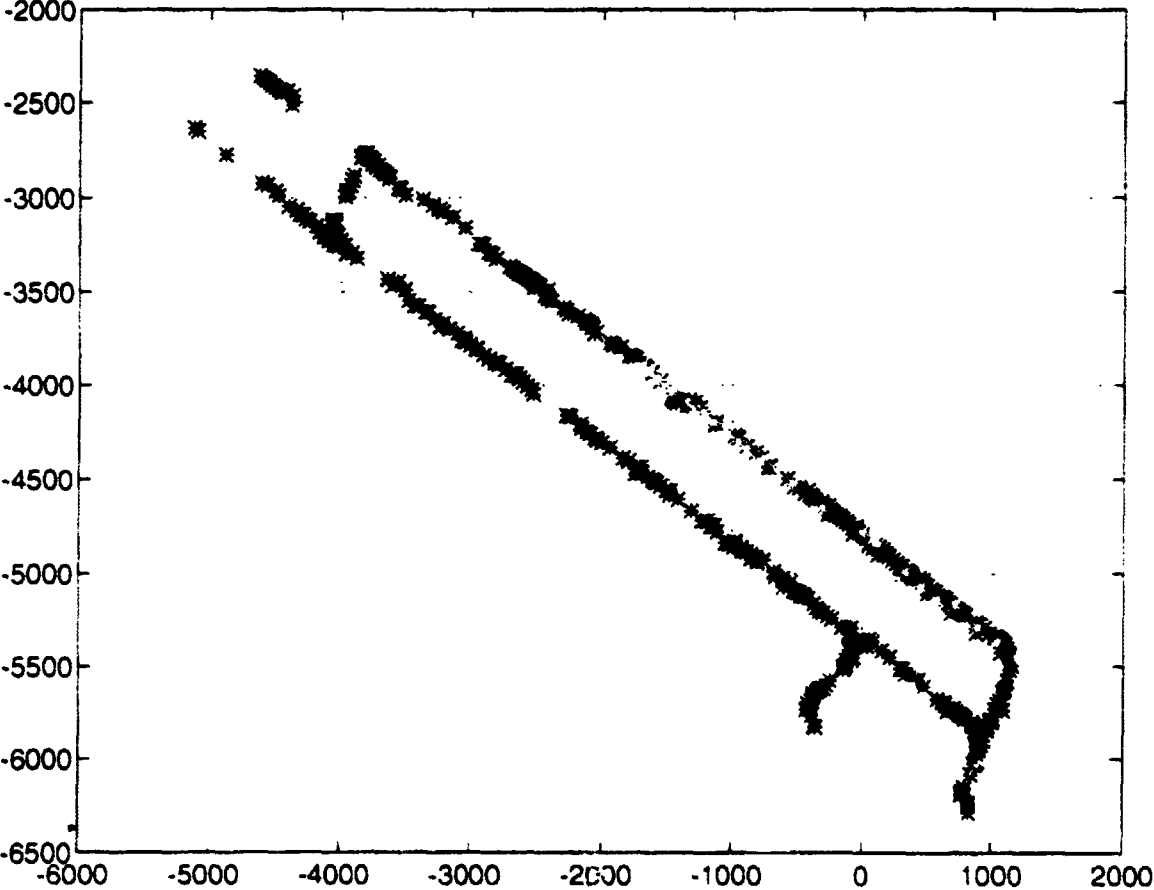
TSRV Ground Tracks June 28 20:07z



Norden Ground Tracks June 28 20:07z



TSRV Ground Tracks June 28 20:07z



APPENDIX B

4260043	16:34:13	39.46279507	-74.590999056
Ownship	16:34:13	39.45155829	-74.568328941
4260043	16:34:14	39.46287159	-74.591031997
Ownship	16:34:14	39.45155829	-74.568328941
4260043	16:34:16	39.46297855	-74.591035433
Ownship	16:34:16	39.45155829	-74.568328941
4260043	16:34:18	39.46303571	-74.591043228
Ownship	16:34:18	39.45155829	-74.568328941
4260043	16:34:19	39.46308340	-74.591009282
Ownship	16:34:19	39.45155829	-74.568328941
4260043	16:34:19	39.46310344	-74.590947172
Ownship	16:34:19	39.45155829	-74.568328941
4260043	16:34:21	39.46314359	-74.590939628
Ownship	16:34:21	39.45155829	-74.568328941
4260043	16:34:22	39.46317561	-74.590930240
Ownship	16:34:22	39.45155829	-74.568328941
4260043	16:34:22	39.46320762	-74.590916578
Ownship	16:34:22	39.45155829	-74.568328941
4260043	16:34:24	39.46326060	-74.590879949
Ownship	16:34:24	39.45155829	-74.568328941
4260043	16:34:24	39.46327803	-74.590868717
Ownship	16:34:24	39.45155829	-74.568328941
4260043	16:34:25	39.46332380	-74.590805098
Ownship	16:34:25	39.45155829	-74.568328941
4260043	16:34:27	39.46336445	-74.590754556
Ownship	16:34:27	39.45155829	-74.568328941
4260043	16:34:27	39.46338163	-74.590739552
Ownship	16:34:27	39.45155829	-74.568328941
4260043	16:34:29	39.46344676	-74.590741480
Ownship	16:34:29	39.45155829	-74.568328941
4260043	16:34:30	39.46349596	-74.590707282
Ownship	16:34:30	39.45155829	-74.568328941
4260043	16:34:30	39.46354944	-74.590674089
Ownship	16:34:30	39.45155829	-74.568328941
4260043	16:34:32	39.46359847	-74.590611560
Ownship	16:34:32	39.45155829	-74.568328941
Ownship	16:34:33	39.45155829	-74.568328941
Ownship	16:34:33	39.45155829	-74.568328941
Ownship	16:34:35	39.45155829	-74.568328941
4260043	16:34:35	39.46374801	-74.590443503
Ownship	16:34:35	39.45155829	-74.568328941
4260043	16:34:36	39.46377407	-74.590412406
Ownship	16:34:36	39.45155829	-74.568328941
4260043	16:34:38	39.46382311	-74.590345351
Ownship	16:34:38	39.45155829	-74.568328941
4260043	16:34:38	39.46382730	-74.590264214
Ownship	16:34:38	39.45155829	-74.568328941
4260043	16:34:40	39.46378966	-74.590179138

7.0 Conclusion

As one can see from the error table, the radar data was the least accurate of the three positions compared with the post processed GPS. However, if the few points that are skewing the mean value in the radar data are ignored, the ASDE Ave becomes closer to the Min. The raw GPS falls in with an overall average of approximately 2.79 feet, which is only a little more than the DGPS. The DGPS has the least overall error with an average of approximately 1.8 feet. This is excellent when one considers that the test aircraft was perhaps 75 feet across. When differential corrections fail, the position of the test aircraft will only be as accurate as the Raw GPS.

Concerning the radar data availability data, at first all the gaps in the data were counted, and the percentage of the total time that the radar data was unavailable was between 75 and 85%. This seemed like a large amount, and it was decided that a closer look at the data was in order.

A large percentage of the gaps in the radar data were two second gaps (i.e. 15:08:25 - 15:08:27). In the target data for the test aircraft, sometimes two positions were sent in the same second - two different packets are stamped with the same time, but contain different ownship (test aircraft) positions. An example of this is shown after the plots. It is possible that the two packets with the same timestamp cause the majority of the two second gaps in the data.

Example: 15:08:09

15:08:10

15:08:10 --> Should be counted as 15:08:11 and two second gap ignored.

15:08:12, etc.

When the two second gaps that are paired with a double timestamp are ignored, the availability of the radar data jumps to between 55 and 60%.

So basically this comes down to how one wants to define availability. If one ignores all gaps in the data that are 19 seconds or less, the radar data was available 100 percent of the time. On the other hand if one does not ignore any gaps in the data (even the two second gaps), the radar data was available only 18% of the time.

It was later discovered, that while the GPS receiver is operating in DGPS mode, there is no Raw GPS data. The DGPS is mirrored to the Raw GPS, and this is why DGPS, and Raw GPS are so close in the error table. In this case the Raw GPS numbers really have no meaning.

**NEXT
DOCUMENT**

TITLE SHEET

**Introducing
Current Technologies**

TIFFANY MITCHELL
LARSS student

BARRY GIBBENS
Mentor

**Technology Applications Group
Technology Transfer Team**

Abstract

The objective of the study was a continuation of the "technology push" activities that the Technology Transfer Team conducts at this time. It was my responsibility to research current technologies at Langley Research Center and find a commercial market for these technologies in the private industry. After locating a market for the technologies, a mailing package was put together which informed the companies of the benefits of NASA Langley's technologies. The mailing package included articles written about the technology, patent material, abstracts from technical papers, and one-pagers which were used at the Technology Opportunities Showcase (TOPS) exhibitions. The companies were encouraged to consult key team members for further information on the technologies.

INTRODUCTION/ BACKGROUND INFORMATION

Since the signing of the Space Act in 1958, the technologies of NASA have proven to contribute to the economic security of the United States. As a part of this legislation,, partnerships between the private sector and NASA have been strongly encouraged. NASA should no longer be solely considered a space center. It's responsibilities have branched out to the private industry, and technology transfer has become a key function at each NASA center.

In addition to its existing partnership with the aerospace industry, NASA Langley proactively seeks non-aerospace partners for R&D collaborations where such collaborations offer significant synergy or benefits from sharing technology. Arrangements will be emphasized with industries which can benefit significantly from introduction of NASA technology for new products, improved products or increased efficiency.
(Agenda for Change, p.7)

This important marketing responsibility is held by LaRC's Technology Applications Group, part of which is the Technology Transfer Team (TTT). The Transfer Team is divided into four specialized sections: Medical/Sensors/Instrumentation/Environment/Energy, Information/Communication, Transportation, Materials/Manufacturing. It is a primary objective of the TTT to "encourage broader utilization of NASA Langley-developed technologies in the American industrial community." *(The Technology Transfer Process, p.1)*

SUMMARY OF RESEARCH

The key purpose of my particular project was to solicit interest in the current technologies which have failed to be utilized or licensed by the private industry. Requests were made to several transfer members to submit a list of technologies which they believed would be beneficial to a commercial market. Two technologies were chosen from the list submitted based on benefits to the commercial market and the existence of a market for the technology. The technologies which were selected were the Blind-Anchor-Nut-Installation-Fixture (BANIF) and Panel Analysis and Sizing Code (PASCO) software.

DESCRIPTION OF TECHNOLOGIES

BLIND-ANCHOR-NUT-INSTALLATION-FIXTURE is "an invention which enables a user to install an anchor nut on the blind side of a component. The potential commercial uses include boat repair, maintenance and repair of transportation systems, and automotive bodywork" (TOPS one-pager, "Blind Fastening Technique")

PANEL ANALYSIS and SIZING CODE provides a graphical interface which simplifies the specification of panel geometry and reduces user input errors. The user draws the initial structural geometry, then uses a combination of graphic and text inputs to refine the structural geometry. The potential commercial use corrugated cardboard boxes. (Abstract, "User's manual for MacPASCO")

APPROACH

After the selection of the technologies, research into each technology began. The team members which specialized in each particular technology aided in my research. Publications by the researchers, one-pagers from the Technology Opportunities Showcase (TOPS) exhibitions, and abstracts from NASA technical papers were obtained through the use of the World Wide Web. Other materials were also acquired from by the Technology Transfer Team members. The reading materials were collected and organized for a mailing package so that the selected market could be informed of the benefits of NASA Langley's technology.

Following the compilation of the mailing material, a specific target market was determined. A discussion with several of the TTT members was held so that an optimal market was chosen. The particular markets were selected because they appeared to be able to receive the most benefits from the technology, would use technology the most resourcefully, and would generate the most funds. The markets which were chosen were as follows: Blind Fastener--Tool Companies, and "PASCO" software-- Corrugated Cardboard Box Companies

With the aid of the librarians at the Technical Library who searched on an extensive database, the addresses of companies which fit into each particular category were gathered. The listings included companies from around the country, examples being Snap-on Incorporated and Black & Decker. A cover letter was included with each mailing package to the companies. They were requested to review all the materials included and contact a specific TTT member if interested in further information regarding the technology, or interested in licensing the technology. At this time responses are being awaited.

**NEXT
DOCUMENT**

PRODUCT ASSURANCE FOR SPACEFLIGHT HARDWARE

**Larss Student: Mike Monroe
Mentor: John Greco**

OSEMA, OMA

ABSTRACT

This report contains information about the tasks I have completed and the valuable experience I have gained at NASA. The report is divided into two different sections followed by a program summary sheet. The first section describes the two reports I have completed for the Office of Mission Assurance (OMA). I describe the approach and the resources and facilities used to complete each report. The second section describes my experience working in the Receipt Inspection/Quality Assurance Lab (RI/QA).

The first report described is a Product Assurance Plan for the Gas Permeable Polymer Materials (GPPM) mission. The purpose of the Product Assurance Plan is to define the various requirements which are to be met through completion of the GPPM mission. The GPPM experiment is a space payload which will be flown in the shuttle's SPACEHAB module. The experiment will use microgravity to enable production of complex polymeric gas permeable materials.

The second report described in the first section is a Fracture Analysis for the Mir Environmental Effects Payload (MEEP). The Fracture Analysis report is a summary of the fracture control classifications for all structural elements of the MEEP. The MEEP hardware consists of four experiment carriers, each of which contains an experiment container holding a passive experiment. The MEEP hardware will be attached to the cargo bay of the space shuttle. It will be transferred by Extravehicular Activity and mounted on the Mir space station.

The second section of this report describes my experiences in the RI/QA lab. I listed the different equipment I used at the lab and their functions. I described the extensive inspection process that must be completed for spaceflight hardware. Included, at the end of this section, are pictures of most of the equipment used in the lab.

There is a summary sheet located at the end of this report. It briefly describes the valuable experience I have gained at NASA this summer and what I will be able to take with me as I return to college. I briefly discuss the experiences I mentioned in the previous three paragraphs along with training classes I attended and courses I completed at the Learning Lab.

OFFICE OF MISSION ASSURANCE (OMA)

Product Assurance Plan

My first project consisted of preparing a Product Assurance (PA) Plan for the Gas Permeable Polymer Materials (GPPM) mission. The purpose of the Product Assurance Plan is to define the requirements for configuration management, reliability, quality assurance, parts, materials, processes, and system safety which are applicable for design, procurement, fabrication, assembly/disassembly, and test operations for Langley Research Center deliverables through completion of the GPPM mission.

The purpose of the GPPM experiment is to use microgravity to enable production of complex polymeric gas permeable materials. This experiment will be put aboard the SPACEHAB module which is integrated into the Orbiter cargo bay. SPACEHAB provides a shirtsleeve environment for performance of multiple experiments.

The material resources I used to accomplish this task were the manual (LHB 5300.1), the handbooks NHB 5300.4(1B) and 5300/4(1A-1), and a PA Plan for a previously completed experiment. The human resources I took advantage of, in the Office of Mission Assurance, to complete the plan were the program assurance manager, GPPM project personnel, payload safety engineer, and the reliability engineer.

The first section of the Product Assurance Plan includes the classification of the payload, the mission success criteria and a list of the Office of Mission Assurance's Product Assurance Services. GPPM is a "Class D" payload. This means that this payload has objectives worth achieving at a cost not to exceed the amount required for a single low cost attempt where single failure points are acceptable and formal verification requirements are limited to those necessary for safety and compatibility. The mission success criteria for the GPPM experiment will be met if it maintains mechanical and electrical integrity from launch through landing and has the capability to enable a variety of sample tube monomer mixtures to polymerize. I worked with the program assurance manager to determine all of the items to be furnished to the Project Leader at appropriate times.

The second section of the PA plan states where the GPPM Project Team Organization can be found and describes the responsibilities of the Product Assurance Engineer. The Product Assurance Engineer is responsible for assuring the overall implementation of the requirements of the PA plan consistent with the intent of the Product Assurance Instruction 5300.1 "Program Assurance: General Policy, Responsibility, Authority, and Implementation."

The reliability assessment and design specifications for the GPPM are included in the third section of the PA plan. I found out, from the reliability engineer, the type of reliability analysis that will be done on GPPM. The GPPM had been flown on previous missions successfully without a reliability analysis being done. Therefore, a reliability analysis does not need to be done for the current experiment. Design data will be reviewed to ensure that quality, reliability, and safety considerations have been factored into the flight hardware design.

The fourth section of the PA plan establishes a Configuration Management System for the control of the GPPM experiment. This section cites the way design changes are dealt with and how parts, materials, and processes are to be accounted. The GPPM Project Manager shall be responsible for providing and implementing a GPPM Configuration Management Plan prior to fabrication of flight hardware. The plan should identify the configuration management system to accurately define and control the configuration of flight hardware, spares, and ground support equipment.

Procurement Program Assurance is covered in the fifth section of the PA plan. The purchase request review, receiving and inspection, the acceptance/rejection of received articles, receipt inspection and supplier documentation requirements are contained in this section.

The sixth section covers parts, material selection, and process control. Parts shall be selected which optimize design and performance to certain extents specified. The Electrical, Electronic, and Electromechanical (EEE) Parts Manager shall approve all EEE parts in the GPPM hardware and is responsible for qualification, screening, testing, and failure analysis as required. The EEE Parts Engineer shall develop the GPPM Parts list and show lot/date codes as appropriate. Fasteners received at Langley Aerospace Research Center will be verified by the Receiving and Inspection Lab per GPPM specifications (I was able to do this task of verifying fasteners at the Receiving and Inspection lab as I will describe under the topic heading "Receipt Inspection/Quality Assurance Lab"). A materials and limited life items list shall be prepared. Metals will be selected using MSFC 522B "Design Criteria for Controlling Stress Corrosion Cracking," as a reference and all GPPM hardware will satisfy outgassing constraints in accordance with JSC 09604F/MSFC-HDBK-527F.

Quality control requirements are contained in the seventh section of the PA plan. Electrostatic Discharge Control (ESD), fabrication control, inspection and testing, assembly and integration, nonconforming articles and material control, bonded stores, metrology control, QA stamp control, the end-item data package and handling preservation and shipping all have requirements included under quality control. Most of these topics' requirements are defined in certain cited handbooks. The end-item data package provides cognizance of the functional characteristics, and flight worthiness of the hardware to be shipped and subsequently maintains configuration accountability.

The eighth and final section describes what will be done for system safety of the GPPM experiment. A reflight assessment will be developed and documented based on the Safety Analysis presented to the Safety Review Panel for previous flights. All safety reviews shall be held in accordance with the phased system as defined in NSTS 13830B.

Fracture Analysis

My second project consisted of preparing a fracture analysis report on the Mir Environmental Effects Payload (MEEP). The MEEP hardware consists of a sidewall carrier and four Passive Experiment Carriers (PEC), each of which contains an experiment container holding a passive experiment. The PEC's will be attached to the cargo bay of the space shuttle. They will be transferred by Extravehicular Activity and then mounted on the Mir space station.

The fracture analysis report is required for the flight certification of Shuttle payloads by NHB 8071.1. The fracture analysis report is a summary of the fracture control classifications for all structural elements of the MEEP. Each component may fit under one of five categories: contained, fail-safe, low risk fracture, low released mass, or fracture critical. The structural elements have been fabricated from materials that have high resistance to stress corrosion cracking (SCC). For each part, the material is listed along with its SCC classification.

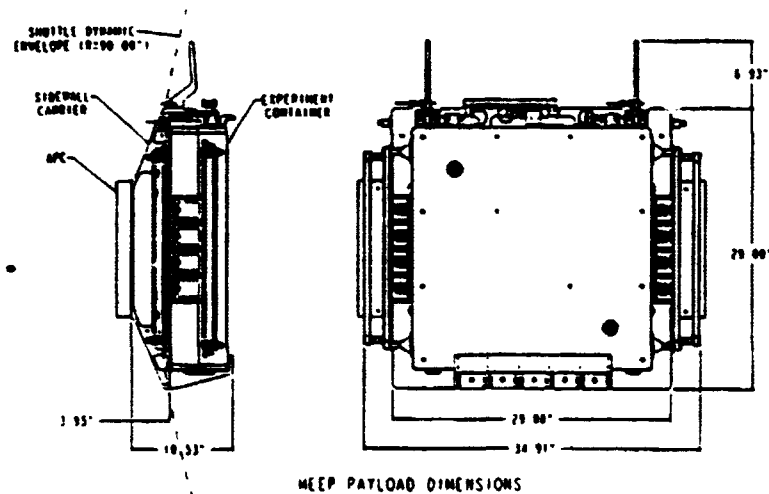
The first step that needed to be taken, in order for me to be able to determine the information needed to complete the requirements stated in the paragraph above, was to obtain the drawings for the hardware under consideration. I obtained the drawings from the aerospace system engineers who drew them. These drawings of the individual structures of the MEEP show the material of which each component is made. I then listed, in my report, the components of the MEEP, followed by the material they are made of and the stress corrosion cracking (SCC) classification of the material. The SCC classification for each material was obtained from the booklet "Design Criteria for Controlling Stress Corrosion Cracking." A classification of 1 indicates high resistance to SCC, 2 indicates moderate resistance, and 3 indicates low resistance.

I then studied the drawings of each component very carefully to determine their fracture classifications. A full-scale model of the MEEP was also available, in the systems engineering building, to study in order to get a better picture of its components. In order to classify each component, I determined fractures that could occur in each component that would cause a worst case scenario. If a component is classified as being contained, it can fracture and not be a threat to the payload of the shuttle, due to it being contained by a surrounding structure. A fail-safe component is designed with redundancy, which means if one part of its structure failed there would still be another structure holding the part in place. Low released mass is a classification given to a structure which does not have the potential to do damage to the shuttle payload if it fails, due to its light weight (Mass < 2.5 lb.). The classification "fracture critical," raises the most concern of all the possible classifications a structure can be labeled. If a structure is fracture critical, it may cause damage to the shuttle if it fails (catastrophic failure). Engineers try to design the structures to contain a minimal number of fracture critical parts. Low risk fracture is a classification which permits hardware which would ordinarily be defined as "fracture critical" to be classified as "non-fracture critical" when the possibility of failure due to a crack-like flaw can be shown to be extremely remote.

Every component of the MEEP was made of either 6061-T6 AL, 7075-T73 AL, A286 SST, or 300 series SST. These are all materials which have high resistance to stress corrosion cracking and therefore, in the analysis, each component was given a SCC

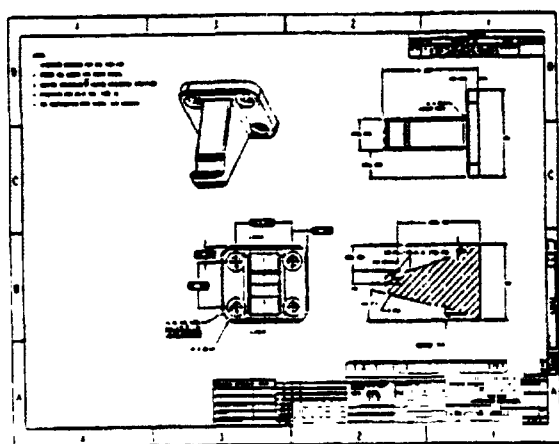
classification of 1. Most of the components of the MEEP were identified during the analysis as being either fail-safe or a low released mass. The attention should be drawn to the two components which were found to be fracture critical. These components are the hook latches located on top of the experiment container and on the sidewall carrier and the latch plate pins which join the latches to the sidewall carrier (drawings of these components along with the entire MEEP structure are shown below). If a crack propagated at the bottom of the hook latch, above where it is bolted on to the structure, causing the component to fail, it would become a projectile. This projectile would weigh more than .25 pounds and has potential to do damage to the shuttle payload (if it weighed less than .25 pounds, it would be considered a low release mass as stated earlier). The latch plate pins are also considered fracture critical since if one failed, the entire latch assembly would become a projectile which weighs much more than .25 pounds. Stricter and more numerous inspections will be done on these fracture critical components.

MEEP Payload Drawing

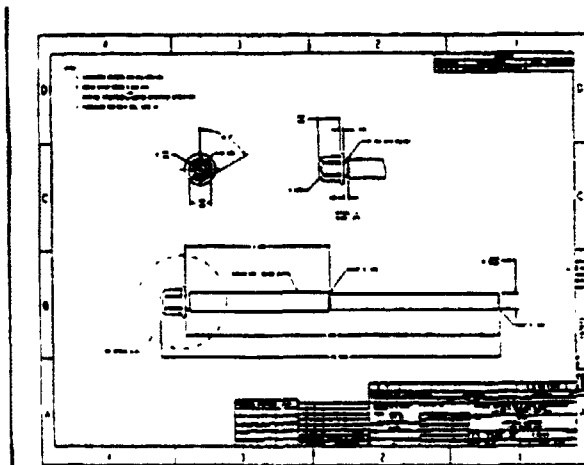


Fracture Critical Components

Hook Latch



Latch Plate Pin



Receipt Inspection / Quality Assurance (RI/QA) Lab

I was fortunate enough to be able to spend some time working with the inspectors at the Receipt Inspection/Quality Assurance (RI/QA) Lab. The inspectors are employed by Mason & Hanger who are contractors at NASA. I conducted various quality inspections and verification tests of incoming stock and spaceflight hardware. I gained experience on the equipment used in the inspection process. The following list shows the equipment I used. There are pictures of most of these machines at the end of this section.

- **Cutting Saw** - cuts a section of material to be mounted by the mounting processing system.
- **Mounting Press** - encapsulates specimens to be metallographically prepared and examined.
- **Grinder** - prepares samples for metallographic examination by using progressively smaller abrasive materials to remove distorted surface material from the sample so it can be studied under a microscope.
- **Stereoscope/Microscope Video package** - allows low and high magnification of prepared samples to view surface coatings and to determine surface discontinuities.
- **Measurement System** - video measurement system which measures coating thickness and non-conformities.
- **EDAX (energy dispersive X-ray fluorescence) system** - Spectra chemical microanalysis system which uses X-ray energy to excite unknown elements causing them to give off their own specific energy which allows each element to be identified in a test specimen.
- **Magnaflux F.P.I. Processing System** - uses florescent penetrant inspection to detect discontinuities exposed to a specimens surface.
- **Hardness Tester** - performs the Rockwell Hardness Test to determine the hardness of a specimen.
- **Micro-hardness Tester** - performs the Rockwell Hardness Test on very small and thin samples.
- **Tensile Tester** - determines the mechanical properties of a specimen, such as, ultimate tensile strength and reduction of area.
- **Laser Thread Measurement System** - non-contact thread measurement system used for determining root radius, flank angles, functional diameter, etc.

In the inspection process, there is a chart that is followed in the lab which specifies the number of samples that must be tested from a certain lot, depending on the number of pieces contained in the lot. The most ideal method would be to test every part in a lot, but this takes too much time and money to be effective. The idea is to choose samples which represent the entire population. NASA follows the "zero-defect" policy. This policy states that if one of the pieces in the lot does not meet its' specifications, the whole lot is rejected. This strict rejection policy gets the manufacturer's attention providing an extra incentive to make parts strict to their specifications.

During my time at the lab, screws were the main items being tested. First, every inspection machine must be calibrated. Then I would pick a designated number of samples out of the lot, referring to a chart. Then I would perform a variety of tests on the samples.

The first test I would perform on these samples is a visual test. This would consist of seeing if they would properly screw into a pre-tapped hole of the screws specified measurement, and simply looking at the screw to see if there were any noticeable defects. Then one sample from each lot would be tested for its proper thread dimensions using the Laser Thread Measurement System. This is a very precise non-destructive test, which virtually eliminates human error. NASA is one of the few places to have purchased one of these devices.

Then a chemical test is performed to see if the sample was made of the material specified. Many times manufacturers have sold zinc coated screws to NASA, while telling NASA they were coated with cadmium. This is because it is cheaper and easier for the manufacturers to coat screws with zinc, and they could still charge cadmium coating prices, if this went undetected. The EDAX machine keeps manufacturers from getting away with delivering pieces made with material other than what was specified in the contract. The EDAX is an X-ray device which can determine the percentage of each element present in a sample.

A tensile test or hardness test should then be done on the sample. A tensile test can be done on most screws and is done to see if it meets or exceeds the minimum tensile strength stated in the specifications. The screw's length and width must be measured before and after the test in order for the elongation and reduction of area to be calculated. This is a destructive test which literally pulls the screw until it breaks apart in order to find it's ultimate tensile strength.

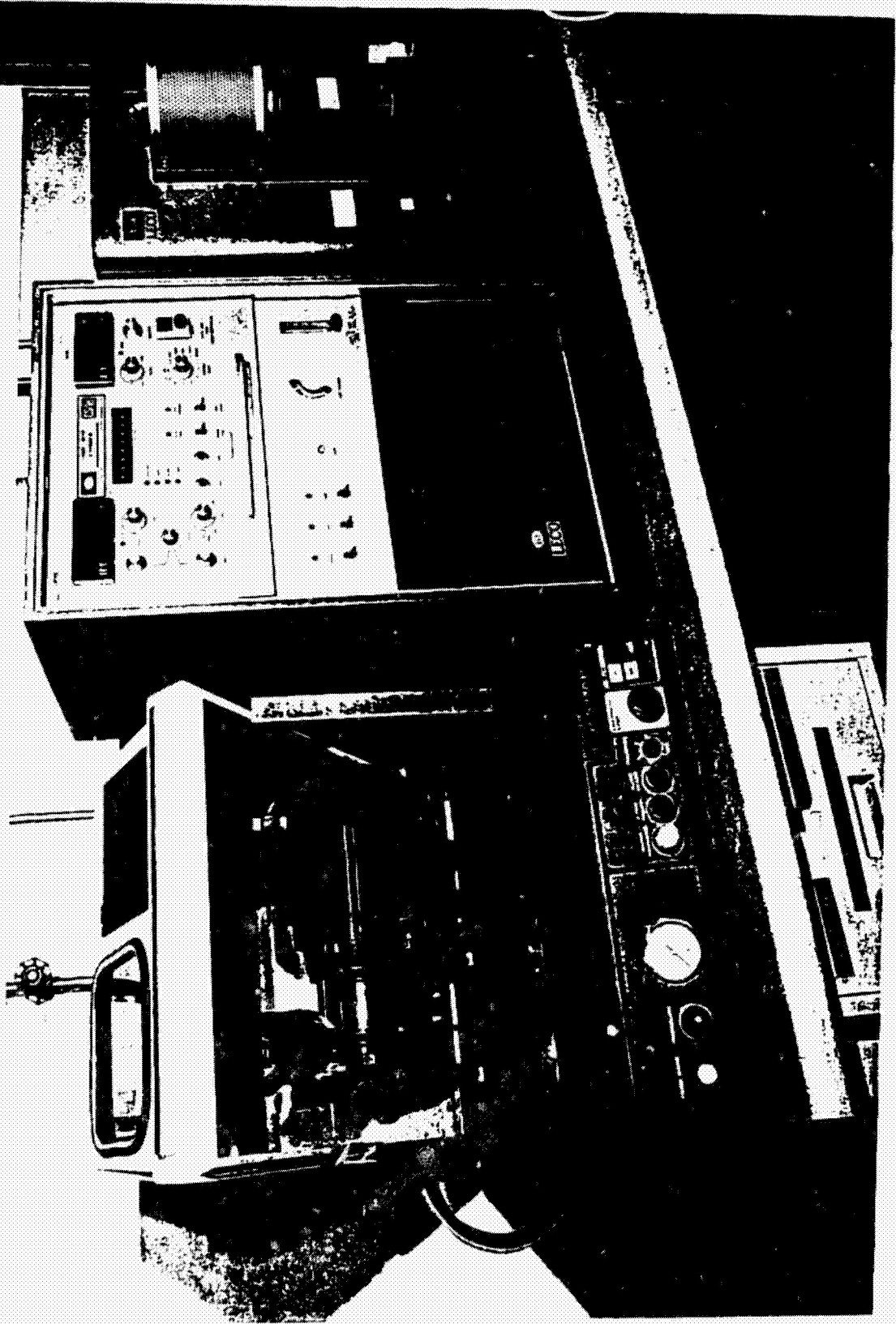
If the screw can not be placed in the tensile test machine, it must be prepared for a Rockwell Hardness test to be executed with either the Hardness Tester or the Micro-hardness tester, depending on the specimen's size. The preparation phase is a rather long process for this test. First the specimen should be cut, using the cutting saw, to about one centimeter long. Then, the specimen is mounted using the Mounting Press. A flat, polished surface, free from obstructions must be exposed in order to do the hardness test. Therefore, a grinder is used to achieve this purpose, using progressively smaller abrasive materials to remove distorted surface material. After this process is finished, the sample can then be tested for hardness. A test for coating thickness can also be done to the specimen after it has been prepared in the way stated.

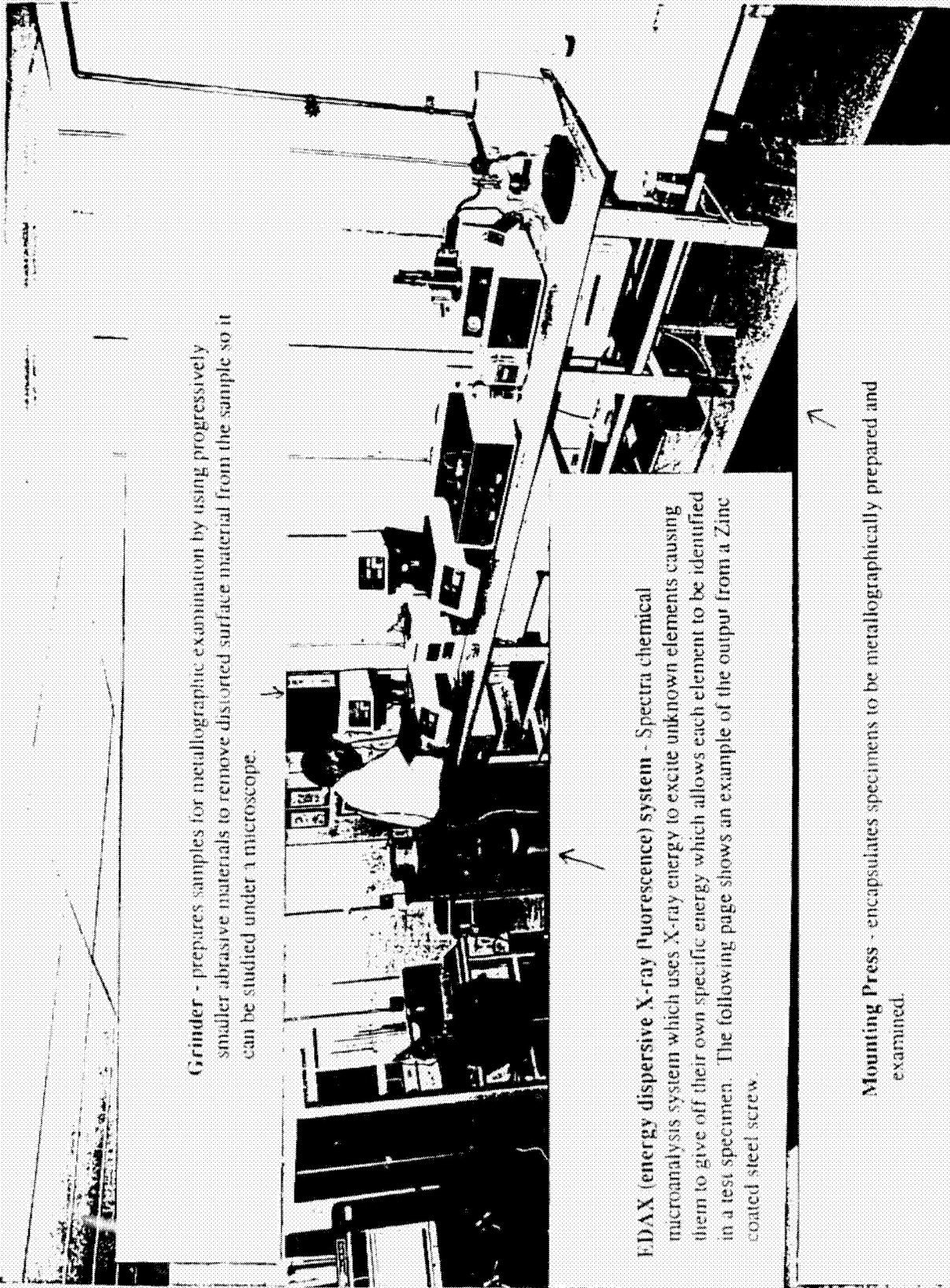
In order to see if a specimen has been coated with the specified amount of material, the Stereoscope/Microscope Video package is used along with the video Measurement system. The specimen is magnified many times with this system. The image of the specimen is shown on a monitor. Pointers can then be toggled around the coating layer of the specimen on the video screen. The system automatically measures the distance between the two pointers, determining the coating thickness of the specimen. This entire system can also be used to show irregularities in the material. The system can print a picture of the image displayed on the monitor to be used for the sake of argument when dealing with manufacturers of faulty components.

The Magnaflux F.P.I. Processing System is used mainly for pressure fittings to see if there are discontinuities on the surface of the specimen. One must be a level III inspector in order to do diagnose faults in specimens, using this test.

With NASA's zero defect policy, if any of the tests mentioned above, shows a result which does not agree with the specifications of the part being examined, all of the parts are rejected. During my stay, only one of the lots I worked with was rejected. It was rejected because there were bolts contained in this same lot made by two different manufacturers. This was made illegal, since the parts lose their tractability causing it to be impossible, at times, to hold a specific manufacturer accountable for the quality of their products.

Cutting Saw - cuts a section of material to be mounted in myrtle mounting processing system.





Grinder - prepares samples for metallographic examination by using progressively smaller abrasive materials to remove distorted surface material from the sample so it can be studied under a microscope.

EDAX (energy dispersive X-ray fluorescence) system - Spectra chemical microanalysis system which uses X-ray energy to excite unknown elements causing them to give off their own specific energy which allows each element to be identified in a test specimen. The following page shows an example of the output from a Zinc coated steel screw.

Mounting Press - encapsulates specimens to be metallographically prepared and examined.

c:\dx4\crf\4294.spc

Label:TEST

Prst:200L

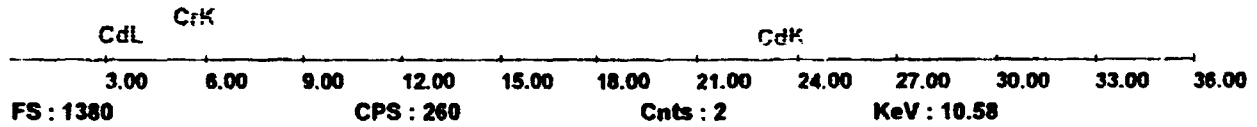
Lsec:200

11:25:14

7-13-95

ZnK

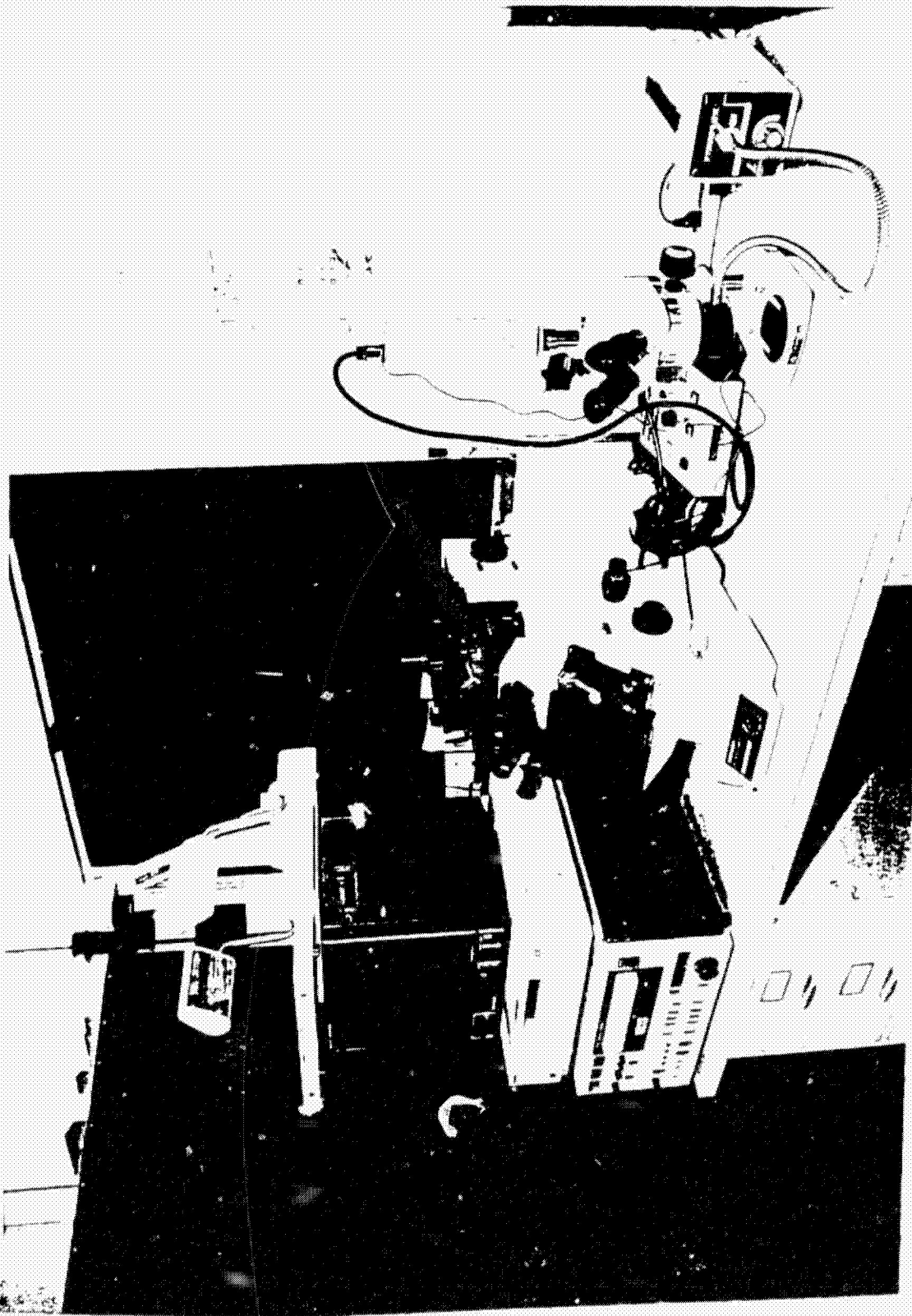
FeK



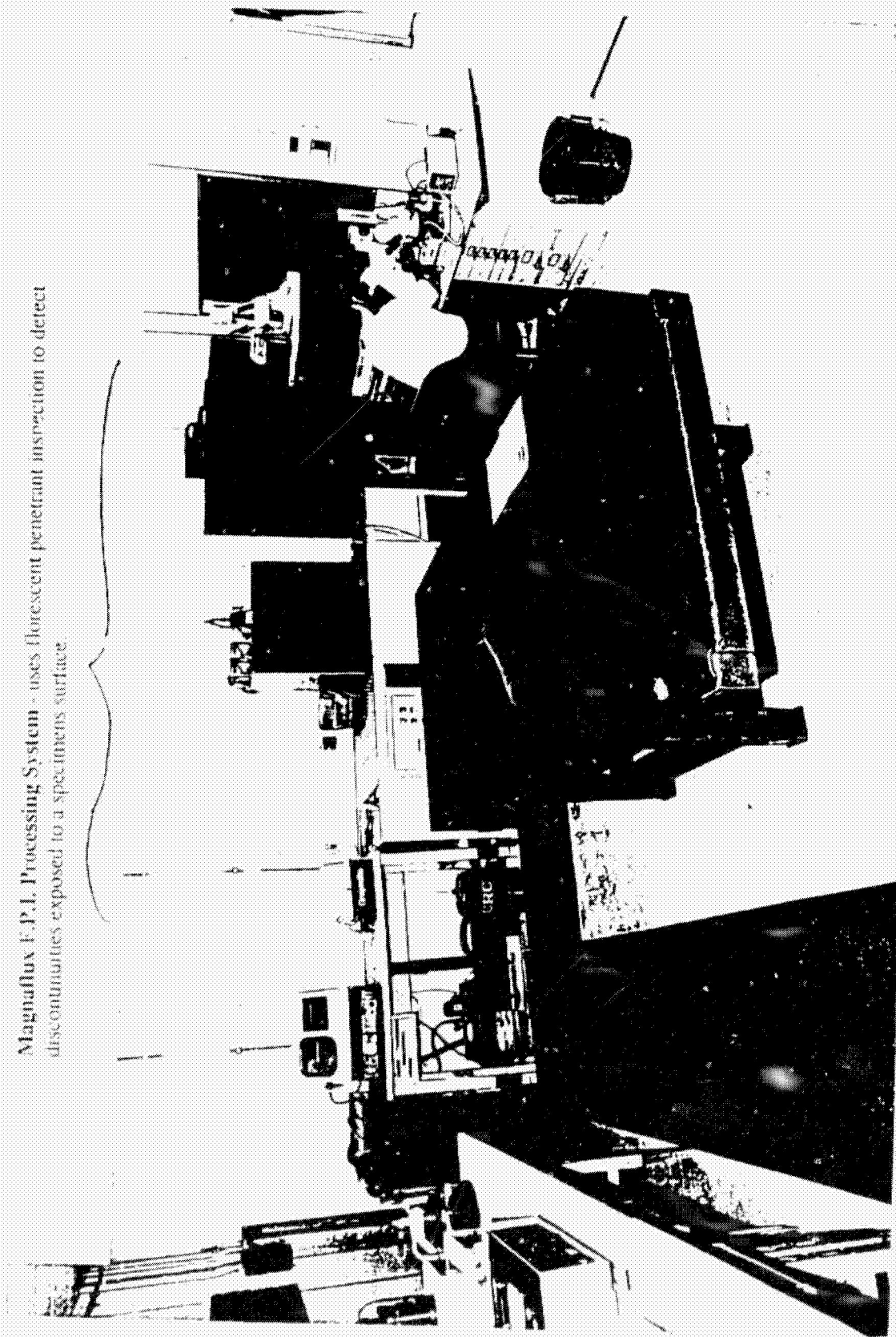
Element	Gross Inten	Inten Error
CdL	0.49	10.15
CrK	3.17	3.97
FeK	94.35	0.73
ZnK	126.19	0.63
CdK	0.20	15.81

This is an example of output from the EDAX (energy dispersive X-ray fluorescence) system which is a spectra chemical microanalysis system that uses X-ray energy to excite unknown elements causing them to give off their own specific energy which allows each element to be identified in a test specimen. The purpose of this specific inspection test was to determine if a screw was coated with zinc as stated in its specifications. The screw was, in fact, coated by zinc as shown by the graph on this page.

Stereoscope/Microscope Video package - allows low and high magnification of prepared samples to view surface coatings and to determine surface discontinuities.



Magnaflex F.P.I. Processing System - uses fluorescent penetrant inspection to detect discontinuities exposed to a specimens surface.



Hardness Tester - performs the Rockwell Hardness Test to determine the hardness of a specimen.



Micro-hardness Tester - performs the Rockwell Hardness Test on very small and thin samples.

Tensile Tester - determines the mechanical properties of a specimen, such as, ultimate tensile strength and reduction of area.



**NEXT
DOCUMENT**

Finite Element Analysis of an Energy Absorbing Sub-floor Structure

Scott C. Moore

Benson Dexter

**National Aeronautics and Space Administration
Langley Research Center**

**Research and Technology Group, Structures Division,
Structural Mechanics Branch**

Abstract

As part of the Advanced General Aviation Transportation Experiments program, the National Aeronautics and Space Administration's Langley Research Center is conducting tests to design energy absorbing structures to improve occupant survivability in aircraft crashes. An effort is currently underway to design an energy absorbing (EA) sub-floor structure which will reduce occupant loads in an aircraft crash. However, a recent drop test of a fuselage specimen with a proposed EA sub-floor structure demonstrated that the effects of sectioning the fuselage on both the fuselage section's stiffness and the performance of the EA structure were not fully understood. Therefore, attempts are underway to model the proposed sub-floor structure on computers using the DYCAST finite element code to provide a better understanding of the structure's behavior in testing, and in an actual crash.

Introduction

The National Aeronautics and Space Administration (NASA), the Federal Aviation Administration (FAA), and several aircraft and avionics manufacturers are currently working in partnership to develop new technologies for use in future general aviation and commuter aircraft. This goal of this research, known as the Advanced General Aviation Transportation Experiments (AGATE), is to revitalize the general aviation and commuter aircraft industry in the United States. There are four major NASA work packages comprising the general aviation element of AGATE: Integrated Cockpit Systems, Propulsion, Sensors, and Controls, Integrated Design and Manufacturing, and Icing Protection Systems. The goal of the Integrated Design and Manufacturing package is to develop lighter, safer, and more affordable certified aircraft structural concepts.

Current Research

NASA Langley Research Center (LaRC) has been conducting impact dynamics research and full scale crash testing for over 20 years. In recent years, NASA impact dynamics research has concentrated more and more on composite materials, which will be used much more extensively in aviation in the future. As part of the Integrated Design and Manufacturing work package of AGATE, LaRC is conducting research into energy absorbing (EA) structures for use in next generation general aviation aircraft. NASA recently acquired two seven seat Learfan aircraft with carbon composite fuselages. One of the aircraft, with the standard metal beam floor structure, was outfitted with energy absorbing seats, side by side with standard FAA Part 132 9g aircraft seats, and crash tested at LaRC's Full Scale Impact Dynamics Research Facility (IDRF) to form a baseline for future tests. At impact, the aircraft was traveling at 31 fps vertical velocity

and 81 fps longitudinal velocity. The maximum vertical accelerations measured in the seat pans were approximately 80g in the standard seats and 40g in the EA seats, compared with the human tolerance level of 50g. However, the test dummies in the EA seats sustained spinal loads of 1600 lbs, above the maximum human tolerance of 1500 lbs. These results demonstrate that, even in a moderate impact such as this one, occupants in EA seats would likely suffer severe injuries or death and occupants in standard 9g aircraft seats would almost certainly be killed.

The next stage in testing is to replace the standard sub-floor structure with an energy absorbing structure and repeat the test. However, before this can occur, a suitable sub-floor structure has to be developed and tested. One structure currently under consideration is a box core flat-faced composite beam. The structure consists of a 0/90 degree fiberglass core with a skin of +/- 45 degree Kevlar for structural integrity and is filled with rigid closed cell PVC foam. The structure, which has achieved a sustained crushing load of 240 lbf per inch length in dynamic testing is mounted directly under standard T-section seat rails. Recently, this structure was installed and tested in a 36 inch long full scale fuselage section from a Learfan aircraft. EA beams were mounted directly to the fuselage and seat rails under standard 9g aircraft seats, which carried standard instrumented crash dummies. The fuselage section was then drop tested in the IDRFS Vertical Testing Apparatus at 30 fps vertical velocity. However, the EA beams did not crush as anticipated.

After the test, some differences between this test and previous tests in metal fuselage aircraft which may have contributed to the problem were uncovered. Because, in this composite fuselage test, the EA beams were attached directly to the fuselage and there were no lateral beams, the relative stiffness of the fuselage section is more important. Also, the stiffness of the fuselage section was later determined to be less than that of the same section when it is part of the entire fuselage. In addition, the energy absorbing floor beams in the fuselage section act differently from how they would in a full length fuselage. These differences are caused by the shorter lengths of the beams and the differences in restraint at the ends of the beams (both ends of the 36 inch EA beams in the fuselage section test were unrestrained, whereas they would be restrained by the rest of the beam in a full length fuselage). It is therefore important to conduct more research into the effects of varying the lengths of fuselage sections and EA floor beams so that fuselage section drop tests can be both better understood and made more representative of full length aircraft fuselages. Efforts are currently underway to model both the fuselage section and the sub-floor structure on computers. The remainder of this paper focuses on computer modeling of the seat rail and energy absorbing floor beam which together form the sub-floor structure.

Finite Element Modeling

Developing an accurate computer model of the sub-floor structure under consideration is desirable because it would allow simulations to be run without the trouble and expense of a full scale test. Although full scale testing is still needed, these simulations could reveal problems, such as the ones that appeared in the fuselage section test, ahead of time, reducing the need for

costly re-tests. Computer models can also be used to simulate the behavior of materials under many different conditions, reducing the need for actual static and dynamic testing. It is hoped that developing accurate Finite Element Method (FEM) computer models of the sub-floor structure under consideration will lead to a better understanding of the structure and help researchers to recognize and correct potential problems before full scale testing is conducted.

DYCAST (Dynamic Crash Analysis of Structures), the FEM computer code used to model the energy absorbing sub-floor structure is a non-linear structural finite element computer code developed by NASA and Grumman Corporation (Ref. 1). Two different DYCAST elements were used to construct the computer model, the SPNG non-linear spring element and the TSEC beam element. The SPNG element is a non-linear crush spring with energy absorption capability. Its behavior is defined by user-input loading and unloading curves. The TSEC element is a beam element with six different integration points and user-input strain hardening and failure criteria. Each integration point can go plastic or reach failure separately. Also, the stiffness of each integration point is deleted from that of the whole beam when that point reaches the failure criteria (Ref. 1).

Modeling Considerations

For the original model used in the static testing, two sets of nodes were defined, along both the X axis and the line where the ground plane intersects the XZ plane (see Figure 1). Note that the X axis and the ground are 8 inches apart and that both the X and Y axes pass through the centroidal axis of the seat rail. The nodes were initially placed one inch apart in the X direction, along, and directly below the entire length of the beam in consideration. TSEC elements were defined between the elements along the X axis and SPNG elements were defined between these nodes, and the nodes directly below them on the ground. Material properties for 7075-T6 extruded aluminum alloy were used, as well as a 32 point Ramberg-Osgood curve to represent the strain hardening and failure characteristics of the material (see Ref. 2).

Because the cross-section of the seat rail was not identical to that of the TSEC beam, it was necessary to calculate the moment of inertia and centroid of the beam manually. The moment of inertia was then input into DYCAST and the thickness of the DYCAST TSEC flange was varied so that the centroid calculated by DYCAST would be at the proper Z coordinate. These calculations are included in spreadsheet form as Appendix A. The section numbers shown correspond to those in Figure 1. Next, a finite beam on an elastic foundation model was used to verify the DYCAST model (see Ref. 3). The DYCAST springs were made linear with $K=7500$ lbf per inch deflection and the DYCAST results and elastic foundation results for deflection at the ends and center, and the moment and maximum normal stress at the center were compared at several loads applied at the center node of the model. A comparison with a load of 2000 lbs is included as Appendix B. It was also necessary to construct a load vs. displacement curve for the SPNG elements used in the model. For static modeling, a simple 5 point curve could be used, however, for the dynamic cases, it was necessary to use a 15 point curve to smooth the rapid

changes in slope because of numerical integration problems which would otherwise result. A typical dynamic spring curve representing a sustained crushing load of 240 lbf/in length is included as Figure 2. On this curve, negative displacements and forces represent and cause, respectively, compression. It should be noted that this curve is for springs used with the 1/2 inch length TSEC elements used in some dynamic models, and that the level portion of the graph is slightly less than half of 240 lbf to account for the fact that there is always one more spring than beam element in each model. The static springs have a similar shape, but level off at slightly less than the 200 lbf/in length value used for the static crushing load (1 inch elements).

Static Model

The first series of tests involved static models with 1 inch elements at lengths of 12 and 24 inches, and loads of 2475 lbf and 4800 lbf, respectively. Graphs of the results are included as Figures 3 and 4. Please note that all seat rail displacement graphs represent only the left halves of the structure. The structures are symmetric about the right edge of the graphs. The models were run on a Digital Equipment Corporation Microvax. All nodes were constrained to allow translation in only the Z direction and rotation about only the Y axis. The translation restriction was imposed because of convergence problems with the static integrator. However, in the actual structure, the elements can also translate in the X direction. For this reason, the results are not representative of the actual material behavior. Therefore it was desirable to create a more accurate model.

Dynamic Model 1

In an attempt to more accurately model the behavior of the sub-floor structure, a dynamic model was created. The model was run at eight different lengths, 12 in, 13 in, 14 in, 16 in, 18 in, 22 in, 26 in, and 36 in, on several Sun Sparc 10 series workstations. The 12 through 16 inch models used 1/2 inch length elements, while the 18 through 36 inch models used 1 inch length elements due to a limit DYCAST imposes on the number of elements and the large amount of processor time required for these models. In each case the load was a 104 lbm point mass applied to the center node of the beam. The beam was then given an initial velocity of 30 fps in the negative z direction. In an effort to further reduce the computer time required, the symmetry of the beams used to represent the whole beam by modeling only the left half. To do this, the strength of the center spring was cut in half and a mass of 52 lbm was applied. The center node was then constrained to no rotation to force symmetry. These models were verified by comparing them to their full length counterparts and the results were identical. All of the other nodes along the beam were allowed translate in both the X and Z directions, and to rotate about the Y axis. A large unloading slope, comparable to the initial slope of the SPNG elements, was

used to make the deformation permanent. A Newmark-Beta implicit integration scheme was originally tried, however system energy errors of greater than 1000% resulted. The Wilson-Theta implicit integrator was then tried, and yielded much better results. This integrator was used for all remaining models, and system energy errors were all less than 5% and usually less than 1%.

Graphs of the 12, 13, 14, 18, 26, and 36 inch models at 4 millisecond increments are included as Figures 5 through 10, respectively. Figures 5 through 7 exhibit unusual behavior at the last three time increments. These are a consequence of the rebound the center node experiences when it reaches the very steep slope towards the end of the load vs. displacement curve and the unloading slopes on the springs. Because this behavior is uncharacteristic of the actual material, deflections after the center has reached the point of maximum Z deflection are indicated on the graphs as hairlines. A more troubling trend, however, is the large X deflection of the ends of the beams in all but the 26 inch case. This is not characteristic of the results of dynamic testing conducted at the IDRFB. The large deflections occurred because the model does not take in to account the strength added to the structure by the EA beam in directions other than the Z direction. The actual structure also resists crushing in the X direction and the +/- 45 degree Kevlar fibers in the beam give it a strong resistance to torsion. Next, an attempt was made to compensate for these factors.

Dynamic Model 2

In an attempt to compensate for the composite beam's X direction crush resistance and resistance to torsion, springs were attached from the end node of the 13 inch model to a point far in the positive X direction (so that only X and not Z deflections of the beam would affect the length of this new spring). Springs with loading curves identical to those used on each beam were then added and the dynamic tests were re-run in a trial and error process until the final X deflection of the end of the beam was close to that observed in a dynamic test of a 13 inch specimen. Similar beam-end X deflections were observed with 13 springs attached to the end (the equivalent of two springs per inch). The model was then run at lengths identical to those used in Dynamic Model 1 with two springs per inch of model length for 12 to 16 inches, and one spring per inch for 18 to 36 inches (the springs were twice as strong for these lengths due to the 1 inch elements). Plots of the displacements and accelerations of the mass at the center of each beam are included as Figures 11 through 16. Upon comparing the results of the 13 inch model (Figure 12) with a specimen from a dynamic test, it was discovered that the Z displacements along the beam were almost identical. While the X displacements were modeled after those of the test specimen, the fact that the Z displacements along the beam were the same indicates that the vertical springs represent the crushing behavior accurately and that the overall model is accurate for the 13 inch length. It can also be assumed that the models accurately represent the behavior of 14 and 12 inch specimens because they are close in length to the 13 inch model which has been verified. However, further research is necessary to determine if the scheme for adding springs to the end in the longer length models correctly represents the behavior of the material. However, even if it doesn't, corrections should be possible by simply adding or deleting springs.

Conclusions

Of the three different types of finite element models attempted, the third one, Dynamic Model 2, has the most promise. It has demonstrated the ability to accurately model the behavior of a test specimen, and with a few more dynamic tests, it could be verified and corrected, if necessary, for other lengths. The Static Model did not accurately represent the behavior of the material, although this is probably because numerical integration problems necessitated limiting the degrees of freedom of the beam beyond what was accurate. However, the static model was useful in that it allowed for verification with elastic foundation theory. Also, Dynamic Model 1 did a poor job of predicting the material behavior because it neglected the stiffness of the energy absorbing beam in other than the Z direction. Although Dynamic Model 2 shows promise, it might also be useful to try and model the sub-floor structure with another more advanced finite element code with the capability to model more complex composite materials. This might provide an even better understanding of the energy absorbing sub-floor structure's behavior.

References

1. Pifko, A. B. and Ogilvie, P. L. DYCAST - A Finite Element Program for the Crash Analysis of Structures. NASA CR 4040, January 1987.
2. Niu, Michael C. Y. I. Airframe Structural Design. Hong Kong: Convilit Press, Ltd., 1993.
3. Hetenyi, M. Beams on Elastic Foundations. Ann Arbor: The University of Michigan Press, 1976.

Appendix A: Moment of Inertia and Centroid Calculations

Seal Track Centroid Calculations

Section	Length in	Width in	Area in ²	Y of Centroid in	Y of Cent * A
1	0.7828	0.0073	0.0057	0.00365	0.02081
2	0.0073	0.0073	0.0053	0.00365	0.19352
3	0.7828	0.0073	0.0057	0.00365	0.02087
4	0.7828	0.0073	0.0057	0.00365	0.02087
5	0.7828	0.0073	0.0057	0.00365	0.02087
6	0.7828	0.0073	0.0057	0.00365	0.02087
7	0.7828	0.0073	0.0057	0.00365	0.02087

Sum = 0.49805 Sum = 0.41153

Y Centroid = 0.82829 in

Seal Track Moment of Inertia Calculations

Moments of Inertia about Y Axis:

Section	I _{yy} in ⁴
1	0.01480118
2	0.18291523
3	0.01858283
4	0.03084882
5	0.03084882
6	0.03084882
7	0.03084882

Moment of Inertia about Centroid:

I_{yy} = 0.38428 in⁴

A = 0.49805 in²

b = 0.82829 in

I_{yy} = 0.02421 in⁴

DYCAST Geometry Calculations

Width of Flange (A1) = 2.53125 in
 Depth of Web (A2) = 1.00000 in
 Thickness of Flange (T1) = 0.00600 in
 Thickness of Web (T2) = 0.00375 in

Current Centroid = 0.82821 in

Desired Centroid = 0.82829 in

NOTE: These values do not represent the actual geometry of the seal rail. They are only dummy values used by DYCAST to determine the centroid of the seal rail.

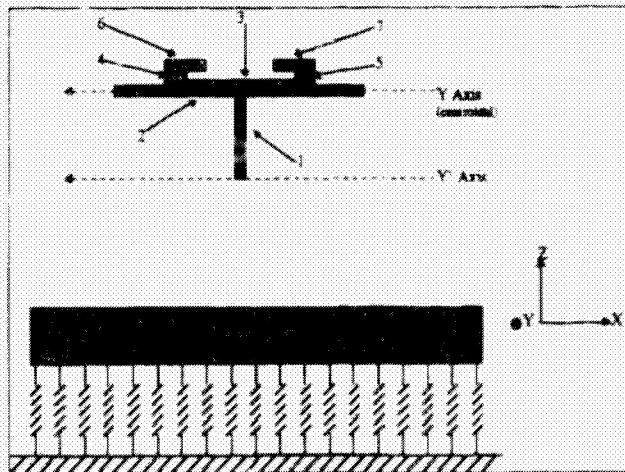


Figure 1: DYCAST Model Geometry

Appendix B: Comparison of DYCAST Results with Elastic Foundation Model

Finite Beam on Elastic Foundation Model

Model Geometry



0.287641 = BETA

Output

-0.00488 = DEFLECTION AT ENDS (in)

DYCAST = 0.12050477
 ERROR = 2.54%

0.048318 = DEFLECTION AT CENTER (in)

DYCAST = 0.044988
 ERROR = 2.35%

1881.05363 = MOMENT AT CENTER (in²lb)

DYCAST = 1788.4
 ERROR = 4.71%

84200.5701 = MAX NORMAL STRESS (psi)
 48000 = YIELD STRESS

DYCAST = 82395
 ERROR = 2.81%

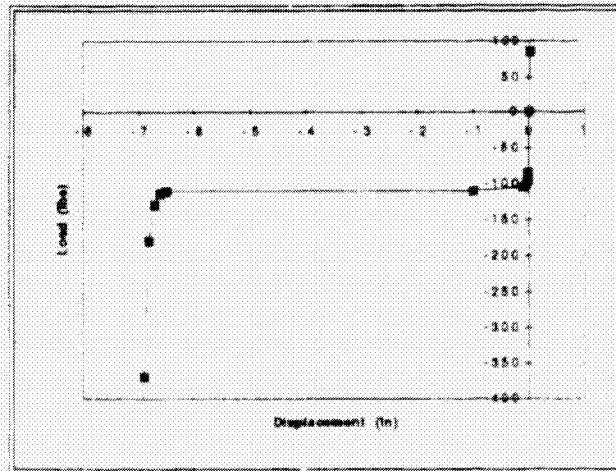


Figure 2: Load vs. Displacement Curve for DYCAST Springs

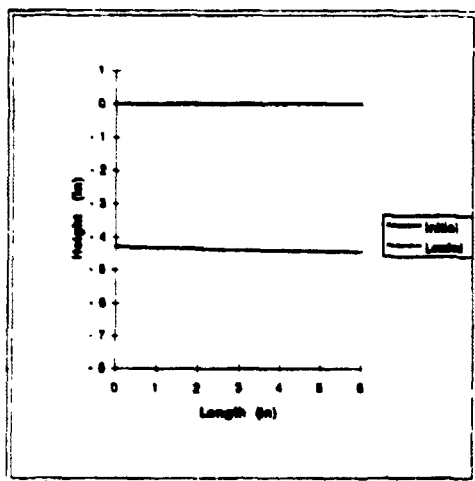


Figure 3: DYCAST Analysis of Seat Rail under Vertical Static Loading
Length = 12 in Load = 2475 Lbs

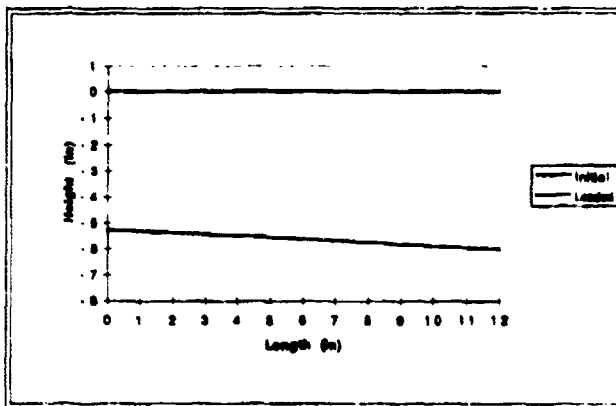


Figure 4: DYCAST Analysis of Seat Rail under Vertical Static Loading
Length = 24 in Load = 4800 Lbs

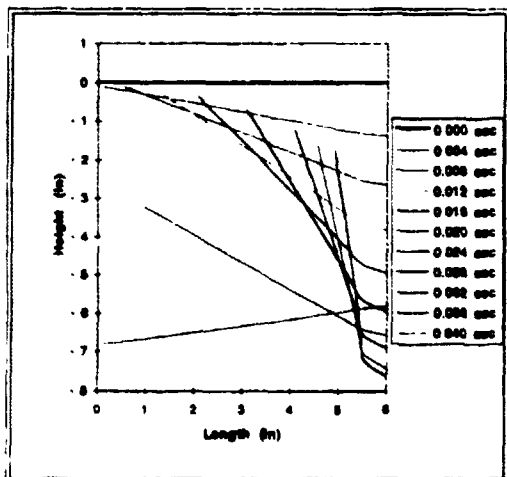


Figure 5: DYCAST Analysis of Seat Rail under Vertical Dynamic Loading
Length = 12 in Load = 104 lbm at 30 fps

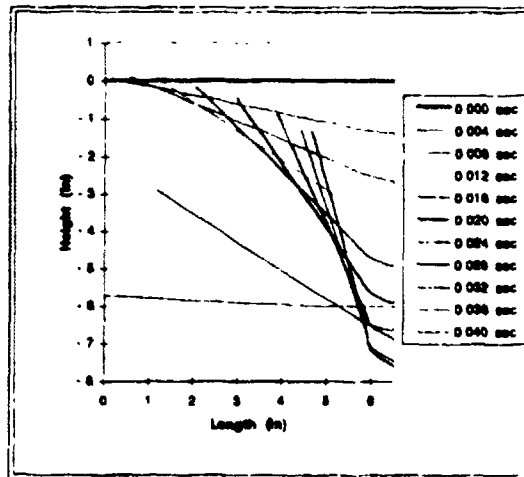


Figure 6: DYCAST Analysis of Seat Rail under Vertical Dynamic Loading
Length = 13 in Load = 104 lbm at 30 fps

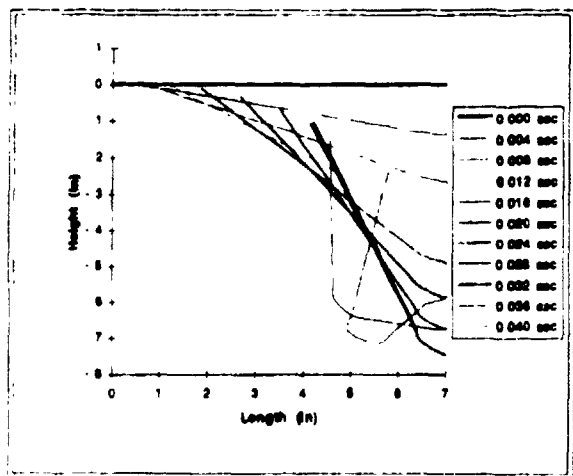


Figure 7: DYCAST Analysis of Seat Rail under Vertical Dynamic Loading
Length = 14 in Load = 104 lbm at 30 fps

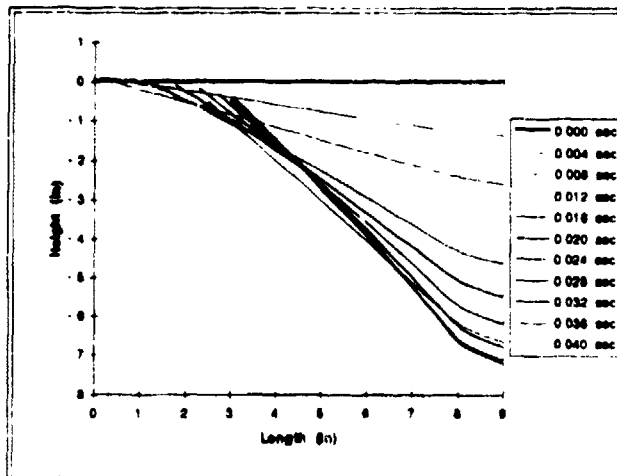


Figure 8: DYCAST Analysis of Seat Rail under Vertical Dynamic Loading
Length = 18 in Load = 104 lbm at 30 fps

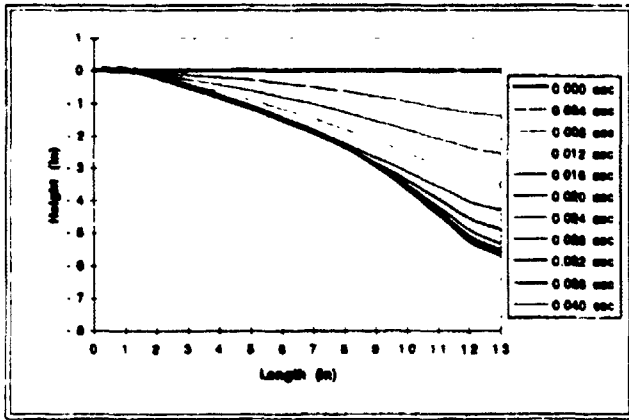


Figure 9: DYCAST Analysis of Seat Rail under Vertical Dynamic Loading
Length = 28 in Load = 104 lbm at 30 fps

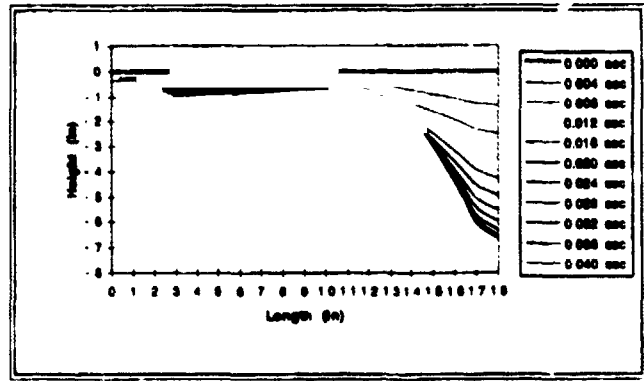


Figure 10: DYCAST Analysis of Seat Rail under Vertical Dynamic Loading
Length = 38 in Load = 104 lbm at 30 fps

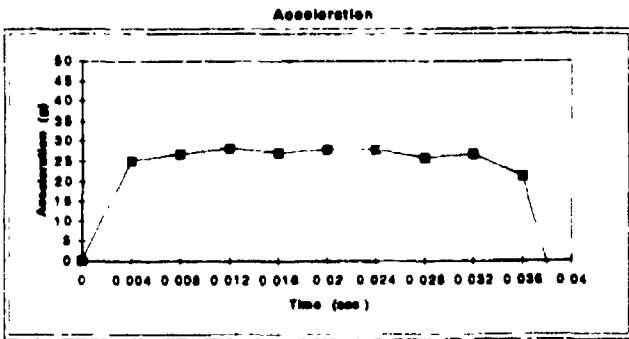
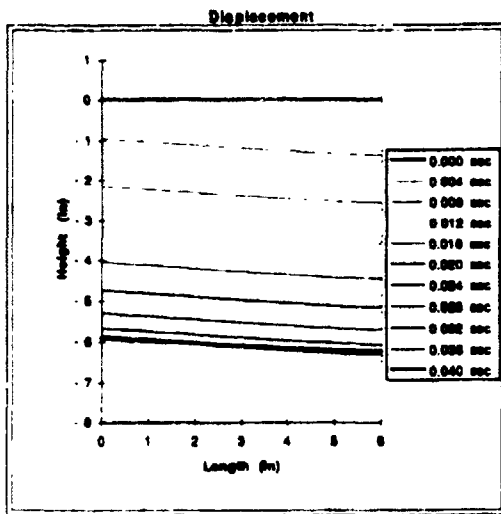


Figure 11: DYCAST Analysis of Seat Rail under Vertical Dynamic Loading
Length = 12 in Load = 104 lbm at 30 fps Ends restrained

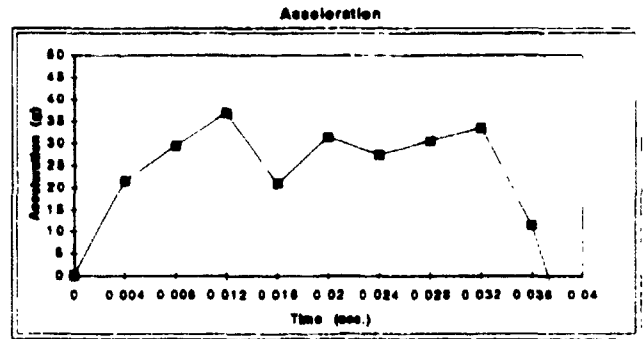
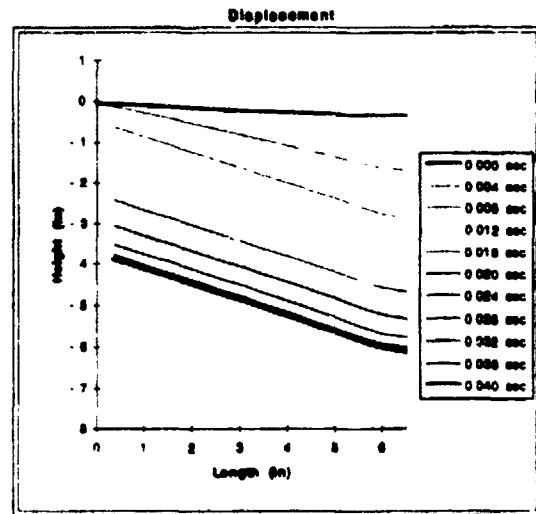


Figure 12: DYCAST Analysis of Seat Rail under Vertical Dynamic Loading
Length = 13 in Load = 104 lbm at 30 fps Ends restrained

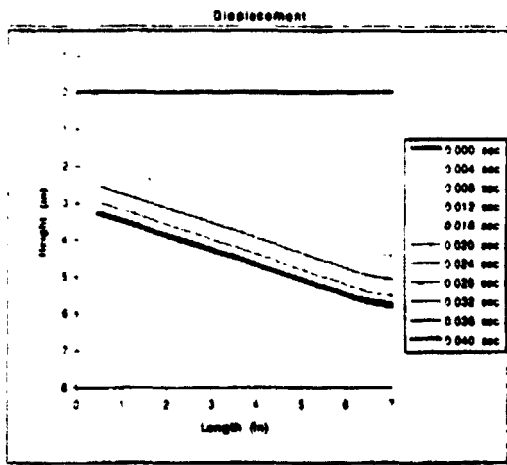


Figure 13. DYCAST Analysis of Seat Rail under Vertical Dynamic Loading
Length = 14 ft. Load = 104 lbm at 30 fps. Ends restrained

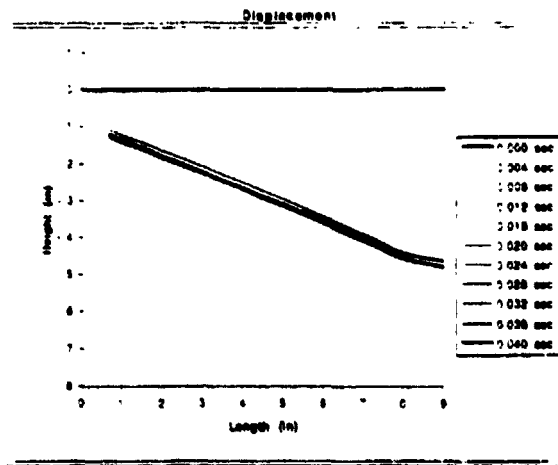


Figure 14. DYCAST Analysis of Seat Rail under Vertical Dynamic Loading
Length = 18 ft. Load = 104 lbm at 30 fps. Ends restrained

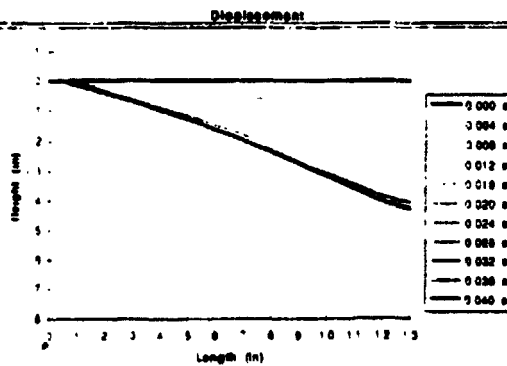
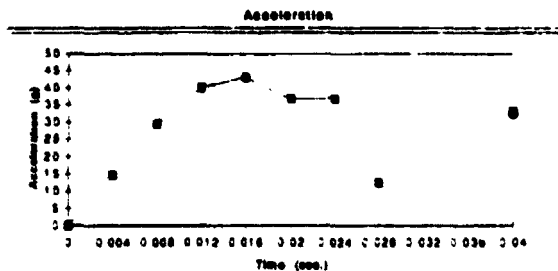
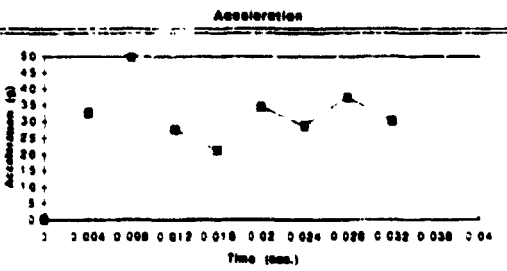


Figure 15. DYCAST Analysis of Seat Rail under Vertical Dynamic Loading
Length = 26 ft. Load = 104 lbm at 30 fps. Ends restrained

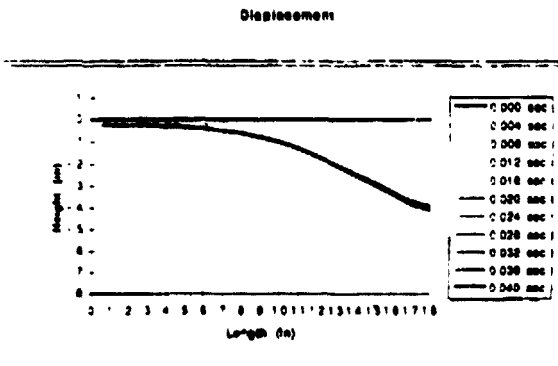
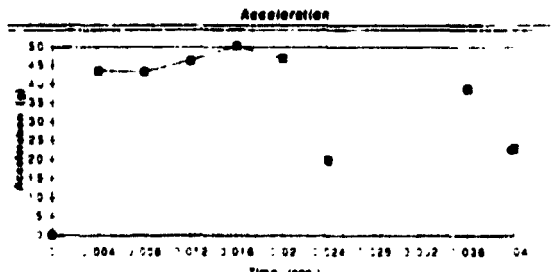
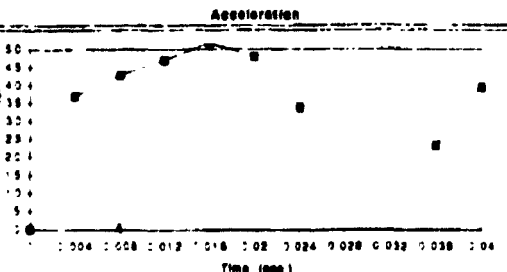


Figure 16. DYCAST Analysis of Seat Rail under Vertical Dynamic Loading
Length = 36 ft. Load = 104 lbm at 30 fps. Ends restrained



**NEXT
DOCUMENT**

Reusable Software Technology

**Timothy E. Morgan
Norfolk State University
1995 Langley Aerospace Research Summer Scholar Program**

**Under the direction of
Calvin Mackey**

**Space and Atmospheric Sciences Program Group
Atmospheric Science Division
Data Management Branch**

Table of Contents

Abstract	4
Introduction	4
Quality Action Team and Reusable Software System	4-5
World Wide Web	5
HyperText Markup Language	5-6
Netscape	6
CERES Software Bulletin's Home Page	6-7
Reusable Software System Home Page	7-8
Informix Tutorial	9
Conclusion	9
Acknowledgments	9
References	10

Abstract

The objective of the Reusable Software System (RSS) is to provide NASA Langley Research Center and its contractor personnel with a reusable software technology through the Internet. The RSS is easily accessible, provides information that is extractable, and the capability to submit information or data for the purpose of scientific research at NASA Langley Research Center within the Atmospheric Science Division.

Introduction

The Reusable Software System provides a repository for reusable software developed by NASA and contractor personnel engaged in atmospheric science research and support activities at the Langley Research Center. This system also provides links to a number of other established software repositories. The RSS was undertaken as a Quality Action Team (QAT) project by Science Applications International Corporation (SAIC) and is presently a joint effort with the staff of the NASA Langley Research Center Atmospheric Science Division.

The World Wide Web (WWW) is the mechanism that allows access to the Reusable Software System. The system consists of a variety of HyperText Markup Language (HTML) documents, also known as home pages, that display text, graphics, as well as sounds. These HTML documents provide information for the entire Internet world. Each HTML document is an element of a growing reusable software technology allowing individuals to combine their efforts and resources to centralizing important and useful software.

Quality Action Team and the Reusable Software System

The objective of the Quality Action Team is to promote the exchange and efficient use of computer software among various groups within the division. The widespread use of workstations, PCs and Macintoshes has generated a growing need for a variety of software and methods for allowing these different platforms to work together. New versions of software packages are being purchased or developed in-house, but not everyone in the division has access to these tools. While proprietary rights may limit the sharing of some of the commercial packages, no such restrictions exist for software developed within the government. Therefore the creation of a system based reusable software technology would provide a company with accessible information that can be extracted and submitted easily. The Quality Action Team addresses the following key issues:

- 1) Reuse/sharing of software developed by Division employees.
- 2) Transfer of unused hardware components among different groups.
- 3) Software quality assurance and virus protection.
- 4) Legality of sharing commercial software packages.

Chuck McKinley serves as Chairman for the Quality Action Team. The members of this team consist of Vince Brackett, Bill Chandler, Patrick Purcell, Chuck Turnitsa, David Ayers, and my mentor

Calvin Mackey. Calvin Mackey and the Data Management Office (DMO) were approached by Chuck McKinley to become a member of the Quality Action Team due to DMO's desire to create their own reusable software technology.

Chuck McKinley and Calvin Mackey with the assistance of DMO and the QAT established the NASA Langley Research Center Atmospheric Science Reusable Software System (RSS). The Reusable Software System is accessible through the World Wide Web on the Internet. The system is accessed through a home page which allows individuals to extract information from the RSS that will be useful in atmospheric research and projects. The RSS Home Page consists of information regarding applications, computer graphics, CASE tools, programming code, site-licensed software, compendium of universal constants, freeware, commercial databases, atmospheric data collections, other repositories, and other resources.

World Wide Web

The Web is an access mechanism layered atop existing network services that provides a consistent view of many different services. The World Wide Web is comprised of three systems: hypertext, the Internet, and multimedia. Hypertext is text within a document which provides a direct link to another document. The Internet is a global system of computer networks. Multimedia is the combination of different presentational technologies to appeal to multiple senses. The WWW is a unique tool which allows you to access not only text but also graphics, sound, or video information from all over the Internet world.

Hypertext MarkUp Language

HyperText Markup Language is a simple markup system used to create hypertext documents that are portable from one platform to another. HTML markup can represent hypertext news, mail, documentation, and hypermedia; menus of options; database query results; simple structured documents with in-lined graphics; and hypertext views of existing bodies of information. HTML is how a WWW browser displays its multimedia documents. The documents themselves are plain text files, also known as ASCII, with special "tags" or codes that the WWW program knows how to interpret and display on your screen. These HTML special "tags" define the structural elements in a document such as headers, citations, addresses, etc.; layout information such as bold and italics; the use of in-line graphics together with the ability to provide hypertext links. HTML, along with the World Wide Web, were invented by Tim Berners-Lee of the CERN High Energy Particle Physics Laboratory in Geneva, Switzerland. HTML allows you to:

- 1) Publish documents to the Internet in a platform independent format
- 2) Create links to related works from your document
- 3) Include graphics and multimedia data within your document
- 4) Link to non-World Wide Web information resources on the Internet

HTML is written in a text editor and by using special HTML commands the user is able to manip-

ulate the text to whatever style or form the individual requires. The HTML commands are simple and easily understandable:

- <H1>, <H2>, . . . , <H6> - Change the size of the font
- <P> - Marks the end of a paragraph
-
 - Starts a new line
- - bold
- <I> - italics
- <U> - underline
- <A HREF> - hyperlink

These commands are just a few of many which allow the user to do numerous things with the document.

The command, <A HREF>, is an extremely important part of HTML. <A HREF> is the hyperlink function that allows quick movement through documents while browsing the Internet. The <A HREF> provides a link to the direct path of a document without the bother of opening command windows and searching for the pathway. The pathway to the HTML document is called the Uniform Resource Locator (URL).

Netscape

A Mountain View, CA - based corporation originally known as Mosaic Communications Corp., Netscape was founded in April 1994 by James H. Clark, founder of Silicon Graphics Inc., and Marc Andreessen, creator of the original NCSA Mosaic prototype. Led by Andreessen and a team of software developers, Netscape launched its beta version in October 1994 and quickly took the world by storm. Netscape's browsers come in three flavors: UNIX, Windows, and Macintosh, all of them virtually identical from the user's perspective.

Netscape sought to stand apart from the masses by supporting features not included in the HTML specifications. Netscape established the inclusion of special extensions, non-standard HTML, that allowed users to format data on pages in a more elegant fashion than had previously been available, such as wrapping text around a graphics image. Other extensions for special features included blinking, scaling the size of the fonts used, and centering were also added.

CERES Software Bulletin's Home Page

The Cloud and Earth's Radiant Energy System (CERES) Software Bulletin's Home Page was the first HTML document. Maria Mitchum, member of the Data Management Office, supplied the bulletins and requested that they be posted on the Internet for easy readable access. The bulletins were sent through email in a file and had to be converted into postscript form. The application Ghostview was needed to display the bulletins on the screen. Ghostview allows the bulletin to be displayed on the screen while the Netscape window remains free. The CERES Software Bulletin's HTML document read the following code:

```

<title>CERES DMS Software Bulletins </title>
<hr>
<h1>Clouds and Earth's Radiant Energy System (CERES)</h1>
<IMG SRC="http://asd-www/tmorgan/news.gif">
<hr>

<h2>CERES DMS Software Bulletins</h2>
<h3>
<ul>
<li><a href="http://asd-www/ceres/CERES_SB_95-01.ps">CERES Bulletins Purpose & Mailing
List</a>
<li><a href="http://asd-www/ceres/CERES_SB_95-02.ps">CERES Standard Routine Prologue</a>
<li><a href="http://asd-www/ceres/CERES_SB_95-03.ps">CERES Release 1 Grid Bulletin</a>
<li><a href="http://asd-www/ceres/CERES_SB_95-04.ps">Revised CERES Standard Routine Pro-
logue</a>
<li><a href="http://asd-www/ceres/CERES_SB_95-05.ps">Release 1 Data Product Module Guide-
lines</a>
<li><a href="http://asd-www/ceres/CERES_SB_95-06.ps">F90 Debugger General Information</A>
<ul>
<li><A href="http://asd-www/ceres/F90-Users-Notes">F90 Users Notes </a>
</ul>
<li><a href="http://asd-www/ceres/CERES_SB_95-07.ps">CERESlib README Guidelines</a>
</ul>
</h3>

<p>
<address>Last Updated Thursday, July 26, 1995 15:15 EST<address>
<a href="http://asd-www/cgi-bin/tem_home.cgi"> <i>Timothy Morgan</i></a>

<hr>
<i><a href="http://asd-www/ceres/docs.html">
Back to On-line Documentation</a></i></ul>

```

This HTML document is located at this URL., <http://asd-www/ceres/bulletins.html>.

Reusable Software System Home Page

Calvin Mackey expressed a need for more HTML features to be incorporate into the Reusable Software System (RSS) Home Page. Calvin Mackey wanted to display the time, date, and the number of times the page had been accessed at the top of the page. To do this two programming languages, awk and perl, had to be used. Awk was used to keep an accurate count of the number of times

the page had been accessed. Perl was used to display the current time and date.

Mark Shipham, member of DMO, provided technical support in the creation of the awk program. The program read the following code:

```
#!/bin/sh
awk '{print (int($1)+1)}' /home/docs/ceres/RSSHOW_MANY > /home/docs/ceres/temp
\mv /home/docs/ceres/temp /home/docs/ceres/RSSHOW_MANY
```

The program called for the creation of a file called how_many. How_many is the file that stores the number of times the page had been accessed. The program calls the file, how_many, adds one to whatever number is currently in the file, then displays that number on the home page.

Calvin Mackey provided technical support in the development of the perl program. The date program read the following code:

```
#!/bin/sh
DATE=/bin/date
echo Content-type: text/plain
echo if [ -x $DATE ]; then $DATE
else echo Cannot find date command on this system.
fi
```

The first line of code, #!/bin/sh, tells the computer this is a perl script file. Without that first line the computer would not recognize the commands that follow. The time is a standard part of every UNIX system and does not need a special perl program but time is still called by the perl program in the RSS HTML document.

When modifications were made to the RSS Home Page, the programs were implemented into the RSS HTML documents. For the programs to work the RSS HTML document had to be moved to a different directory, cgi-bin. This directory allows all executable programs to run therefore the RSS HTML document had to be converted into a perl script file, RSS1.cgi. The code that was added to the document allowed the computer to read the text in the new directory. Key commands such as echo, #!/bin/sh, and #!/bin/csh were recognized by the computer as perl commands. These lines were recognized as awk and perl programming code:

Date and Time (Perl Program)

```
echo ""date -u '+It is %h %d, 19%y and the current time is %H:%M Z (GMT).'"
```

Access Number (Awk Program)

```
echo ""/home/docs/htbin/RSSCOUNT""
echo "<B> cat /home/docs/ceres/RSSHOW_MANY`</B>"
```

Since the RSS HTML document had been converted to a perl script file, a new file had to be created to call the document to the screen. The new file, named RSS, calls the document to be executed through the cgi-bin directory. The RSS file also resides in the cgi-bin directory. The RSS Home Page

is founded at this URL, <http://asd-www/cgi-bin/RSS>.

Informix Tutorial

Calvin Mackey also requested the Informix Tutorial be transferred into a HTML document. Informix is a relational database management system (DBMS) that allows the user to create tables of data and to relate them to each other based upon common fields. Informix is needed by the ERBE/CERES project for tracking purposes.

The Informix tutorial was installed on WWW to provide easy access and increase the learning-curve efforts of new members of the ERBE/CERES project. The Informix tutorial is informative and descriptive allowing the viewer full comprehension of the material. When all revisions are completed, the tutorial will be placed in on the RSS Home Page.

Conclusion

The CERES Software Bulletin Home Page, the Reusable Software System Home Page, and the Informix Tutorial are a part of the reusable software technology that is a vital part of Langley Research Center. Each HTML document offers employees of NASA, contractor personnel, as well as Internet users the opportunity to be informed and educated on the many research projects at NASA. Placing this wealth of knowledge on the Internet provides easy access, extractable information, and submitable information to increase the communication and broaden the research tools at Langley Research Center.

With the motto "better, faster, cheaper" at the front of a new era, a reusable software technology, like the Reusable Software System at Langley Research Center, will become increasingly more important as projects and research require software that has already been created. The Reusable Software System will provide NASA Langley Research Center with the technology to incorporate the many technical research projects in a central location. The Atmospheric Science Division of NASA Langley Research Center has realized the importance of reusable software technology therefore the Reusable Software System is a step in a positive direction.

Acknowledgments

I would like to thank my mentor Calvin Mackey for the time and patience he has shown me during my internship at NASA. I would also like to thank the members of Data Management Branch for the warm and caring attitude they showed to the LARSS students that were employed here over the summer.

References

- Berners-Lee, T. & Connolly, D. Hypertext Markup Language - 2.0. August 4, 1995.
World Wide Web Document (URL) <http://www.w3.org/hypertext/WWW/MarkUp/html-spec/html-spec.txt>
- Schlenoff, C. The World Wide Web. June 29, 1994.
World Wide Web Document (URL) <http://elib.cme.nist.gov/fasd/pubs/schlenoff94/www2.html>
- Seidman R. "Netscape Vs. The World." WebWeek. Meckler Corp. Vol 1, Issue 1.
May 1995.
- TQM Steering Committee. Quality Action Team to address technology transfer.
November 4, 1995. (SAIC Memo)

**NEXT
DOCUMENT**

13-34

**ELIMINATING FLOW SEPARATION AND REDUCING VISCOUS DRAG
THROUGH BOUNDARY LAYER ANALYSIS AND MANIPULATION**

Matthew D. Oser (LARSS Student)

Richard L. Campbell (Mentor)

Research and Technology Group

Aerodynamics Division

Transonic/Supersonic Aerodynamics Branch

ABSTRACT

As both computers and flow-analyzing equations have increased in sophistication, computational fluid dynamics (CFD) has evolved into a fixture for advanced aircraft design. While CFD codes have improved in accuracy and efficiency, their ability to encompass viscous effects is lacking in certain areas. For example, current CFD codes cannot accurately predict or correct for the increased drag due to these viscous effects at some flow conditions. However, by analyzing an airfoil's turbulent boundary layer, one can predict not only flow separation via the shape factor parameter, but also viscous drag via the momentum thickness. Various codes have been written which can calculate turbulent boundary layer parameters. The goal of my research is to develop procedures for modifying an airfoil (via its local pressure distribution) to eliminate boundary layer separation and/or to reduce viscous drag. The modifications to the local pressure distribution necessary to achieve these objectives will be determined using a direct-iterative method installed into a turbulent boundary layer analyzer. Furthermore, the modifications should preserve the basic characteristics of the original airfoil.

ELIMINATING FLOW SEPARATION AND REDUCING VISCOUS DRAG THROUGH BOUNDARY LAYER ANALYSIS AND MANIPULATION

As both computers and flow-analyzing equations have increased in sophistication, computational fluid dynamics (CFD) has evolved into a fixture for advanced aircraft design. While CFD codes have improved in accuracy and efficiency, their ability to encompass viscous effects are lacking in certain areas. For example, current CFD codes cannot accurately predict or correct for the increased drag due to these viscous effects at some flow conditions. However, by analyzing an airfoil's turbulent boundary layer, one can predict not only flow separation via the shape factor parameter, but also viscous drag via the momentum thickness. Various codes have been written which can calculate turbulent boundary layer parameters. My research project involved developing a procedure for modifying an airfoil (via its local pressure distribution) to eliminate boundary layer separation and/or to reduce viscous drag. The modification to the local pressure distribution necessary to achieve these goals would be determined using a direct-iterative method.

My research project required a turbulent boundary layer analyzer. I selected a code, written by Gary Warren, which utilizes Green's direct lag-entrainment method. This code solves for boundary layer parameters, such as displacement thickness, momentum thickness (Θ), and shape factor (H), based on inputted free stream conditions, local pressure (C_p) distribution, and an initial value of Θ . Unfortunately this code was written in FORTRAN, while I had learned C. I therefore borrowed a FORTRAN manual and spent my first few nights learning FORTRAN.

My first task was to edit the code to input data from a more convenient data file. The code originally input data from an archaic namelist that was time-consuming to modify. With this task accomplished, I needed to run some test cases in order to verify the code's accuracy. I found an AGARD report that contained experimental boundary layer data for various airfoil configurations. I selected three test cases: The first case exhibited completely attached flow, the second case exhibited flow that neared separation, and the third case produced separated flow. The code yielded very accurate theoretical data for the first two cases. One drawback of the direct lag-entrainment method is its inability to produce accurate boundary layer data for separated flow cases. However, my code remained fairly accurate for even the third test case. Confident in the boundary layer analyzer, I was ready to proceed with my research.

In order to examine the effects alterations to the C_p distribution would have on the H distribution, I needed an easy way to qualitatively compare my calculated data. The original code output data into a large table. It was difficult, and very time-consuming, to compare various tables from different test cases. I therefore modified my code to graph both C_p and a user specified boundary layer parameter versus x/c location. As a result, I could quickly compare multiple sets of data. I also required a convenient method for modifying the inputted C_p distributions. I chose to approximate each C_p distribution with a system of linear segments joined together at "control points." (Figure 1) I altered the code to present the user the option of inputting a C_p distribution via these control point coordinates. I also created an option which allows the user to interactively move one of the control points using a mouse.

After these modifications, I was ready to contrast H distributions produced by various C_p distributions. I chose a base-line C_p distribution composed of five linear segments as defined by six control points (Figure 1). I created dozens of test cases by varying the height and/or slope of these segments. After observing the resulting changes in the H distributions, I developed some fundamental conclusions. I observed that a change in the C_p distribution has no effect on the H distribution (or any other boundary layer parameters' distributions) upstream of the change. I also concluded that the sharp increase in H near the shock is determined by the pressure gradient across the shock. Furthermore, I observed that in front of the shock, a decrease in C_p causes an increase in H. Behind the shock, however, a decrease in C_p typically results in a decrease in H.

Armed with a qualitative understanding of the relationships between C_p and H, I sought to develop a procedure for modifying an existing C_p distribution to return a desired H distribution. Since H is often used as a separation criterion, I would then be able to construct a C_p distribution with fully attached flow. I first looked to develop a routine for reducing the rise in H due to the shock. By raising the C_p value of control point three ($C_p(3)$), I could decrease the strength of the shock, and thus diminish the rise in H due to shock. Unfortunately, adjusting only control point three would change the area under the C_p distribution, and thus alter the lift coefficient. However, by simultaneously lowering the C_p value of control point two as I raised the C_p value of control point three, I would decrease the shock strength while conserving the area under the C_p curve. Thus the rise in H due to the shock would be lowered without upsetting the lift coefficient. In order to install this procedure into my computer code, I needed an expression to quantitatively predict this increase in $C_p(3)$ requisite for a desired decrease in the maximum value of H within the shock region. After trial-and-error, I selected an expression of the form:

$$\Delta C_p(3) = A * H * \Delta H_{max} + B * H * (\Delta H_{max})^2$$

Since this expression is an approximation, I had to make the procedure iterative within the code. Despite being iterative, the procedure requires little CPU time to achieve a high degree of accuracy. (Figure 2.) It is also worthy to note that this shock-adjusting procedure can be used to increase a shock's strength if desired.

In order to remove any flow separation that occurred after the shock region, I planned to "locally" adjust the C_p value at each point where H exceeded some specified $H_{separate}$. This technique differs from the previous "shock-reducing" method where C_p values upstream of the separation point were modified. Early attempts to predict a local change in C_p that would yield a desired change in H were unsuccessful. Unfortunately, multiple C_p values exist which produce a single desired value of H. My code needed to predict a change in C_p that would not only produce a desired H value, but also preserve the characteristics of the Θ distribution. (While there are various C_p values that will produce a desired H, there exists a unique C_p value that will produce both the desired H and Θ values). With continued investigation and trial-and-error, I developed an expression of the form:

$$\Delta C_p = A * (\Delta H / H) + B * (\Delta H^2 / H)$$

which accomplished this with reasonable accuracy. (Figure 3.) With procedures for both reducing H within and after the shock region, my code could now redesign an airfoil to avoid separation at

specific free stream conditions. I now aspired to devise a process for reducing an airfoil's viscous drag.

While H predicts flow separation, the value of Θ at the trailing edge ($\Theta_{t.e.}$) of the airfoil predicts viscous drag. In order to minimize viscous drag, one must minimize $\Theta_{t.e.}$ (viscous drag also depends on $H_{t.e.}$, but lowering $\Theta_{t.e.}$ has the greatest influence on the reduction of viscous drag). Thus, I required a procedure for redesigning a C_p distribution around a desired value of $\Theta_{t.e.}$. At the same time, I wanted the basic characteristics of my C_p distributions to remain fixed. In order to accomplish this, I first scaled the existing Θ distribution so that Θ at the trailing edge of the airfoil would equal a user specified target value. Thus, the new target Θ distribution would maintain the same characteristics of the original Θ distribution. I now only needed a procedure for modifying an existing C_p distribution to produce this desired target Θ distribution. I once again chose to use a direct iterative method. After much experimentation, I developed an expression of the form:

$$\Delta C_p = A*(\Delta\Theta/\Theta) + B*(\Delta\Theta^2/\Theta)$$

This expression produced an accurate estimation of the required change in C_p needed to produce a desired change in Θ . After installing this iterative procedure into my code and running some test cases, I was pleased with the results. Designing to a target Θ distribution is much more efficient than designing to a target H distribution: it requires fewer iterations (and therefore less CPU time) to achieve a desired tolerance. Figure 4 shows an example where I have used this new procedure to reduce the drag of an airfoil by nearly five counts.

With separate methods for redesigning a C_p distribution to produce both desired H and Θ distributions, I now sought to create a procedure for redesigning an airfoil to simultaneously produce both target boundary layer distributions. Unfortunately, it is sometimes impossible to design an airfoil to meet two stringent criteria. Therefore, one of the criteria must take precedence over the other. Then, if a C_p cannot be modified to produce both boundary layer design criteria at a given x/c location, the code will insure that at least the primary design constraint is met. With few alterations to my existing code, I installed this procedure. Basically, the code modifies the existing C_p distribution to remove any secondary criterion violations. Once this has been accomplished, the code checks for primary criterion violations. If the code encounters any such violations, it readjusts the C_p distribution accordingly.

One drawback of these various methods for reducing separation and viscous drag is the tendency for the value of C_p at the trailing edge ($C_{p,t.e.}$) to become increasingly smaller. Typically, $C_{p,t.e.}$ for a given airfoil is fixed around a value of 0.1. I needed a procedure for redesigning an airfoil, with the added constraint of keeping $C_{p,t.e.}$ constant. Unfortunately, this added constraint created the possibility for even more cases with "no solutions." However, I felt this constraint was too important to over-look. Therefore, I devised a fairly simple subroutine that uses triangulation to adjust the C_p distribution after the shock until this trailing edge constraint is met. (During this stage of my research, I determined that a linear C_p distribution after the shock results in the lowest value of $\Theta_{t.e.}$) I even included the option of maintaining constant lift and moment coefficient by adding or subtracting a parabolic increment to the C_p distribution as needed. Figure 5 illustrates an example of this lift coefficient conserving technique. Readjusting the C_p

distribution to constrain C_p *t.e.* unfortunately can create more boundary layer parameter violations (H and/or Θ may once again exceed their specified limits). One would then have to redesign the C_p distribution to eliminate the new violation, which in turn could cause another C_p *t.e.* violation. Continuing this iterative procedure will cause eventual convergence on the solution, assuming one exists.

My completed code meets all of the original project goals. It can eliminate flow separation about an airfoil, as well as reduce an airfoil's viscous drag. Despite utilizing direct-iterative procedures, the code remains efficient. However, installation of a proven boundary layer analyzer that uses the *indirect* lag-entrainment method would eliminate the need for most of the iterations. Unfortunately, no such analyzer was available during the course of my research. Regardless, the UNIX based workstations I used for my research provided more than enough processor speed to run my program swiftly.

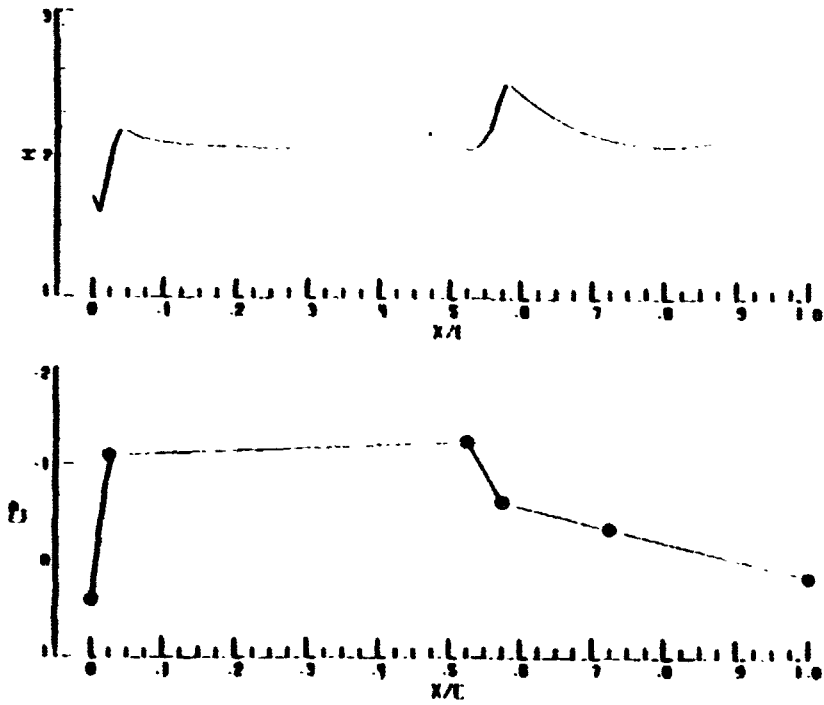
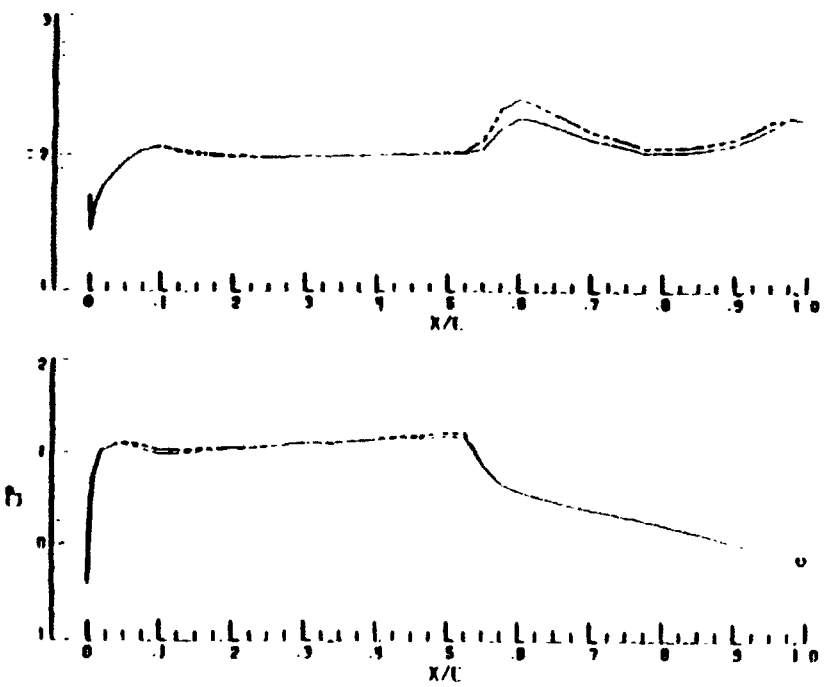


Figure 1.



(In the remaining figures, the dashed-lines represent the original distributions, while the solid-lines represent the adjusted distributions.)

Figure 2.

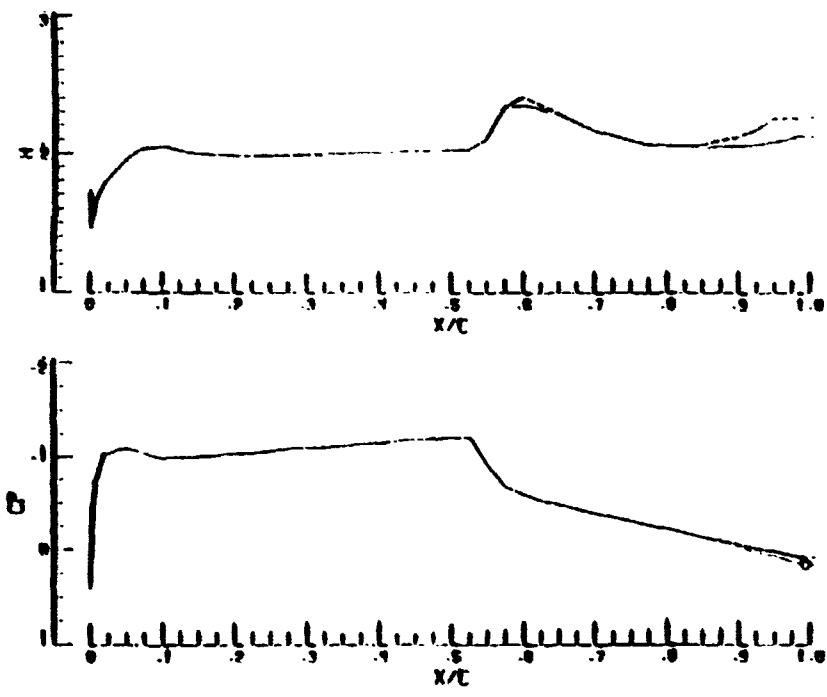


Figure 3.

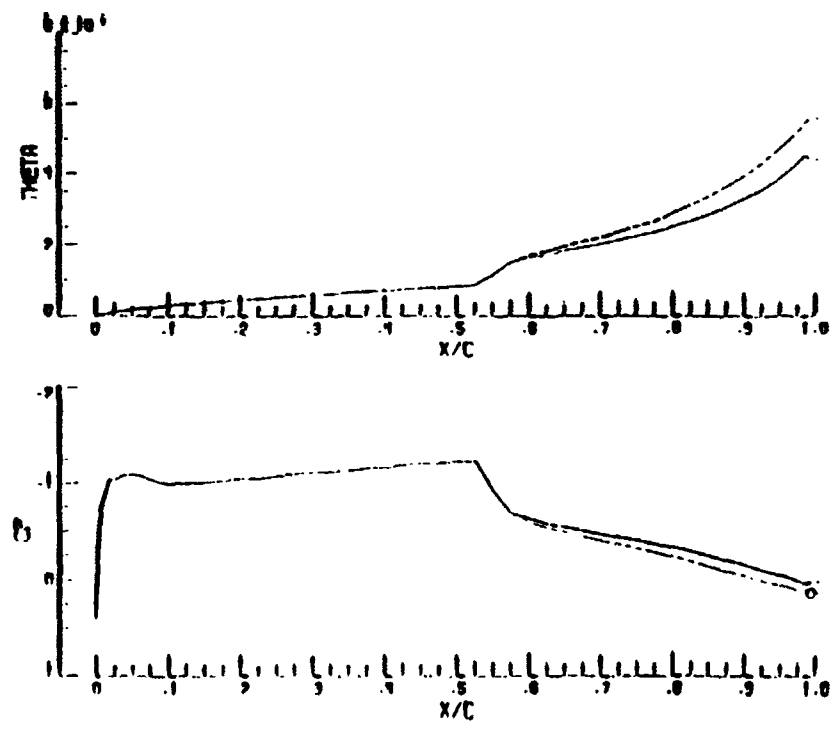


Figure 4.

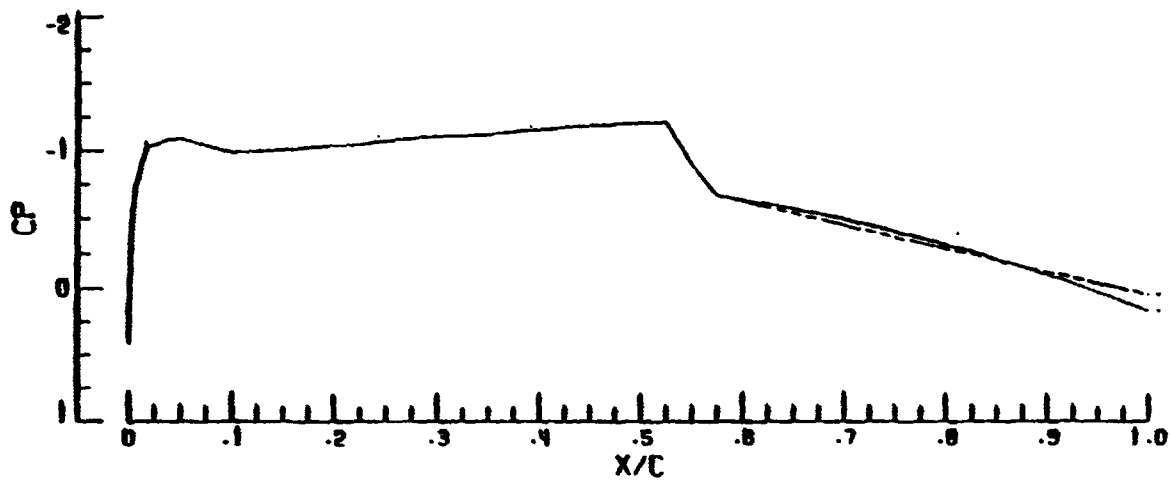


Figure 5.

**NEXT
DOCUMENT**

174-55

ELECTRONIC PHOTOGRAPHY

Meredith Lyndsay Payne
Mentor: Dr. Thomas E. Pinelli

Internal Operations Group
Scientific and Technical Information Division
Visual Imaging Branch

Abstract

The main objective of my time spent at the NASA Langley Research Center was to assist in the production of electronic images in the Electronic Photography Lab (EPL). The EPL is a new facility serving the electronic photographic needs of the Langley community.

Introduction

The purpose of the Electronic Photography lab is to provide Langley with access to digital imaging technology. Although the EPL has been in operation for less than one year, almost 1,000 images have been produced. The decision to establish the lab was made after careful determination of the centers needs for electronic photography. The LaRC community requires electronic photography for the production of electronic printing, Web sites, desktop publications, and its increased enhancement capabilities. In addition to general use, other considerations went into the planning of the EPL. For example, electronic photography is much less of a burden on the environment compared to conventional photography. Also, the possibilities of an on-line database and retrieval system could make locating past work more efficient. Finally, information in an electronic image is quantified, making measurements and calculations easier for the researcher.

Approach

One of the main goals of the lab is quality consistency through standardization. Although many steps in producing the master image file require subjectivity, there are rigid protocols throughout. There are three very basic steps in the production of an electronic image; capture, processing, and output.

Capture

An image can be captured by one of three methods. The first, and most common, is film capture. Photographic film, negatives or transparencies, are captured using a high resolution (5000 pixel linear CCD array) film scanner. The Leafscan 45 is capable of scanning film sizes from 35mm to 4x5 inches. The approximate maximum sampling frequency of the scanner is 5000 pixels per inch (ppi) for 35mm, 2500 ppi for 70/120/220mm, and 1200 ppi for 4x5 inch films. The resulting image files generally are between 60 and 105 MB.

The second, and least common, method of image capture in the EPL is reflective material scans. The Epson ES 800C flatbed scanner is used for photographic prints, it has a 400 pixel linear CCD array. Because of the lower resolution, the flatbed is used only when other options have been exhausted.

Scanning films and prints can be very time consuming. The average 6x7 cm film scan takes approximately 30 minutes. Fortunately, electronic capture is also an option. The Kodak DCS460 electronic camera has a 2000 x 3000 pixel CCD area array and the images download easily onto the EPL computers. The camera has successfully been used by the lab to capture images for publications and Langley Web sites. Other advantages of electronic capture are: the complete bypass of chemical processing, instantaneous results, and the economical advantage of lower, long-range material costs. The specific DCS camera used for the above mentioned projects was on loan to the lab while waiting for one on back order. However, when the camera arrived it was found during testing, the CCD array had defective pixels and has since been sent back to the manufacturer. A replacement is expected soon.

Processing

Once the image is in electronic form, the processing stage begins. The final file produced in this phase will be called the "Master Image File" (MF). From this file, any type of desired output is created and the file itself will be of the highest possible quality and image integrity. The

purpose of processing the image is to optimize detail and maintain best possible color and tonal quality.

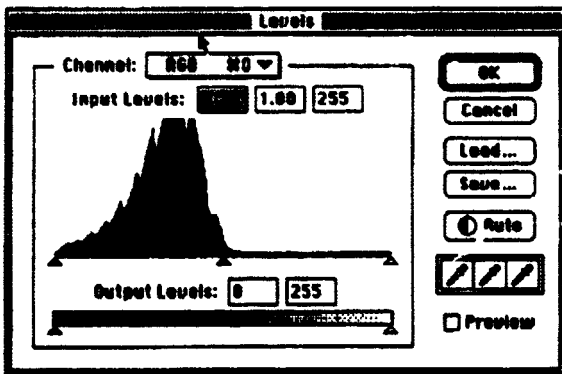


Figure 1 Uncorrected levels.

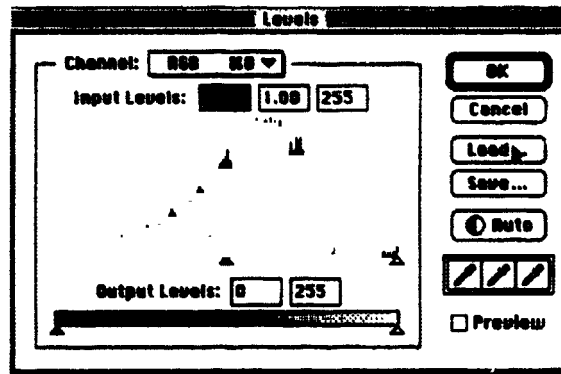


Figure 2 Corrected levels.

The electronic file is brought into the Photoshop 3.0 image processing program, named by its "L number," and the designation that it is a "raw file." The image has 256 levels of grey including pure white and black. These levels, if not already well distributed, are adjusted to maximize tonal range (see Figures 1 and 2). Tonal corrections are always made first because poor tonal distribution can also affect color shifts. The changes in the levels are saved in a separate file and applied to the image. If the image needs further modification in either color or tone, the corrections are made by adjusting the curves.

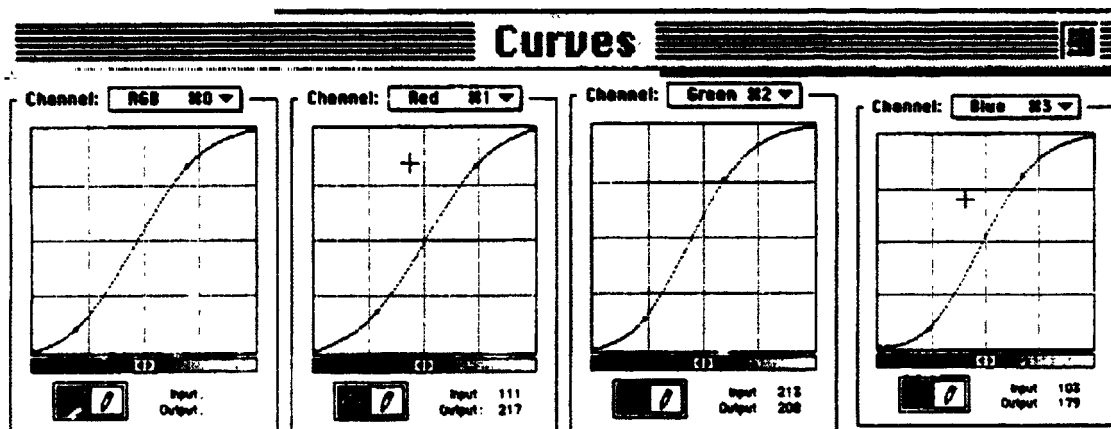


Figure 3 Examples of image curves.

There are four curves for the image, one for each red, green, and blue channel as well as one for the combination of the three (see Figure 3). The combined RGB curve is used to alter contrast, while the individual channel curves are used to compensate for color shifts. Just like in conventional color printing, each channel affects two colors - the color of the channel and its opposite (red/cyan - green/magenta - blue/yellow).

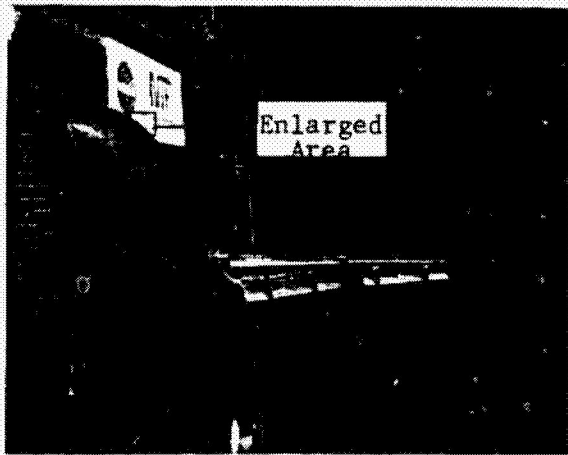


Figure 4 Example image.

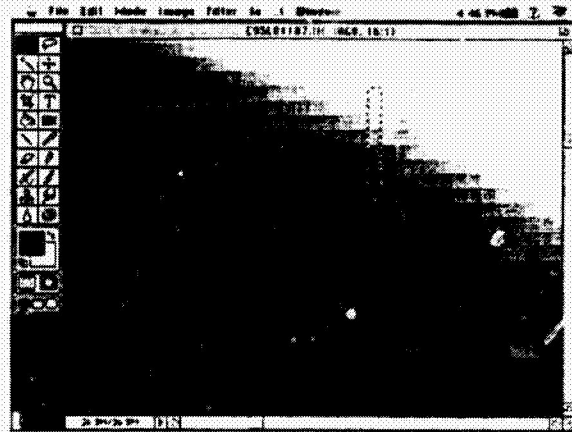


Figure 5 Enlarged area.

Once the image density and color are corrected the MF size is determined. The image file is examined under high magnification of approximately 16:1. An image file will be reduced if an edge transition (from an area of critical focus) spans over five pixels and single grains span over 3 pixels (see Figure 5). Reducing such an image by spatially resampling will not result in significant information loss. Should an image to be reduced be determined as excessively grainy, a median filter is applied before file size reduction. After the file is tone/color corrected and the final file size is applied to the image, a second file is created with the "In Process" designation.

The next step in image processing is to print the electronic file and make final decisions on the tone and color quality. Although the monitors are carefully calibrated, the characteristics of the phosphors change throughout the course of a day. It is also suggested that the human eye is more critical with printed material than with CRT screens. The file is printed on the Fujix Pictography 3000, photographic quality color printer. Currently the Fujix cannot print files larger than 30 MB, so the "in progress" file is reduced to 320 ppi with a width of 4.5 inches. Before the file is sent to the printer, a curve Look-up Table (LUT) is applied to compensate for the density differences between the CRT screens and the Fujix prints. The print is viewed under the MacBeth SpectraLiteII using the three main light sources - incandescent, daylight, and fluorescent. If the image needs further correcting the levels and curves are adjusted and applied to the original raw file and a new "in progress" file is created.

The final, and sometimes most time consuming, step in image processing is the removal of dust and scratches. Spotting is performed on the "in progress" file that has been determined to be of good image quality. Unintended marks are most problematic in film scanned images. In addition to dust and scratches, some of the older negatives have damage to the emulsion such as cracking and mold. The spots are removed by copying a similar part of the image over the blemish. At this point the file is saved as a master image file and permanently stored on CD. From this master file the original requesters output, and any other future output, is made.

Output

The most common uses for electronic files have been halftone images, Fujix prints & transparencies, TIFF files for documents, and monitor files for Web pages. Another option in the EPL includes film negatives and transparencies from the Solitaire Image Recorder. The Solitaire writes the image to film, either negatives or transparencies, and will accept film sizes of 35mm and 4x5 inches. All these different outputs can be created from the same master image file by simply applying a curve to compensate for the output device. A curve can also be applied to the master image file for quality output on almost any device that can be calibrated.

Equipment

The Electronic Photography Lab has five workstations. Three stations are designed for image processing, one is designated for printing, and the last is used to write electronic images to photographic film. The stations are labeled by names of colors for ease of identification.

"Magenta" - Scanning/Image Processing

- Power Macintosh 8100/80 (264 MB RAM/ 250MB Hard Drive)
- Apple 19" multi-scan color monitor
- Andataco 2.3 GB external hard drive
- PLI 1.3 GB 5.25" Magneto Optical drive
- Tahoe 128 MB 3.5" Magneto Optical drive
- Leafscan 45 film scanner (35mm -> 4x5 inch formats)
- APC Smart UPS 1250 battery back-up/surge protector

"Cyan" - Image Processing/CD Writer Output

- Power Macintosh 8100/80 (264 MB RAM/ 250MB Hard Drive)
- Apple 19" multi-scan color monitor
- Andataco 2.3 GB external hard drive
- Tahoe 128 MB 3.5" Magneto Optical drive
- PLI 1.3 GB 5.25" Magneto Optical drive
- Pinnacle Micro CD writer
- APC Smart UPS 1250 battery back-up/surge protector

"Yellow" - Image Processing/Print Scanning

- Power Macintosh 8100/80 (264 MB RAM/ 250MB Hard Drive)
- Apple 19" multi-scan color monitor
- Andataco 2.3 GB external hard drive
- Tahoe 128 MB 3.5" Magneto Optical drive
- PLI 1.3 GB 5.25" Magneto Optical drive
- Epson ES 800C flatbed color scanner
- APC Smart UPS 1250 battery back-up/surge protector

"Blue" - Image Output

- Macintosh Centris 650 (136 MB RAM 80MB hard drive)
- Apple 13" multi-scan color monitor
- APS 730 MB external hard drive
- Tahoe 230 MB 3.5" Magneto Optical drive
- PLI 1.3 GB 5.25" Magneto Optical drive
- APC Smart UPS 1250 battery back-up/surge protector
- Fujix Pictography 3000 printer

"Red" - Image Output

- Macintosh Centris 650 (136 MB RAM 80MB hard drive)
- Apple 13" multi-scan color monitor
- Andataco 2.3 GB external hard drive
- Tahoe 230 MB 3.5" Magneto Optical drive
- APC Smart UPS 1250 battery back-up/surge protector
- Solitaire Image Recorder film writer

Server

- Macintosh IIx
- 2.3 GB external hard drive

"Grey" - Electronic Photography Support/Word Processing

- Macintosh PowerBook 540c (36 MB RAM 500 MB hard drive)
- MicroSystems PCMCIA drive

With the exception of the server, all the computers are equipped with Adobe Photoshop version 3.0 for image retrieval, processing, and output. AppleShare is used to connect the EPL computers to the server and the Langley community. Mathematica was used to create the curves applied to files for output, it is not used on a daily basis.

Conclusion

The EPL meets its goal of "supporting the acquisition, analysis, documentation, and communication of research by providing direct digital image capture; image scanning, processing, and enhancement; and optimized device dependent imaging protocols for output." The personnel and equipment in the lab will be forever-changing with technology in order to fulfill this mission.

**NEXT
DOCUMENT**

Technology Transfer: A Contact Sport

Written by **Nina Paynter**

Mentored by **Marisol Romero**

Technology Applications Group

"Put on your tennis shoes, get out there, and meet people!"

-loosely paraphrased from Dr. Joseph S. Heyman

Technology transfer is a dynamic process, involving dynamic people as the bridge between NASA Langley Research Center and the outside world. This bridge, for non-aerospace applications, is known as the Technology Applications Group. The introduction of new innovations and expertise where they are needed occurs through a "push" and "pull" process. A "push" occurs when a new technology is first developed with high commercial potential and then a company is found to license or further develop the technology. The "pull" process occurs through problem statements. A company or group will submit a written statement of what they need and the shortcomings of commercially available technology. The Technology Transfer Team (T3) reviews these problem statements and decides where NASA Langley can offer assistance. A researcher or group of researchers are then identified who can help solve the problem and they are put in contact with the company. Depending upon the situation in either method, a Space Act Agreement (SAA), or outline of the responsibilities for each party, is developed.

My mentor, Marisol Romero, developed a two-part project for me, centered around the process of handling problem statements. The first part was to follow through the answering of a problem statement, to develop a technology for someone and deliver it. The second part was to create a database of the expertise at Langley so that the T3s would know whether the Center could handle incoming problems and, if so, find a researcher whose expertise matched the need. In the creation of this database, I would have the opportunity to gain an overview of the center, as well be exposed to a number of engineering disciplines.

As the first part of my project, I assisted in answering a problem statement from an Adult Day Care Center in Virginia Beach. One of the patients, a young woman with cerebral palsy, needed a better computer interface. Her only method of communication was to select a word from a list, vocalized and recorded by computer. The switch she had been using to select a word required an attendant, and was difficult to use when her head position varied. For this project, Marisol asked Bruce Little, from the Fabrication Division, to mentor me. After a site visit to better understand the specifications of the project, Bruce Little and I sat down to design a solution. This was my first time designing and building a device, and Bruce Little was exceptionally receptive to my ideas. He made me feel like a team member rather than a simple observer of his work. We asked advice from people in several different areas of the center, and brought together pieces and ideas from all of them to make a "Chin Mouse".

A "Chin Mouse" device is a helmet mount with an adjustable arm extending underneath the chin. At the end of the arm is the microswitch apparatus, which is activated by a depressible platform. The helmet is fully padded, and can be adjusted in height and width, while the arm can be attached to either side. This provides the flexibility needed, while allowing independent access to the computer. The "Chin Mouse" is also easily adaptable for others with similar handicaps.

After the fabrication, I encountered the next step in the technology dissemination process, the legalities of intellectual property. I wrote and submitted an Invention Disclosure, and have followed the beginnings of the patent process with vested interest. More important than a possible patent, however, is the fact that our invention helped this young woman. Marisol, Bruce and I went to present it to her, and she seemed pleased

with it. (see attached photo and letter) The story has also been picked up by Channel 3 news and local papers, which provides positive community publicity for Langley and the technology transfer process.

In this particular case Marisol drew upon her previous contacts to choose Bruce Little for this project. This is the way that most problem statements are matched with researchers, ensuring cooperation but not taking full advantage of the Center resources. In order to allow the T3s to explore resources beyond their personal contacts, Marisol saw the need for the second part of my project: to gather information about the expertise at Langley and organize it into a database which can be searched for keywords to match a problem statement with a person who can support it.

I approached this second portion of my project by first was to gathering the functional statements of each group, division, and branch. This provided a fairly specific view on the type of research each section of the center was performing. Along with this information, I also received a detailed breakdown of the resources of the Fabrication Division, cataloging the type of personnel as well as each machine. This particular document also included the Fabrication Divisions of Ames, Dryden and Lewis, allowing us to possibly redirect a problem statement to a more appropriate facility. From this more general information, I was then able to begin interviewing specific people. This is the intended level of the database, in order to pinpoint an actual person to contact. I met the people I interviewed in three ways: through personal introduction, through further exploration of technologies Marisol was working with, and through problem statements I was given to work on. The people of this center were wonderful in their willingness to take the time to explain their work to me, and in this way I expanded my knowledge of the possible fields of engineering.

Marisol first introduced me to Milfred Thomas, who runs the Optical Damage Testing Laboratory. He is a laser expert, and to illustrate his work he allowed me to assist in the construction of a laser head. I was also given the opportunity to help him in the design and fabrication of a flow-measurement mount and power supply. Through Bruce Little I met Lisa Jones, an aerodynamic engineer studying crashworthiness, who provided a literal overview of the center while she explained her job from the top of the Impact Dynamics and Crash Testing facility. In working with Diane Flynn, a fellow LARSS student, I became well versed in composites, starting with a brief lecture on the subject by Paul Hergenrother, who works with composites and adhesives. Next, Dr. Ruth Pater, the Senior Polymer Scientist in the Materials Division, gave me a tour of her lab and a description of one of her inventions: the High Performance Polyimide, LaRC RP 46. Finally, Phil Ransone and Phil Glaude explained the carbon-carbon piston concept, providing a background on engines as well as the material.

While Marisol was currently working on the process of matching companies to several technologies, I was also able to observe the commercialization process, and became acquainted with several of the "hot" technologies. To gain a better understanding of these technologies, and to add to my database, I visited a few of the "hot" labs. The inventor of the Extended Attention Span Training system and the Crew Response Evaluation Window, Dr Alan Pope, gave me an overview of his work as well as that of the entire branch. The Crew/Vehicle Integration Branch works on the human factors issues, trying to create machine systems that complement and enhance human capabilities. Another new technology of interest is the piezoelectric material THUNDER, which I was introduced by Richard Hellbaum, Robert Fox, and Robert Bryant. This group of an electrical engineer, a microelectronics technician, and a chemist, respectively, are developing applications for this material which moves when voltage is applied to it, with a better displacement for energy input ratio than available elsewhere. Lastly, James McAdoo explained to me his

highly marketable method of Digital Mammography, a faster, better way to scan tissue using a mosaic of CCD's to generate high resolution digital images.

I was also given several specific problem statements to look at, and in my search to find researchers I added to my database. One of the problems was from a textile machinery manufacturer, who wanted a system for monitoring the alignment of a pocket on a shirtfront before sewing. I went to the Data Visualization and Animation Lab (DVAL), and found their expertise so useful that I arranged for them to present their work to several interested members of TAG including Joe Heyman, the Deputy Director. The DVAL team works in scientific visualization, which is applicable to everything from producing presentation quality videos to computational fluid dynamics. The next problem involved diagnosis of premature infants with Retinopathy of prematurity, an eye disease resulting from abnormal retinal development and causing blindness. The difficulty arises in the observation of the retina and the display of the information gathered. Surgeons are using a video camera to record the retina, but are unable to compile the running film into a usable map of the blood vessel system. Complications arise from the lack of a point-of-reference for the images on the film, as the infants move their eyes. For this problem I went to Donald Cahoon, in the Atmospheric Sciences Division. He is an expert on remote sensing and offered to relay several suggestions to the requestor. The last person I met through problem statements was John Companion, who I approached for help on more than one occasion. He works in Non-Destructive Evaluation, developing items such as a Tissue Simulating Gel and a Bladder Scanner for volume measurement.

Throughout the completion of my project, I met several other people whom I cannot fit into neat categories in my database. I was allowed to sit in on a meeting between the THUNDER team and representatives from McDonnell Douglas, during which I was able to watch ideas being thrown out as they were thought of, and in trying to follow the discussion I learned more than in most lectures. I was also able to meet the incoming class of astronauts when they visited Langley. I spoke with David Williams, who give me a personal perspective on the selection and the requirements of job which symbolizes NASA in the eyes of most people. I met the entire staff of TAG, an energetic and focused group. First and foremost is my mentor Marisol Romero, a member of the Technology Transfer Team in the Medical, Instruments, Sensors, Environmental, and Energy (MISEE) sector. She works with medical technologies and has an electrical engineering background. She was my guide and the hub of my network. I also gained a more in-depth and international perspective on technology transfer from another T3, Lance Bush, whose unique insight into technology transfer stems from his background as a space craft designer and his interactions with people involved in space policy throughout the world.

I have worn out my tennis shoes in ten weeks here, and I feel I have gained a broad perspective of NASA Langley Research Center and the Technology Transfer Process. Working through a problem statement provided me with the necessary procedural background to appreciate the need for a database to improve and expedite the process. My work is only a foundation, and its impact cannot be judged yet. Ideally, it will reflect the unique, multidisciplinary aspects of this center for TAG to draw upon. The future lies in communication and cooperation, and Langley is taking steps, in its tennis shoes, toward that goal.





City of Virginia Beach

VIRGINIA BEACH ADULT DAY PROGRAM
(804) 473-5681

400 INVESTORS PLACE SUITE 107-109
VIRGINIA BEACH VIRGINIA 23452

Charlie Blankenship
NASA Langley Research Center
Technology Applications Group
MS 200
Hampton, VA 23666

July 20, 1995

This letter is in reference to the development of the Chin Mouse by Marisol Romero, Bruce Little, and Nina Paynter. The Chin Mouse will be utilized by our clients who possess extreme motor impairments to access a computer, as well as small appliances. The advent of affordable computer technology has created a multitude of opportunities for persons with severe disabilities to interact with their environment. However, there are numerous variables which limit use and affect accuracy, such as range of motion and positioning. These factors greatly influence motoric ability to access. Commercially available devices did not address the need for flexibility in positioning or range of motion for Jennifer. Flexibility is the primary characteristic which differentiates the Chin Mouse from other devices. It can be easily adjusted to adapt its use for numerous individuals with severe motor disabilities.

The most difficult aspect of my work as a special educator for individuals with severe and profound disabilities is individualizing programming and equipment to best meet the needs of my clients. It is often the case commercially available products are insufficient. Products designed such as the Chin mouse with flexibility to adapt to changing needs are few and far in between. Manufacturers are more apt to produce products which address the needs of the majority of disabilities, rather than a specific impairment. This philosophy is understandable. Therefore, a tremendous need exists for assistive technology which addresses the needs of a few, but can be easily modified to be utilized by many. Marisol Romero, Bruce Little, and Nina Paynter have accomplished this.

Their professional expertise has improved the quality of Jennifer's life by providing the opportunity for Jennifer to access a computer independently.

On a personal level they acknowledged Jennifer with dignity and respect. An aspect of their visits that truly impressed me was the fact they spoke directly to Jennifer. They did not appear intimidated by her disability. They were also aware of the need to maintain confidentiality.

Please continue your community service program. The need for technical expertise and collaboration among organizations is overwhelming for our disabled population. Technical expertise is imperative to further assist individuals to achieve their greatest potential.

With Sincere Appreciation,



Rosann Fox
Clinician II

pc: Carol Smith

**NEXT
DOCUMENT**

**Fabrication of Fabry-Perot Interferometer Sensors
and Characterization of their Performances
for Aircraft Inspection**

LeRuth Pendergrass* and Dr. Robert S. Rogowski

**Non-Destructive Evaluation Sciences Branch
Fiber Optics Group
MS 231
NASA Langley Research Center
Hampton, VA 23681**

***Langley Aerospace Research: Summer Scholar**

Abstract

This work provides the information for fabricating Fabry-Perot Interferometer sensors and their performances. The Fabry-Perot Interferometer sensors developed here will be used for the detection of flaws in aircraft structures. The sequel also contains discussion of the experimental setups for the Ultrasonic technique and the Fabry-Perot Interferometer.

Introduction

In order to make the type of fiber optic sensor in this work, a single mode fiber and capillary tube were used. A fiber is a glass filament with a core having a slightly higher index of refraction than the surrounding cladding and a buffer layer which surrounds the cladding layer. A fiber is also used as input and output signals. The capillary tube is a hollow core optical fiber tube where the fiber is inserted.

The purpose of this study is to fabricate fiber optic sensors in a cost effective way to be able to detect damage such as corrosion and disbond in the walls of aircraft. In choosing a specific fiber optic sensor the format in which the final output is available is an important concept to consider. In this experiment, an extrinsic Fabry-Perot fiber optic sensor was designed to develop a Fabry-Perot Interferometer Sensor. The performance of the Fabry-Perot sensor was characterized using a multimeter, and an optical microscope. The 1300nm laser light source was used to observe the performance of the Fabry-Perot Interferometer by showing the amplitude changes, due to temperature variation as a function of time.

This work provides additional information for fabricating and characterizing the performance of Fabry-Perot sensors. Many research groups and individuals are either working on or have worked on this same type of project, but in more detail or different aspects. The fiber and electro-optics Research Center in correlation with the Materials Response Group of Virginia Tech have done an analysis of macro-model composites with Fabry-Perot optic sensors [1]. This particular experiment shows how useful macro-model composites, with Fabry-Perot fiber optic sensors, are in measuring strain concentrations introduced by damage events. The department of mechanical engineering at the University of Maryland did research on the phase-strain temperature model for structurally embedded interferometric optical fiber strain sensors with applications [2]. The fiber and electro-optics research center and Bradley department of electrical engineering at Virginia Tech did research on the Fabry-Perot fiber optic sensors in full scale fatigue testing on an F-15 aircraft [3]. This experiment deals with strain and temperature being applied to a interferometric optical fiber sensor and the optical phase changes that occur.

Even though there are many groups and individuals working with fiber optic sensors, in support of this particular work the sources mentioned above were used along with help from my mentor and individuals in the fiber optics group at NASA.

Experimental Procedure

The simplest configuration of the extrinsic Fabry-Perot Interferometer consists of two plane, parallel, highly reflecting surfaces separated by some distance (air gap), see figure 1 [4]. In the construction of the Fabry-Perot fiber optic sensor a single mode fiber ($\lambda_0=1300\text{nm}$) was used as the input/output fiber and as a reflector to form an air gap. The buffer layer, of two pieces of single mode fiber, was removed using a razor and a radio solvent (a solvent used to remove and loosen cemented cones). The buffer layer was removed because the diameter of the fiber was too large to fit into the capillary tube. After the fiber was taken out of the solvent and wiped off, the ends of the fiber were cleaved with a cleaver. The cleaving had to be parallel in order for the energy reading to be more accurate. The portable fiber splicer (model pfs 330) was used to confirm if the fiber ends were cleaved correctly.

One end of each piece of fiber was put into the capillary tube. Since the capillary tube has a $155\mu\text{m}$ inner diameter and the fiber optic core and cladding has a $125\mu\text{m}$ diameter, each piece of fiber must be $15\mu\text{m}$ away from both edges of the tube. The other two ends of the fiber were put into the splicemates. This setup is shown in figure 2. In this setup the light coming from the laser through the fiber goes into the photodetector and the output (energy reading) is obtained from the multimeter. When an acceptable energy reading was obtained epoxy was applied to both ends of the capillary tube. After the epoxy cured the sensor was characterized using the optical microscope. The optical microscope captured images of the sensors on the computer, making sure an air gap was present, see figures 3-5. The reflection and transmission methods were used to test the quality or performance of the sensor. In the reflection method the coupler was used to help the signal go back to the photodetector. In the transmission method a coupler was not used. Tests were run on the Fabry-Perot sensors in effort to obtain changes in amplitude due to temperature variations as a function of time. These results are shown in figures 6-10. These tests were run using the experimental application. Two sources of temperature were used to determine the change in temperature, which led to the change in amplitude as shown on the graphs, shown in figures 6-10. When there was a small fluctuation and then a change in temperature occurred and the fluctuation became large, the variation of temperature versus time was acceptable. If the quality of the Fabry-Perot sensor was good, the flaws in the aircraft structures were able to be measured using the ultrasonic technique and the Fabry-Perot Interferometer sensor. The aluminum is held together by epoxy and if any detachment takes place or loosens the sensor or transducer can detect the damage. In the ultrasonic technique two transducers were used to find the waveform propagated ultrasonically through the aluminum, see figure 11. In the Fabry-Perot Interferometer sensor setup, the sensor, placed between two transducers, was used to find the amplitude changes within the aluminum, see figure 2.

Experimental Setup and Results

The experimental setup for this project consisted of a 1300nm laser used as a light source, a photodetector used as a detector, a coupler used to help measure transmitted optical power and reflection, and a Norland Products, Inc. splicemate used to connect the sensor to the coupler (all of these devices are shown in figure 2) [5]. A Reicher Austria Nr. 362257 Optical Microscope was used to capture images of the fiber optic sensor revealing the air gap, these images are shown in figures 1, 3, 4, & 5. A Hewlett Packard 3478A multimeter was used to show the output amplitude reading obtained from the sensor (readings are shown in figures 6-10). A solder iron was used as a source of temperature, a CT-03 Cleaver was used to form parallel cut fibers, and a Portable Fiber Splicer model PFS 330 was used to confirm the parallelism of the cleaved fiber.

Experiments were performed using Fabry-Perot sensors. The Fabry-Perot fiber optic sensors shown in figures 1 and 3 were used to obtain experimental results. If an energy reading less than .5volts occurred, the performance of a sensor was not acceptable. Sensor number three contained a low energy reading of .046millivolts. This could have been caused by the size of the air gap. In an air gap the light is dissipated by the air, which means the larger the air gap the smaller the intensity, and the smaller the air gap the more light can pass through the two fibers. Another cause of low energy readings could have been because of a misalignment between the two pieces of fiber in the capillary tube. The problem occurred in sensor number three because of a large air gap, shown in figure 1. Tests were run on sensor number three, despite the low energy reading, to further justify the malfunction in performance of the sensor. Figures 6 and 7 show the amplitude changes due to temperature as a function of time for sensor number three. As mentioned in the procedure, when a small fluctuation occurs and then there is a change in temperature and the fluctuation becomes large, the variation of temperature versus time is acceptable. Shown in figure 6 there is really no type of amplitude change to make this test run acceptable, and in figure 7 the amplitude decreases at a temperature change instead of increasing. Sensor number four contained an initial energy reading of -1.28volts and a final reading of -1.69volts. This sensor, shown in figure 3, was of good quality and therefore could be further tested. In figures 8-10, amplitude changes due to temperature variation as a function of time are shown for sensor number four. In figure 8, when a temperature change occurred, the amplitude increased. In figure 9, the temperature did not have any type of effect on the sensor, which caused a great amount of fluctuation. And lastly in figure 10, a solder iron was used as a source of temperature to indicate amplitude changes. The Fabry-Perot sensors shown in figures 4 and 5 are just two of the first sensors fabricated during this project. Figure 4 shows a misalignment and figure 5 is a good quality sensor but it was broken so it was not used for testing.

Acknowledgments

Research on this project was supported by the fiber optics group in the Non-Destructive Evaluation Sciences Branch of NASA Langley Research Center. I would like to personally thank the entire fiber optics group for all of the support and help throughout

my project. Lastly, I would like to thank Dr. Nurul Abedin for being patient and inspiring throughout this project.

Discussion

The testing of damage such as corrosion and disbond that occurs in aircraft structures can not be accomplished without first fabricating and characterizing the performance of the Fabry-Perot Interferometer sensor. This particular project indicated the experimental procedure used to complete fabrication and characterization of the Fabry-Perot Interferometer sensor. The actual testing of damage in aluminum or aircraft structures was not performed, but the setups for the ultrasonic technique and the Fabry-Perot Interferometer sensor were completed. Figure 11 shows the setup for the ultrasonic technique. If a waveform is not shown on the Lecroy 9400A Dual Digital Oscilloscope, there is indication that a crack or disbond has formed in the aluminum. Figure 2 shows the setup for the Fabry-Perot Interferometer sensor. If the voltage reading from the multimeter changed or approached zero, there is indication of a crack or disbond in the aluminum. The readings from the multimeter and the oscilloscope relate because when there is a waveform on the oscilloscope there is a voltage reading on the multimeter and when there is not a waveform, the reading on the multimeter is zero or very close to zero.

References

1. Carman, G. R., Claus, R. O., B. Fogg, B. R., Lesko, J. J., Miller, W. V., Reifsnider, K. L., and Vengsarkar, A. M., "Analysis of Macro-Model Composites with Fabry-Perot Fiber Optic Sensors," Fiber Optic Smart Structures and Skins IV, vol.1588, 14-25, 1991.
2. Sirkis, J. S., "Phase-Strain-Temperature Model for Structurally Embedded Interferometric Optical Fiber Strain Sensors with Applications," Fiber Optic Smart Structures and Skins IV, vol.1588, 26-43, 1991.
3. Claus, R. O., Gunther, M. F., Murphy, K. A., Vengsarkar, A. M., "Fabry-Perot Fiber Optic Sensors in Full-Scale Fatigue Testing on an F-15 Aircraft," Fiber Optic Smart Structures and Skins IV, vol.1588, 134-142, 1991.
4. Hecht, Eugene, "Hecht Optics," Addison-Wesley Publishing Company, Reading, Massachusetts, 1987.
5. Fiber Optics Handbook, third edition, Hewlett Packard, Republic of Germany, 1989.

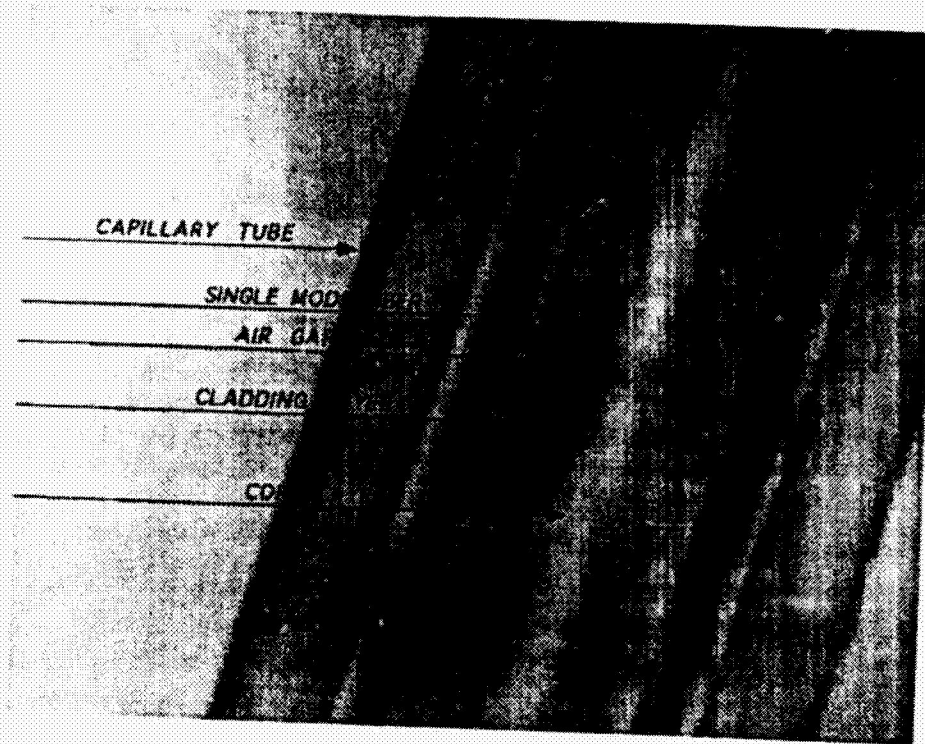


Figure 1 The Fabry-Perot Interferometer Sensor(sensor number three) characterized using the optical microscope.

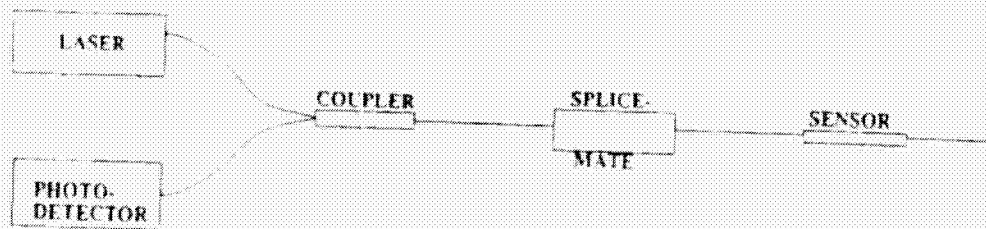


FIGURE 2. EXPERIMENTAL SETUP FOR FABRY-PEROT INTERFEROMETER INSPECTION

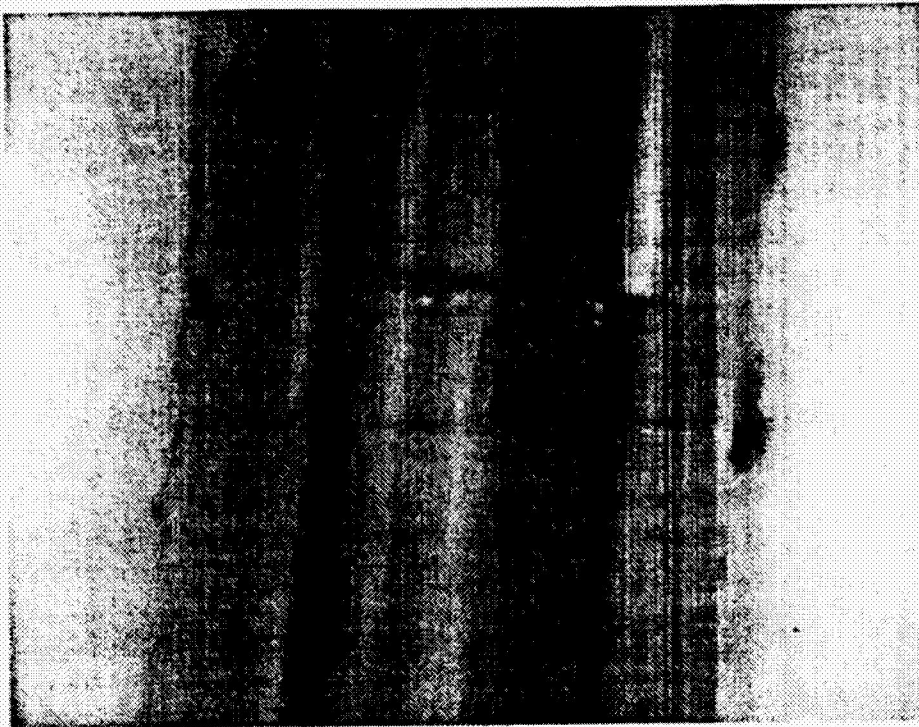


Figure 3. Characterization of the Fabry-Perot Interferometer Sensor(sensor number four) using the optical microscope.

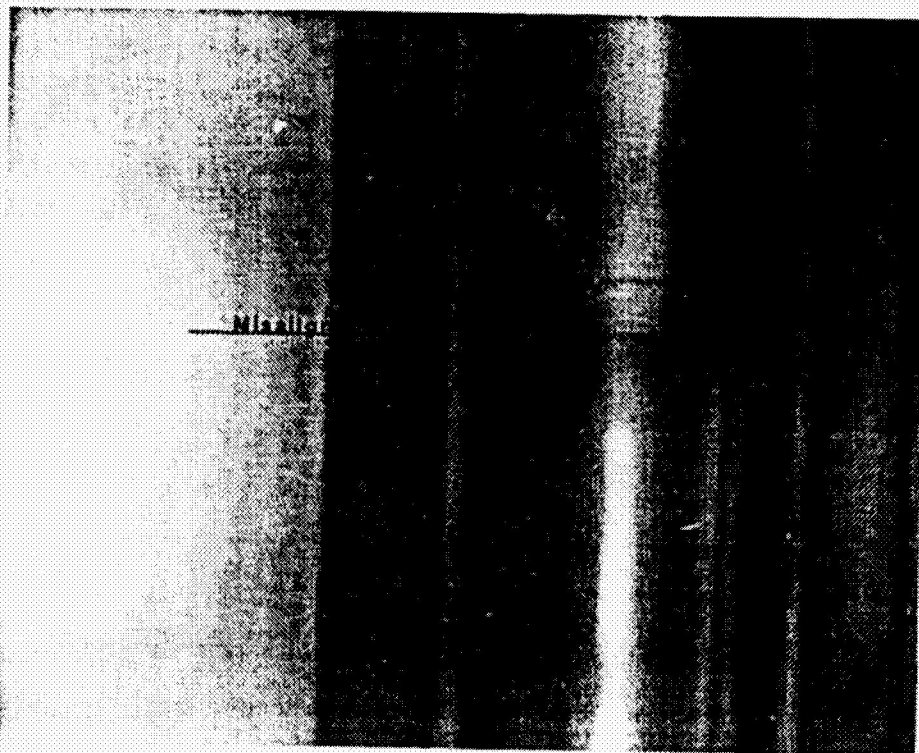


Figure 4. Characterization of the Fabry-Perot Interferometer Sensor(sensor number one) using the optical microscope.

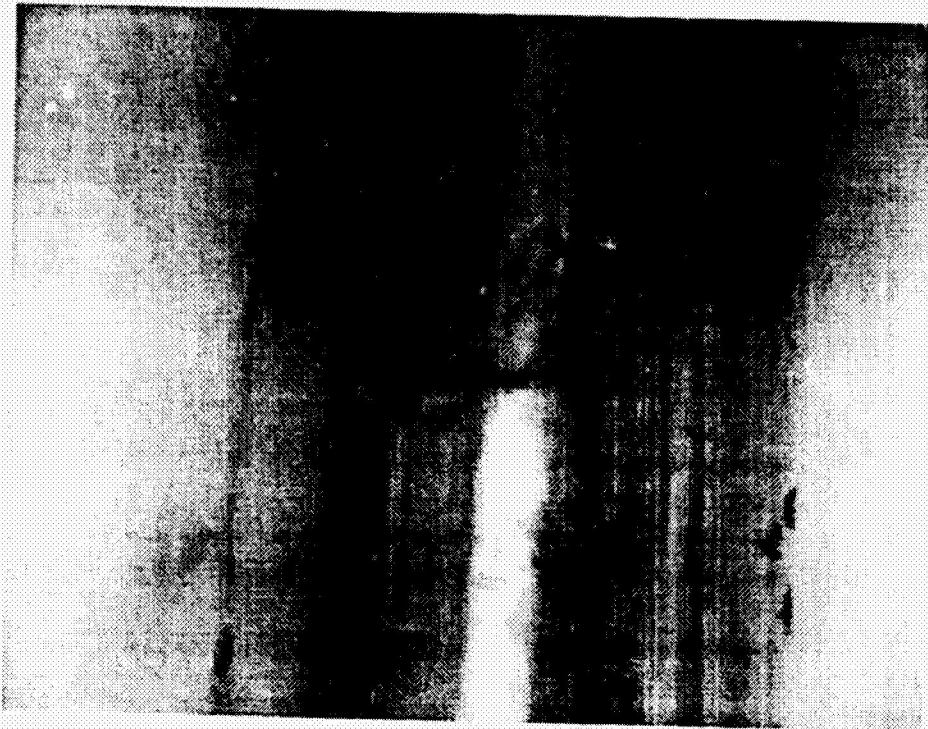


Figure 5. Characterization of the Fabry-Perot Interferometer Sensor(sensor number two) using the optical microscope.

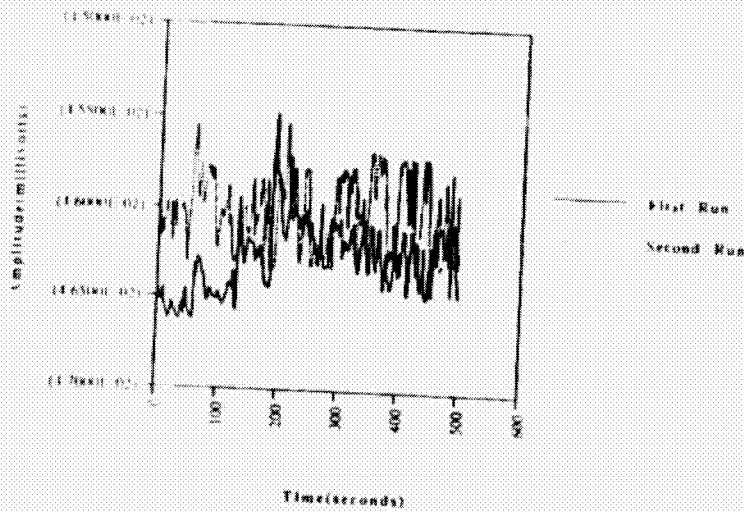


Figure 6. Amplitude changes due to temperature variation as a function of time(Reflection method using sensor number three).

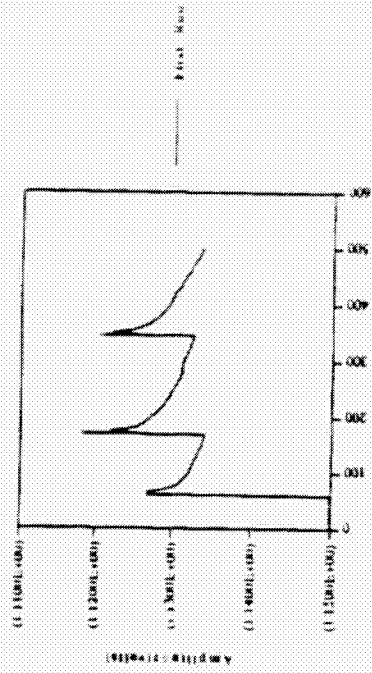


Figure 8. Amplitude changes due to temperature variation as a function of time (Transmission method using sensor number four).

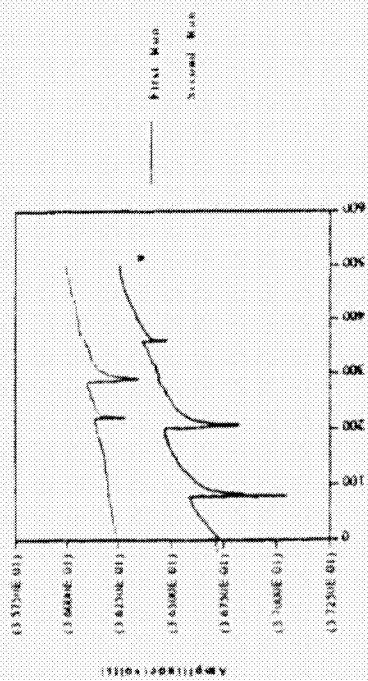


Figure 7. Amplitude changes due to temperature variation as a function of time (Transmission method using sensor number three).

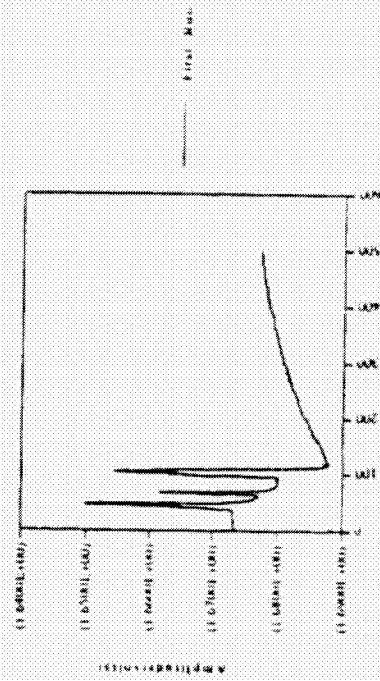


Figure 10. Amplitude changes due to temperature variation as a function of time (Reflection method using sensor number four).

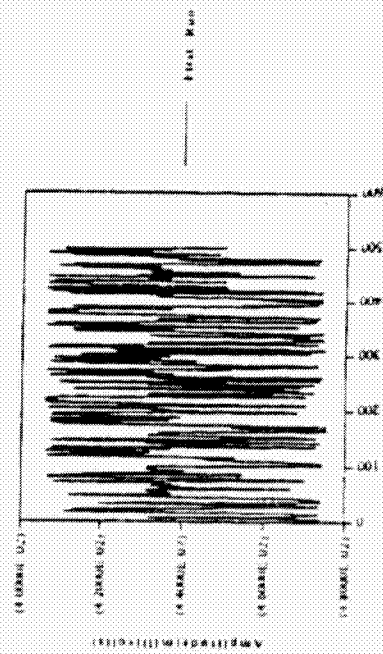


Figure 9. Amplitude changes due to temperature variation as a function of time (Reflection method using sensor number three).

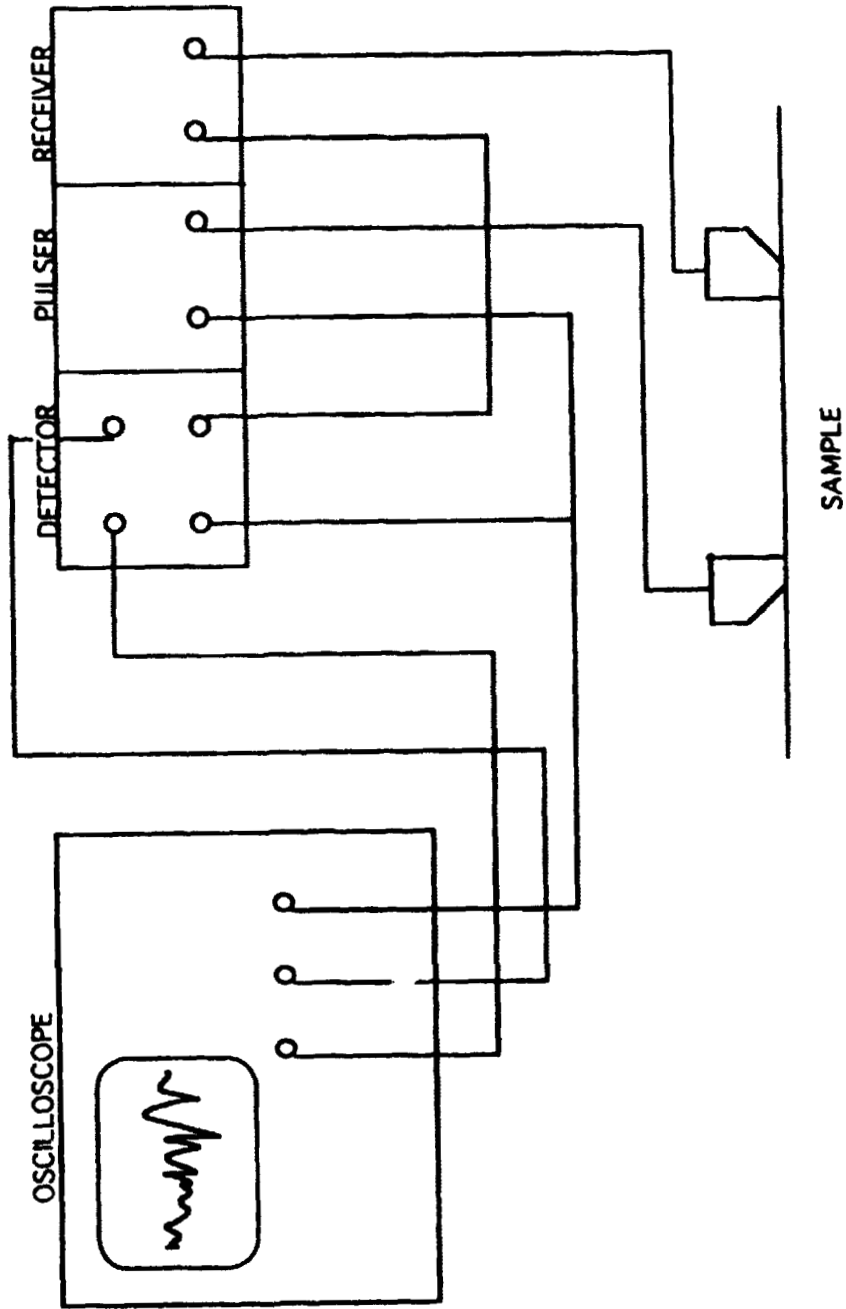


Figure 11. EXPERIMENTAL SETUP FOR ULTRASONIC INSPECTION

**NEXT
DOCUMENT**

17-01

**PERFORMANCE COMPARISON OF A MATRIX SOLVER
ON A HETEROGENEOUS NETWORK
USING TWO IMPLEMENTATIONS OF MPI:
MPICH AND LAM**

BY:
Jennifer Phillips

MENTOR:
Jerrold M. Housner

RESEARCH AND TECHNOLOGY GROUP
STRUCTURES DIVISION
Computational Structures Branch

◆ ABSTRACT

Two of the current and most popular implementations of the Message-Passing Standard, MPI, were contrasted: MPICH by Argonne National Laboratory, and LAM by the Ohio Supercomputer Center at Ohio State University. A parallel skyline matrix solver was adapted to be run in a heterogeneous environment using MPI. The Message-Passing Interface Forum was held in May 1994 which led to a specification of library functions that implement the message-passing model of parallel communication. LAM, which creates its own environment, is more robust in a highly heterogeneous network. MPICH uses the environment native to the machine architecture. While neither of these free-ware implementations provides the performance of native message-passing or vendor's implementations, MPICH begins to approach that performance on the SP-2. The machines used in this study were: IBM RS6000, 3 Sun4, SGI, and the IBM SP-2. Each machine is unique and a few machines required specific modifications during the installation. When installed correctly, both implementations worked well with only minor problems.

◆ INTRODUCTION

With the current downsizing and new philosophy of "faster, better, cheaper" companies can no longer afford large powerful machines like the CRAY, yet they still require the computing power provided by such systems. The current direction of the computational sciences is to utilize the power of the machines already in use by engineers. Workstations have given engineers powerful and accurate tools with which to design aircraft such as the Boeing 777. These same machines are also giving engineers the ability to perform the large scale computations which were previously done on large machines.

A single workstation could spend days slowly grinding through a large computation, but with the use of parallel communications, many workstations can be linked together and provide the power of a single large computer. This concept has led to many types of communication software facilitating the production of massively parallel machines. The most common types of communication are MPL, the message passing library for the IBM machines, and Parallel Virtual Machine or PVM which was designed as a message passing library for heterogeneous networks. PVM has recently been used in a parallelized Navier-Stokes CFD code at McDonnell Douglas. With the success and development of such software, a decision was made to standardize the communication protocol.

In May 1994, the first conference was held to create a new standard for message passing. This forum produced the Message-Passing Interface Standard [Ref. 1] or MPI-1. The best attributes of the existing message passing libraries were assessed and combined. MPI-1 is currently a standard by which to create message passing libraries. It in itself is not software; it is left to the implementors to write the code. While this standard currently contains message passing information and control, I/O is being considered for MPI-2, and dynamic process control (e.g. MPI_Spawn) is still under controversy. The beauty of the standard is that programs written in MPI can be used on any architecture and with any implementation.

There are currently about five implementations of MPI freely available (see resource list). The two most common and best supported are MPICH and LAM. These two implementations will be profiled and contrasted in the following. The machines used in this study were:

- IBM RS6000
- (3) Sun 4
- SGI Indigo
- IBM SP-2

These machines were accessed from a Macintosh IIfx using MacX.

◆ IMPLEMENTATIONS

Both implementations require the use of the remote shell command, 'rsh,' and thus require all machines in the available network, including the root machine, to appear in the .rhosts file of the user.

◆ LAM VERSION 5.2

The Ohio Supercomputer Center's implementation, Local Area Multicomputer or LAM (which is a subset of the greater Trollius system), creates a similar environment to PVM. LAM is a message passing library with it's own environment. LAM's implementation of MPI amounts to a separate set of libraries that interact with LAM's environment. To run an MPI program in LAM it needs to be compiled with a FORTRAN/C compile script provided by Ohio State. The environment must then be set up by "starting the engine" or running the LAM deamon on all the machines in the desired network.

◆ OPERATION

Once the engine is running LAM is fairly simple to use. However, for heterogeneous networks the executable must lie in the user's path. The program is run with a command line execution that includes the script executable (mpirun), options, the nodes which it will be run on, and the program executable. The program name is assumed to be the same on all machines. There is no way to easily deal with different executable names or paths. For a heterogeneous environment any I/O to the program must have a specified path name or be located in the directory from which LAM was booted. (For the root computer this will be the directory from which 'lamboot' was run. For other computers in the network, it is the user's home directory.)

◆ INSTALLATION

The installation is pretty straightforward as laid out in the Installation Guide [Ref. 2]. An environment variable must be set up to define the location of the executables and this location must then be placed in the user's path. This location is *different* from the location of the source code, since the source code may be eliminated once LAM is properly built. The last thing required before running the 'make' is linking the 'config' file to the proper architecture configuration file.

The only problem encountered during the installation was the necessary addition of the '-Bstatic' option to the C compiler (cc) and the FORTRAN compiler (f77) in the 'config' file on 'sunny.larc.nasa.gov' (Sun4) and 'csmsun.larc.nasa.gov' (Sun4). These machines require this option as a result of a problem with their shared libraries.

For a permanent network installation LAM should be installed in the path `/usr/local/lam` or `/usr/local/lam5.2` etc. In order to do this, the `TROLLIUSHOME` environment variable must be set to this path as well as the home variable in the config file. Once set, run:

```
make install
```

and the source directory may be deleted.

◆ MPICH VERSION 1.0.10

MPICH uses an environment already installed on the machine which gives rise to its chameleon nature and the CH in its name. MPICH relies on the environment already created on various machines, such as p4 on workstation and MPL/EUI on IBM machines. Argonne National Laboratory has created libraries to make MPI take advantage of the native message passing routines already on the computers. To run a MPI program with MPICH an appended makefile (created by MPICH) is required to initialize certain environment variables.

◆ OPERATION

MPICH is also fairly easy to run. It also uses a script executable (`mpirun`) followed by options and the program executable. MPICH does not require the listing of nodes/computers to be run on in the command line, however it does require the `'-np'` option at a minimum to specify the number of processes. When enlisted, MPICH looks for all the machines with the same architecture as the root computer (these are listed in a file in MPICH) and the processes are dispersed among them. In order to run on a heterogeneous network, the process file or proggroup (`PI####`) needs to be created by the user. This process file contains the computer's network name, the number of processes assigned to that computer and the full path name of the executable, as well as the user's login name on heterogeneous machines. Since the full path name of the program is specified, the program names and paths may vary on other machines without being placed in the user's path.

A generic proggroup file was created containing all of the machine names available; unused machines were then commented out as necessary for each machine.

◆ INSTALLATION

Installation of MPICH is also fairly simple; see the MPICH Installation Guide [Ref. 3]. MPICH supplies a configuration script, `configure`, that can be run with or without flags that specify options such as the architecture, device and C compiler used. This `configure` script creates the makefiles, which simply need to be built. The following variations were made for the workstations used. The IBM RS6000, borg-07, is a stand alone workstation and does not contain the MPL/EUI libraries, thus the device and communications protocol used were p4. On the SP-2, the `configure` was unable to successfully use the `mpCC` or C++ compiler, so the `-cc=mpcc` option was used to specify the C compiler. This had no effect to subsequent programs since MPICH is written in C and the sparse solver is written in FORTRAN. Finally, the two Sun4 workstations, sunny and csmsun, required a modification to their configuration files. MPICH requires use of the shared libraries on these Suns so the static or non-shared library option was not successful (i.e. `configure -cc="cc -Bstatic" -fc="f77 -Bstatic"`). An additional library reference is needed for the shared libraries. There is no specific flag to specify the libraries for the `configure` file, therefore the script was directly modified and the shared libraries were added to the primary list of parameters (i.e. `LIBS=-lc.1.8.1` and `-lc.1.9.1`, respectively for sunny and csmsun). In addition, subsequent makefiles required this option as well.

For a permanent network installation MPICH should be installed in the path /usr/local/mpi or /usr/local/mpi-1.0.10 etc. This installation is performed by the following command:
 make install PREFIX=/usr/local/mpi-1.0.10
 ln -s /usr/local/mpi-1.0.10 /usr/local/mpi

THE SPARSE SOLVER

The matrix solver used for this study was a vectorized skyline sparse solver written by Majdi A. Baddourah. This particular solver has been tested in various forms including PVM and MPL on the SP-2. For previous benchmarks and performance see the Computational Structures Branch Web page (see resource list).

Since MPI's subroutines are similar to existing parallel communicators, few changes had to be made to the solver. For example, the standard send FORTRAN syntax is provided below for the native message-passing library of the IBM machines (MPL), Parallel Virtual Machine (PVM), and MPI.

```

MP_SEND( outgoing_message, msg_length(bytes), destination, data_type )
PVMFINITSEND( encoding, error_code )
PVMFPACK( outgoing_message, first_element#, msg_length(items), stride, error_code )
PVMFSEND( task_identifier_of_destination_process, msg_tag, error_code )
MPI_SEND( outgoing_message, msg_length(items), data_type, destination, msg_tag,
          communicator, error_code )
  
```

MPI is a combination and reordering of the other two, allowing the simplicity of MPL with the heterogeneous capability of PVM. The main program was edited to reflect MPI's initialization and finalize routines; MPI_Init()¹, MPI_Comm_Rank()², MPI_Comm_Size()³, and MPI_Finalize()⁴. All other communication references were dealt with as subroutines. One other change was made to the factorization and back solving subroutines. MPL requests the number of bytes being sent while MPI requires the number of items, thus variables such as 'nbyt' were essentially divided by the number of bytes per item to reflect the number of items only.

The send subroutine was modified to use the standard MPI send, MPI_Send()⁵. Other options for different types of sending routines were considered, but deemed unnecessary. One of these possibilities was a synchronous send, which will not complete until not only the message buffer is safe to be reused but also the matching receive has been posted. The standard send is a blocking send, where the send will not complete until the message buffer is able to be reused. This standard send was also the fastest send, especially for large messages. This modification was a little tricky since the send and receive subroutine were called for both integer and real data types. MPL accepts a range of numbers to specify a certain data type, e.g. the integers 1 to 100000 represent real numbers and larger integers represent integers. The original data type was used as the message tag and then changed to an MPI data type, e.g. MPI_Real⁶. Using this message tag will also prevent mismatches in send and receive pairs.

¹ MPI Standard page 196 line 20 MPI_INIT(ierror)
² MPI Standard page 142 line 5 MPI_COMM_RANK(communicator, rank, ierror)
³ MPI Standard page 141 line 28 MPI_COMM_SIZE(communicator, size, ierror)
⁴ MPI Standard page 196 line 34 MPI_FINALIZE(ierror)
⁵ MPI Standard page 16 line 26 MPI_SEND(buffer, nelements, datatype, destination, tag, communicator)
⁶ MPI Standard page 17 line 12 Fortran: REAL

The global sum subroutine was modified to make use of `MPI_Allreduce()`⁷, which not only performs a user defined function but also sends the result to all of the machines in the network. Here, the user defined function, vector addition, was slightly modified to the form expected by MPI. This modification only involved reordering the arguments.

The two communication ring subroutines, integer and real data types, were initially modified to use the `MPI_Sendrecv()`⁸ routine. `MPI_Sendrecv()` will send and receive the same buffered information in either direction, which should prevent deadlock. Deadlock occurs when one machine is attempting to send and the receiving machine is also attempting to send, thus not allowing the completion of either send call. Unfortunately, this created problems and was abandoned.

Finally, the subroutine used for timing the program, or profiling, was changed from a C subroutine using `gettimeofday()` to `MPI_Wtime()`⁹. `MPI_Wtime()` returns wall-clock time in seconds similar to `gettimeofday()`.

The makefiles for the solver are generally straight forward, the header information for both LAM and MPICH was either copied or generated by the software. Initially, the makefiles were not finding the MPI library, this was temporary fixed by editing the environmental variable `LIB_PATH` to reflect the location of `libmpi.a`. This is not necessary, however, if the makefiles are created with the correct path for each MPI implementation. Also, LAM 5.2's include file for FORTRAN, `mpif.h`, was originally written in C, this facilitated the need for extra lines in the makefile, i.e. the preprocessor `cpp` was required of all files containing the include file. This was subsequently changed after an inquiry to the implementors of LAM. This change may now be included as a patch and will most likely appear in the next version to be released.

◆ PERFORMANCE TESTING

There have been previous studies in the performance of MPI as compared to other parallel libraries. "Performance Comparison of MPL, MPI, and PVMc" [Ref. 4] compared the performance of PVMc, MPICH, MPI-F, and MPL. As expected MPL performed the best, but IBM's vendor's version of MPI, MPI-F, practically matched MPL performance. The free-ware version of MPI, MPICH, was a close second followed by PVMc. Also, "Some early performance results with MPI on the IBM SP1" [Ref. 5] found MPI-F to closely match MPL and MPICH followed closely behind.

The solver was run for various combinations of processors using LAM and the p4 directories in MPICH. The SP-2 was used as the primary control machine, since it was the original source of the solver's program with MPL. For each matrix tested, the solver was run on the SP-2 using, MPL, MPICH, and LAM for two to six processors or nodes. In addition various other combinations of machines were used for each of the matrices up to the entire network of all six machines available. The matrices tested were a simple beam consisting of 24 equations, a test matrix of 840 equations, a plate with a hole in it with 1,802 equations and a model of the High Speed Civil Transport with 16,152 equations.

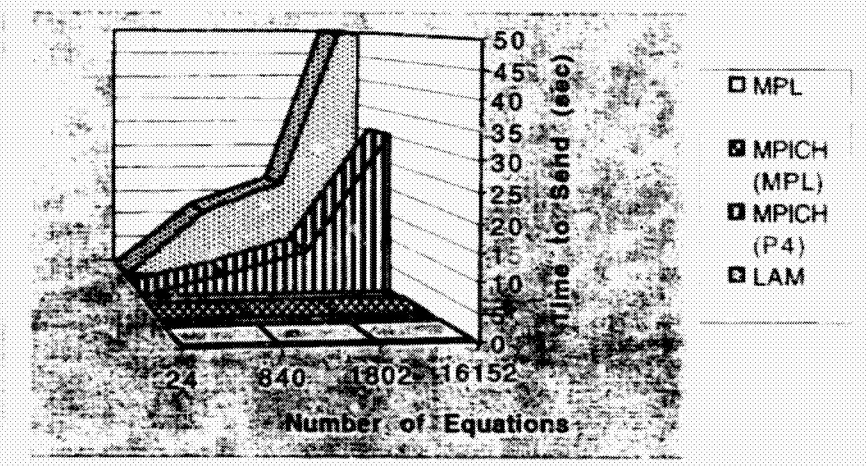
As a basis for a comparison, all four matrices were run on the SP-2 and compared in Figure 1. The send time in the factorization is compared for the solver running with MPL, MPICH using the native MPL, MPICH using p4, and LAM. The SP-2 was tested with p4 because, for this particular network p4 interacted the most consistently with the other machines. Figure 1 shows MPICH with MPL a close second to MPL itself.

⁷ MPI Standard page 122 line 14 `MPI_ALLREDUCE(sendbuffer, recvbuffer, nelements, datatype, operation, communicator)`

⁸ MPI Standard page 57 line 4 `MPI_SENDRECV(sendbuffer, sendnelements, sendtype, destination, sendtag, recvbuffer, recvnelements, recvtype, source, recvtag, communicator, status)`

⁹ MPI Standard page 195 line 19 `FUNCTION MPI_WTIME()`

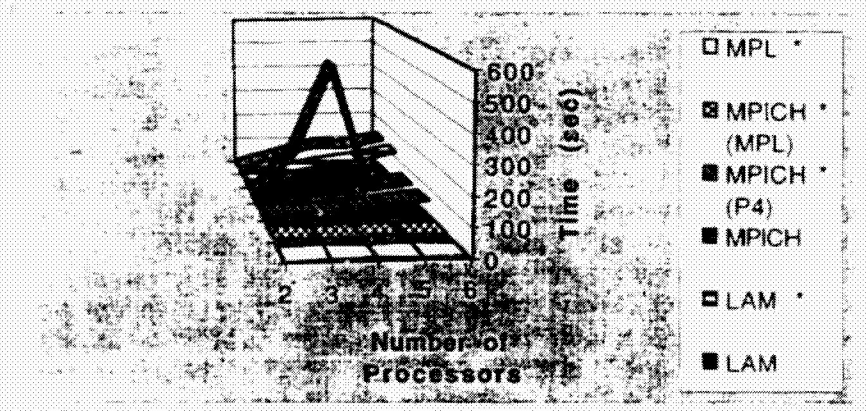
Figure 1. Send Times on Poseidon



Please note the graph is not to scale and is a bit skewed. Figure 1 does not yet suggest scalability as all graphs are climbing through the increase in number of equations, however, it has been shown that MPICH using native libraries will become as scalable as the native libraries themselves.

Figure 2 demonstrates the total factor time for the SP-2 as well as an average of many other heterogeneous configurations. This figure demonstrates the increase in communication time in the heterogeneous network. This is primarily due to the relative speeds and memory of each machine as the time varies with the number of processors and not with the degree of heterogeneity.

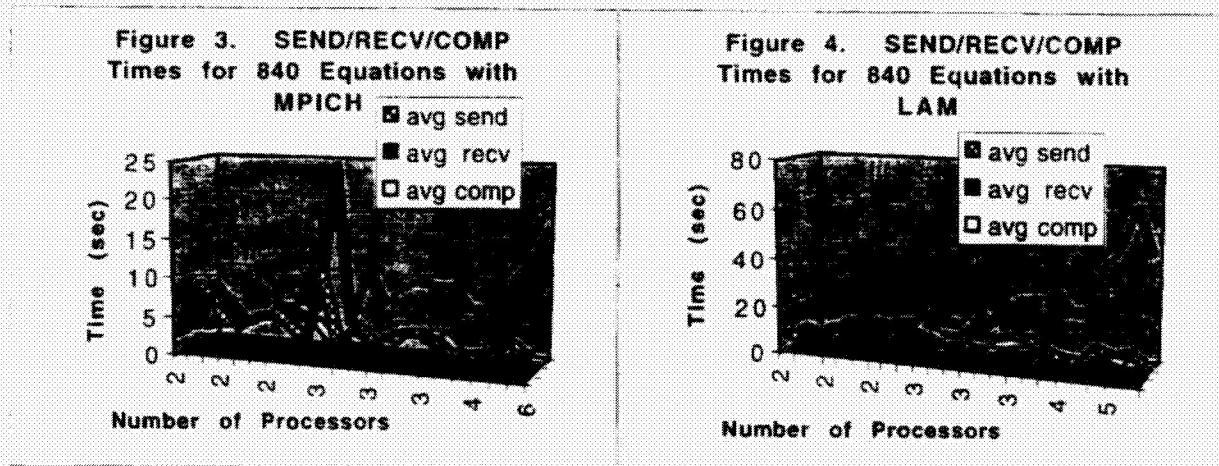
Figure 2. Factor Times for 1802 Equations



The largest peak stems from a largely heterogeneous network using MPICH and p4. This curve drops off quickly because this network could not handle larger matrices thus, the last data points are for the SP-2 alone and not an average of many networks.

As mentioned above, the time is dependent on the individual machine and thus the over all time can vary great depending on the machines in the network. Figure 3 shows the send, receive, and compute time for the 840 equations. The general trends are for send time to decrease with an increasing number of nodes which can be explained by the decreasing message size. The compute time also decreases with increasing nodes, which was expected since the relative work load is

decreasing. Finally, the receive time increases dramatically. This is mostly likely due to down time waiting for other machines in the network.



The large peaks represent very heterogeneous networks, i.e. at least three different architectures, and usually contain a Sun. It is also interesting to note that the order of networks configurations is the same in both Figure 3 and 4. Figure 4 lacks the large peaks found in Figure 3, but the overall time is much greater. The length of the send and receive times was also dependent on the degree on heterogeneity and the speed of the machine being sent to or receive from. The compute time remained relatively constant per machine, differences resulting from load on the machine. For large matrices, i.e. the high speed civil transport, LAM's performance begins to approach MPICH's performance using p4, however, neither approaches MPICH using native message-passing.

◆ CONCLUSIONS

The choice of implementation should be based on user preferences, i.e. what type of control the user is more comfortable with and the importance of time and performance. LAM is more robust in a heterogeneous environment than MPICH, however, MPICH provides much better performance than LAM. LAM may also allow dynamic process control in the future which is not available with MPICH. For a semi-homogeneous environment, e.g. cluster of IBM RS6000's, MPICH using the native message-passing would be the best choice. For a program developer on a heterogeneous network, LAM offers the most ease of control and stability.

Further testing with larger matrices should be done. This, however, should not be done on the local Suns, since they do not provide the hardware necessary to efficiently run them. A similar performance to that of the SP-2 should be attainable on the IBM RS6000 cluster. In addition, optimization can be done to further increase the performance of the solver using MPI. The X windows interfaces, e.g. MPE and Xmpi, provide an aide to this task.

◆ RESOURCES

◆ REFERENCES

- [1] Message Passing Interface Forum, *MPI: A Message-Passing Interface Standard*. Computer Science Dept. Technical Report CS-94-230, University of Tennessee, Knoxville, Tennessee, 5 May 1994.
- [2] GDB. *LAM for Fortran Programers. (LAM Installatio.. Guide)* Ohio Supercomputer Center, The Ohio State University, July 20, 1994
Ohio LAM version 5.2
- [3] Patrick Bridges, Nathan Doss, William Gropp, Edward Karrels, Ewing Lusk, Anthony Skjellum. *User's Guide to MPICH, a Portable Implementation of MPI. (Installation Guide to MPICH)* Argonne National Laboratory, 5 May 1995.
MPICH version 1.0.10
- [4] Bill Saphir and Sam Fineberg. *Performance Comparison of MPL, MPI, and PVMe*. NAS Scientific Consulting Group, 21 October 1995.
- [5] William Gropp and Ewing Lusk. *Some early performance results with MPI on the IBM SP1 - EARLY DRAFT*. Argonne National Laboratory, 5 June 1995.
- [6] Ed Karrels and Ewing Lusk. *Performance Analysis of MPI Programs*. Argonne National Laboratory, (1995).
- [7] William Gropp, Ewing Lusk, and Anthony Skjellum. *Using MPI: Portable Parallel Programming with the Message-Passing Interface*. MIT Press, 1994.

◆ FTP SITES

MPICH source code info.mcs.anl.gov/pub/mpi/mpich.tar.Z
CHIMP source code ftp.epcc.ed.ac.uk/pub/chimp/release/chimp.tar.Z
LAM source code tbag.osc.edu/pub/lam/lam52.tar.Z

Test Code repository info.mcs.anl.gov/pub/mpi-test

◆ MAILING LISTS

mpi-bugs@mcs.anl.gov *MPICH bugs and information (William Gropp)*
trollius@tbag.osc.edu *LAM bugs and information (Raja Doaud)*
mpi-comm@cs.utk.edu *the MPI Forum discussion list*

◆ NEWS GROUP

comp.parallel.mpi

MPI newsgroup

◆ WWWEB PAGES

Message-Passing Interface

<http://WWW.ERC.MsState.Edu/mpi/>

MS State's MPI resource web page

The MPI Resource Center

<http://www.epm.ornl.gov/~walker/mpi/index.html>

Oak Ridge National Laboratory's MPI resource web page

Message Passing Interface

<http://www.mcs.anl.gov/~jmpi/>

Argonne National Laboratory's MPI resource web page

Papers Related to MPI

<http://www.epm.ornl.gov/~walker/mpi/papers.html>

MPI Paper's from Oak Ridge's page

LAM - MPI Network Parallel Computing

<http://www.osc.edu/lam.html#MPI>

Ohio State's MPI/LAM information page

The LAM companion to "Using MPI..."

<ftp://c isr.anu.edu.au/pub/papers/meglicki/mpi/tutorial/mpi/mpi.html>

*Center for Information Science Research,
Australia National Lab's MPI/LAM tutorial*

Getting Started with MPI on LAM

<http://www.osc.edu/Lam/lam/tutorial.html>

Ohio State's MPI/LAM installation & boot-up tutorial

MPICH Home Page

<http://www.mcs.anl.gov/mpi/mpich/index.htm>

Argonne National Lab's MPICH information page

Web pages for MPI and MPE

<http://www.mcs.anl.gov/Projects/mpi/www/index.html>

Argonne National Lab's MPI (MPE) man pages

Computational Structures Branch

<http://olaf.larc.nasa.gov/>

Benchmarks for matrix solvers on various platforms

**NEXT
DOCUMENT**

19-07
1-5

A Study of How Stitch Placement Affects the Open Hole Tension Strength of Stitched Textile Composite Materials

Kathleen A. Pierucci

Clarence C. Poe

Keith Furrow

**Research And Technology Group
Materials Division
Mechanics And Materials Branch
Langley Research Center
Hampton, Virginia**

August 8, 1995

Abstract

This paper investigates the relationship between open hole tensile strength and distance between a hole and a stitch in a textile composite material. Tension tests were completed on various specimens with widths of 1 in., 2 in. or 3 in. and a constant width to hole diameter ratio of 4. The composites tested were warp knits with AS4 fibers and 3501-6 resin. Test results show a small percent change of net strength with stitch location. However, due to the large scatter in data, the small 6% change in net strength is considered negligible.

Introduction and Background

There is strong interest in using composite materials for primary airplane components. The chief advantage of composites over presently used metals is the low density of composites compared to the high density of metals. The overall weight of an airplane would be reduced thereby reducing fuel consumption. Another advantage of using composites is the stiffness of the material. By using composites, future airplane wings will have a higher aspect ratio of length to width because of the increased stiffness of the wings. This results in a more economical plane because high aspect ratio wings reduce the drag on an aircraft. The third advantage of composites over metals is that composite strength and stiffness can be tailored. Components of an aircraft will need extra strength in certain directions depending on the design of the component. Anisotropic composites can have increased strength and stiffness in different directions by laying extra fibers in the directions of the needed extra strength.

Although there are many benefits in using composite materials, the present cost of manufacturing composites is high compared to the costs of manufacturing metals. As a result, an effort has been made to develop cheaper methods of fabricating composites without a large decrease in strength or stiffness. One of these new methods being researched is mechanically stitching dry textile preforms. Fibers in the dry fabric are oriented in different directions, depending on where the most strength is needed, and then sewn together by machine. After being stitched together, the material is cut to the desired size and shape. Resin is used to harden the material, and bind the layers together. This was accomplished by resin transfer molding (RTM), in which the material is impregnated with resin and cured. This new method has been proven to be more cost effective than present manufacturing techniques. Stitching has also been found to reduce delamination after impact.

Before stitched composites can be used regularly in commercial aircraft, the mechanical properties of composites must be tested. Further tests are needed to determine the ability to machine and fabricate final products from stitched composite parts. One concern about the fabrication of the final components was the effect of hole placement near a stitch. The area surrounding a stitch tends to have a pocket for resin which may make that area weaker than the rest of the material. Since higher stress concentrations exist around a hole, there was concern over whether the material would be weaker in this area if a hole was drilled in a resin enriched area near a stitch. Therefore, the combination of high stresses between a hole and a stitch needed to be examined. Open-hole tension tests determined if the distance between the edge of a hole and a stitch affected the ultimate strength of a specimen.

Materials

All of the specimens tested were warp knit with 44% AS4 fibers in the $\pm 45^\circ$ and 0° directions and 12% AS4 fibers in the 90° direction. The A specimens had all seven layers stitched at once, whereas the H1 specimens had the $\pm 45^\circ$ and 0° layers stitched together as a group, and then a layer of 90° was stitched between two groups of $\pm 45^\circ$ and 0° .

Each row of stitches was sewn at 0.25 in. from the previous row in all three specimen widths. Different stitch diameters were considered for testing. The diameter of the stitches for the

H1, A1, and A2 specimens was 0.0313 in. (1/32). This type of stitch was tested for the three width sizes of 3 in., 2 in., and 1 in. However, for the A3 specimens a smaller stitch diameter of 0.156 in. (1/64) was tested. The reason for testing a small diameter stitch was a small diameter might leave a smaller area or pocket than a large diameter stitch. Since resin tends to collect in pockets near a stitch, a small area around a stitch was believed to collect less strength-reducing resin than a large area around a stitch. However, this small diameter stitch was tested only in the 1 in. wide composites.

Different diameter holes were core drilled into the specimens. This type of drilling involves a cylindrical-shaped drill-bit grinding a hole through the material. The ratio of the width to the hole diameter of each specimen was kept constant at 4. The hole diameters were 0.25 in., 0.5 in., and 0.75 in for the width sizes of 1 in., 2 in., and 3 in. respectively. The edge of the holes were located either touching a stitch, close to a stitch, or far from a stitch. For each specimen width, at least 3 specimens were tested with each hole location. A sample specimen can be seen in Figure 1.

Procedures

Each specimen was measured, with a caliper, for width, thickness, diameter, and distance of the longitudinal tangent of the hole from the nearest stitch. The width and thickness were needed to calculate the cross sectional area of the specimen. The thickness of the specimen was measured on both sides of a hole, and the average of the two measurements were recorded as the thickness. The diameter of the drilled hole was measured to check for consistency. The distance of the longitudinal tangent of the hole from the stitch was measured in order to compare the hole placements of each sample.

After each specimen was measured, the ends of the specimens were taped to protect the grips of the tension machine. The specimen was placed squarely in the lower grip of the tension machine and the upper grip was maneuvered around the upper portion of the specimen and closed. The machine applied a load to the specimen at a rate of 0.05 in./min. until fracture. The ultimate tensile load was recorded from each experiment for later comparison. Specimens were tested in groups according to the width, and then hole placement with the largest specimens tested first.

The tension testing machine for the largest specimens of 3 in. width was a Materials Testing Machine (MTS) Hydraulic Fatigue Test System, with a 100 KIP capacity. The machine was controlled with a MTS 458.20 microconsole. For the two smaller widths of 2 in. and 1 in., a MTS Hydraulic Fatigue Test System, with a 50 KIP capacity and MTS 458.20 microconsole was used for testing. A computer was connected to the microconsoles to read the output signals. The data acquisition software program plotted the load vs. the grip stroke.

Results

The net open-hole tensile strength of the each specimen versus the distance of the edge of the hole from the stitch was graphed. The net strength allowed for specimens of different cross sectional areas to be compared. Calculations of the net strength were made by the following formula:

$$(1) \quad \text{Net Strength} = \text{Load} / ((\text{Width-Diameter}) * \text{Thickness})$$

The average net strength of all the specimens by type, by size, and by the location of the edge of the hole can be seen in Table 1. The net strength was used to calculate the percent of scatter in the data. The difference between the highest and lowest net strengths of specimens with the same size, stitch diameter, and stitch technique were divided by the net strength of the highest specimen as in the following equation:

$$(2) \quad (\text{Highest net strength} - \text{Lowest net strength}) / \text{Highest net strength}$$

For the largest width size of 3 in., both the H1 and the A2 specimens were graphed together for comparison between materials. As can be seen in Figure 2, the distance between the edge of the hole and the stitch did not affect the ultimate strength of either material. The average strength of the H1 material with the edge of the hole close to the stitch (HC), was compared with the average of the H1 with the edge far from the stitch (HF). Although there was a slight 2.3% decrease in the average strength of the H1 specimens from HC to HF, Figure 2 shows the scatter of the data points was as high as 7.4%. With this high percentage of scatter, it can not be concluded that the strength changed significantly when the distance between the edge of the hole and the stitch decreased. The average net strength of the A2 specimens with the edge close to the stitch (A2C) was 79.33 ksi, and the average net strength of the specimens with the hole far from the stitch (A2F) was 73.82 ksi. The A2 specimens similarly showed a decrease in average net strength of 6.9%, but with as much as a 10.5% scatter of data. Since the scatter of data was higher than the change from A2C to A2F, it was concluded that the change was negligible. Figure 2 also shows that the open-hole tension strength of the H1 and A2 Specimens are similar even though the H1 has a different stitching technique

Results from the tests with the 2 in. wide H1 and A1 specimens are shown in Figure 3 and Figure 4. In Figure 3, the average net strength of the H1 with the edge close to the stitch (HC) was 78.24 ksi. This strength is 1.8% less than the average net strength of 79.65 ksi for the H1 with the edge far from the stitch (HF). The percent scatter of the points was 11.4%, which was higher than the decrease in net strength of 1.8%. As a result, the change in strength was negligible when compared to the higher percent scatter of data. As can be seen in Figure 4, the average net strength of the A1 specimens that had the edge close to the stitch (A1C) was 86.04 ksi. The average net strength of the A1 specimens that had the edge far from the stitch (A1F) was 86.28 ksi, which was less than 1% higher than the A1C specimens. This change in average net strength was especially low when compared to the other tests. Since the 21.7% scatter of data was significantly higher than the change of net strength, the change in net strength was considered to be negligible. The average strengths of the H1 for the 2 in. wide specimens was lower than the A1 specimens even though the H1 had a different stitching technique.

The results of the 1 in. wide specimens can be seen in Figure 5, Figure 6, and Figure 7. In Figure 5, the H1 specimen with the tangent close to the stitch (HC) had an average net strength of 90.65 ksi. This net strength was 5.7% lower than the net strength of 96.16 ksi for the H1 with the edge far from the stitch (HF). However, the scatter of data was 15.5% which was higher than the percent change in the net strengths of the specimens. The change in strength from HC to HF was considered to be negligible since the percent scatter of data was higher than the percent change in strength. In Figure 6 it can be seen that the A1 specimen with the edge close to the stitch (A1C) had an average net strength of 93.97 ksi. The A1C net strength was 8.0% lower than the average net strength of 102.17 ksi for the A1 specimen with the edge far from the stitch (A1F). However, since the scatter of data was 13.5%, the 8.0% change on net strength was considered negligible. A third set of tensile tests was conducted with 1 in. wide A3 specimens. These specimens had a smaller stitch diameter of 0.0156 in. as compared to the stitch diameter of 0.0313 in. used in the A1 and H1 specimens. As can be seen in Figure 7, the average net strength of the A3 specimens with the edge close to the stitch (A3C) was 94.25 ksi. This net strength was 7.8% lower than the average net strength of 102.17 ksi for the A3 specimen with the edge far from the hole (A3F). The scatter in data was 12.4%, which was more than the change in net strength.

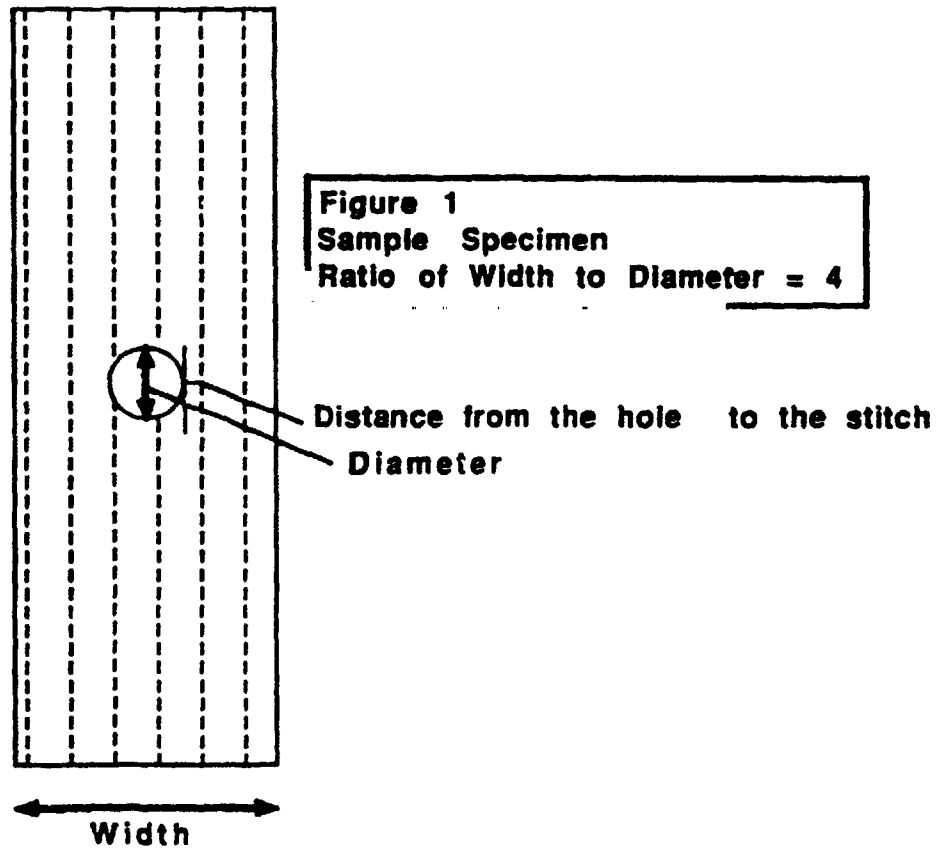
Conclusions

In conclusion, all the specimens had a percentage of scatter higher than the percent change in net strength. As a result, there was no significant change in strength due to hole location near a stitch. Future tests should focus more on why the percent scatter of data was so high, and more tests with hybrid material. Hybrid material uses the same stitching technique as the H1 specimens but has stronger IM7 fibers in the 0° direction.

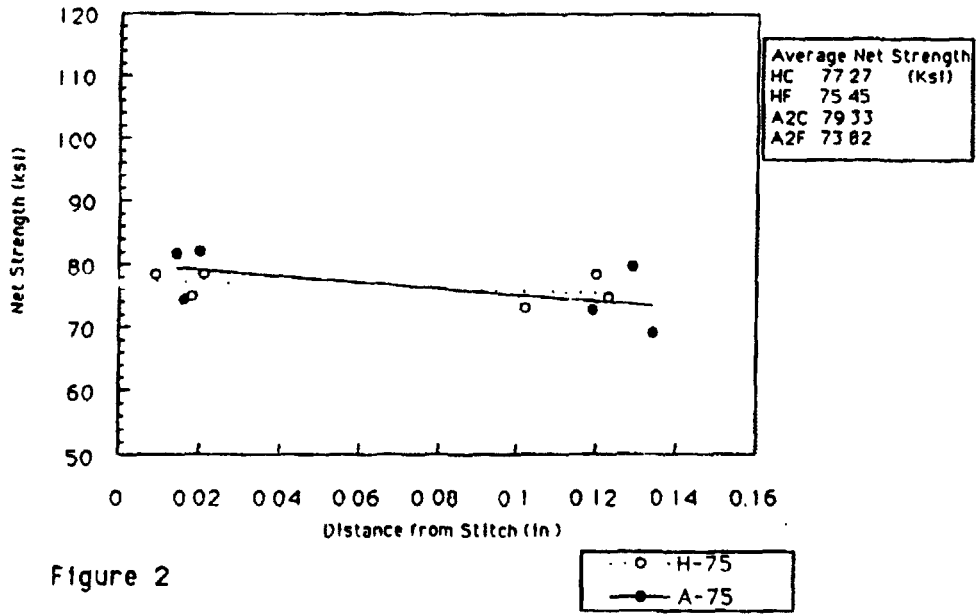
References

Hawley, Arthur V., "Development of Stitched / RTM Primary Structures for Transport Aircraft," NASA Contractor Report 191441, NASA Contract NS1-18862, July 1993.

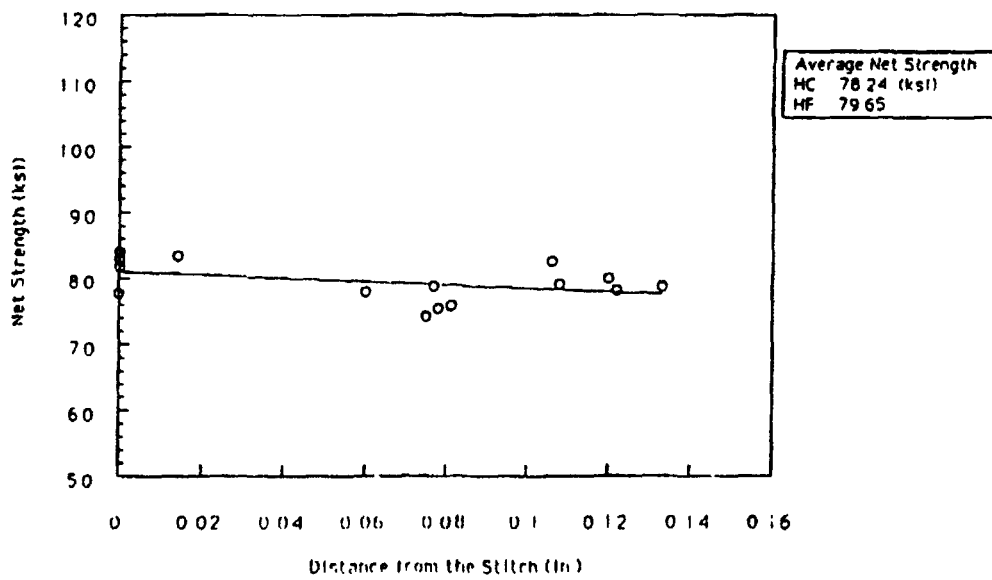
Table 1					
Material	Width (in.)	Ave. Net Strength (ksi)	Material	Width (in.)	Ave. Net Strength (ksi)
Hybrid Close (HC)	3	77.27	Hybrid Close (HC)	1	90.65
Hybrid Far (HF)	3	75.45	Hybrid Far (HF)	1	90.16
A2 Close (A2C)	3	79.33	A1 Close (A1C)	1	93.97
A2 Far (A2F)	3	73.82	A1 Far (A1F)	1	102.17
Hybrid Close (HC)	2	78.24	A3 Close (A3C)	1	94.25
Hybrid Far (HF)	2	79.65	A3 Far (A3F)	1	102.17
A1 Close (A1C)	2	86.04			
A1 Far (A1F)	2	86.28			



Net Strength Vs. Distance of the Hole from the Stitch for H-75 and A-75



Net Strength Vs. Distance of the Hole from the Stitch for All H150



Net Strength Vs. Distance of the Hole from the Stitch for All A150

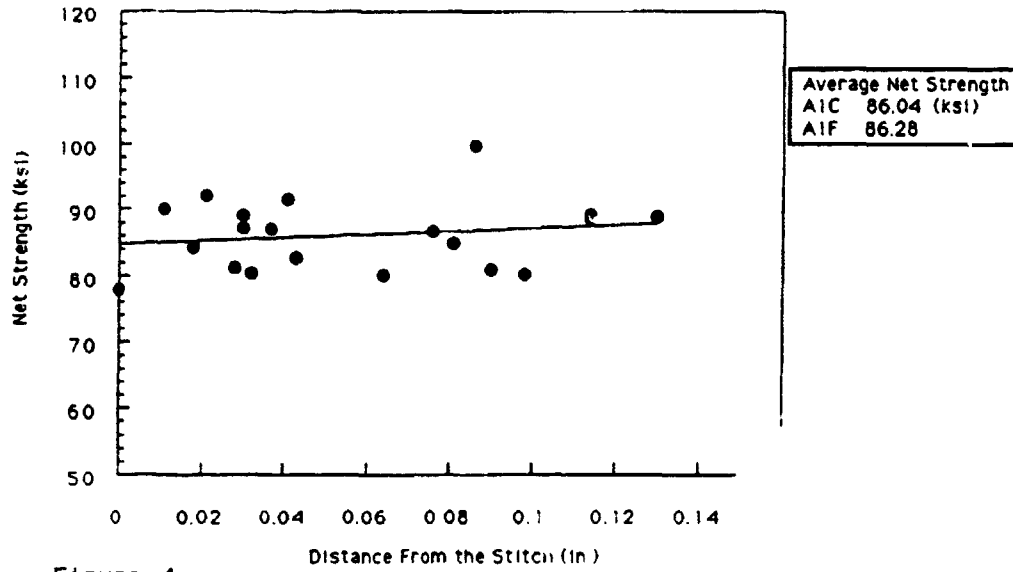


Figure 4

Net Strength Vs. Distance of the Hole from the Stitch for All H125

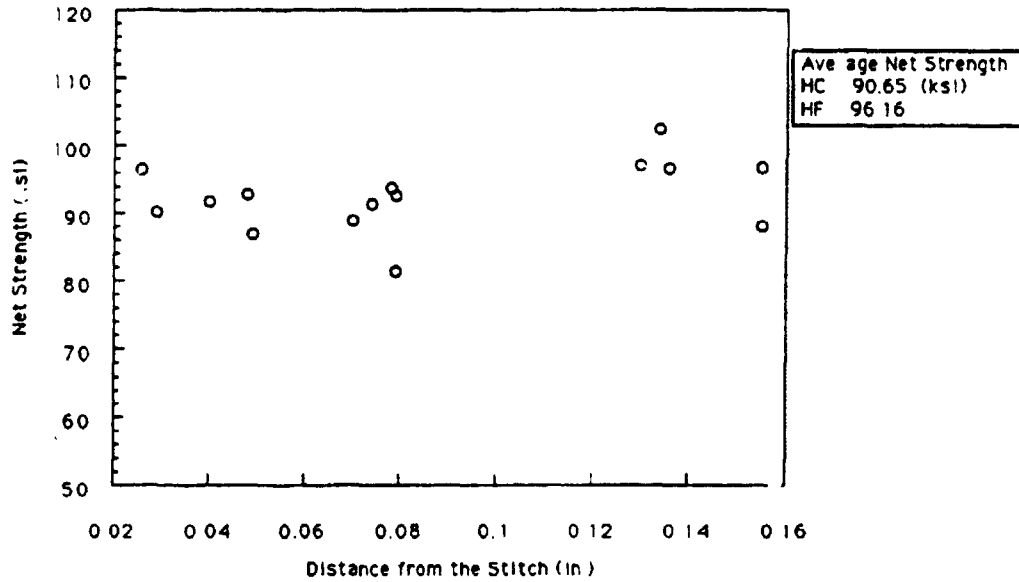


Figure 5

Net Strength Vs. Distance of
the Hole from the Stitch for All A125

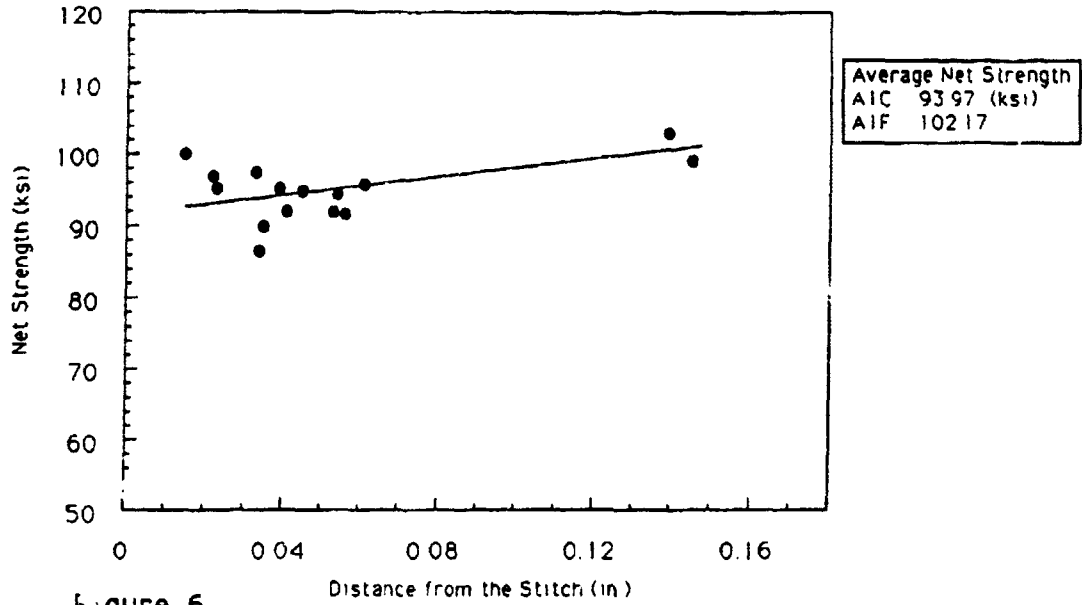


Figure 6

Net Strength Vs. Distance of
the Hole from the Stitch for All A325

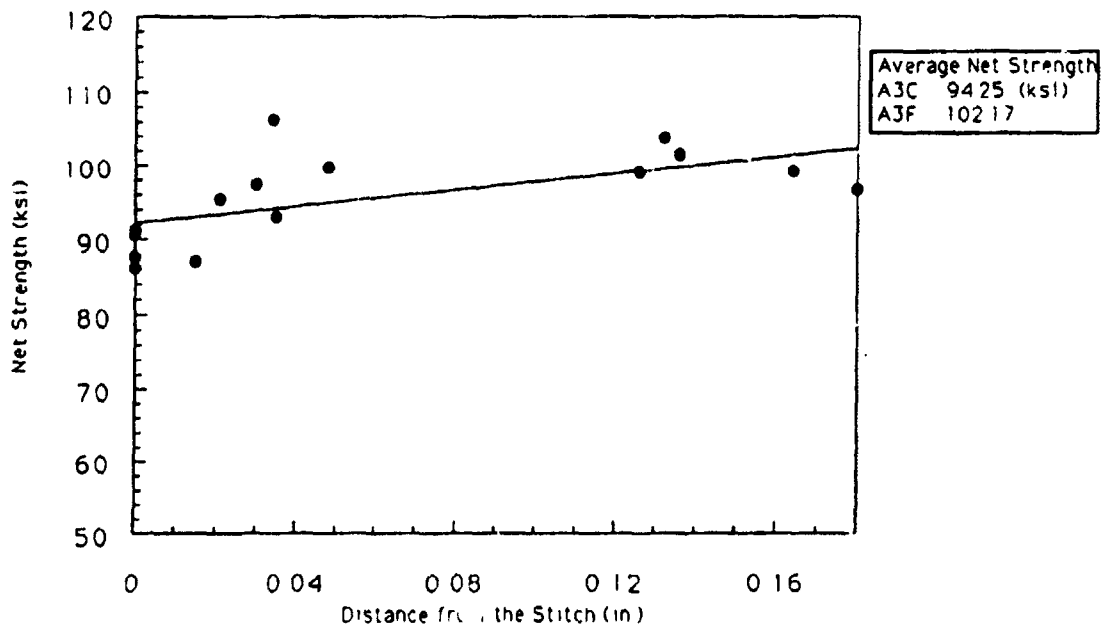


Figure 7

**NEXT
DOCUMENT**

TAG CD-ROM

Myrna Syamara Rivera

Stuart Pendelton

Technology Applications Group

ABSTRACT

The purpose of this project was to produce a CD-ROM for the Technology Applications Group. The CD was being developed to allow interested people, organizations, or companies to view the technologies available to them that were developed by NASA research. The CD's main audience however, is any small business. The CD will give the small business an opportunity to see what technologies are available in an inexpensive manner. Most companies probably have a CD-ROM drive on their computers but may not have access to the internet. By using only the internet to inform on the technology, NASA was not considering a large segment of the population. The CD-ROM can now cover that group of the population.

INTRODUCTION

One of the main focuses of the Technology Applications Group (TAG) is to transfer technology from NASA to industry. To aid in the transfer of technology, TAG decided to inform the public of the available technologies through two means. The first is through the internet and the second is by way of CD-ROM. Although a large portion of the population does have access to the internet, many individuals and small companies cannot afford to use it. On the other hand, many people and companies have access to a CD-ROM drive or are able to purchase one at an affordable price. It is these people who we want the CD-ROM to reach.

SUMMARY

APPROACH

I arrived in the TAG office two weeks early to develop a plan and design for our CD-ROM. We had initially intended on killing two birds with one stone by embedding the Netscape or MOSAIC browser into the CD-ROM along with a translator. The translator was to translate our data into HTML. So, the information which we obtained and the screens which we made would have been viewable not only on the CD-ROM, but also on the world wide web. We were unable to get Netscape to work with us, however after several weeks of working with MOSAIC, they decided to work with us. Unfortunately, by the time MOSAIC reached their decision, time had come for us to get started one way or another and we started without MOSAIC. Next year however, the next group will be able to embed the MOSAIC browser into their CD. This year, our work can only be viewed via CD-ROM.

EQUIPMENT

My group was chosen for this program as a result of our knowledge of HTML. We however, could not apply what we already knew and had to start from scratch. We had to learn how to use new software and hardware. The hardware included: Macintosh computers, CD-ROM writer, and scanner. Our software included: MicroSoft Word, FoxPro, Adobe Premiere, Adobe Illustrator, ColorIt, Impact, PageMaker, and Photoshop.

RESULTS

We have developed a CD-ROM which will be completed within the next two weeks. I believe that it was a good first attempt. Teams that work on this project on the future will hopefully be able to take this much further than we have taken it. Hopefully, they will already have more knowledge on the use of the hardware and software and will not have to spend as much time learning how to use the software before getting started.

Also, the next team will probably have a better understanding of what is to be developed because they have something on which they can already go on, our CD.

**NEXT
DOCUMENT**

***Correlations of Different Surfaces Tests,
Tire Behavior Math Model for the High
Speed Civil Transport (HSCT)
and
Michelin Tire Properties Tests for
Boeing 777***

Iván Román

Robert H. Daugherty

Structures Division

Structural Dynamics Branch

Aircraft Landing Dynamics

Abstract

In the surfaces correlation study, several different volumetric and drainage measurement techniques for classifying surface texture were evaluated as part of a major study to develop and improve methods for predicting tire friction performance on all types of pavement. The *objective* of the evaluation was to seek relationships between the different techniques, and to relate those results to surface frictional characteristics. We needed to know how each of the tests could be related to each other.

Another of my assigned projects was to make a tire behavior math model for the High Speed Civil Transport (HSCT) using the same methods used for the space shuttle a few years ago. A provided third order equation with two variables was used. This model will also be used for studies with the Boeing 777. Only a few changes will be necessary to adapt it for this other aircraft, which is the newest offered by Boeing.

In my final project I was involved with testing the tires for this new aircraft using the Aircraft Landing Dynamics Facility (ALDF) test carriage within the carriage house (Bldg. 1261) at LaRC. A 50 inch diameter radial tire manufactured by Michelin Aircraft Tire Corporation had to be tested to double overload of 114,000 pounds. The rated load of each tire is 57,000 pounds, but Boeing required tests assuming failure of a companion tire that could have cost Michelin approximately \$12 million to build a facility to provide the required test capability. Here at LaRC, only minimum modifications to the facility were required to perform this specific test.

Introduction of Correlations

It has long been recognized that the texture characteristics of a pavement surface can directly influence the frictional forces which pneumatic tires can develop for accelerating, steering, and braking. Many different devices and techniques have been developed to provide quantitative measurement of surface texture, and these efforts have identified two texture classifications, micro- and macrotexture. In general, microtexture consist of the fine, small-scale surface features such as those found on individual stone particles, whereas macrotexture encompasses the coarse, large-scale roughness of a pavement surface-aggregate matrix. Results from studies to evaluate the effects of speed on tire friction have indicated that the slope of the friction-speed gradient curve is primarily a function of the surface macrotexture. On that basis, it would appear that an assessment of both surface micro- and macrotexture characteristics is necessary to relate texture measurements with tire frictional performance.

Explanation of Some Equipment and Test Procedures

Comparative measurements were collected in this study using several different pavement classification techniques which included *volumetric types, drainage devices, a skid resistance tester, and another which uses light beam calibration procedures.* Surface preparations were followed during the operation of each technique on sixteen different concrete and asphalt surfaces located at Langley Research Center (NASA), Wallops Flight Center (NASA) and at Cranfield University. For each technique, a stiff, wire-bristle brush was applied vigorously to the surface test area prior to measuring to remove all loose stones, debris, and other contaminants. A minimum of six measurements were taken at different locations on a given surface. Data was collected using all the techniques on the same test area of a given surface. For each technique, an average value was calculated from the individual measurements taken on each test surface. A general description of some of the different equipment and test procedures used for the various techniques follows.

Volumetric Methods:

The volumetric methods involved spreading a known volume of a given material on a pavement surface to fill all voids, measuring the area covered, and computing values of the average texture depth by dividing the material volume by the spread area. The dissimilar material properties required different measurement procedures, as well as different equipment.

The sand patch method was developed at the British Road Research Laboratory, and is one of the first methods used to determinate surface texture. The technique used in this procedure consists of pouring a known volume of fine, dry sand on the pavement, spreading it over a circular area, and using a hard round puck similar to that used in ice hockey, leveling the sand with the tips of the asperities (peaks). A small, open-ended, wood frame provided the test surface area with protection from the wind during each sand patch application. The *average surface texture depth* is obtained by *dividing the volume of sand used by the area covered*.

Another method used in this study is the grease patch method. For this method a metal cylinder with an internal volume of about 16,000 mm³ (aprox. 1 cubic inch) is used. The actual volume is not critical, provided it is accurately known. Suitable dimensions based on an accurate 1 inch internal diameter pipe would be a diameter of 25.4 mm and a length of 32.3 mm. Other secondary requirements are a putty knife, a tight fitting plunger, a rod to expel the grease from the cylinder, a rubber faced aluminum or wooden squeegee some 30-40 mm in width, and masking tape. In this method the test cylinder is first packed with any general purpose grease using the putty knife in such a way as to avoid entrapping air and the ends are squared off using the putting knife. Two parallel lines of masking tape are placed at right angles to and at one end of the test area and worked in the voids in the surface to the levels of the peaks of the surfacing and in a rectangular shape between the parallel masking tape. Care is to be taken so that no grease is left on the masking tape or squeegee. Measure the volume of the test cylinder and the dimensions of the grease patch. The average surface depths of the voids is given by the equation:

$$\text{Surface_Texture_}(mm) = \frac{\text{Volume_of_Grease_}(mm^3)}{\text{Area_Covered_}(mm^2)}$$

Two spreaders were available - NASA and Cranfield. The NASA spreader consist of a flat piece of metal approximately 40 mm by

150 mm to which a strip of rubber has been stuck to act as the squeegee. The Cranfield spreader is shaped like a shepherd's crook with a wooden handle and metal head on to which the 40 mm wide rubber squeegee has been stuck. As part of the objectives I tried to determine the differences between both set of values.

Drainage Methods:

The basic static water drainage meter, commonly referred to as an *outflow meter*, consists of a transparent plastic cylinder to contain water and a brass base plate with a rubber ring attached to the bottom face. The cylinder is placed on the pavement and loaded so that the rubber ring will contact the surface aggregate particles in a way similar to that expected of a tire tread element. Water is poured into the cylinder, and a clock measures the time required for a known volume of water to escape through the pores or grooves in the pavement and between the rubber ring and the pavement surface.

Skid Resistance Tester:

The British pendulum skid resistance tester is a dynamic pendulum impact-type tester used to measure the energy lost when a rubber slider edge is propelled over a test surface. The British Pendulum Number (BPN) values measured for flat surfaces represent the frictional properties obtained with the apparatus using recommended procedures. Since pavement surface temperature measurements were taken during all test, the average BPN values on each test surface were temperature-corrected by a nonlinear factor established during a British Road Research Study.

Other:

The Texture Van, developed by Penn State University, is a test where a computer collects data from a frame grabber that looks at a 3 mm by 51 mm rectangular beam of light that is flashed onto the pavement. This produces a shadow effect on both edges which are called Leading and Trailing edges. RMS (Root Mean Square) values are calculated from these edges to be used in results.

Another kind of test was the Texture Beam. It has two types of measuring devices, an infrared laser and a LVDT for measuring texture. The beam has a trolley that is motor powered and carries the measuring devices. A computer collects the data and is displayed in real time.

As part of my work, I did not actually conduct these types of tests. Rather, I had to study and learn how each of these tests work so as to make the best correlation between the different tests.

Results

From all the data collected I made different charts that provided me with a visual meaning of the data and how the different tests are related. With Tom Yager's (Senior Project Engineer) and Robert H. Daugherty's (my mentor) help I could find some of the outlying points and which tests are related or similar. Also, I had to work with the equations for the best curve fit to each correlation. One tries to obtain the nearest value of r to 1 ($r=1 \implies$ the best curve fit), but one must keep in mind the real meaning of the curve obtained. I conducted comparisons between the different tests which were made the last year on similar surfaces. Generating more charts showed the differences found between all the values.

The first of my other two projects involved an HSCT tire model consisting of a worksheet made in MS-Excel to calculate a curve fit to a set of bi-cubic test data. The worksheet could be modified for different coefficients, yaw angles, and rated load factors. As soon as the required data was obtained, MatLab was used to make two different matrices (one for the positive side and one for the negative side) using the sign conventions for the yaw angle and side forces used in LaRC to plot the graphs requested. After this, John Tanner (NASA Engineer) used another plotting software to make a 3D surface using the data sets that the model provided.

My other project with the Michelin tires was slow. We had a few problems with the adhesive used in the sand paper to increase the friction on the surface. A new kind of adhesive used in France for the same purpose was procured to continue the tests. As soon as we obtained the adhesive we started again. Michelin needs three main kinds of tests; *a) Unyawed Relaxation Length - Zero yaw, pull side load up to 47,000 pounds, roll tire forward slowly,* *b) Yawed Relaxation Length - Yaw tire up to ± 18 degrees, no side pre-load, roll*

tire forward slowly and c) Breakaway Friction - Pull static load up to 80,000 pound with tire stationary required from Boeing.

As part of this project I was involved in taking data and operating the track data system in the Instrument Room. The procedures consisted of the Test Engineer (Robert H. Daugherty) informing the technician what load to apply to the test article for each test. He had to be on the phone with me to advise me when to commence and cease taking data.

I was learning about how the data system used works. Also I had the opportunity to see how can you make the plots needed and how to extract the data that you need from the system. On one occasion I had the opportunity to see a strange behavior on one of the plots made by the computer. This behavior suggested there was a problem in test wheel axle, and upon physically looking at the axle a small metal spacer had failed.

This testing will continue for another month.

**NEXT
DOCUMENT**

The Use of the Internet to Support General Aviation Research

by

James H. Rowbottom

**Mentor: Gretchen L. Gottlich
Information Systems Division
Advanced Computer Systems Branch
NASA Langley Research Center**

Abstract

For the past few years, innovation in the field of General Aviation (GA) has declined. The reason for this decline has not been because of a lack of ideas, but rather a lack of funds necessary to convert these ideas into reality. NASA implemented the Small Business Innovative Research (SBIR) program in an effort to promote new technology in General Aviation. Under this program, small business with good ideas present them to NASA who reviews them and determines their value potential in the GA market. If the company's idea proves worthy, NASA subsidizes their research in three phases that include the research, testing, development, and production of their product. The purpose of my internship this summer was to use the Internet to promote the work of SBIR companies globally to prospective investors.

The Use of the Internet to Promote General Aviation Research

My studies as an Aviation Professional major at Norfolk State University have instilled in me a desire to follow the latest innovations being researched in General Aviation equipment. As an active duty member of the U.S. Navy and an aspiring Naval Aviator, seeking ways to make flying safer by improving equipment and reducing pilot workload are the primary focuses of my education. My internship at NASA Langley Research Center (LaRC) offered me a chance to promote new aviation technology on the Internet, an interactive global network of multimedia communications that is accessed daily by thousands of individuals and businesses all over the world.

When I first arrived at NASA, I could not even define the word "Internet". My knowledge of it consisted of knowing it existed and that I knew nothing about it. My new mentor and boss for the next ten weeks invited me to a class she was implementing at NASA that taught the basics of the Internet, and how to use a World Wide Web browser. I sat down at a MacIntosh (all I had ever used was a PC based computer) and jumped into this electronic realm of no return. What I found was that the Internet had been revolutionized; it was no longer just a text-based system of mumbo-jumbo but now there were images, sound, video, and more information than I could want in a lifetime. This was called the World Wide Web (WWW) and was a new way of searching the Internet. Needless to say, I got overwhelmed my first day and became frustrated because I knew I was going to be a useless piece of baggage on this project.

I chose to go for it anyway. I spent the next week staring at the 21" monitor of my "personal" MacIntosh Centris 650 (which I still didn't know how to operate yet), and "surfing", not sure of what I was looking for. I buried my face for hours in a MacIntosh user manual and got myself familiar with my new information platform. I also spent countless hours trying to learn Hypertext Markup Language (HTML), the programming language used to author home pages on the World Wide Web. Once the basics were learned, I began to produce work.

The two SBIR companies Tonette Scott and I worked with were Vision Micro Designs, Inc. and Innovative Aerodynamic Technologies. Our assignment was to produce home pages promoting their aviation research and complete the pages prior to the annual Experimental Aircraft Association (EAA) Fly-in Convention scheduled for July 27-Aug 2. For the first week or so, we struggled to get all the information necessary to produce home pages for the companies. At the same time, we were given the assignment of structuring and teaching a World Wide Web class to the faculty of NASA LaRC. Since only three weeks had passed since my first surfing experience, this was going to be a chore. Nevertheless, we tucked our shoulders and took on our assignments head-on.

The WWW classes proved to be the most challenging part of the internship. Tonette and I sat down and discussed the things that made learning the Web difficult for us and developed a class around this. Our classes for the most part consisted of individuals with little to no Internet experience. Since the WWW is now the way NASA transfers technology and information within and outside the base, it is essential that NASA employees learn to use this tool. Over the course of eight weeks, Tonette and I taught up to six class per week, up to ten students per class, and successfully educated (some more than others) over 300 NASA faculty and visiting elementary school teachers from all over the country. The very positive feedback we received from the forms filled out by each of the students reassured me that my handicapped efforts were not in vain.

While continuing to teach the classes, Tonette and I continued to work on the Web pages. Numerous hours were spent learning more HTML, typing and revising information, scanning images on the color scanner in the Data Visualization Lab (I also had to learn how to use a scanner and Adobe Photoshop), and loading the files and links into a web server. One week before the airshow, we had completed the home pages and had become NASA Langley resources for World Wide Web information and instruction.

The final and most exciting experience of my internship came when I was awarded travel funds and a flight line pass to the Oshkosh airshow. Tonette and I traveled on Friday morning to Oshkosh and helped support the efforts of the NASA World Wide Web team who displayed our home pages and presented NASA's developments in information technology transfer using the World Wide Web. Our booth was visited by a majority of the estimated 1,000,000 pilots and airshow enthusiasts who attended, including NASA Administrator Dan Goldin. Our presentation was extremely successful and we received extremely positive feedback from Administrator Goldin, as well as from Thayer Sheets, the director of the NASA SBIR program.

After returning from the airshow, the remainder of our internship was spent improving the WWW class, teaching the class, and researching the various General Aviation applications of the Internet.

**NEXT
DOCUMENT**

5200

1-11-11

Aviation Research and the Internet

LARSS Student: Antoinette M. Scott
Mentor: Gretchen L. Gottlich
Information Systems Division (ISD)
Advanced Computer Systems Branch (ACSB)
NASA Langley Research Center

Objective: To promote the importance of aviation research, by use of the Internet.

The Internet is a network of networks. It was originally funded by the Defense Advanced Research Projects Agency or DOD/DARPA and evolved in part from the connection of supercomputer sites across the United States. The National Science Foundation (NSF) made the most of their supercomputers by connecting the sites to each other. This made the supercomputers more efficient and now allows scientists, engineers and researchers to access the supercomputers from their own labs and offices. The high speed networks that connect the NSF supercomputers form the backbone of the Internet.

The World Wide Web (WWW) is a menu system. It gathers Internet resources from all over the world into a series of screens that appear on your computer. The WWW is also a distributed. The distributed system stores data information on many computers (servers). These servers can go out and get data when you ask for it.

Hypermedia is the base of the WWW. One can "click" on a section and visit other hypermedia (pages). Media, the type of data you would find on the Internet, can be ASCII text, a postscript @ file, an audio file, a graphic image, or any other sort of data that can be stored in a computer file.

Our approach to demonstrating the importance of aviation research through the Internet began with learning how to put pages on the Internet (on-line) ourselves. We were assigned two aviation companies; Vision Micro Systems Inc. and Innovative Aerodynamic Technologies (IAT). We developed home pages for these SBIR companies which can now be seen on-line (<http://beginning.larc.nasa.gov/oshkosh/vm1000.html/> and <http://beginning.larc.nasa.gov/oshkosh/iat.html/>).

The equipment used to create these pages were the UNIX and Macintosh machines. HTML Supertext software was used to write the pages and the Sharp JX600S scanner to scan the images.

As a result, with the use of the UNIX, Macintosh, Sun, PC, and AXIL machines, we were able to present our home pages to over 800,000 visitors at the EAA Fly-in Convention in Oshkosh, Wisconsin. Over half of the visitors were pilots. We were not only to display our home pages, but gave them hands on experience on how to use the Internet to benefit their needs in aviation research. We were able to locate weather information for any state, Fixed Based Operators (FBO's), Federal Air Regulations (FAR's) and much more data that would benefit pilots.

Before our research began, who would have ever thought of using the Internet as a tool for aviation research? Now the question is, "How can you live without it"?

**NEXT
DOCUMENT**

..7
/.

**Development of a Pressure Sensitive Paint System With Correction
For Temperature Variation**

Student: Kantis A. Simmons

Mentor: Dr. Billy T. Upchurch

**Internal Operation Group
Experimental Testing Technology Division
Acoustic, Optical, and Chemical Measurement Branch**

DEVELOPMENT OF A PRESSURE SENSITIVE PAINT SYSTEM WITH CORRECTION FOR TEMPERATURE VARIATION

Kantis A. Simmons*
NASA Langley Research Center (LARSS)

Donald M. Oglesby*
Old Dominion University

Billy T. Upchurch*
NASA Langley Research Center

ABSTRACT:

Pressure Sensitive paint (PSP) is known to provide a global image of pressure over a model surface. However, improvements in its accuracy and reliability are needed. Several factors contribute to the inaccuracy of PSP. One major factor is that luminescence is temperature dependent. To correct the luminescence of the pressure sensing component for changes in temperature, a temperature sensitive luminophore incorporated in the paint allows the user to measure both pressure and temperature simultaneously on the surface of a model. Magnesium Octaethylporphine (MgOEP) was used as a temperature sensing luminophore, with the pressure sensing luminophore, Platinum Octaethylporphine (PtOEP), to correct for temperature variations in model surface pressure measurements.

* Undergraduate Summer Research Student, Norfolk State University, Department of Chemistry, Norfolk, VA 23450

* Research Professor, Department of Chemistry and Biochemistry, Old Dominion University, Norfolk, VA 23539-0126

* Senior Research Scientist, Langley Research Center, MS 234, Hampton, VA 23861-0001

INTRODUCTION:

Measuring surface pressure on a wind-tunnel model is an important analytical tool in fluid mechanics. The most common technique used to measure pressure is the use of pressure taps. The use of pressure taps is a complex and expensive process. Efforts to find more effective ways to measure model surface pressure have led to the development of pressure sensitive paint (PSP).

Pressure Sensitive Paint is a luminescent paint which consist of a luminophore (fluorescent or phosphorescence chemical) that is dissolved in a polymer/solvent matrix. The luminophore is chosen from those which are quenched by oxygen. The paint mix is applied to the surface of the model and allowed to cure. The pressure is then determined by measuring the light emitted from the illuminated model. The intensity of the emitted light is inversely proportional to the oxygen's partial pressure, and may be represented by a modified form of the classical Stern-Volmer equation.

$$\frac{I_{ref}}{I} = A + BP \quad (1)$$

The " I_{ref} " is the emission intensity at some reference pressure. " I " equals the emission intensity at air pressure " P ". " A " is the y-intercept and " B " represents the slope of the plot of I_{ref}/I vs. pressure.

When using a PSP in a wind tunnel, I_{ref} is experimentally measured and a calibration curve is established by measuring " I " as a function " P ", using pressure taps on the model to measure the calibration pressures.

Peterson and Fitzgerald first reported the use of fluorescence quenching by oxygen for flow visualization of oxygen and nitrogen gas streams, but did not extend their concept to air pressure measurements (1). Russian researchers published the use of PSP for air flow visualization and pressure measurement in wind tunnels (2). NASA-Ames in conjunction with the University of Washington, used platinum octaethylporphine in a polydimethylsiloxane paint matrix for luminescent barometry in a wind tunnel (3). Crites of McDonnell Douglas, presented a thorough summary of measurement techniques based on the oxygen quenching of the fluorescence and phosphorescence luminophores (4).

Pressure Sensitive Paint has proven to be a valuable technique for measuring global pressure, but the accuracy and reliability has not yet been established. Some of the deficiencies that need to be remedied are: (1) PSP luminescence is temperature dependent. (2) All PSP's undergo some photodegradation, but there are some that are worse than others. (3) PSP luminescence is illumination intensity dependent, and an internal reference luminophore is needed to correct for variations in illumination.

We have chosen to focus our research efforts on developing a pressure sensitive paint system to correct for model surface temperature variations.

Research Plan. The conceptional approach of our research is to incorporate a luminophore in the paint which responds only to temperature changes and thus enable the user to measure temperature at any point on the model surface. By knowing the surface temperature and the emission/temperature function for the pressure sensing luminophore, a correction may be made

for the effect of temperature on the pressure sensing luminophore. Candidate temperature sensing luminophores (TSL) that are compatible with proven pressure sensing luminophores (PSL) will be investigated.

There are certain requirements that a TSL must have for it to be considered a compatible luminophore. First, the excitation wavelength of the TSL must be compatible with the excitation wavelength of the PSL. The emission wavelength of the TSL must not overlap the emission wavelength of the PSL. The emission peaks should be separated by at least 50 nm. The TSL must be chemically compatible with both the PSL and the paint matrix. Finally, a good TSL must be spectroscopically compatible with the PSL. This means that one luminophore must not excite the other luminophore.

EXPERIMENTAL:

Chemicals: Radelin 1807-Zinc Cadmium Sulfide [(Zn,Cd)S:Ag:Ni] (Luxton Co., Mountain View, CA.) were used as supplied without further purification. The phosphors of Ruthenium (II)-(4,7-diphenyl-1,10-Phenanthroline), Platinum octaethylporphine (PtOEP) and Magnesium Octaethylporphine (MgOEP), (Porphyrin Products Inc., Logan, Utah) were used as supplied. Polymers used in paints included Poly(2-ethylhexylmethacrylate-co-isobutylmethacrylate) (University of Washington, Seattle, WA), and silicone rubber (RTV-118, General Electric Co.). Solvents (toluene and acetone) were analytical grade or better (Sigma Aldrich Co.).

The dual luminophore paint was prepared as following: 500 ppm of PtOEP and 300 ppm of MgOEP were dissolved in a 1 part IEMA (polymer) to 10 part toluene.

Method: Two proven pressure sensing luminophores, Ruthenium bathophenanthroline (RuB) and Platinum octaethylporphine (PtOEP), were considered in this study. Candidate temperature sensing luminophores were selected from published spectral characteristics. These published properties were compared to spectral characteristics of the two PSL's as shown in Table I. Two of the phosphors; Radelin 1807-Zinc Cadmium Sulfide [(Zn,Cd)S:Ag:Ni], and the Magnesium octaethylporphine [MgOEP] were chosen for study with either of the two pressure sensing luminophores.

Candidate luminophores were tested by studying each of them separately. The luminophore (either the TSL or PSL) was dissolved in a solvent/polymer matrix and sprayed on a square piece of aluminum, the material of the model, and then allowed to cure. Spectral analyses were run on a Perkin Elmer LS50B spectrofluorimeter. The emission and excitation spectra were determined for each sample. The degree of oxygen quenching was determined by measuring emission intensity as a function of air pressure in the sample cell. Emission intensity as a function of air pressure was measured for 6,8,10, 12, and 14.7 psia at 25, 30, 35, 40, and 45°C.

RESULTS & DISCUSSION

The Radelin-1807 phosphor proved to have a poor temperature response ($\Delta E/\Delta T \approx 2$ unit/°C). Also, this TSL was not compatible with either the Ruthenium bathophenanthroline or the Platinum octaethylporphine, due to unacceptable spectral overlap. The MgOEP phosphor showed acceptable temperature sensitivity results

($\Delta E/\Delta T = 18.8$ units/°C) (Figure 3). Preliminary measurements of temperature response suggested that MgOEP as a TSL would correct for temperature variation with the pressure sensing

luminophore PtOEP.

The MgOEP and PtOEP (dissolved in IEMA/Toluene) as dual luminophores were studied on the LS50B. MgOEP fluoresces at 580 nm and can be excited by light around 407 nm. PtOEP can be excited at 382 nm and emits at 644 nm, this is 60 nm away from MgOEP. The emission and excitation spectra of the two are shown in Figures 1 and 2.

Oxygen Quenching. Oxygen quenching was measured by reading the emission intensity output at 5 different air pressures. This enabled the creation of Stern-Volmer Plots (Figure 4) at various temperatures from 25°C to 45°C. From this data, the intercepts and the slopes of the Stern-Volmer plots at each temperature were established (Figure 4).

As may be seen from Figure 4, both the slope and the intercept change with temperature because I_{ref} at 25°C was used for all plots. Since both the intercept and slope change, it is necessary to establish their temperature relationship. A plot of intercept vs. temperature and a plot of slope vs. temperature are shown in Figures 5 and 6. Although the changes in these two Stern-Volmer parameters versus temperature are not exactly linear, to a first approximation a linear function may be assumed.

Temperature Response. Emission intensity as a function of temperature for the MgOEP, at different pressures is shown in Figure 3. The emission intensity from the paint at 580 nm was read, and the surface temperature was calculated using the equation

$$T = -\frac{I-a}{b} \quad (2)$$

where a = intercept and b = slope of the plot of average emission versus temperature. This plot shows that MgOEP is independent of pressure, because of the similarity of each line (Figure 3).

To exemplify the improvement of accuracy by this dual luminophore, we compare a system without correction to one using a temperature correction. Suppose there is an unknown temperature increase during the experiment, but we are assuming that the temperature has remained at 28°C. The emission intensity for PtOEP was read to be 155 units and that for MgOEP to be 1287 units. Since we are operating off the Stern-Volmer calibration curve at 28°C (Figure 4), we would calculate the pressure to be 16.1 psia using Equation 1. This would result in a 61% error in the calculated pressure, since the experimental pressure value was actually 10 psia. Using the same emission intensity as above for both MgOEP (1287) and PtOEP(155). We apply temperature correction (Equation 2) to the MgOEP emission; we calculate the corrected temperature to be 36.4°C. From Figure 5 we use the corrected intercept equation to calculate a new corrected intercept "A", to be 0.596. We use the corrected slope equation (Fig. 6) and calculate the new slope "B", to be 0.106. With the new intercept and the new slope, we determine the new corrected pressure to be 10.8 psia. Since the experimental pressure was 10 psia, this represents an 8% error compared to an error of 61% without correction. This 8% error is due to a combination of experimental error and our assumptions regarding linearity of the data.

CONCLUSION

Although a dual luminophore, temperature/pressure sensing paint gives more accurate measurements of pressure at a model surface. This paint combination still has two deficiencies that need further investigation. The photodegradation of MgOEP at 300 ppm and PtOEP at 500

ppm needs to be improved. The photodegradation decay slope of this formulation is -2.18 intensity units per minute. This might be improved by changing the ratio of the concentrations of both luminophores without affecting the intensity output.

Due to the different excitation peaks of both the MgOEP (407 nm) and PtOEP (382 nm), a broad band filter must be used for lamp illumination in a wind tunnel setting.

We have shown that the inclusion of a temperature sensitive luminophore in a PSP can significantly improve accuracy when changes in temperature occur. This will enhance the accuracy of global pressure measurements, and bring us closer to the goal of using PSP for accurate, discrete pressure measurements, an essential step towards replacing pressure taps.

REFERENCES

1. J.I. Peterson and R.V. Fitzgerald, *Rev. Sci. Instrum.* 51(5), 1980, 670-671.
2. M. M. Ardasheva, Translated from *Zhurnal Prikladnoi Mekhaniki i Tekhnicheskoi Friziki*, No. 4, 1985, 24-31. (0021- 8944/85/2604-G469) - Plenum Publishing Corp.
3. J. Kavandi, J. Callis, M. Gouterman, G. Khalil, D. Wright, D. Burns, and B. McLachlan, *Rev. Sci. Instrum.* 61 (11), 1990, 3340-47.
4. Crites, R.C., "Pressure Sensitive Paint Techniques," *Measurement Techniques*, Von Karman Institute of Fluid Dynamics, Lecture Series VKILS 1993-05, April 19-23, 1993.
5. D.M. Oglesby, C.K. Puram, and B.T. Upchurch, "Optimization of Measurements with Pressure Sensitive Paints", NASA Technical Memorandum 4695.

TABLE I

TEMPERATURE INDICATING PHOSPHORS

**** Literature Study ****

PHOSPHOR	EXCITATION WAVELENGTH	EMISSION WAVELENGTH	PtOEP Em= 644 nm COMPATIBLE	Ru(Ph ₂ phen) ²⁺ Em= 600 nm COMPATIBLE
EuTTA	345 nm	612 nm	maybe	no
Mg ₂ (F)GeO ₄ :Mn	290 nm	658 nm	no	yes
La ₂ O ₃ S:Eu	254 nm	514 nm	yes	yes
Radelin 1807, (Zn,Cd)S	365 nm	540 nm	yes	yes
Sylvania 243, Sr ₂ P ₂ O ₇ :Sn	270 nm	460 nm	no	yes
MgOEP	407 nm	580 nm	yes	maybe
Conducting Polymers	440 - 490 nm	630 - 670 nm	maybe	maybe

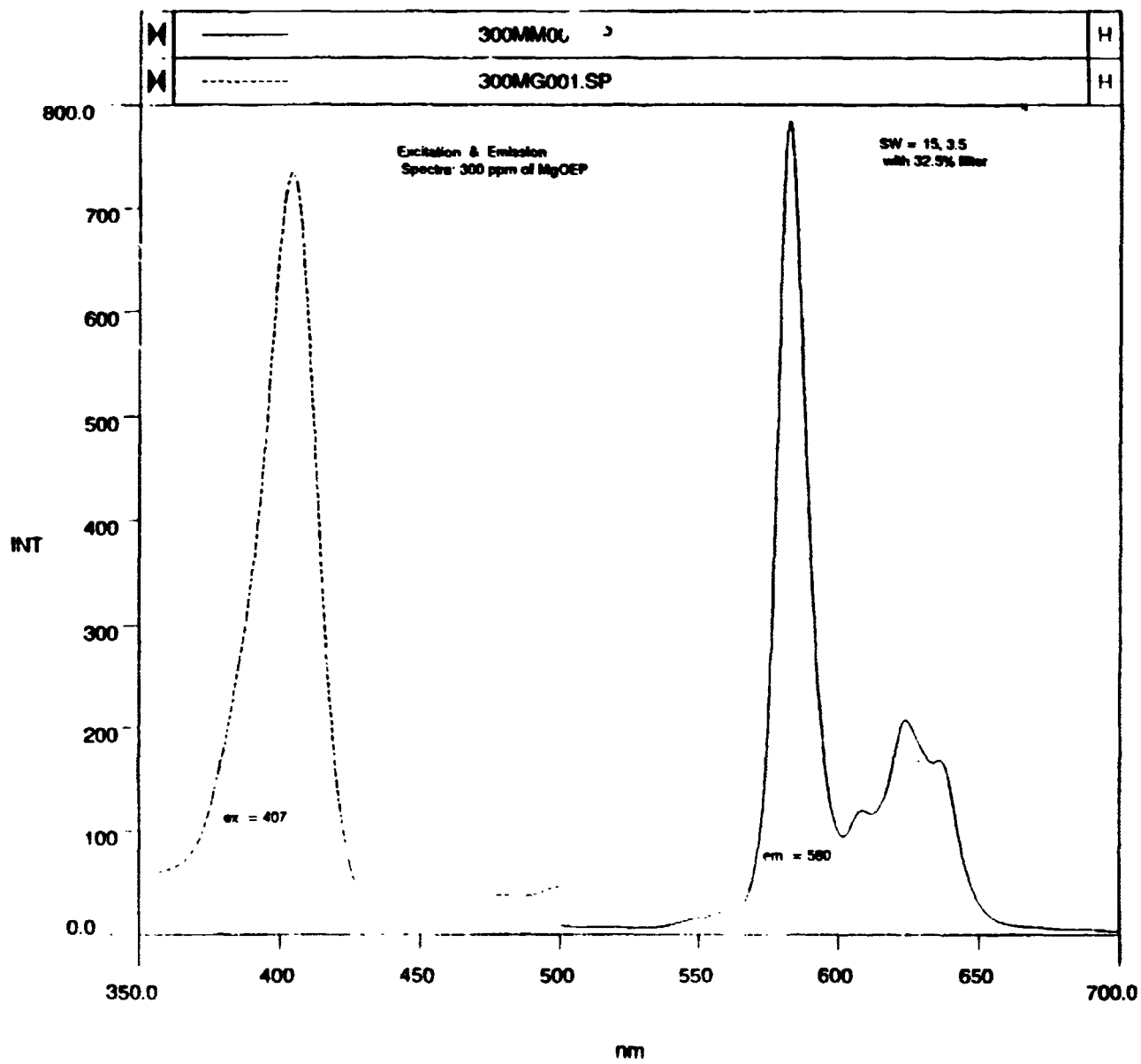


Figure 1. Excitation and Emission Spectra of MgOEP

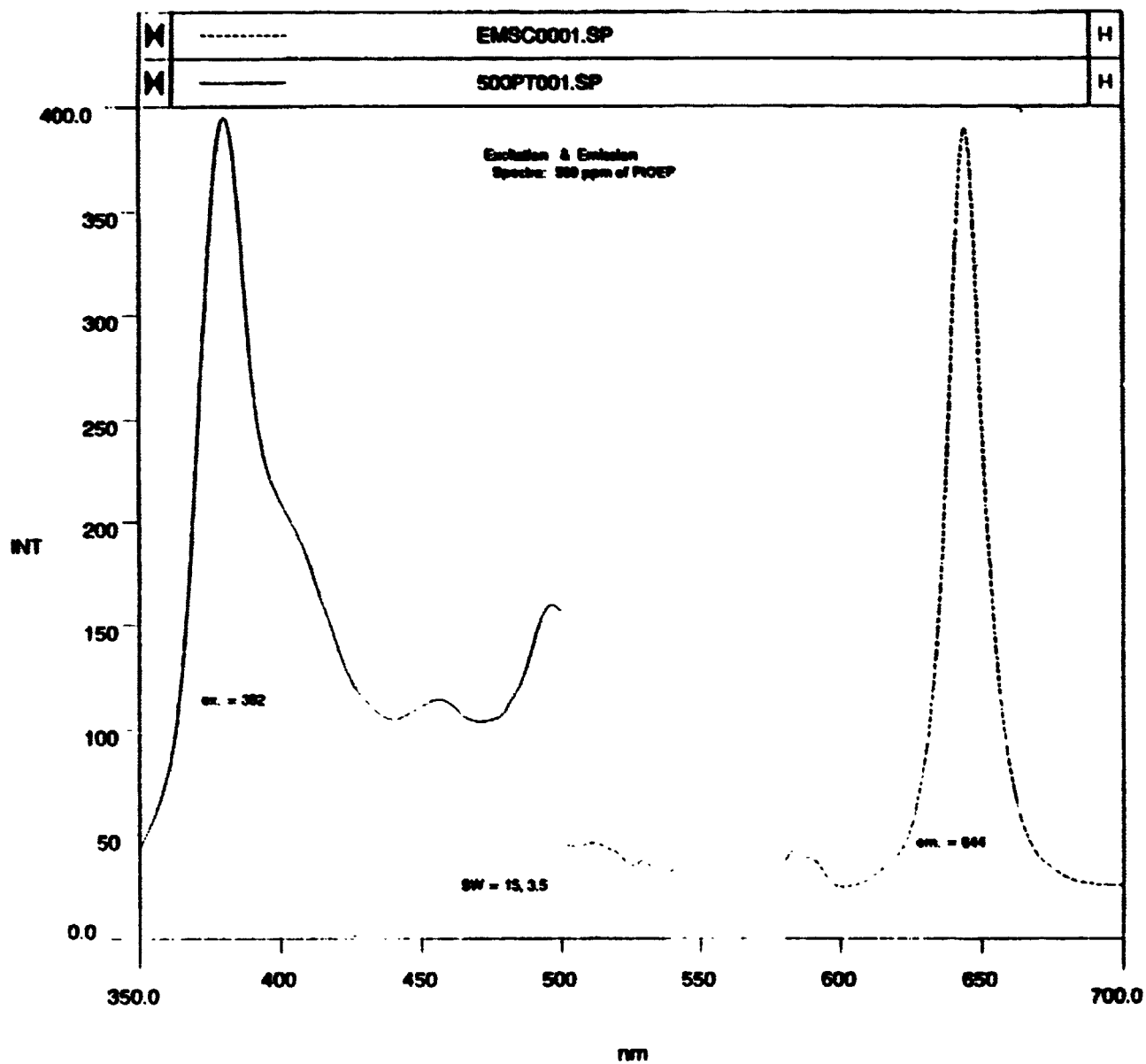


Figure 2. Excitation and Emission Spectra of PtOEP

Temperature Response of Different Preparation
 (1 part HEMA, 10 part tol., PEO/P (500ppm) & BzO/P (300ppm)

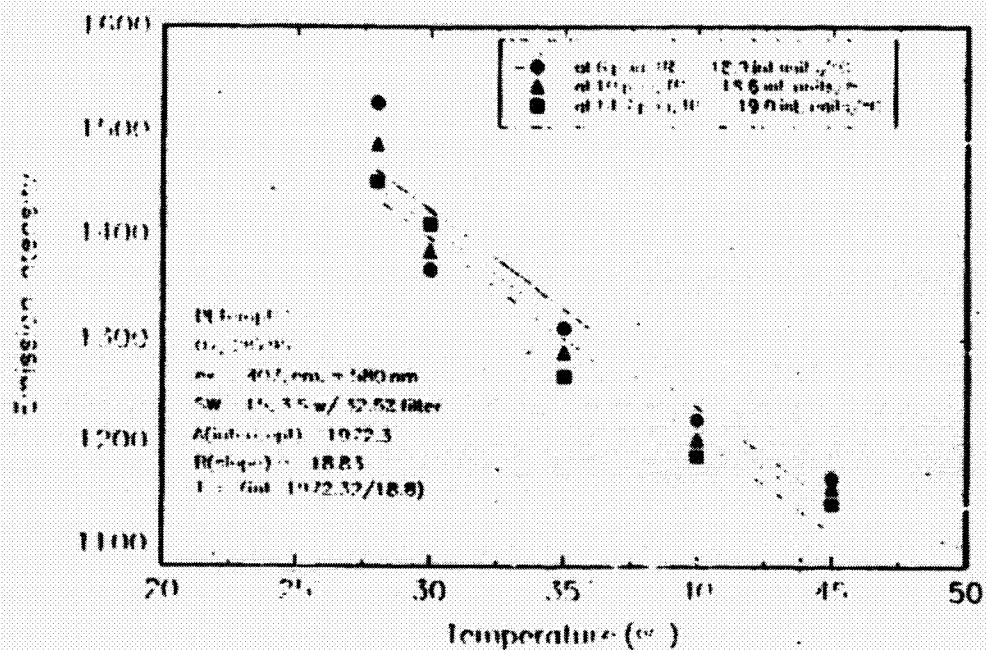


Figure 3.

Stern-Volmer Plot of Different Temperatures
 (1 part HEMA, 10 part tol.), PEO/P (500ppm) & BzO/P (300ppm)

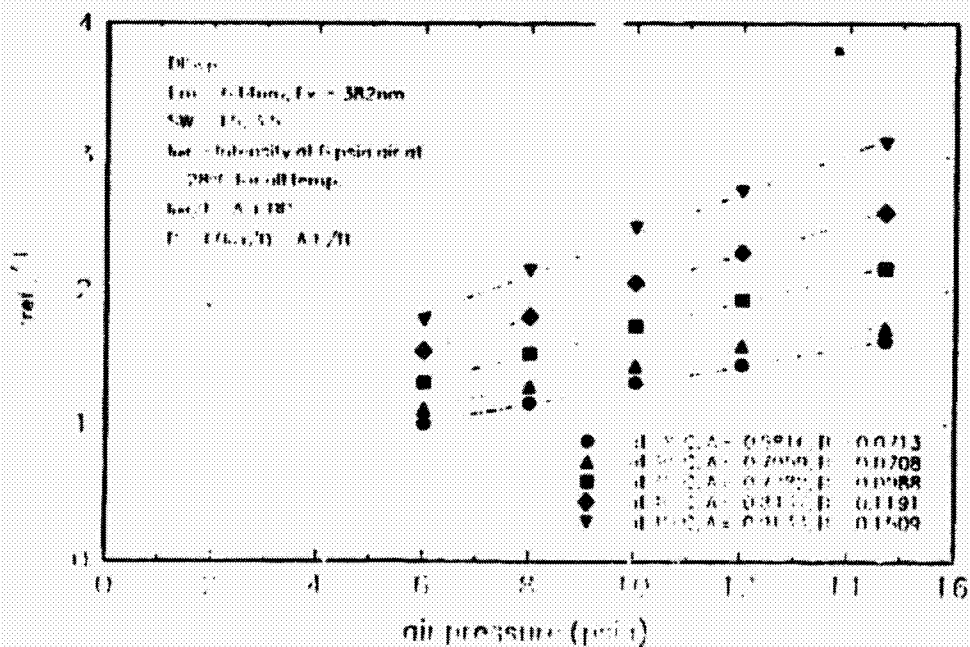


Figure 4.

Stern - Volmer Intercept for P10LP
 (1 part HEMA/10 part tol.), P10LP (500ppm) & MgO1P (300ppm)

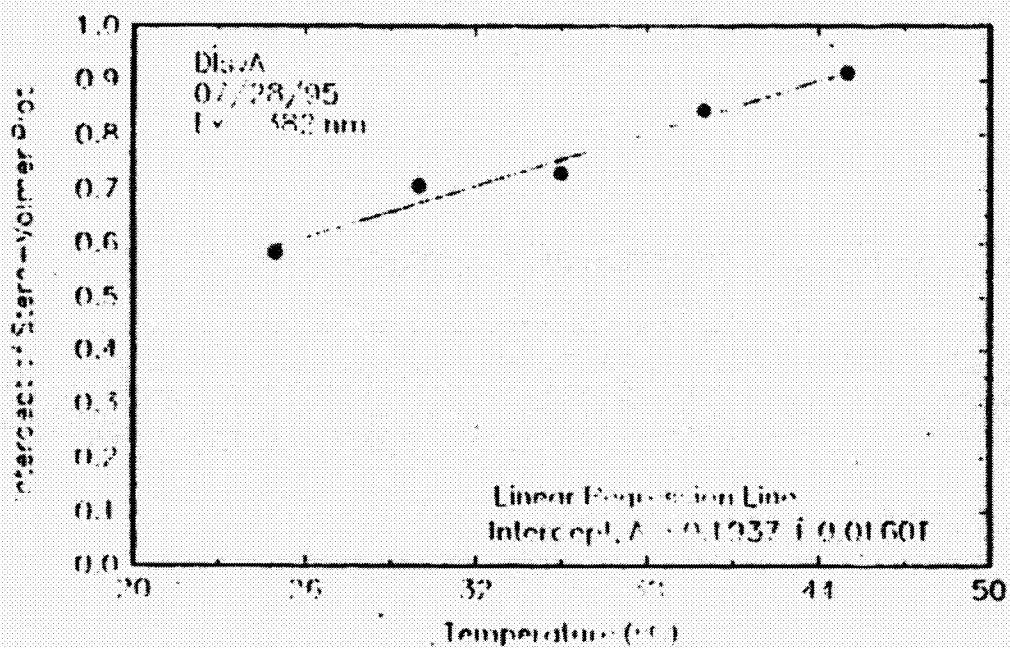


Figure 5.

Stern - Volmer Slope for P10LP
 (1 part HEMA/10 part tol.), P10LP (500ppm) & MgO1P (300ppm)

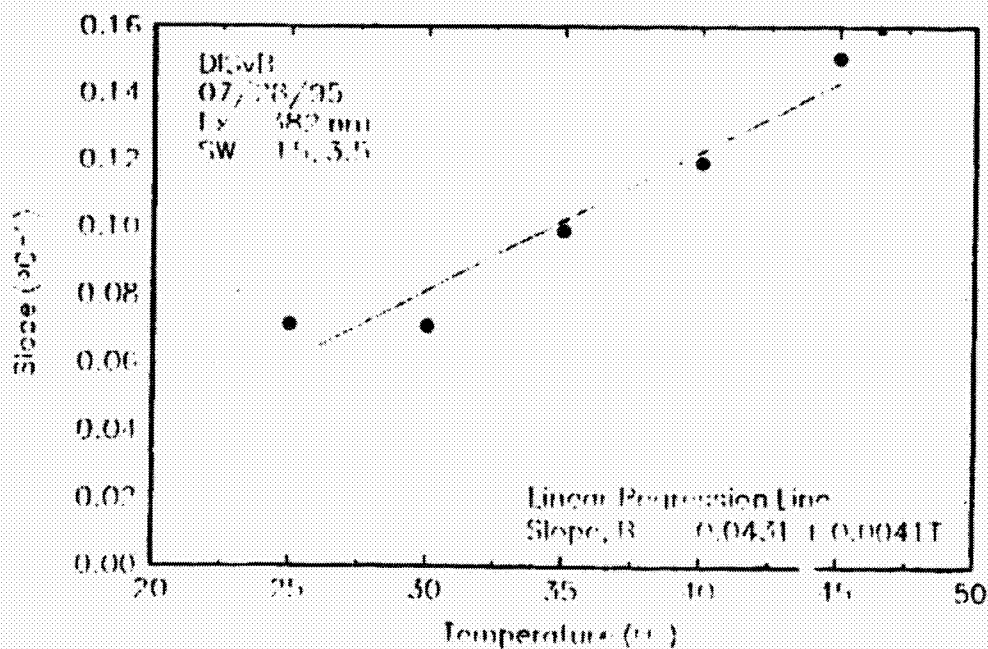


Figure 6.

**NEXT
DOCUMENT**

TOPIC: TECHNOLOGY TRANSFER

STUDENT: NANETTE R. SMITH

MENTOR: ROBERT L. YANG

BRANCH: TECHNOLOGY APPLICATIONS GROUP

ABSTRACT

The objective of this summer's work was to attempt to enhance TAG's ability to measure the outcomes of its efforts to transfer NASA technology. By reviewing existing literature, by explaining the economic principles involved in evaluating the economic impact of technology transfer, and by investigating the LaRC processes our William & Mary team has been able to lead this important discussion.

In reviewing the existing literature, we identified many of the metrics that are currently being used in the area of technology transfer. Learning about the LaRC technology transfer processes and the metrics currently used to track the transfer process enabled us to compare other R&D facilities to LaRC.

In the working paper "Measuring the Economic Impact of Technology Transfer From a National Laboratory: A Primer," we discuss and diagram impacts of technology transfer in the short run and the long run. Significantly, this paper serves as the basis for analysis and provides guidance in thinking about what the measurement objectives ought to be.

By focusing on the SBIR Program, valuable information regarding the strengths and weaknesses of this LaRC program are to be gained. A survey was developed to ask probing questions regarding SBIR contractors' experience with the program. Specifically we are interested in finding out whether the SBIR Program is accomplishing its mission, if the SBIR companies are providing the needed innovations specified by NASA and to what extent those innovations have led to commercial success.

We also developed a survey to ask COTRs, who are NASA employees acting as technical advisors to the SBIR contractors, the same type of questions, evaluating the successes and problems with the SBIR Program as they see it. This survey was developed to be implemented interactively on computer.

It is our hope that the statistical and econometric studies that can be done on the data collected from all of these sources will provide insight regarding the direction to take in developing systematic evaluations of programs like the SBIR Program so that they can reach their maximum effectiveness.

INTRODUCTION

The Technology Applications Group (TAG) is fairly new to LaRC, having only been formed within the last two years. Our work this summer was geared toward enhancing TAG's ability to measure the outcomes of its efforts to transfer LaRC technology. Our work began last semester as we reviewed the TAG mission statements and organizational charts. During our first weeks at NASA, we extensively reviewed the existing literature pertaining to the measurement of technology transfer and its impact on the economy and throughout the summer we continuously attempted to broaden our understanding of the TAG transfer process by observing and talking with the individuals involved in the transfer activities.

Our paper "Measuring the Economic Impact of Technology Transfer From a National Laboratory: A Primer" laid the ground work for guiding our discussions regarding technology transfer measures. The paper provides guidance in thinking about measurement objectives and the associated metrics to use when attempting to measure the impact of technology transfer on the economy, and it discusses many of the limitations and difficulties in the measurement process.

Combining the economic theory with what we learned from our research and observations, we outlined a potential list of metrics that are specific to TAG at LaRC. This list included input, output and outcome measures and does not speak to the measurement process, which is complex and dynamic as it requires the cooperation and coordination of many people at all levels in an organization.

As an example of performance evaluation, we turned our focus toward a project to investigate a specific program. The Small Business Innovation Research Program (SBIR) was chosen. In this effort, we wrote, designed, and developed two surveys this summer to gather data about the participants of the SBIR Program. By statistically analyzing the data that we collect, it is our hope to provide information that will maximize the effectiveness of the SBIR Program as well as show by example the advantages that organizations can have in decision making when the relevant metrics are analyzed.

In each of the following sections of this paper we briefly discuss each element of our work here at NASA this summer.

SECTION I

BRIEF DESCRIPTION OF SOME OF THE DISCOVERIES MADE IN REVIEWING THE LITERATURE

In reviewing the existing literature, we identified many of the metrics that are currently being used in the area of technology transfer. Researchers agree that basing current policy on past studies is difficult because the average time lag between the discovery, development, production and marketing of an innovation is 15-20 years. They also agree that advances in technology have a positive effect on the economic growth of a nation, but they disagree on how large the effect is.

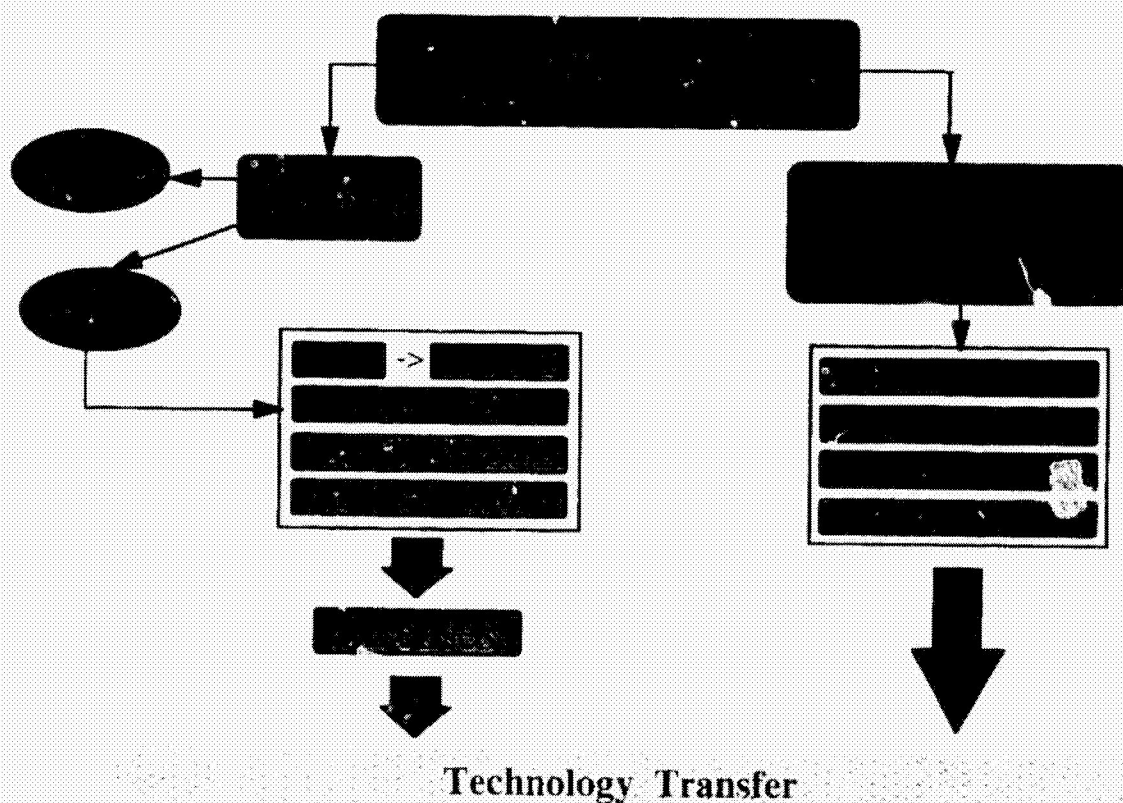
Researchers agree that there are different facets of R&D that overlap. Applied science research leads to more commercial production, pure science research may often lead to "break through discoveries" that may take a long time to develop into commercial products. "Push technologies" are usually less marketable than "pull technologies." Pull technologies refer to innovations that have been discovered as a result of consumer or producer demand, push technologies refer to innovations that have not been fully developed and lack production and/or marketing momentum.

SECTION II

INVESTIGATION OF THE LaRC TECHNOLOGY TRANSFER PROCESS

The technology available to TAG for transfer requires a "push" strategy and therefore the objectives and relevant metrics must be designed to capture TAG's effectiveness in assisting in the development of innovations into marketable products. The diagram below summarizes the TAG transfer process. At each stage of this diagram, metrics can be developed to determine whether specific objectives are being met effectively.

LaRC TECHNOLOGY TRANSFER PROCESS DIAGRAM



By tracking the activities in the transfer process and analyzing the data continuously over time, the most successful strategies can be identified and used to improve the overall effectiveness of TAG.

SECTION III

METRICS DISCUSSION

The best metrics are associated with clearly stated objectives. If a program or a job description is not precise in its expectation of what is to be accomplished, the relevant metrics cannot be adequately identified. Clear objectives are a most important element of evaluating success. Equally important are consistent, quantifiable measures that are systematically collected, analyzed and that the resulting information is used in determining future decisions.

METRICS THAT MAY BE USEFUL TO NASA LaRC

- **Input Metrics**
 - Number of spin-offs and spin-ons
 - Number of patents
 - Number of TOPS exhibits (patentable/non-patentable, patented/not patented, licensed/not licensed)
 - Number of COOPPRs
 - Number of contacts (post technology transfer)
 - Number of contacts (pre technology transfer)
 - Time spent on technology transfer
 - Use of facilities
- **Output Metrics**
 - Number of MOAs/MOUs and number of MOAs/MOUs leading to commercialization
 - Number of university/industry partnerships
 - Technical briefs/papers (published, requested, presented)
 - Technical problems solved
 - Number and dollar value of licenses and sublicenses
 - Number of software packages released
- **Outcome Metrics**
 - Number and dollar value of commercialization from TOPS, COOPPRs, Cooperative Agreements, MOAs, MOUs, SAAs and SBIRs
 - Commercial sales
 - Royalties
 - Cost savings
 - Productivity gains
 - User satisfaction
 - Short-run economic impact on income and employment

This was a tentative grouping of metrics that were presented during the 10 week summer session. Thoughts on these and other metrics are not complete. The important discussion should include metrics like these, but as mentioned earlier, metrics are only part of the process.

SECTION IV - THE PRIMER

Having identified the need for a discussion of the economic implications of the discussions that were taking place at NASA about the impact that technology has on the economy, a primer was written. My contribution to this effort was in creating the graphical representations of the concepts discussed in the paper. A full copy of the paper is enclosed along with this final report. The executive summary follows.

MEASURING THE ECONOMIC BENEFITS OF TECHNOLOGY TRANSFER FROM A NATIONAL LABORATORY: A PRIMER

Robert Archibald, Professor of Economics
David Finifter, Professor of Economics
and Director of the Thomas Jefferson Program in Public Policy
Nanette Smith, Graduate Student
Thomas Jefferson Program in Public Policy

- Executive Summary -

One measures the economic benefits of a particular event by comparing the state of the economy after the event has happened to the state of the economy assuming the event had not happened. Given this understanding of economic benefits, in this paper we reach the following conclusions about the economic benefits of technology transfer from national labs.

- In the long run, successful technology transfer increases the productivity of the country. As a result the per capita income generated by the U. S. economy will rise. Technology transfer from national labs will spur economic growth.
- In the long run, the number of jobs in the economy is unaffected. The characteristics of the jobs are different, however. On average, the real compensation of jobs will increase, and therefore technology transfer does create higher paying (better) jobs.
- In the long run, the economic competitiveness of U.S. firms will be enhanced, i.e., the balance of trade will be improved.
- In the short run, outcomes are less clear. The results of increases in technology transfer activity depend upon the stage of the business cycle and in any case are only temporary.

These conclusions have clear implications for the measurement efforts being undertaken at NASA labs. To directly measure the benefits of technology transfer, NASA labs need to focus on the long run consequences of their activities.

SECTION V

SURVEYS

By studying the SBIR Program information might be provided that could help to maximize its effectiveness. This study can also be useful in demonstrating by example the advantages that organizations can have in decision making when the relevant metrics are analyzed. The SBIR Program awards contracts to small businesses who present a viable case for doing research that NASA solicits. These contracts are awarded in two phases. A Phase I contract is awarded to begin the research, a Phase II contract is awarded after the Phase I has been completed, it is the second step in the process and may result in a product or process that can not only be used by NASA, but also may become commercially successful. If a company is awarded a Phase I or Phase II contract, a NASA employee is assigned to the project as a COTR to provide technical assistance.

Our team developed and sent a survey to the companies who participated in the 382 SBIR contracts awarded from 1985 to present. The objective of the survey is to collect data from the SBIR firms regarding the success of their innovation that can be analyzed to gain insight in answering the following questions. Did their solicitation result in an innovation that was or could be used by NASA? Did their innovation result in a commercially viable product? Did the SBIR award impact the economy?

Since COTRs can also provide valuable information about the SBIR Program, we developed a second survey to be completed by COTRs. This survey was developed to be implemented interactively on computer.

Enclosed are copies of the two surveys and a print out of the automated survey input screens.

Ideas Generated From the Study:

Economic Impact of Technology Transfer

Idea 1

Counting the number of jobs that are generated by technology transfer is a political argument for justifying the continued funding of federal labs, but it is a short run and incomplete argument that does not reflect the long run benefits of increasing the nation's global competitiveness, gross domestic product per capita, and quality of life as Congress determines how it will allocate shrinking federal resources. See "Measuring The Economic Impact of Technology Transfer From a National Laboratory: A Primer" which was developed by the William & Maury team this summer to explain the economic theory behind this claim.

Idea 2

By changing the contracting process to require that contractors provide NASA with the information needed to better estimate the potential economic benefit of the transfer, communities could be better served. As firms forecast potential profit and report on actual profit that results from NASA research, the NASA contribution becomes more tangible and measurable. The information needed should include data that will indicate the potential savings and/or profits that will and do result from the transferred technology. Other questions to investigate are: Who benefits beyond the company receiving the innovation, what is the benefit, and how much is it? How long does/did each step in the process take?

How do the benefits/costs vary over time? Are there losers, if so who are they and how much do they lose? To capture the economic impact of technology transfer it will require a long term informational commitment between NASA and the contracting firm. How can NASA staff better maintain this information link?

Toward TAG Metrics

Idea 1

Assigning personnel to analyze the metrics being captured and to develop the evolution of the performance measurement process could enhance TAG's ability to quantify the success of its technology transfer efforts. The analyst(s) should be able to link metrics to organizational objectives in order to evaluate the strengths and weaknesses of the technology transfer processes. The analyst(s) should be able to identify additional information requirements and be able to recommend and implement adaptations to the measurement process. By being able to discern process patterns allows for discoveries to be made that could lead to increased transfer activity.

Idea 2

When a NASA technology is being considered for licensing by more than one firm could a bidding process increase the probability of its commercial success? By opening the licensing for bidding, increased commitment toward commercialization may occur as an outcome of the higher cost to the firm that wins the bid. The bidding process also permits NASA to get a feel for the market value of the innovation being transferred, thus gaining insightful information that could be used in future technology transfer efforts.

SBIR/STTR Programs

Idea 1

Could the SBIR/STTR Programs be improved to enhance commercialization of technology? An analysis of the SBIR/STTR Programs might help to determine whether solicitation topics written for SBIR/STTR contracts can or should be focused more toward "applied" R&D, which may result in increased commercial activity.

Idea 2

Investigating the possibility of incorporating problem statements into SBIR/STTR program might lead to increased commercial activity as R&D efforts are focused on process or product improvement. This might be accomplished by matching SBIR/STTR firms with problem statement firms through personal contact or through solicitation write-ups.

**NEXT
DOCUMENT**

7

**Characteristics of Three-node Smoothing Element
Under Penalty Constraints**

Seth S. Sobel
LARSS Student
Integrated Science And Technology
James Madison University
Harrisonburg, VA

Dr. Alexander Tessler
Computational Structures Branch
NASA Langley Research Center
Hampton, VA

**Research and Technology Group
Structures Division
Computational Structures Branch**

Abstract

The project is based upon research of Tessler et al. (1994) on an improved variational formulation for post-processing stress predictions in Finite Element Analysis. The methodology, called Smoothing Element Analysis (SEA), employs a three-node smoothing finite element. The present effort focused on verifying the basic *constant strain criterion* for the three-node smoothing element subject to a set of internal *penalty constraints*. The convergence characteristics of the element are assessed by first deriving the constrained form of the assumed element stress and stress gradient fields, and then by verifying the validity of the constant strain criterion once the element penalty constraints are explicitly imposed. The analytical investigation is carried out with the use of the symbolic manipulation code *Mathematica*.

Introduction

An improved variational formulation called Smoothing Element Analysis (SEA), developed by Tessler et al., (1994), serves as a foundation for the enhancement of finite-element obtained deformation and stress response. In the case of stress predictions, C^1 -continuous stress field from a finite element solution is enforced into a C^1 -continuous stress field with continuous stress gradients. These enhanced results are ideally suited for error estimation since the stress gradients can be used to assess equilibrium satisfaction. The approach is employed as a post-processing step in finite element analysis. The variational statement combines the discrete-least squares, and penalty-constraint functionals, thus enabling automated recovery of smooth stresses and stress gradients.

The practical issues whose adequate resolution is essential for a successful application of the approach are:

(1) The SEA mesh and the number of the discrete stresses extracted from the Finite Element Analysis (FEA) mesh should be properly interrelated in order to produce a determined system of SEA equations. To fulfill this requirement, Tessler et al. (1994) proposed specific guidelines. An automated generation of the SEA mesh may also be necessary to make the post-processing transparent to the user.

(2) The FEA stresses need to be extracted at the discrete elemental locations that are best suited for the recovery. Optimal (i.e., superconvergent) Barlow points and Gauss integration points have been successfully used.

(3) The smoothing element should not exhibit *locking* — a pathological stiffening phenomenon commonly exhibited in penalty-constrained elements. In this connection, a judicious choice of the element shape functions is key to avoiding *locking*.

The purpose of this effort is investigate the influence of penalty constraints on the characteristics of the smoothing element used in Tessler et al. (1994). Particularly, the convergence characteristics of Tessler's smoothing element are assessed by way of deriving the constrained form of the assumed element stress and stress gradient fields, and by verifying the validity of the constant strain criterion once the element penalty constraints are explicitly imposed. This analytical investigation is facilitated by the use of the symbolic manipulation code *Mathematica*.

Error Functional

In this section an error functional proposed by Tessler et al. (1994) for a two-dimensional plane formulation is reviewed. It is assumed that within a two-dimensional region $\Omega = \{\mathbf{x} \in \mathcal{R}^2\}$, where $\mathbf{x} = \{x_i\}$, $i=1,2$, represents a position vector in Cartesian coordinates, a finite element-derived stress field $\sigma^h(\mathbf{x})$ has been obtained by means of a discretization of Ω with characteristic element size h . The smoothed stress field, $\sigma^s(\mathbf{x})$, is to be constructed from $\sigma^h(\mathbf{x})$ via a variational formulation. The variational statement involves scalar quantities only, and so each component of $\sigma^h(\mathbf{x})$ is smoothed independently. Hence, in the following reference is made only to components σ^h and σ^s . The finite element stress field is sampled at \mathbf{x}_q , $q = 1, 2, \dots, N$, to obtain the set of stresses $\{\sigma_q^h\}$, i.e., $\sigma_q^h \equiv \sigma^h(\mathbf{x}_q)$. The sampled stresses are those extracted at the Gauss integration points, Barlow points, or other element locations in the finite element analysis. To minimize the error functional, we adopt the finite element methodology and therefore discretize Ω with n_e "recovery" or "smoothing" finite elements such that $\Omega = \cup_{e=1}^{n_e} \Omega^e$, where Ω^e is the domain of smoothing element e . Within our recovery element model, we use C^0 -continuous interpolation functions for the stress, σ^s , and the independent quantities θ_i^s , $i=1, 2$, whose mathematical interpretation will be readily established. The error functional to be minimized can be written as

$$\Phi = \frac{1}{\gamma} \sum_{q=1}^N w_q [\sigma_q^h - \sigma^s(\mathbf{x}_q)]^2 + \lambda \sum_{e=1}^{n_e} \int_{\Omega^e} \rho(\mathbf{x}) [(\sigma_{,x}^s - \theta_x^s)^2 + (\sigma_{,y}^s - \theta_y^s)^2] d\Omega \quad (1)$$

where w_q and $\rho(\mathbf{x})$ are the appropriate weight functions; γ is a normalization factor; λ is a dimensionless parameter; and a comma denotes partial differentiation. Because the highest partial derivative in equation (1) is of order one, the field variables need only be approximated with C^0 -continuous shape functions.

The first term in equation (1) represents a discrete least-squares functional in which the squared 'error' between the smoothed stress field and the sample data is computed for all sampled stresses. The term can be normalized in several different ways; presently, the normalization factor equals the total number of the sampled stresses, i.e., $\gamma = N$. The discrete weights w_q are introduced so that sample data known to be of higher accuracy can be assigned more weight than less accurate data.

The second term in equation (1) represents a penalty functional which, for λ sufficiently large, enforces the derivatives of the smoothed stress field $\sigma_{,i}^s$ to approach the corresponding θ_i^s variable pointwise, i.e.,

$$\sigma_{,i}^s \rightarrow \theta_i^s \quad (i=x,y) \text{ in } \Omega^e \quad (2)$$

Theoretically, the greater the value of λ , the closer the correlation between σ^s and θ^s , where C^1 continuity of σ^s is achieved as $\lambda \rightarrow \infty$. In practice, λ needs to be sufficiently large in order to enforce conditions (2), yet it should not be excessively large to cause ill-conditioning of the *smooth* solution. Because θ^s are interpolated with continuous functions, the smoothed stress field, for all practical purposes, is C^1 continuous. The weight function $\rho(\mathbf{x})$ is introduced in the functional to allow the enforcement of C^1 continuity to be somewhat relaxed in certain regions of Ω and more strictly enforced in others, if so desired. Also note that by specifying the weights w_s and $\rho(\mathbf{x})$ to vanish in regions outside a given domain of interest, a *local* or *patch* analysis is admitted. Presently, we only consider the special case where $w_s = 1$ and $\rho(\mathbf{x}) = 1$, that is all stress data are treated equally and the C^1 continuity is enforced throughout the Ω domain.

Assumed Element Fields

Although the functional (1) admits C^0 -continuous shape functions for the field variables σ^s , θ_x^s , and θ_y^s , the constraints (2) impose certain restrictions on the suitable choice of shape functions. In a similar plate theory formulation, constraints of this type are known to cause *locking* (i.e., severe stiffening) when conventional isoparametric interpolations are used. (In the present context, *locking* would manifest itself in a smoothed stress field, σ^s , that grossly underestimates the 'true' stress distribution.) When σ^s is interpolated with a polynomial one degree higher than those for the θ_x^s and θ_y^s variables, using *anisoparametric* interpolations, the *locking* effect is alleviated or completely eliminated (Tessler, 1985).

Another important consideration is the nodal configuration that is best suited for the smoothing element. It turns out that a three-node triangle is well-suited for this purpose because (a) from a modeling standpoint, it represents the most versatile element topology, and (b) it permits a one-to-one linear mapping between the global and element local (area-parametric) coordinates, thus allowing a straightforward identification of the sampled stress data within the smoothing element.

The anisoparametric interpolations for a three-node element involve quadratic approximation of σ^s and linear approximations of θ_x^s and θ_y^s which can be expressed in matrix form as

$$\sigma^s = \mathbf{z}\sigma^c + \mathbf{m}\theta_x^c + \mathbf{l}\theta_y^c, \quad \theta_i^s = \mathbf{z}\theta_i^c \quad (i=1,2) \quad (3)$$

where σ^c , θ_i^c are 3x1 vectors of nodal degrees-of-freedom (dof), \mathbf{z} is selected as a row-vector of a linear shape function, and \mathbf{m} and \mathbf{l} are selected as row-vectors of quadratic shape functions. Their explicit forms given in terms of area-parametric coordinates are

$$\mathbf{z} = \{z_1, z_2, z_3\}, \quad \mathbf{m} = \{m_1, m_2, m_3\}, \quad \mathbf{l} = \{l_1, l_2, l_3\} \quad (3.1)$$

where

$$z_i = \frac{1}{3A}(c_i + b_i x + a_i y), \quad m_i = \frac{1}{3}(a_k z_i z_j - a_j z_i z_k), \quad l_i = \frac{1}{3}(b_j z_i z_k - b_k z_i z_j)$$

$$a_i = x_k - x_j, \quad b_i = y_j - y_k, \quad c_i = x_j y_k - x_k y_j \quad (i=1,2,3, \quad j=2,3,1, \quad k=3,1,2)$$

and A denotes the area of a triangular element.

Note that these interpolations are consistent with a three-node element which has only three dof per node, even though σ^e is quadratic and θ_i^e are linear functions. Moreover, equations (3) ensure that the gradient of the smoothed stress, $\sigma_{,i}^e$, is the same degree polynomial as that representing θ_i^e , i.e., they are both linearly distributed across Ω^e . This naturally leads to a reasonable expectation that penalty constraints (2) can be adequately fulfilled without over constraining (*locking*) the element.

Edge Penalty Constraints

A straightforward manipulation of the two constraint equations in (2), in which equations (3) are introduced, produces three edge-wise constraints per element. For the element edge defined by nodes i and j , the edge constraint equation has a simple form in terms of the nodal dof corresponding to the edge (Pomeranz, 1995; Tessler, 1985):

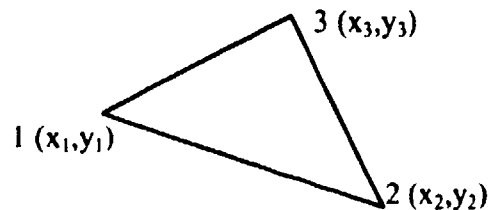
$$\sigma_i^e - \sigma_j^e \rightarrow \frac{1}{2}(x_i - x_j)(\theta_{xx}^e + \theta_{yy}^e) + \frac{1}{2}(y_i - y_j)(\theta_{xx}^e - \theta_{yy}^e) \quad (4)$$

where x_k and y_k ($k = i, j$) are the nodal coordinates.

The three edge constraint equations ensure that there are only six independent dof per element, thus properly describing the complete parabolic field of σ^e . They also facilitate a simple calculation of the total number of independent dof in the mesh. The key aspect of these constraints is that they control the mechanisms of *locking*. Their assessment in the context of assembly of elements can provide proper insight into preferable discretization patterns for such elements. For example, a fully non-locking behavior is achieved by producing SEA meshes made of quadrilateral *macro-elements* that are formed with four triangles in a cross-diagonal pattern.

Constant Strain Criterion

Let us consider an arbitrary triangular element as shown in the diagram below.



The satisfaction of the *constant strain criterion* in the finite element method ensures convergence of the method as the mesh is refined. In this case, it is expected that each individual finite element accommodates constant strains. Mathematically, the criterion is verified by summing up on all shape functions for each field that is approximated, and the resulting sum should add up to unity. This can be readily verified for the unconstrained element fields in (3).

The constraint equations for the edges of this element can be written as follows.

Edge 1-2

$$\sigma_1 - \sigma_2 = \frac{1}{2} \left((x_1 - x_2)(\theta_{x1} + \theta_{x2}) + (y_1 - y_2)(\theta_{y1} + \theta_{y2}) \right)$$

Edge 2-3

$$\sigma_2 - \sigma_3 = \frac{1}{2} \left((x_2 - x_3)(\theta_{x2} + \theta_{x3}) + (y_2 - y_3)(\theta_{y2} + \theta_{y3}) \right)$$

Edge 3-1

$$\sigma_3 - \sigma_1 = \frac{1}{2} \left((x_3 - x_1)(\theta_{x3} + \theta_{x1}) + (y_3 - y_1)(\theta_{y3} + \theta_{y1}) \right)$$

(5)

Using Mathematica, the three constraint equations are solved for σ_1 , σ_2 , and θ_{x3} . When these solutions are substituted into the original definitions for σ^i , θ_x^i , and θ_y^i , the following expressions of the three element fields are derived

$$\begin{aligned} \sigma^i &= g_1 \sigma_3 + g_2(x) \theta_{x1} + g_3(x) \theta_{x2} + g_4(x, y) \theta_{y1} + g_5(x, y) \theta_{y2} + g_6(x, y) \theta_{y3} \\ \theta_x^i &= d_1(x) \theta_{x1} + d_2(x) \theta_{x2} + d_3(x, y) \theta_{y1} + d_4(x, y) \theta_{y2} + d_5(x, y) \theta_{y3} \\ \theta_y^i &= e_1(x, y) \theta_{y1} + e_2(x, y) \theta_{y2} + e_3(x, y) \theta_{y3} \end{aligned} \quad (6)$$

where g , d , and e are shape functions whose expressions are summarized in the Appendix.

To verify the constant strain criterion for the resulting element fields, the summation of the g , d , and e shape functions is carried out with the use of Mathematica. The resulting equations are as follows

$$g \equiv \sum_{i=1}^6 g_i = 1 + x - x_3 + y - y_3, \quad d \equiv \sum_{i=1}^5 d_i = 1, \quad e \equiv \sum_{i=1}^3 e_i = 1 \quad (7)$$

Note that both θ_x^i and θ_y^i fulfill the constant strain criterion for a finite size element since $d = 1$ and $e = 1$. On the other hand, g only approaches unity in the limit as the element size diminishes to zero, i.e.,

$$x \rightarrow x_3, \quad y \rightarrow y_3 \quad (8)$$

giving rise to $g \rightarrow 1$. Thus, the element convergence is ensured as the smoothing mesh is refined.

Conclusions

The project has been a continuation of the research of Tessler et al. (1994) on an improved variational formulation for post-processing stress predictions in Finite Element Analysis. The effort focused on verifying the basic *constant strain criterion* for the three-node smoothing element subject to a set of internal *penalty constraints*. The convergence characteristics of the element were assessed by first deriving the constrained form of the assumed element stress and stress gradient fields through a process of simplifications using *Mathematica*. The element penalty constraints were explicitly imposed using the formulas set out by Tessler et al. (1994). Then the validity of the constant strain criterion for the element was verified. As the smoothing mesh is refined, the constant strain criterion is satisfied.

References

Tessler, A., Riggs, H. R., Macy, S. C., 1994, "A variational Method for Finite Element Stress Recovery and Error Estimation," *Computer Methods in Applied Mechanics and Engineering*, Vol. 111 pp. 369-382.

Tessler, A., 1985, "A Priori Identification of Shear Locking and Stiffening in Triangular Mindlin Elements," *Computer Methods in Applied Mechanics and Engineering*, Vol. 53, pp.183-200.

Pomeranz, S., 1995, Personal Communication.

Wolfram, S., 1988, *Mathematica™ A System for Doing Mathematics by Computer*, Addison-Wesley Publishing Company, Inc., Redwood City, CA.

Appendix

The following are the shape functions in (6) as solved by Mathematica™.

$$g_1 = 1$$

$$g_2 = ((-x + x_3)(x - 2x_2 + x_3))/(2(-x_1 + x_2))$$

$$g_3 = ((x - x_3)(-x + 2x_1 - x_3))/(2(x_1 - x_2))$$

$$g_4 = (x_1x_2y^2 - x_2^2y^2 - x_1x_3y^2 + x_2x_3y^2 - 2x^2x_1y^2 + 2x^2x_2y^2 + 2x_1x_3y^2 - 2x_2^2x_3y^2 + x^2y_1y^2 - 2x^2x_2y_1y^2 + 2x_2^2x_3y_1y^2 - x_3^2y_1y^2 - x^2y_2^2 + 2x^2x_1y_2^2 - 2x_1x_3y_2^2 + x_3^2y_2^2 + 2x^2x_1y_3 - 2x^2x_2y_3 - 2x_1x_2y_3 + 2x_2^2y_3 - x^2y_1y_3 + 2x^2x_2y_1y_3 - 2x_2^2x_3y_1y_3 + x_3^2y_1y_3 + x^2y_2y_3 - 2x^2x_1y_2y_3 + 2x_1x_3y_2y_3 - x_3^2y_2y_3 + x_1x_2y_3^2 - x_2^2y_3^2 - x_1x_3y_3^2 + x_2x_3y_3^2)/(2(-x_1 + x_2)(-x_2y_1 + x_3y_1 + x_1y_2 - x_3y_2 - x_1y_3 + x_2y_3))$$

$$g_5 = (-x_1^2y^2 + x_1x_2y^2 + x_1x_3y^2 - x_2x_3y^2 + 2x^2x_1y^2 - 2x^2x_2y^2 - 2x_1x_3y^2 + 2x_2^2x_3y^2 - x^2y_1^2 + 2x^2x_2y_1^2 - 2x_2^2x_3y_1^2 + x_3^2y_1^2 + x^2y_1y_2 - 2x^2x_1y_1y_2 + 2x_1x_3y_1y_2 - x_3^2y_1y_2 - 2x^2x_1y_3 + 2x_1^2y_3 + 2x^2x_2y_3 - 2x_1x_2y_3 + x^2y_1y_3 - 2x^2x_2y_1y_3 + 2x_2^2x_3y_1y_3 - x_3^2y_1y_3 - x^2y_2y_3 + 2x^2x_1y_2y_3 - 2x_1x_3y_2y_3 + x_3^2y_2y_3 - x_1^2y_3^2 + x_1x_2y_3^2 + x_1x_3y_3^2 - x_2x_3y_3^2)/(2(-x_1 + x_2)(-x_2y_1 + x_3y_1 + x_1y_2 - x_3y_2 - x_1y_3 + x_2y_3))$$

$$g_6 = ((-x_1y + x_3y + x^2y_1 - x_3y_1 - x^2y_3 + x_1y_3)/(2(-x_1 + x_2)) + (x_2y - x_3y - x^2y_2 + x_3y_2 + x^2y_3 - x_2^2y_3)/(2(-x_1 + x_2)) + ((-x + x_3)(y_1 - y_2)(-x_1y + x_2y + x^2y_1 - x_2^2y_1 - x^2y_2 + x_1y_2))/(2(-x_1 + x_2)(x_2y_1 - x_3y_1 - x_1y_2 + x_3y_2 + x_1y_3 - x_2^2y_3)) + ((x_1y - x_2y - x^2y_1 + x_2^2y_1 + x^2y_2 - x_1y_2)(y - y_3))/(2(x_2y_1 - x_3y_1 - x_1y_2 + x_3y_2 + x_1y_3 - x_2^2y_3)))$$

$$d_1 = (x - x_2)/(x_1 - x_2)$$

$$d_2 = (x - x_1)/(-x_1 + x_2)$$

$$d_3 = (((-x_1y + x_2y + x^2y_1 - x_2^2y_1 - x^2y_2 + x_1y_2)(y_2 - y_3))/((-x_1 + x_2)(-x_2y_1 + x_3y_1 + x_1y_2 - x_3y_2 - x_1y_3 + x_2^2y_3)))$$

$$d_4 = ((x_1y - x_2y - x^2y_1 + x_2^2y_1 + x^2y_2 - x_1y_2)(-y_1 + y_3))/((-x_1 + x_2)(x_2y_1 - x_3y_1 - x_1y_2 + x_3y_2 + x_1y_3 - x_2^2y_3))$$

$$d_5 = ((y_1 - y_2) * (-x_1 * y_1 + x_2 * y_1 + x_3 * y_1 - x_2 * y_2 - x_3 * y_2 + x_1 * y_2)) / ((-x_1 + x_2) * (-x_2 * y_1 + x_3 * y_1 + x_1 * y_2 - x_3 * y_2 - x_1 * y_3 + x_2 * y_3))$$

$$e_1 = (x_2 * y_1 - x_3 * y_1 - x_1 * y_2 + x_3 * y_2 + x_1 * y_3 - x_2 * y_3) / (x_2 * y_1 - x_3 * y_1 - x_1 * y_2 + x_3 * y_2 + x_1 * y_3 - x_2 * y_3)$$

$$e_2 = (x_1 * y_1 - x_3 * y_1 - x_1 * y_2 + x_3 * y_1 + x_1 * y_3 - x_1 * y_3) / ((-x_2 * y_1) + x_3 * y_1 + x_1 * y_2 - x_3 * y_2 - x_1 * y_3 + x_2 * y_3)$$

$$e_3 = (-x_1 * y_1 + x_2 * y_1 + x_3 * y_1 - x_2 * y_2 - x_3 * y_2 + x_1 * y_2) / ((-x_2 * y_1) + x_3 * y_1 + x_1 * y_2 - x_3 * y_2 - x_1 * y_3 + x_2 * y_3)$$

Notation

In the above expressions, $x_1 = x_1$, $y_1 = y_1$, $x_1^2 = x_1^2$, and the asterisk (*) denotes multiplication.

**NEXT
DOCUMENT**

**Langley Research Center - Soluble Imide
(LaRC-SI)**

by

David Stang - LARSS

Carl Voglewede Mentor

**Internal Operations Group
Fabrication Division
Electronic Technology Branch
Microelectronics and Sensor Development Section
Building 1238**

15 August 1995

Abstract

This report is about my LARSS experiences at NASA Langley Research Center. My experiences entailed experimenting and developing uses for the new thermal plastic developed by Dr. Robert Bryant called the "Langley Research Center - Soluble Imide" (LaRC-SI). The three developments that I worked on are the use of the LaRC-SI as a dielectric for thin film sensors, as an adhesive to place diamonds on surfaces to increase thermal conductivity, and as an intermediate layer to allow the placement of metal on aluminum nitride.

Introduction

The LaRC-SI was developed by Dr. Robert G. Bryant, a chemical engineer at NASA Langley Research Center. This new multi-purpose, self-bonding thermoplastic material has won the R&D 100 award for being one of the 100 most significant new technical products of 1994. The R&D 100 award is presented annually by *Research and Development* magazine to those who have contributed the most significant products for advancing science and technology during the year.

The unique properties of this material is that it is an amorphous thermoplastic. This means that it can be reformed at elevated temperature and pressures. It can be applied in the form of a spray, spin, dip coating, paint, or spread with a doctors blade. The LaRC-SI has excellent adhesive and dielectric properties. It can also be recycled. Potential applications for this material are resin for mechanical parts such as gears, bearings and valves, advanced composites like carbon fiber, high strength adhesives, thin film circuits, and as a dielectric film for placing electrical components on conductive materials.

My stay as a LARSS student at Langley Research Center was involved in helping develop applications for the LaRC-SI. There were three areas of concentration. The first was the application of using the LaRC-SI as a dielectric to place thin film sensors on models for use in wind tunnels. The second area of concentration was to use the LaRC-SI to apply diamonds to a surface in order to transmit heat energy away from the heat source. The last experiment was the use of LaRC-SI as an intermediate layer to allow metal to be placed on aluminum nitride.

Thin Film Sensors

Thin film sensors are used on models to measure air speed while in a wind tunnel. This measurement is used to find out when laminar air flow changes to turbulent air flow on a model. The sensor consist of a thin conductive film with a constant current passing though it. With a flow of air across it, the thin conductive film cools and the resistance goes down. This results in a smaller voltage across the film. When the air flow is reduced, the thin conductive film

heats up and the resistance goes up resulting in a larger voltage drop. The voltage drop is therefore an indication of the air speed.

The best way to put thin film sensors on a model is to deposit the metal sensors directly onto the model. The idea is to make the sensors as thin and smooth as possible so that it is not intrusive to the flow of air. In order to deposit metal on the model, a layer of dielectric material needs to be placed on the model to prevent the thin film sensors from shorting out on the model. The current material used for a dielectric is a polyimide made by DuPont. It works but it causes some problems because it cures at 500°F (Solder melts at ≈450°F and some model materials melt at < 500°F). My project consisted of determining if the LaRC-SI could be used as a dielectric for thin film sensors and then finding the lowest curing temperature.

Most of the time spent on this project was consumed by polishing small aluminum coupon plates by hand. There is definitely an art to polishing aluminum so that it has small uniform scratches that all go the same way. Also a large number of coupons were polished because every failed attempt of fabricating the thin film sensors resulted in re-polishing the coupon. The reason for the coupon surface needing to be so smooth and flat was due to the small size of the sensors.

The next problem was spraying the LaRC-SI in a humid environment. The LaRC-SI was dissolved in a solvent called NMP (1-Methyl-2-pyrrolidinone). In a humid environment, the NMP would react with the moisture in the air and would glob up resulting in clogging the air gun nozzle or depositing on the coupon. This was undesirable since a smooth even layer of LaRC-SI was needed on the coupon. Different ratios of LaRC-SI and NMP were tried. Also experiments of mixing NMP and Xylene was tried. The recipe that resulted was to mix the LaRC-SI and NMP in a 1:9 ratio by weight. This solution was mixed until all of the LaRC-SI was dissolved. This mixture was diluted by mixing 2:1 solution and NMP by volume. Finally, 10 drops of Xylene was added for every 10 mL of solution. This mixture was also sprayed early in the morning when the air conditioner was not tasked beyond its ability to minimize the moisture in the air.

Another problem was the forced air convection ovens in which the coupons were placed to cure the LaRC-SI. The forced air caused two problems. First it would make ripples in the LaRC-SI as it was drying due to the air currents. Second, it would circulate dust around in the oven which would eventually deposit on the LaRC-SI as it was drying. The first attempt was to cover the coupons with aluminum shelves to minimize the air flow on the coupons. This solved the ripple problem, but dust was still being deposited on the coupons. Next, large petri dishes were used in which the coupon could be placed in the dish. The first attempt did not work because the petri dish cover did not allow enough air flow to allow the NMP to escape as it was evaporating. After some thought, cardboard spacers were added to the petri dish to raise the cover up to allow the NMP to escape, but not to far up to allow a large amount of air flow (and thus dust) into the dish. This modification worked when the baking temperature and time were raised from 125°F for 30 minutes to 140°F for 45 minutes between each layer of LaRC-SI applied.

In my final batch of coupons, the LaRC-SI mixture was prepared as described above. Four layers of LaRC-SI were applied to four polished coupons with each layer consisting of two coats each. Each layer was dried at 140°F for 45 minutes in a large petri dish. After the four layers were applied, each coupon was baked for two hours at 150°F, 200°F, 300°F, and 400°F respectfully. The coupons were placed in an E-Beam evaporator. 3,000 Angstroms of nickel and then 10,000 Angstroms of copper were evaporated onto the coupons while simultaneously using the ion beam gun. The thin film sensors were then patterned using standard photolithography procedures. The sensors were checked for quality control with a Reichert microscope and an ohmmeter. Hard wire leads were then soldered onto the copper sensor leads. This allowed the sensors to be hooked up to an anemometer. The anemometer stresses the sensor electrically. The results from the anemometer test are shown in tables 1 through 4.

Coupon cured at 400°F.

Sensor	R _G (Ω)	R _T (Ω)	R _S (Ω)	R _L (Ω)	R _{TA} (Ω)	Set (%)	R _{TA} (Set) (Ω)	VA (V)	R _{TA} (After) (Ω)	R _D (Ω)	Comments
1	>20M	11.8	8.5	3.3	10.48	120	11.82	?	14.50	4.1	blown open blown open
					14.50	130	16.74	569			
2	>20M	12.2	9.9	2.3	10.97	120	12.70	.63			
3	>20M	11.6	9.9	1.7	11.75	120	13.76	9.3	11.75	0.00	
					11.75	130	14.77	10.9	11.75	0.00	
					11.75	140	15.77	12.1	11.70	0.05	
					11.70	150	16.70	13.0	11.64	0.06	
					11.64	160	17.60	13.7	11.63	0.01	
					11.81	120	13.77	11.8	11.81	0.00	
4	5.6M	11.8	9.8	2.0	11.81	130	14.75	13.7	11.85	0.04	
					11.85	140	15.79	15.3	11.86	0.01	
					11.86	150	16.79	15.6	11.97	0.11	
					11.97	160	17.90	8.1	12.01	0.04	
					10.95	120	12.90	9.6	10.95	0.00	
5	>20M	11.1	9.9	1.2	10.95	130	13.88	11.1	10.96	0.01	
					10.96	140	14.86	12.4	10.94	0.02	
					10.94	150	15.81	12.4	10.89	0.05	
					10.89	160	16.70	14.2	10.84	0.05	
					10.36	120	12.30	10.6	10.34	0.02	
6	>20M	9.4	9.8	2.0	10.34	130	13.23	12.3	10.35	0.01	
					10.35	140	14.21	13.7	10.36	0.01	
					10.36	150	15.19	14.7	10.37	0.01	
					10.37	160	16.17	8.5	10.35	0.02	
					10.37	160	16.17	8.5	10.35	0.02	

Table 1

Coupon cured at 300°F

Sensor	R _G (Ω)	R _T (Ω)	R _S (Ω)	R _L (Ω)	R _{TA} (Ω)	Set (%)	R _{TA} (Set) (Ω)	VA (V)	R _{TA} (After) (Ω)	R _D (Ω)	Comments
1	>20M	11.2	8.6	2.6	11.02	120	12.70	9.3	11.03	0.01	
					11.03	130	13.56	10.8	11.04	0.01	
					11.03	140	14.42	12.0	11.01	0.03	
					11.01	150	15.22	13.0	11.01	0.01	
					11.01	160	16.06	13.9	12.98	1.97	
											Unstable

2											Not measured
3	>20M	10.8	9.0	1.8	10.62	120	12.38	9.2	10.63	0.01	
					10.63	130	13.56	10.8	110.63	0.00	
					10.63	140	14.16	12.0	10.61	0.02	
					10.61	150	15.02	13.0	10.56	0.05	
					10.56	160	15.82	13.9	10.48	0.08	
4	>20M	10.7	10.1	0.6	10.46	120	12.43	9.8	10.46	0.00	
					10.46	130	13.42	11.5	10.46	0.00	
					10.46	140	14.40	12.6	10.46	0.00	
					10.46	150	15.39	13.6	10.46	0.00	
					10.46	160	16.38	8.7	10.45	0.01	
5	>20M	11.1	9.9	1.2	11.01	120	12.97	8.3	11.01	0.00	
					11.01	130	13.95	9.7	11.02	0.01	
					11.02	140	14.95	10.8	11.02	0.00	
					11.02	150	15.93	11.7	11.07	0.05	
					11.07	160	16.99	12.6	11.13	0.06	
6	>20M	11.0	10.2	0.8	10.91	120	12.93	8.0	10.89	0.02	
					10.89	130	13.92	9.3	10.95	0.06	
					10.95	140	15.01	10.4	10.94	0.01	
					10.94	150	16.01	11.1	10.83	0.11	
					10.83	160	16.85				

open - 844Ω

Table 2

Coupon cured at 200°F

Sensor	R _G (Ω)	R _T (Ω)	R _S (Ω)	R _L (Ω)	R _{TA} (Ω)	Set (%)	R _{TA} (Set) (Ω)	VA (V)	R _{TA} (After) (Ω)	R _D (Ω)	Comments
1	>20M	11.7	9.5	2.2	11.50	120	13.36	7.6	11.51	0.01	
					11.51	130	14.30	8.9	11.52	0.01	
					11.52	140	15.25	9.8	11.51	0.01	
					11.51	150	16.17	10.6	11.48	0.03	
					11.48	160	17.05	11.4	11.48	0.00	
2	>20M	11.9	10.1	1.8	11.77	120	13.76	6.94	11.77	0.00	
					11.77	130	14.76	8.10	11.77	0.00	
					11.77	140	15.76	9.0	11.96	0.19	
					11.96	150	17.04	9.8	17.18	5.22	
3	>20M	11.7	10.1	1.6	11.71	120	13.73	6.4	11.71	0.00	Unstable
					11.71	130	14.74	7.5	11.71	0.00	
					11.71	140	15.75	8.2	11.94	0.23	
					11.94	150	17.11	9.0	16.46	4.52	
4	>20M	11.5	10.1	1.4	11.31	120	13.29	6.7	11.31	0.00	Unstable
					11.31	130	14.28	7.7	11.31	0.00	
					11.31	140	15.27	8.6	11.57	0.26	
					11.57	150	16.66	9.3	11.82	0.25	
					11.82	160	17.08	8.9	11.57	0.25	
5	>20M	11.8	10.8	1.0	11.59	120	13.71	5.4	11.66	0.07	
					11.66	130	14.86	6.24	11.63	0.03	
					11.63	140	15.88	3.7	12.28	0.65	
					12.28	150	17.92				
6	>20M	10.8	10.0	0.8	10.58	120	12.54	6.3	10.58	0.00	blown-1kΩ
					10.58	130	13.51	7.3	10.58	0.00	
					10.58	140	14.49	7.4	13.48	2.9	

Table 3

Coupon cured at 150°F

Sensor	R _G (Ω)	R _T (Ω)	R _S (Ω)	R _L (Ω)	R _{TA} (Ω)	Set (%)	R _{TA} (Set) (Ω)	VA (V)	R _{TA} (After) (Ω)	R _D (Ω)	Comments
1	>20M	12.1	9.7	2.4	11.92 13.26 14.15	120 130 140	13.82 16.52 18.85	7.7 4.3	13.26 14.15	1.34 0.89	open >20MΩ not measured
2											
3	>20M	11.9	10.1	1.8	11.96 13.75	120 130	13.99 17.34	5.6 9.7	13.75 26.7	1.79 12.9	Unstable
4	>20M	11.8	10.3	1.5	11.70	120	13.74	3.8	16.30	4.6	
5	>20M	11.1	10.0	1.1	10.96 12.20 12.61	120 130 140	12.93 15.53 17.21	7.2 3.80	12.20 12.61	1.24 0.41	open >20MΩ
6	>20M	10.1	9.3	0.8	9.94 10.96	120 130	11.77 14.01	6.6 8.7	10.96 13.20	1.02 2.24	

Table 4

Notes:

- R_G: Resistance from sensor to aluminum coupon
- R_T: Total resistance
- R_S: Sensor resistance
- R_{TA}: Total resistance as measured from anemometer
- Set: Rating at which anemometer is set to cause overheating in sensor
- VA: Voltage measurement from anemometer
- R_D: Change in resistance after overheating setting by anemometer

The 160% set on the anemometer is a severe test. Taking this into consideration, the coupons that were cured at 400°F and 300°F were successful. The coupon cured at 200°F had 4 of the 6 sensors go bad when tested at 150%. More tests can be conducted later to determine a more exact temperature at which the LaRC-SI can be cured. This should be in the range of 200°F to 300°F

Electrically, the LaRC-SI material has allowed the placement of thin film sensors on aluminum at curing temperatures as low as 300°F. Two other items need to be taken into consideration: one, how well the LaRC-SI adheres to the model, and two, the smoothness of the finish of the LaRC-SI

The LaRC-SI needs to adhere well to the model. It should not flake off. In the 150°F coupon, the LaRC-SI flaked off in large chunks when using an instrument to scrape it off. Although not as severe, the LaRC-SI also flaked off on all of the other coupons in smaller pieces.

The surface of the LaRC-SI also needs to be smooth so that it does not disrupt the flow of air over the model. All of the coupons tested had ripples due to the LaRC-SI shrinking when it was dried. The coupon baked at 150°F was the worst while the others had ripples that were not as severe.

Thermal Properties

The idea for this project came from the Fall 1994 issue of *UAB Scientist*. It stated that diamonds are the best known thermal conductors, but it is difficult to adhere to metals, ceramic, and plastics. The heat transfer capability of diamond is >1200 W/mK and recently it has been manufactured with a heat transfer capability of >2000 W/mK. This is compared to 326W/mK of copper which is an electrical conductor - a problem in some applications. An improvement in thermal heat transfer and dissipation is needed in the electronics community. After being handed some diamond dust by Dr. Robert Bryant, I wrote a proposal to investigate the heat transfer properties of diamond dust adhered to a surface with LaRC-SI. The experiment was to show that diamonds could be applied to a surface to transfer heat energy from a heat source to a heat sink.

An obstacle to this experiment is that the LaRC-SI is a thermal insulator. Since it is used as an adhesive, it will exist as a thin boundary between the diamonds. This thin layer will minimize the undesirable thermal properties of the LaRC-SI. Also, the thermal heat transfer capability of diamonds is so large that if the number is reduced by a factor of five, the heat transfer capability will still be large.

The experiment was conducted as follows. 600 Grit and 1200 Grit diamonds were placed on 2" x 2" 60 mil alumina ceramic plates by using LaRC-SI. Thermal measurements were taken after using the following methods of placing the diamonds on the ceramic plates.

- 1) Sprayed LaRC-SI and then sprayed the 600 or 1200 grit diamonds. Cured at 125°F for 30 minutes between layers. Placed three layers of LaRC-SI and diamonds onto the ceramic plates.
- 2) Followed the procedure in step 1 but also baked at 500°F for 2 hours after the third layer was placed on the ceramic plate.
- 3) Followed the procedure in step 1 but then baked at 500°F for 2 hours in a vacuum. The surrounding air pressed the diamonds while the LaRC-SI was curing so that the diamonds are closer together.
- 4) Sprayed the LaRC-SI on the ceramic plate but then sprinkled the diamonds on. Used the baking methods in steps 1 and 3.
- 5) Mixed the 600 grit and 1200 grit diamonds together. Sprayed the LaRC-SI on the ceramic plate but then placed the diamonds on by using forced air to agitate the diamonds onto the ceramic plates. Used baking methods described in steps 1 and 3.
- 6) Mixed the LaRC-SI and diamond mix together and painted the mixture onto the ceramic plates. Followed the curing methods as described in steps 1 and 3.

The thermal properties were measured by using the following setup. A 10 Ω power resistor was mounted on the test plate using a silver paint (Dynalot 340). Three thermocouples were used to

take measurements at various locations at 1 cm apart. Two versions of the placement of thermocouples were used. They are shown in figure 1. Measurements were taken every 20 seconds for 20 minutes. The power resistor was operated at 5.0 Volts which resulted in a heat source of 2.5 watts. A box was placed over the plate to minimize the effects of thermal variations due to drafts.

The temperature differences between the thermocouples was used for comparing the rate of heat transfer. The results were compared to a plain alumina plate and to a alumina plate with three layers of LaRC-SI that was cured at 500°F

This method of measuring heat transfer is crude, but it does give an indication of heat transfer and can be later sent to VMI which has the proper equipment setup to measure the heat transfer coefficient.

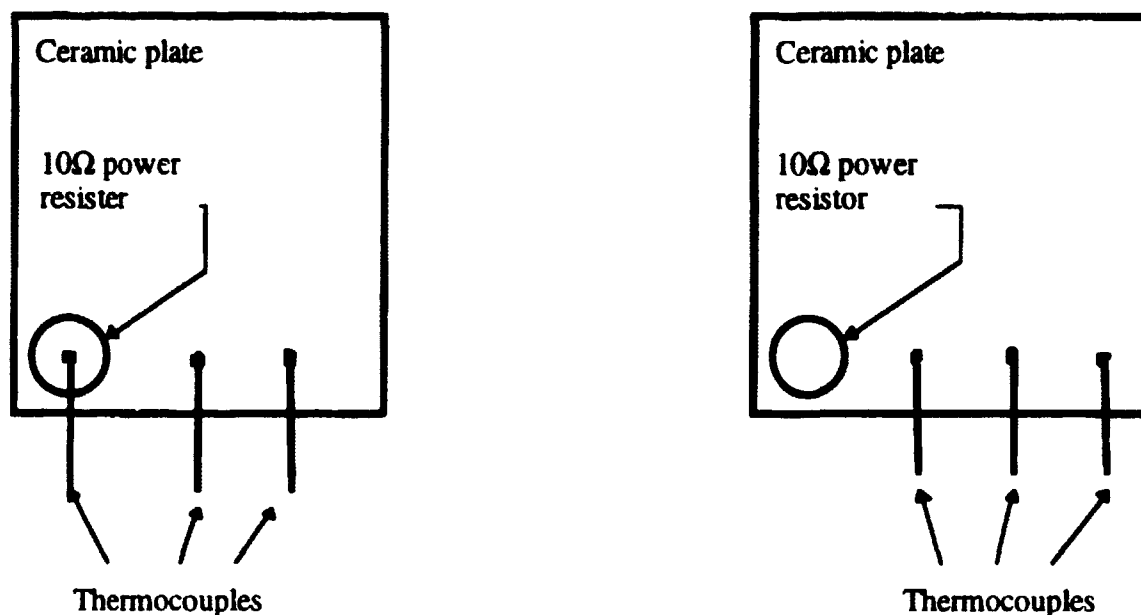


Figure 1. Thermocouple placement on ceramic plates.

Due to a limited amount of diamond dust and time, a more thorough experiment was not performed. Results were positive but not as good as expected. The heat transfer increased when the sample was heated to 500°F and was the best when baked with a vacuum. A graphical result of the increase in heat transfer is shown in Figure 2. The best size diamonds to use was inconclusive. One of the problems was that too much diamond dust was deposited on some samples. The key for best heat transfer is going to be when there is just enough diamonds so that they are all touching with just enough LaRC-SI to pull them all together. Too much diamond dust and the LaRC-SI does not pull all the diamond dust together and leaves air pockets. Too much LaRC-SI and the heat does not get transferred by the diamonds.

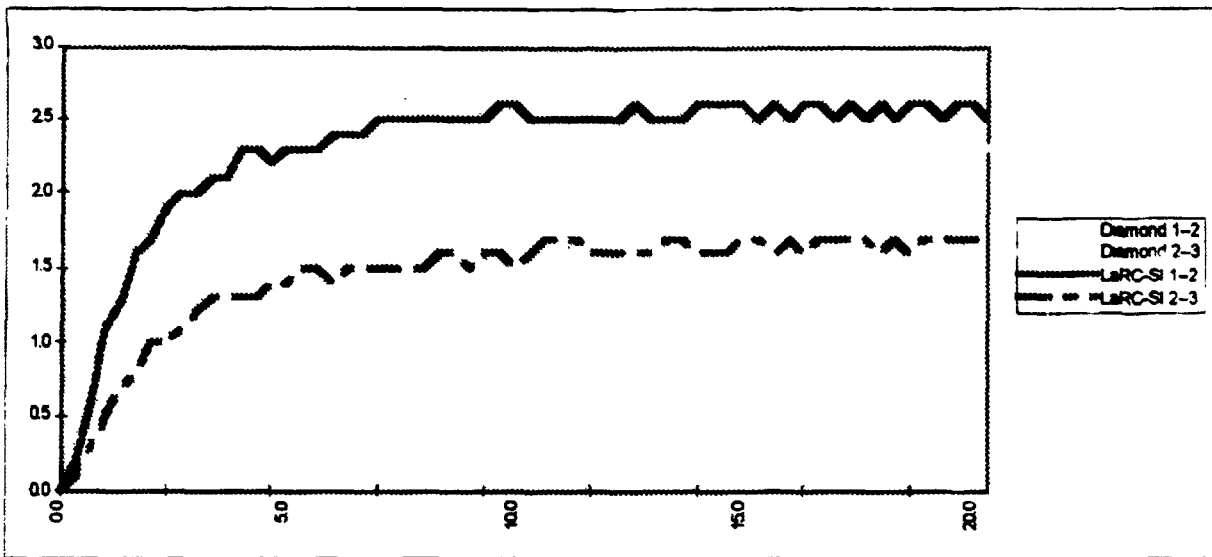


Figure 2. A Graphical Representation of Increased Heat Transfer

Applying Metal to Aluminum Nitride

Aluminum nitride is a ceramic that metal traditionally does not adhere. It is also a good heat conductor. Because of its thermal properties, it has been considered as a substrate for microelectronics. My experiment was to see if LaRC-SI could be used as an intermediate boundary to place metal on aluminum nitride.

Three layers of LaRC-SI was sprayed onto aluminum nitride plates. The mixture that was used was the same as used for the thin film sensors. Between each layer, the sample was dried at 125°F for 30 minutes. The ceramic plates were then baked at 500°F for two hours. 3,000 Angstroms of nickel and 10,000 Angstroms of copper were then evaporated onto the plates

As a check to see that the LaRC-SI really held the metal to the aluminum nitride, a tape pull test was performed. Also a more severe test was done by performing a tape pull test after the test plates were submerged in liquid nitrogen. Both test resulted positively. No metal was pulled off.

Conclusion

The LaRC-SI is an exciting new thermal plastic that has many potential applications. My stay at Langley Research Center involved exploring three of these applications. Due to the time limit of 10 weeks, all of the possibilities on these applications could not be explored.

This is also the first time that I have researched anything that is this complex and time consuming. Thanks to my Mentor, Carl Voglewede, he allowed me a great amount of freedom that I have not experience before in the workplace. I was allowed to make the decision on what equipment was needed and how an experiment was to be performed. This has definitely has been a learning experience.

References

- Bryant, Robert G., "A Soluble Copolyimide", Polymer Preprints, Papers presented at the San Diego, California Meeting, American Chemical Society, The Division of Polymer Chemistry, Inc., Volume 35, Number 1, March 1994.
- Crall, Richard F., "Thermal Management," Advanced Packaging, Winter 1993, p 12-6.
- Davidson, Jim L., et al., "Microelectronic Materials What the Experts Say!" Inside ISHM, International Society For Hybrid Microelectronics July/August 1992, Volume 19, No 4, p 5-9
- Fox, Robert L., "Electronic Management Through New Materials and Electronic Packaging #49"
- Garrou, Philip, and Arne Knudsen, "Aluminum Nitride For Microelectronic Packaging," Advancing Microelectronics, ISHM, The Microelectronics Society, January/February, 1994, Volume 21, No 1, p 6-10.
- Incropera, Frank, and David DeWitt, Fundamentals of Heat Transfer, Joh: Wiley & Sons, New York, 1981.
- Moravec, Thomas J. and Arjun Partha, "Diamond Takes The Heat," Advanced Packaging, October 1993, p 8-11
- Norwood, David, et al., "Diamond - A New High Thermal Conductivity Substrate for Multichip Modules and Hybrid Circuits," IEEE, 1993.
- Peckrell, D J , et al , "Diamond Substrates," Advanced Packaging, Summer 1992, p 16-20
- Shealy, David, et al., "Lasers and Micro-Optics," UAB Scientist, Fall 1994, p 12-3
- Sussmann, R. S et al., Properties of Bulk Polycrystalline CVD Diamond, The Institution of Electrical Engineers, Savoy Place, London, 1993.

**NEXT
DOCUMENT**

THE CALIBRATIONS OF SPACE SHUTTLE MAIN ENGINES HIGH PRESSURE TRANSDUCERS

A Technical Report

written by

Christopher S. Steward

Mentor: Dr. Allan J. Zuckerwar

**Internal Operations Group
Experimental Testing Technology Division
Acoustic, Optical, and Chemical Measurement Branch**

ABSTRACT

Previously, high pressure transducers that were used on the Space Shuttle's Main Engine (SSME) exhibited a severe drift after being tested on the SSME. The Experimental Testing Technology Division (ETTD) designed some new transducers that would not exhibit a severe drift over a short period of time. These transducers were calibrated at the Test Bed at Marshall Space Flight Center (MSFC). After the high pressure transducers were calibrated, the transducers were placed on the SSME and fired. The transducers were then sent to the NASA LaRC to be recalibrated. The main objectives of the recalibrations was to make sure that the transducers possessed the same qualities as they did before they were fired on the SSME. Other objectives of the project were to determine the stability of the transducers and to determine whether the transducers exhibited a severe drift.

INTRODUCTION

A multichannel high pressure transducer using miniature piezoresistive silicon pressure sensors has been designed and developed in the ETTD. It was developed to measure fuel and oxidizer pressure of SSME. The transducer is able to accurately measure pressure to within 0.25% full scale up to 30 MPa for LH₂/GH₂ and LOX/GOX in NASA Launch Vehicles. The pressure sensor unit consists of four silicon piezoresistive pressure sensor dice bonded to two aluminum nitride substrates with Indium or Au/Sn. Three of these high pressure transducers were tested last year on a shuttle engine at Test Bed (MSFC). After four runs these transducers were taken off and are being recalibrated at Langley Research Center.

PROCEDURE

Part I :

In Part I of my project, one of the high pressure transducers were mounted on the cold head in Cryogenic chamber. A Platinum Resistance Thermometer (PRT) was also placed inside the Cryogenic chamber along with the transducer. I brought the pressure from 0psi to 1,000psi and back down to 0psi in 1,000psi increments. During this time, I measured and recorded the output voltages of the 4 pressure sensors and the PRT at each 1,000psi increment. A constant current source was sent through the PRT to obtain an output voltage from it as well. The output voltage from the PRT could be used to determine the exact temperature in the Cryogenic chamber.

Part II :

In Part II of my project, The high pressure transducer remained mounted on the cold head inside the Cryogenic chamber. First, I raised the temperature to 1,000psi and let it stabilize. Next, I lowered the temperature from 295k (Room Temperature) to 10k in 10k increments. I measured and recorded the output voltages from the PRT and the 4 pressure sensors individually at each increment.

PRESSURE SENSOR CALIBRATION SHEET

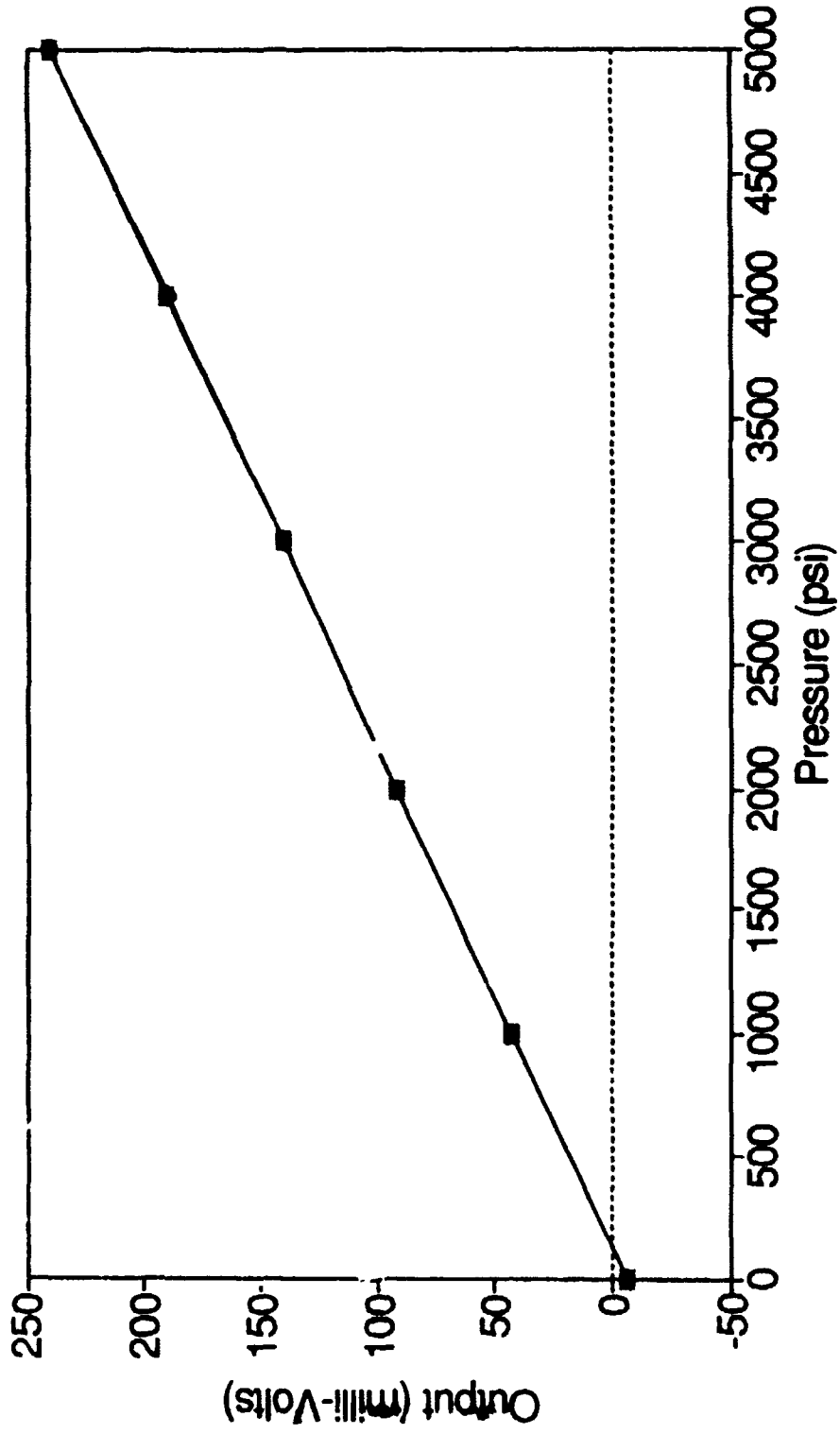
Date : June 26, 1995
Sr. No.: SSME #5
Die : After Testing at MSFC
Medium : R.T. (3rd Run)
Input : 5 volts
File : Sensor #1

TCS. Pressure	BFSL	-----Run #1-----		-----Run #2-----	
	Rm Temp Outputs	Rm Temp Outputs	Error %FSO	Rm Temp Outputs	Error %FSO
0	-6.279	-5.9985	0.1144	-6.0329	0.1003
1000	42.777	42.7590	-0.0073	42.6810	-0.0391
2000	91.832	91.6520	-0.0734	91.5430	-0.1178
3000	140.888	140.7300	-0.0644	140.6090	-0.1137
4000	189.944	190.0890	0.0591	189.9500	0.0024
5000	238.999	239.3700	0.1513	239.2270	0.0930
4000	189.944	190.0310	0.0355	190.0690	0.0510
3000	140.888	140.7630	-0.0510	140.6730	-0.0877
2000	91.832	91.5790	-0.1031	91.6280	-0.0832
1000	42.777	42.7180	-0.0241	42.6810	-0.0391
0	-6.279	-6.0329	0.1003	-6.0413	0.0969

Max Static Error :	0.1513	%FSO	TCO(%F/C
Std Dev of Error :	0.0596		TCS(%F/PC)
Avg Static Error :	0.0456	%FSO	
Max Nonrepeatab'ity :	-0.0583	%FSO	
Sensitivity :	0.0098	mV/psi/V	S(mV/P/V):
Thermal Span :	1.7906	%FSO/C	
Remarks :			

TEST FOR MSFC TRANSDUCER #5

Room Temp., Sensor #1,



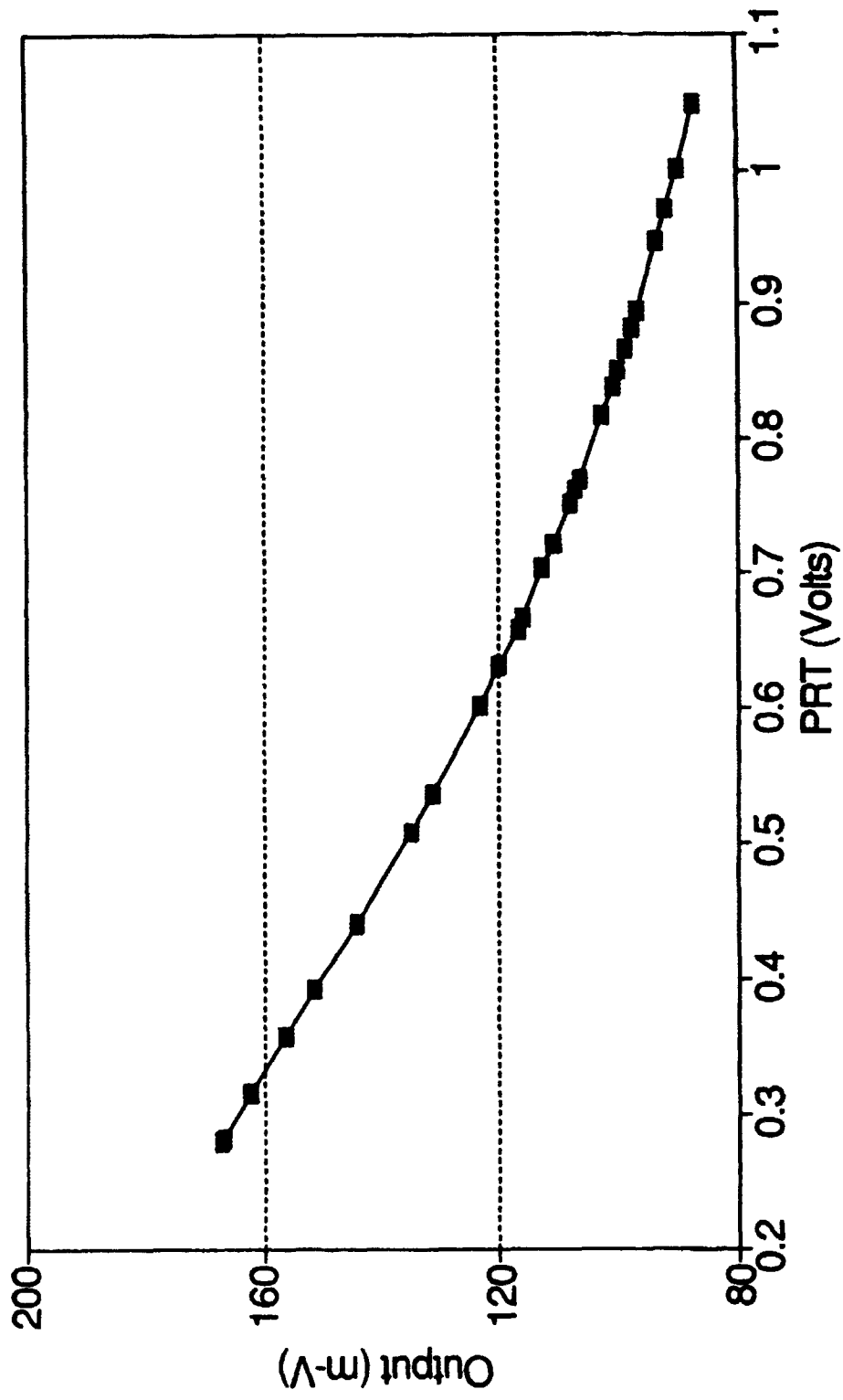
PRESSURE SENSOR CALIBRATION

Pressure =2000 psi

PRT (Volts)	Output (m-V)
1.0487	87.250
1.003	89.957
0.97258	91.782
0.94757	93.336
0.89432	96.788
0.88192	97.677
0.86723	98.761
0.85126	99.945
0.83784	100.976
0.81728	102.571
0.77001	106.440
0.76305	107.090
0.75223	108.032
0.72154	110.822
0.70378	112.508
0.66879	115.857
0.65784	116.994
0.63160	119.798
0.60171	123.208
0.53720	131.177
0.50971	134.852
0.44180	144.110
0.39173	151.243
0.35815	156.052
0.31458	162.156
0.28190	166.404
0.27898	166.780

PRESSURE SENSOR CALIBRATION

Pressure = 2000 psi



EQUIPMENT and FACILITIES

Equipment:

Positive-Shutoff Pressure Controller/Calibrator (PPCK) - a self-contained pneumatic pressure setting system intended for use in calibrating and testing all sorts of pressure measuring devices.

Multimeter (5) - a high performance 5-1/2 digital instrument designed for general purposes or systems applications.

Digital Temperature Controller (Model 9650) - a device used in calibrations to control the temperature in a Cryogenic chamber.

Compressor Module (Model HC-4 MK1) - The HC-4 MK1 compressor module is a single-stage, water-cooled rotary compressor designed to deliver high-pressure, oil-free helium gas to Cryogenic refrigerators.

Facilities:

The high pressure transducers were calibrated in the Component's Verification Building (1248B)

FUTURE WORKS

Future development involves the advanced engineering design to incorporate diagnostic and signal conditioning electronics into a Cryogenic pressure sensor for applications at the MSFC's Space Shuttle Main Engine (SSME) Test Facility. The new "Smart" Sensor requirements are required to integrate Cryogenic pressure sensor into the data system at the test facility.

CONCLUSION

After I completed my project, I was very pleased with my results. Although previous high pressure transducers exhibited a severe drift, the new LaRC developed transducers exhibited only a limited finite drift. All 12 of the pressure sensors in the three transducers followed the earlier calibrations profile very closely. We were able to observe a long term stability of less than 0.5% of full scale output for six months. During the calibration experiment, I was able to conclude that the pressure and output voltage of the pressure sensors were directly proportional. I was also able to conclude that the temperature inside the Cryogenic chamber and the output voltage were inversely proportional.

**NEXT
DOCUMENT**

15 17
/ -

**THE DEPENDENCE OF THE CHANGE IN THE COEFFICIENT OF
THERMAL EXPANSION OF GRAPHITE FIBER REINFORCED
POLYIMIDE IM7-K3B ON MICROCRACKING DUE TO
THERMAL CYCLING**

**Melissa C. Stewart
CraigW. Ohlhorst**

**Research and Technology Group
Materials Division
Environmental Interactions Branch**

ABSTRACT

Composite IM7-K3B was subjected to a simulated high speed aircraft thermal environment to determine the effects of microcracking on the change in CTE. IM7-K3B is a graphite fiber reinforced polyimide laminate, manufactured by Dupont. The lay-up for the material was $[0,90]_{3s}$. The specimens were placed in a laser-interferometric dilatometer to obtain thermal expansion measurements and were then repeatedly cycled between -65°F and 350°F up to 1000 cycles. After cycling they were scanned for microcracks at a magnification of 400x. The material was expected not to crack and to have a near zero CTE. Some microcracking did occur in all specimens and extensive microcracking occurred in one specimen. Further testing is required to determine how closely the CTE and microcracking are related.

INTRODUCTION

Researchers are currently investigating polymer matrix composites as a material for use in the narrow dimensional confines of supersonic aircraft. These composites show many desirable traits such as high stiffness and small changes in the coefficient of thermal expansion.

This study reports thermal expansion data for a graphite fiber reinforced polyimide (IM7-K3B) and examines the dependence of the change in CTE of the composite on microcracking. This microcracking is due to thermal cycling and has been shown to significantly alter physical properties of a composite, sometimes seriously affecting its dimensional stability [1].

EXPERIMENTAL PROCEDURE

Eight specimens of IM7-K3B, produced and manufactured by Dupont, were selected for thermal expansion testing: 1 [0]₁₂, 1 [90]₁₂, 1 [0]₂₄, 1 [90]₂₄ and 4 [0/90]_{3s} lay-ups. This report covers data from the initial testing of the four 12-ply [0/90]_{3s} symmetric crossplies.

The specimens were 7.5cm(3 in.) x 2.5cm(1 in.) with one polished edge. Each specimen had twelve 0.0127cm (0.005 in) plies. Each specimen was roughly 0.1524 cm(0.06 in) thick. A 2.54 cm(1 in.) section in the middle of the polished side of each specimen was examined for microcracking using an optical microscope at a magnification of 400x at 0, 25, 100, 500 and 1000 thermal cycles. The specimens were measured for the axial CTE at the same intervals.

The thermal expansion measurements were obtained using a laser-interferometric dilatometer at NASA Langley Research Center. This setup has a 1 microstrain resolution and measures the expansion of the specimen with respect to a NIST quartz standard [2]. The temperature range that the IM7/K3B specimens were exposed to was -54 °C (-65 °F) to 121 °C (250 °F).

A small scale thermal cycling chamber at NASA Langley Research Center was used to simulate the high speed aircraft thermal environment. One thermal cycle consisted of three steps. The first step started at 27 °C (80 °F) and rose to 177 °C (350 °F). The second dropped from 177 °C (350 °F) to -54 °C(-65 °F) and the final step brought the temperature back up to 27°C (80 °F.) The specimens were in direct contact with liquid Nitrogen during the cooling step.

RESULTS

Although testing is incomplete, initial data shows recognizable trends. Figures 1 through 4 display the CTE verses the number of cycles for each specimen. In each case the slope appears to be slightly negative, which indicates that the material shrinks as the number of thermal cycles increases. Specimen #2 is currently the only specimen of the four that has been tested for CTE after 1000 cycles, so the upward turn after 500 cycles shown in Figure 2 may be characteristic of the material. Comparison with CTE data from the other three specimens will reveal more conclusive results.

CTE data at 1000 cycles is currently unavailable for specimens 2,3 and 4.

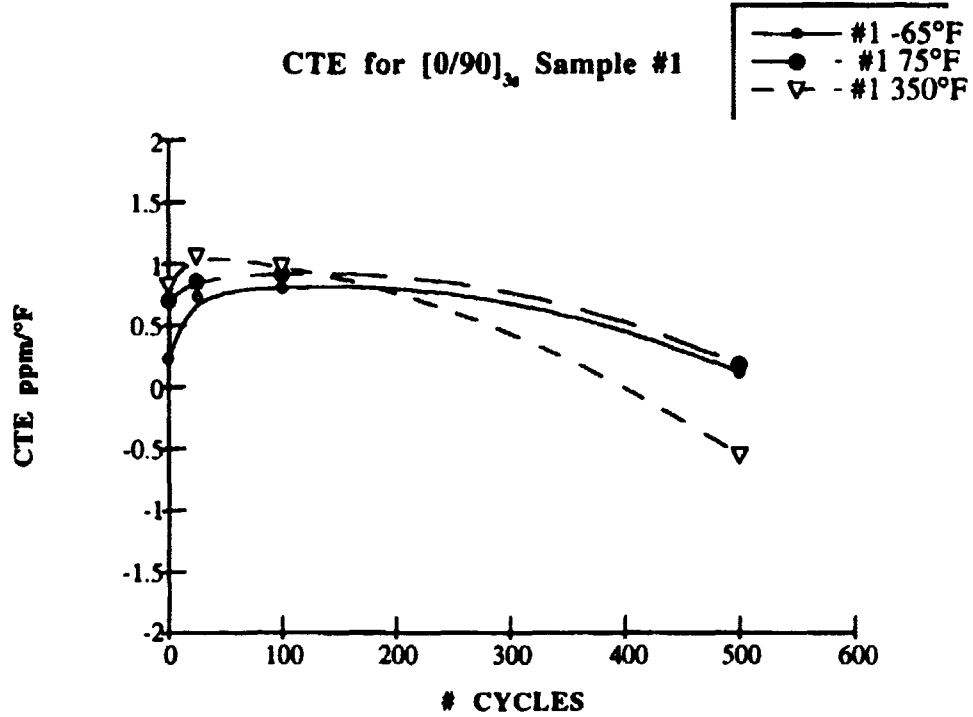


Figure 1 High temperature CTE data this specimen at 500 cycles was extrapolated. This may account for the deviation of the CTE at 350°F

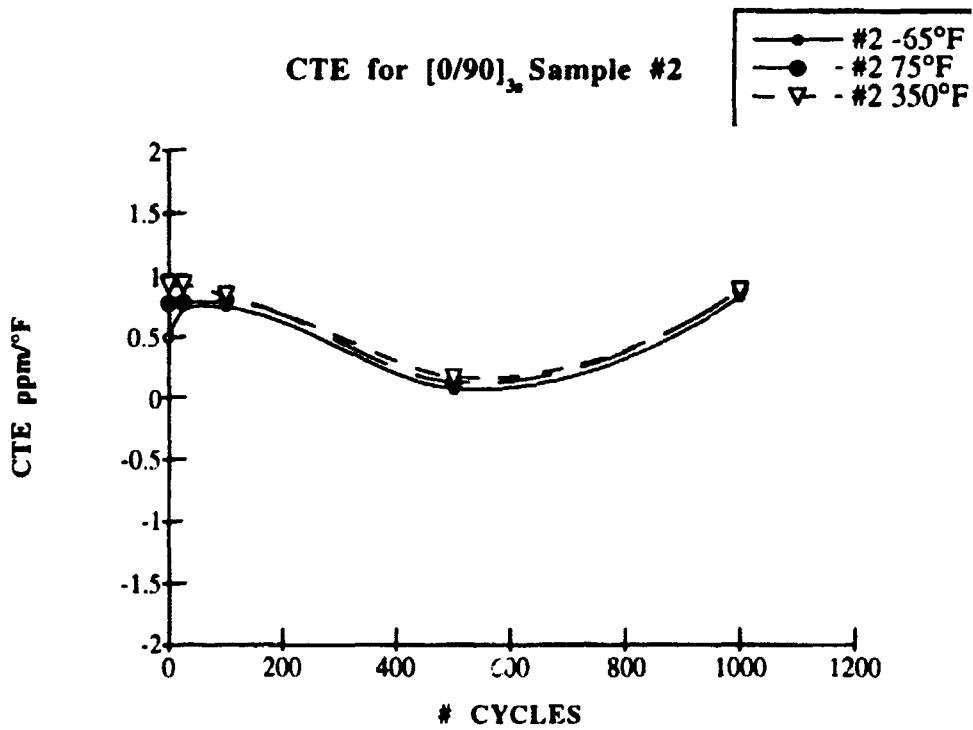


Figure 2 Notice upward turn after 500 cycles.

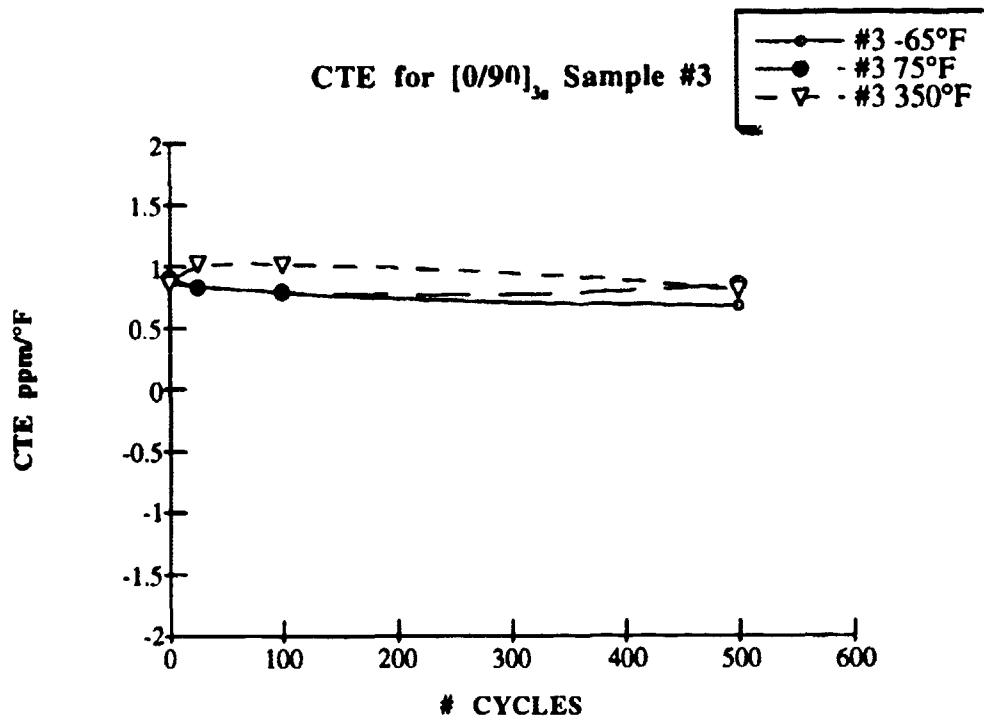


Figure 3

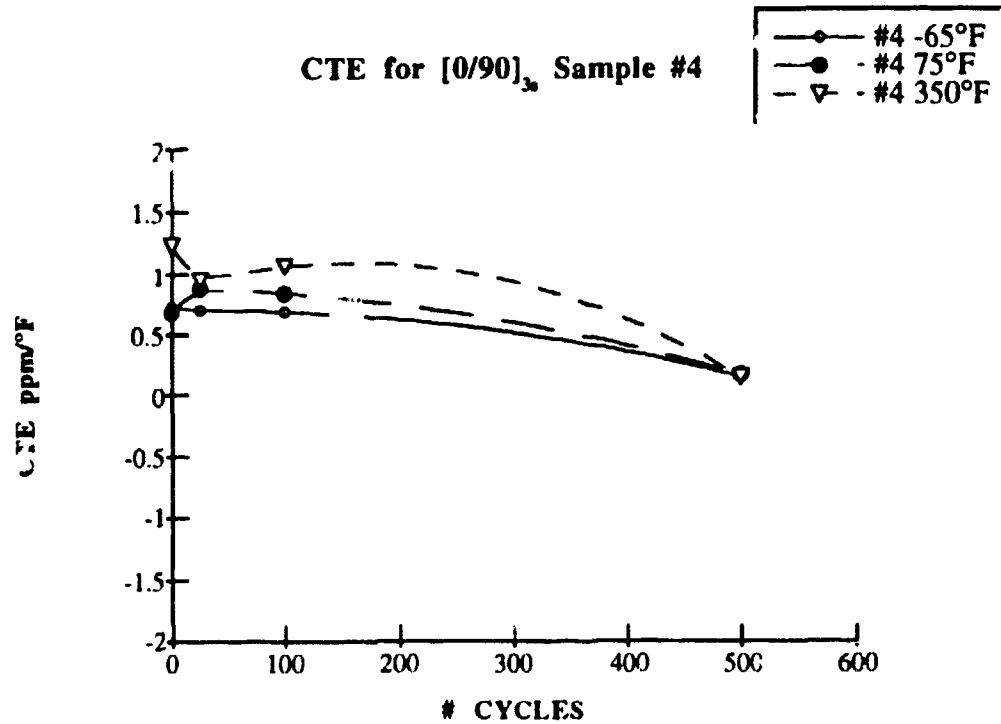


Figure 4

Figures 5 and 6 show the development of microcracks with increasing numbers of thermal cycles. Only data from the 90° plies is reported because microcracking occurs parallel to the 0° plies and cannot be seen by scanning the side of a specimen. The microcracking behavior of specimens 2, 3 and 4 is fairly uniform and appears to reach a limit of approximately 15 cracks/in. At this time only samples 2 and 4 have completed 1000 thermal cycles. Sample 3 is expected to behave similarly, but sample 1 shows radical differences in both the number of microcracks and the rate of microcracking. Possible explanations for this unexpected behavior include damage during fabrication, nonuniform thickness, and possible temperature surges during testing. All of these can contribute to microcracking.

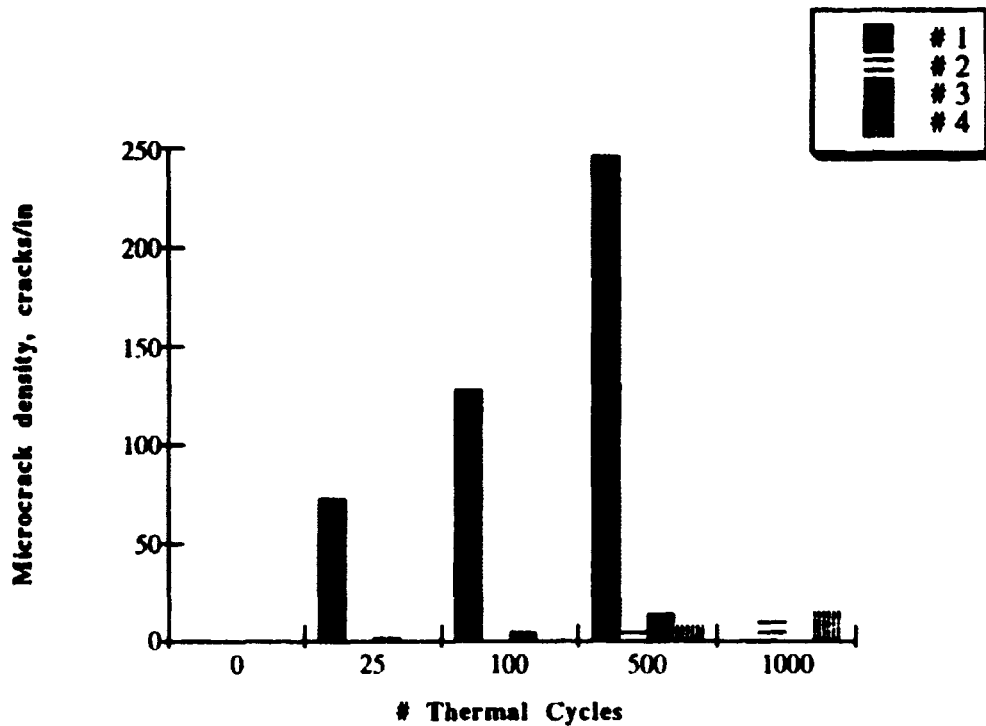


Figure 5 Sample #1 shows a large deviation from the behavior of the other specimens. Possible explanations for the behavior are damage during manufacturing and nonuniform specimen thickness.

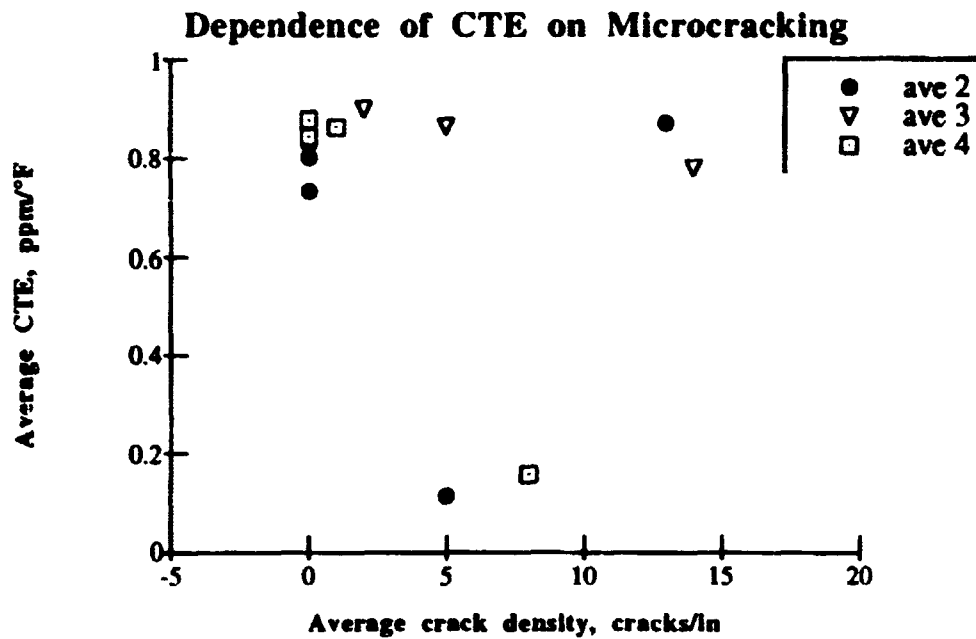


Figure 8

CONCLUSIONS

The thermal expansion of four specimens of IM7-K3B up to 500 thermal cycles has been measured and compared. Additional tests are needed to acquire microcracking and CTE data for 1000 cycles.

In each of the four specimens, the CTE decreased initially as the number of thermal cycles increased. Specimen #2 showed an upward turn after 500 cycles, but no information is currently available for specimens 1,3 and 4.

All specimens began with no visible microcracking, however microcracking did occur in all specimens at some point. The particularly high rate of cracking in specimen #4 should be investigated further at some point. Possible areas to investigate are the manufacturing and cutting process, the location of the specimen in the original panel and the uniformity of the ply thickness.

REFERENCES

1. B. Knouff, S.S. Tompkins, N. Jayaraman, "The Effect of Microcracking Due to Thermal Cycling on the Coefficient of Thermal Expansion of Graphite Fiber Reinforced Epoxy-Cyanate Matrix Laminates", 25th International SAMPE Technical Conference, Volume 25, Advanced Materials: Expanding the Horizons, October 26-28, 1993, Philadelphia, PA pp:610-621.
2. S.S. Tompkins, D.E. Bowles, and W.R. Kennedy, "A Laser-Interferometric Dilatometer for Thermal-Expansion Measurements of Composites", Experimental Mechanics 26, (1), 1, (1986)

**NEXT
DOCUMENT**

ANALOG PROCESSING
ASSEMBLY FOR THE
WAKE VORTEX LIDAR
EXPERIMENT

Edwood G. Stowe

Phil Brockman, mentor
Internal Operations Group
Flight Electronics Division
Sensors Technology Branch

Abstract

The Federal Aviation Administration (FAA) and NASA have initiated a joint study in the development of reliable means of tracking, detecting, measuring, and predicting trailing wake-vortices of commercial aircraft. Being sought is an accurate model of the wake-vortex hazard, sufficient to increase airport capacity by reducing minimum safe spacings between planes. Several means of measurement are being evaluated for application to wake-vortex detection and tracking, including Doppler RADAR (Radio Detection and Ranging) systems, 2-micron Doppler LIDAR (Light Detection And Ranging) systems, and SODAR (SOund Detection And Ranging) systems. Of specific interest here is the lidar system, which has demonstrated numerous valuable capabilities as a vortex sensor. Aerosols entrained in the vortex flow make the wake velocity signature visible to the lidar; (the observable lidar signal is essentially a measurement of the line-of-sight velocity of the aerosols). Measurement of the occurrence of a wake vortex requires effective reception and monitoring of the beat signal which results from the frequency-offset between the transmitted pulse and the backscattered radiation. This paper discusses the mounting, analysis, troubleshooting, and possible use of an analog processing assembly designed for such an application.

Background

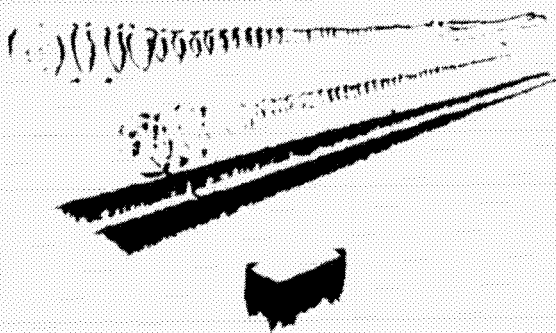
LIDAR As an Operational Vortex Sensor

CO₂ lidars have been used to study wake vortices since the early '70s. The basic Doppler lidar consists of a very stable single frequency laser, interferometer, transmit-receive optics, infrared detector, range-angle scanner, velocity-frequency analyzer, data-algorithm processor/display, and recorders. Aerosol particles scatter the transmitted radiation in all directions, and their motion with the atmosphere Doppler shifts the frequency from that of the transmitted pulse. The backscattered radiation is collected by optics and mixed with a small portion of the original transmitted beam. The total radiation resulting from this mix fluctuates at a beat frequency. This beat frequency is a measure of the wind velocity at that point. The Doppler lidar measures wind velocity components in the sensor line-of-sight (along the laser beam). A family of such velocity measurements produces what is called a signature of that vortex. From that signature, researchers can acquire vortex characteristics such as position and strength.

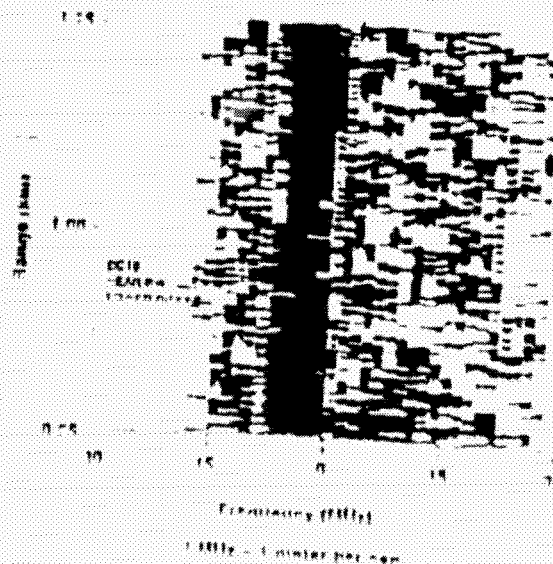
The current wake vortex lidar being developed is a pulsed solid state 2 micrometer system. In a pulsed lidar range information is provided by the two-way time of flight of light. Thus the range of the measurement is $c/(2t)$ where c is the speed of light and t is the time from pulse initiation. The range resolution is dependent on the pulse length. The challenge of the analog processor is to measure a series of stream of data. The length of the streams is a milliseconds and the rate of the streams is dependent on the pulse rate of the lidar, typically 100 - 200 pps.

Lidar provides high-resolution velocity field measurement, and recent successful vortex measurements (Memphis & Denver, Stapleton) have demonstrated numerous other capabilities, including real-time tracking and display. The pictures below depict an example of the trailing wake vortices of a landing aircraft, the measurement geometry of a pulsed lidar system, and the spectrum signature produced from the data acquired.

Example of Measurement Geometry



Velocity vs. Range for Single Line-of-Sight



- Lidar scan produces velocity profile along each line of sight
- Family of velocity profiles produces characteristic signature
- Signature allows extraction of vortex strength, position, and motion

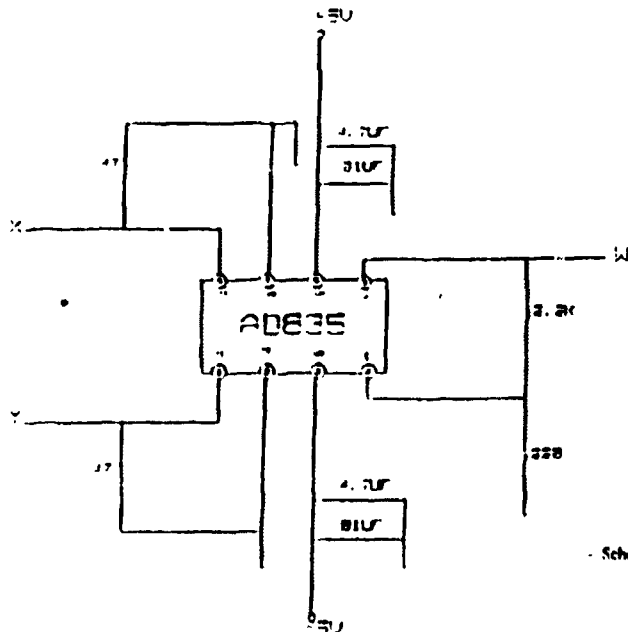
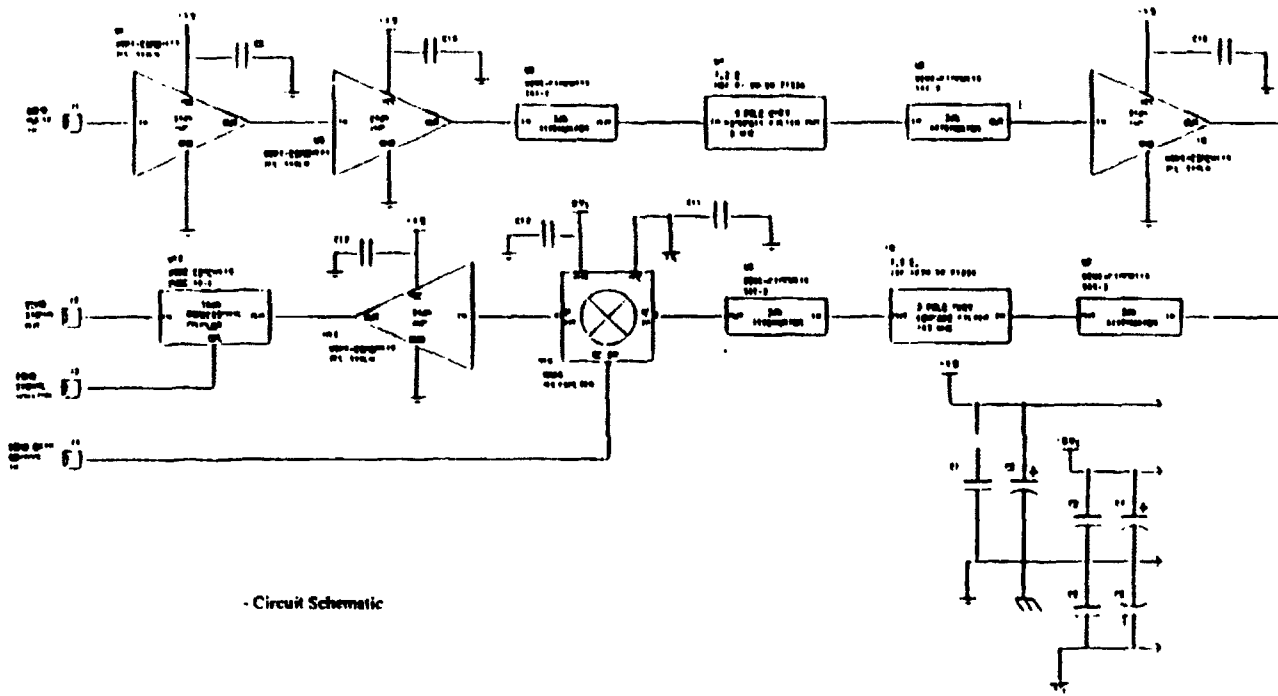
Research / Analysis

For my summer internship project, I investigated an analog processing assembly that is the RF section of the data acquisition system. This assembly receives the heterodyne lidar echo output from the lidar detector/preamp and conditions the signal for input to the A/D converter. The signal occupies a bandwidth from DC to 180 MHz centered at 105 MHz with an amplitude of a few microvolts. The analog signal must be amplified, filtered, and gain-controlled using distributed stages prior to digital processing. A block diagram of the signal processor is shown on the following page. Each element is individually packaged in a small box with SMA coax signal connectors and power terminals. My first task was to mount and interconnect the individual components in a compartment, then analyze the performance of the various stages and test a signal through both the individual elements and the entire circuit. The summer research/analysis was thus divided into the following three phases: (1) Mounting of Circuit, (2) Analysis & Troubleshooting, and (3) Run Sample Data Acquisitions Using LabVIEW.

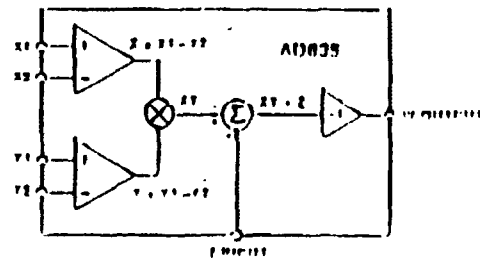
Circuit Description

The analog processing assembly (schematic on following page) is an RF (Radio Frequency) circuit. It generates a 117 dB output of 200 megahertz and consists of the following elements (listed with brief function description and input impedance):

- (4) 24 dB broadband linear low-noise amplifiers
 - signal amplification; 50Ω
- (4) 3 dB fixed attenuators ("pads")
 - power level & noise reduction; 50Ω
- (1) 10 dB directional coupler
 - provides 2 output signals from one input; 50Ω
- (1) 1 dB, .5 MHz passive highpass filter
 - passes high frequencies & attenuates low frequencies;
- (1) 1 dB, 163 MHz lowpass filter
 - passes low frequencies & attenuates high frequencies;
- (1) 3 dB, 4-quadrant voltage output analog multiplier
 - generates linear product of 2 voltage inputs; $100\text{ k}\Omega\parallel 2\text{ pf}$ (schematic pictured on following page)



FUNCTIONAL BLOCK DIAGRAM



- Schematics for voltage controlled multiplier

Twelve elements make for twelve stages in the circuit. The amplifiers and multiplier are DC voltage controlled and each power line includes a capacitor to separate the ground from any DC voltage. The analog multiplier functions as a wideband amplifier; its gain/loss depends on the DC voltage, which ranges from 0 to 1 volt. The attenuators, or pads, reduce noise/power levels before and after each stage of filtration.

This circuit's RF response makes it susceptible to problems such as stray oscillations and noise, mainly because it deals more with amplitude modulation than frequency modulation. An amplitude-modulated signal is more prone to be disrupted by sources of random electromagnetic waves (ie. electrical machinery and electrical storms).

Phase 1: Mounting

The schematic was designed prior to the beginning of my internship. The circuit that I mounted and analyzed this summer receives and monitors the echo pulse. It processes the echo pulse through various stages of amplification, attenuation, and filtering; the result is a signal which can be directed to an analog/digital converter or directed as input to an oscilloscope for test measurement and analysis. A 17" x 10" aluminum chassis was used for mounting the components. The initial challenge was to mount the circuit within this limited space while still leaving room for adjustment and possible modification. Every step in this phase (as with the entire project) required care and deliberation. The holes drilled in the chassis could not be misplaced, and the various elements needed to be secured to the chassis without damage. SMA cables were assembled in the lab, as were the input/output wires and connectors. All needed to be checked for impedance mismatches that might distort the signal. Care had to be taken to insure that each element, connector, and wire was grounded to the chassis and/or the power source.

After laying out the circuit within the chassis, I marked and sized the holes for securing the elements, the input, output, monitor leads, and the front panel. The holes were cut out using a drill press in the machine shop. All of the screws and washers used are brass rather than steel to insure that good contact was made with the circuit elements and the chassis. A power source filter was mounted on a smaller circuit board between the power connector and each component for the ground, +15v, +5v, and -5v sources from outside the chassis. Each wire running from the power source was "pigtailed" with a groundwire and soldered to the appropriate amplifier or the multiplier. The pigtailed wires were crimped and the wires grounded to the chassis with internal-teeth washers under various screws. An additional input was added for the DC-gain source; this and the signal inputs/outputs were also pigtailed and grounded. For the time being, capacitors #11 and #12 were left out of the circuit until necessary; #3 - #6 may provide enough of what capacitance the circuit requires.

Finally, the entire circuit (now secured to the chassis) had to be ohmed to make certain elements were grounded to the chassis, power could reach the amps without hindrance, and impedance hadn't been added by any of the methods used to secure the circuit elements in their places. The coax cables were connected between the elements to insure there was sufficient space, and then the cover was drilled & fitted to make sure nothing prevented it from mating the chassis easily.

Phase 2: Analysis & Troubleshooting

For my analysis, I used a Hewlett Packard Function Generator and a Tektronix 4-Channel Digital Oscilloscope, as well as 3 separate power sources to power the +15v, -5v & +5v, and the DC level for the multiplier. In order to check for impedances in the circuit, I used the Fast Fourier Transform function of the oscilloscope. FFTs allow you to transform a waveform from a display of

its amplitude vs time to one that plots the magnitude or phase angle of the various frequencies the waveform contains with respect to those frequencies. Put simply, FFTs display the amount of signal or noise as a function of frequency within a signal..

This phase required the most investigation. I tested the circuit stage-by-stage to see how cleanly the signals went through and met with a bit of success. The signals were going through, but there were numerous artifacts and impedances that needed to be explored. I completed the stage-by-stage testing and prepared to test a signal's passage through the entire circuit. The following is a brief listing and description of the problems that were exposed and are currently being investigated :

- Stray Oscillations
- Too much Noise
- Mysterious Artifacts
- Insufficient Shielding
- Damaged Elements
- Insufficient Attenuation

The first problem observed was a lack of constant impedance in the highpass filter, indicated by a tiny rift (1.5 dB) in the FFT waveform. Further study called for the ordering of a new filter; for the impedance change could not be compensated. Stray oscillations, noise, mysterious artifacts, and shielding came next. There were approximately 10 db of excess noise indicated by the FFT due to low level spot oscillations alone. A possible source explored was signal radiation coupling to the coax pigtail groundwires on the chassis mount SMA connectors; their length may have added to the impedance. I shortened these, but some oscillations remained. Another possibility was that the some cables were used cables, and we are building new ones. Other possibilities are insufficient shielding between input & output connectors or a damaged element.

Another problem arose when testing the multiplier for gain control. Again, there were several decibels of extra noise indicated by the FFT. In addition, the DC voltage seemed to have no effect on the noise level of the signal. The integrated circuit multiplier was found to be defective and has been replaced. Several variations of the circuit are also being investigated (ex. minus an amplifier, 6 dB pads instead of 3 dB).

There are numerous factors that could affect the complete circuit and/or the individual elements in various ways. These are to be expected in high frequency work; therefore, extreme care must be taken in design and layout. Based on my analysis, the assembly is now being modified to correct the problems detected.

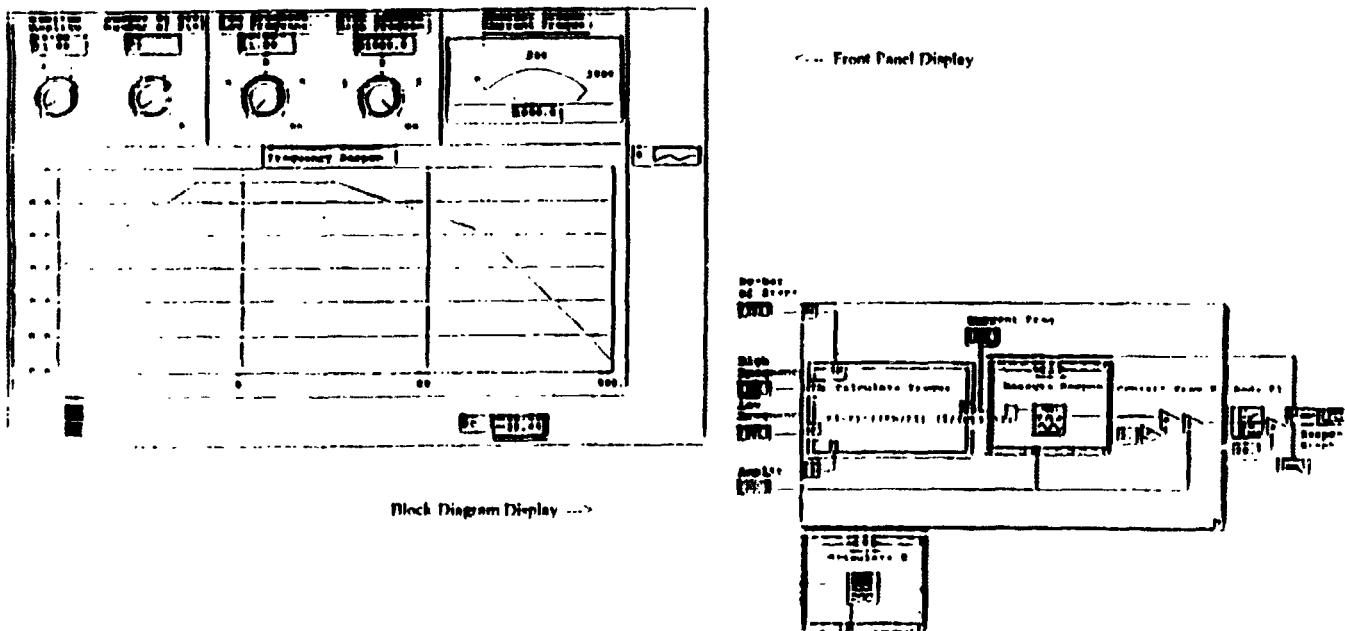
Phase 3: LabVIEW

The first phases of circuit testing were done by manually controlling the signal sources and recording the measurements by hand. To automate this process, I explored using a computer based instrument control & data acquisition program called LabVIEW. The time required to explore the signal artifacts discussed previously limited my time to apply LabVIEW to the testing; however, since part of the purpose was exposure to automated testing, I worked with the program.

LabVIEW, much like C, BASIC, or National Instruments LabWindows, is a program development application. However, while those programming systems use text-based languages to create lines of code, LabVIEW uses a graphical programming language called G to create programs in block diagram form. It relies on symbols rather than language to describe programming actions; its programs are called virtual instruments (VIs) because their appearance and operation imitate actual instruments (examples on following page). LabVIEW contains application-specific libraries for data-acquisition, GPIB and serial instrument control, data analysis, data presentation, and data storage. This is perhaps its most valuable feature - its ability to acquire data from almost any source. Various plug-in boards are available with combinations of analog, digital, and timing inputs/outputs. The hardware line also includes a wide variety of signal conditioning modules for thermocouples,

resistance temperature detectors, voltage and current inputs, and high current digital inputs/outputs. With its many features, LabVIEW adheres to the concept of modular programming. Users can divide an application into a series of tasks and continue subdividing until a complicated application becomes a series of simple subtasks. A VI can be written to accomplish each subtask and then combined with another block diagram to accomplish the larger task. The final top-level VI is a collection of subVIs representing application functions, each of which can be run separately. Debugging is easy. In essence, LabVIEW is much the conventional language, just with pictures.

The LabVIEW programming system allows researchers to sit at a terminal and communicate with a function generator and an oscilloscope. From a computer, they are able to tell the generator what signal to send out and ask the oscilloscope what signal came back. This will reduce the number of instruments that have to be read from 3 to 1. The LabVIEW front panel displays any and all information regarding the input and output signals. From these programs can be written to manipulate the acquired data in whatever way the researchers desire. LabVIEW makes it possible to do all of this from one computer terminal.



Conclusion

The circuit was breadboarded and analyzed with indicated modifications currently being implemented. This analog processing assembly will become part of the Wake Vortex Lidar data acquisition system which will be used in field tests to measure wake vortices. Presently, researchers are developing a trailer to house various transportable "test-bed" lidar systems. Field experimentation will be run from this trailer.

**NEXT
DOCUMENT**

11-2
11-7

Parallel Processing with Digital Signal Processing Hardware and Software

Student

Corey V. Swenson

Mentor

Robert L. Jones

Group

Research and Technology

Division

Information and Electromagnetic Technology

Branch

Systems Integration

Parallel Processing with Digital Signal Processing Hardware and Software

Abstract

The assembling and testing of a parallel processing system is described which will allow a user to move a DSP application from the design stage to the execution/analysis stage through the use of several software tools and hardware devices. The system will be used to demonstrate the feasibility of the Algorithm To Architecture Mapping Model (ATAMM) dataflow paradigm for static multiprocessor solutions of DSP applications. The individual components comprising the system are described followed by the installation procedure, research topics, and initial program development.

1.0 Introduction / Background Information

1.1 Multiprocessing of Digital Signal Processing Algorithms

Digital Signal Processing (DSP) systems are used to realize digital filters, compute Fourier transforms, execute data compression algorithms, and many other compute-intensive algorithms. The recent explosion of DSP products on the market reflects the advancements made in DSP technology. The increasing complexity of this DSP technology, especially in real-time systems, has increased computational requirements and created a need for faster, more powerful systems. As a result, government and industry are turning to multiprocessor solutions to meet these needs. In order to take advantage of multiprocessor architectures, the processes of a DSP application must be effectively mapped onto multiple processors. Such mapping procedures are currently in the design stage and are not yet perfected. One mapping procedure, the dataflow paradigm, has been implemented in the Dataflow Design Tool, created by my mentor Robert L. Jones III.

1.2 Dataflow Design Tool

The Dataflow Design Tool for multiprocessor scheduling was developed to facilitate the design of multiprocessor solutions to a number of computational problems, including DSP algorithms and control law. The tool analyzes the computational problem, represented as a dataflow graph, and determines the performance bounds, scheduling constraints, and resource requirements for solving the problem. The tool utilizes the dataflow paradigm to model computational problems. This model uses graphical nodes to represent schedulable computations, direct edges to

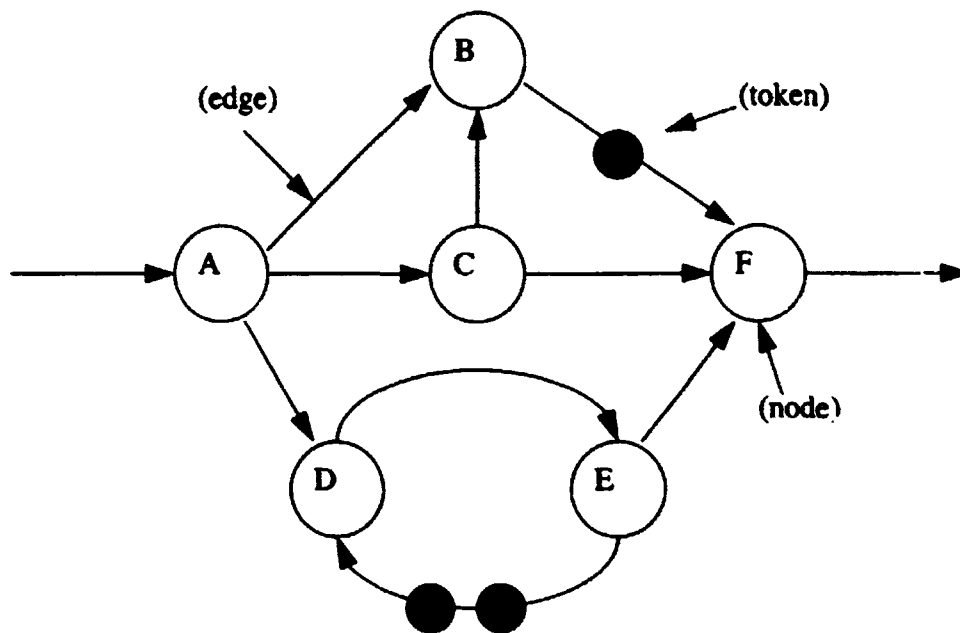


Figure 1. *Dataflow Graph*

describe the dataflow between nodes, and tokens to indicate the presence of data. A dataflow graph is shown in Figure 1.

1.3 Process Scheduling

After an applications algorithm has been modeled, there are two methods for scheduling tasks in a multiprocessor system: static and dynamic. The dynamic scheduling system, shown in the dotted region of Figure 2, has already been implemented and tested with the ATAMM and Dataflow Design Tool on a Generic VHSIC (very high speed integrated circuit) Spaceborne Computer (GVSC). In dynamic scheduling, the tasks to be performed are assigned to a specific processor at *run-time*. Therefore, the system is not dependent on any individual processor, giving it a high degree of fault tolerance. If one processor fails, the algorithm will still execute predictably, only at a degraded level of performance. Dynamic scheduling also gives the system more flexibility. The drawback of dynamic scheduling is its high overhead. Since it is not known at compile time which processor will be producing a token or which processor will be receiving it, more communication is needed between processors, causing delays and a larger overhead.

The static scheduling system, shown in the solid outline in Figure 2, is the system to be constructed and tested as my LARSS project. In static scheduling, the tasks to be performed are assigned to specific processors at *compile-time*, allowing the programmer to decide which processors perform which tasks. For deterministic DSP algorithms, a priori knowledge can be gathered from the model to make costly decisions about scheduling, communication, and synchronization at compile-time. Thus, making these costly decisions at compile-time minimizes the run-time overhead, allowing more time to be spent doing useful work. However, this system is more rigid and inflexible. It is also less fault-tolerant than dynamic scheduling since the failure of a single processor results in the inability of the system to complete the execution of the algorithm.

The ultimate goal in building and testing these two systems is to thoroughly understand all aspects of each, and through innovative design, create a system which implements a combination

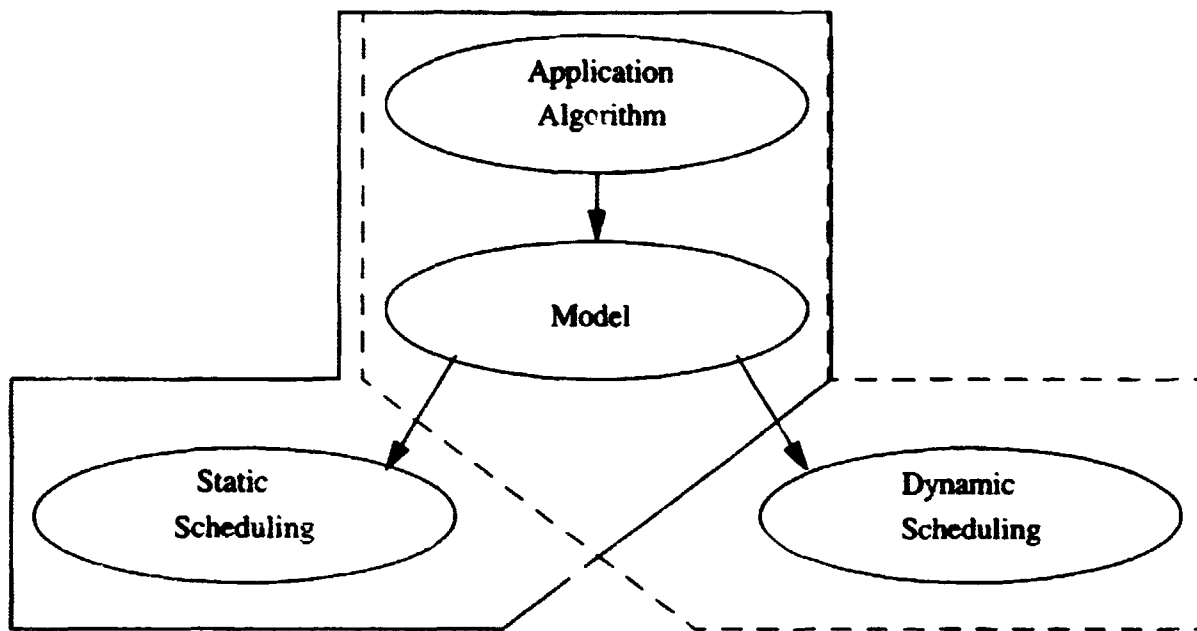


Figure 2. *Process Scheduling*

of static and dynamic scheduling. The resulting system will have a high degree of fault-tolerance and flexibility as well as minimal overhead.

2.0 Summary of Study

2.1 Approach

The multiprocessor system was to utilize in-house models/tools in combination with commercial-over-the-shelf (COTS) software and hardware to realize a suitable testbed. Part of the testbed construction included the selection, installation, setup, and integration of suitable COTS components with state-of-the-art and versatile features that lend themselves to modeling by ATAMM. The in-house models/tools consist of the ATAMM (model) and the Dataflow Design Tool. The COTS tools consist of Hypersignal¹ model capture, automatic code generation, and real-time display; the SPOX² operating system's real-time and multiprocessing functions; and Pentek's³ state-of-the-art digital signal processing boards and debugging software.

When the in-house and COTS components are integrated, the system can be viewed as layers stacked on top of one another to form the system as shown in Figure 3. The application is first created using the Hypersignal graphical software Block Diagram and the code is created with the

1. copyright by Hyperception, Inc. 9550 Skillman, LB 125 Dallas, TX 75243

2. copyright by SPECTRON Microsystems, Inc. 320 Storke Road, Santa Barbara, CA 93117

3. Pentek, Inc. 55 Walnut Street Norwood, NJ 07648

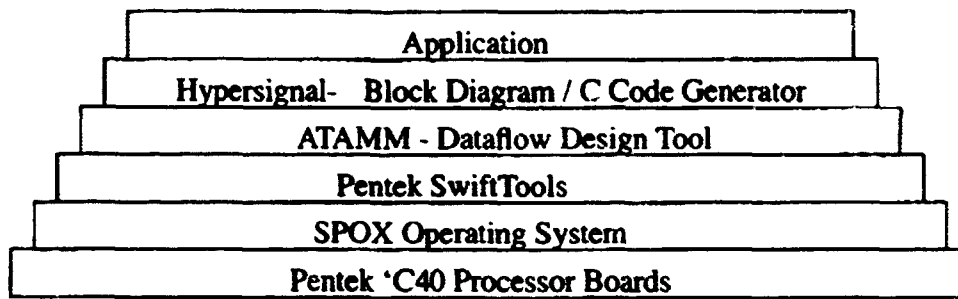


Figure 3. Layered System

C Code Generator. Working with the Block Diagram graphical representation and the dataflow paradigm, the Dataflow Design Tool determines the performance bounds, scheduling constraints, and resource requirements of the application. Using this information, the C code is modified to execute efficiently on the optimal number of processors using Pentek's SwiftTools software. Also, SPOX Operating System (OS) functions may be added to the code to optimize multiprocessor performance. Finally, the code is compiled using the Texas Instruments (TI) optimizing C compiler, downloaded to the Pentek 'C40 boards, and executed.

2.2 Equipment

2.2.1 Hardware Components

Gateway 2000 PC. The Gateway PC contains the software Hypersignal. Through this software the user can create a DSP application, simulate the execution, and see the output. The user can also download the DSP algorithm to a DSP PC/C31 board inside the computer where it is executed. The output may be sent back to the PC and displayed in real-time with the Hypersignal software. The PC can also send an analog signal out or receive an analog signal in via the DSP card. In this way, the PC can receive and display the signal that is processed by a separate computer or computers.

PC/C31 Board. The Loughborough Sound Images' LSI PC/C31 board with A/D D/A daughter module contains a Texas Instruments TMS320C31 processor onto which algorithms can be downloaded via Hypersignal software. The board is also an interface between the Hypersignal software and an external analog signal source. Analog signals come into the PC via the PC/C31 board and are displayed with the RT-2 software.

RadiSys Embedded PC. The RadiSys EPC-5 is a PC/AT compatible embedded CPU module which rests in a card cage along with three Pentek boards. The embedded PC (EPC) has a 66 MHz Intel486 DX2 processor and a VMEbus interface to communicate with the Pentek boards. The EPC contains the SPOX OS and SwiftTools software which allows the user to communicate with the Pentek boards as well as modify and debug C code.

Pentek Model 4202 MIX Baseboard. The 4202 MIX Baseboard is one of the three Pentek boards in the card cage with the RadiSys EPC. The VMEbus, which is part of the card cage, runs along the back of the card cage. The MIXbus runs through the middle of the Pentek boards and is not part of the card cage but part of the Pentek boards. The 4202 converts all of

Pentek's MIX modules into standard VMEbus boards. The 4202 allows communication between the EPC and MIX modules, which are not necessarily connected to the VMEbus.

Pentek Model 4249 Filtered A/D-D/A Converter. The 4249 A/D-D/A converter is the second of the three Pentek boards in the card cage and can support sampling rates of up to 1 MHz. An analog input signal is filtered, sampled by the 12-bit D/A converter, and stored in the 1024 sample FIFO, ready for transfer along the MIXbus to another module. A digital signal received from the MIXbus is put into another 1024 sample FIFO, ready for transfer through the 12-bit D/A converter and low pass filter to the analog output.

Pentek Model 4270 Quad TMS320C40 Digital Signal Processor Board. The 4270 board is the last Pentek board in the card cage. The 4270 contains four Texas Instruments TMS320C40 processors, 4 MBytes of Local SRAM, and 4 MBytes of Global SRAM. Algorithms are downloaded from the EPC onto one or any number of processors on the 4270. The 4270 can send/receive data to/from the 4249 A/D-D/A in its execution of the algorithm.

Hewlett Packard 3312A Function Generator. The HP Function Generator creates the original signals (sinewaves, squarewaves, etc.) to be used by the system. The Function Generator and other hardware subsystems transmit signals through coaxial cable.

2.2.2 Software Components

Hypersignal for Windows. Hypersignal is a collection of software applications which address many scientific and engineering problems involved in signal processing. This software allows the user of the system to graphically design and simulate an application as well as analyze the results in real-time.

Block Diagram. Block Diagram allows the user to design an application by connecting any number of predefined software building blocks. The user can then compile and run the project, simulating the execution of a real system. Block Diagram also allows the user to build a project using real-time building blocks. These blocks can read in a signal from the outside world, process the signal, then send the signal back out. Many software building blocks are included with the software, but custom blocks may be designed by the user.

Block Wizard. The Block Wizard software simplifies the task of creating new user-defined blocks for use in Block Diagram. The user defines the parameters for the new block and Block Wizard generates the text files necessary for compilation. The user then writes the code to perform the desired task, inserts it into one of the generated files, and compiles the files. The new block function is now ready for use.

C Code Generator. The C Code Generator creates the C source code that represents the algorithm designed with Block Diagram. This code can then be cross-compiled for a particular DSP chip and executed.

RT-2. The RT-2 software provides tools for storing and analyzing real-time signals. The Digital Scopes are used to view an input signal in real time. The displays and controls look identical to an actual oscilloscope. The Spectrum Analyzer displays an input signal in the frequency

domain in real time. The Digital Recorder allows the user to store a real-time signal continuously and then regenerate the signal in real-time at their convenience. Also, the stored waveform can be loaded and viewed by the Graph Analysis software which allows detailed analysis of the signal.

Pentek SwiftTools. SwiftTools is a software development environment for Pentek devices. Through this software, the user can debug and edit C source code. The user can step through the source code, executing one line at a time, while setting breakpoints, viewing register contents, and viewing symbol addresses and values. Through these actions, the user can find design errors within the code. The software also serves as an interface between the EPC and the Pentek boards. This enables the user to download the executable code onto the DSP chips after compilation. The user can stop and start the execution of the program on the DSP chips through the SwiftTools software.

SPOX OS. SPOX is a DSP operating system designed to meet the needs of high-end DSP microprocessors by allowing developers to work with objects relating to signal processing and through general purpose features such as device-independent I/O, interrupt management, and multi-tasking support. SPOX enables the use of the high level C language in real-time signal processing, releasing the full potential of the latest DSP hardware through sophisticated applications.

2.3 System Construction

2.3.1 Installation and Testing

The following Hypersignal software was installed on the Gateway PC:

- Block Diagram
- Block Wizard
- C Code Generator
- RT-2

After installation, Block Diagram examples included with the software were executed on the PC. Several block worksheets were designed and executed using various block functions to ensure the software was loaded properly. Execution of real-time block functions on the 'C31 board required proper configuration, after which real-time block examples were tested.

The following software was installed on the Radisys EPC:

- SwiftTools
- SPOX OS
- TI Optimizing C Compiler
- DSPTools

Prior to running SwiftTools, a configuration program called PNCFG was used to relay information to SwiftTools concerning the Pentek boards used in the system. After configuration, a program was compiled, downloaded to the 'C40 boards, and executed, showing that SwiftTools, the TI Compiler, and the DSPTools were all installed properly. The SwiftTools debugger was used to find errors in a test program for the 4249 A/D-D/A board, which was also shown to be installed correctly. The SPOX software included a sanity check program to test its installation. Upon execution, the program displayed a message on the screen confirming proper installation.

2.3.2 Installation Delays

Several problems and delays were incurred during installation of the software. For instance, the Unix version of the SPOX manual was received rather than the DOS version, delaying its installation. Upon receiving the correct SPOX manual, it was realized that the wrong SPOX software version was received as well. A new version was sent but still had the wrong executable files. After receiving new files, the test program finally worked properly. The Hypersignal software has a security button attached to the printer port which was not recognized by the C Code Generator. A new button was sent along with new versions of the C Code Generator and Block Diagram. The new C Code Generator could recognize the new button, but was incompatible with the new Block Generator. A third version of the C Code Generator was sent and worked properly, but the new Block Diagram did not include any real-time block functions to run on the 'C31 board. The SwiftTools PNCFG program was difficult to configure. The Pentek boards had to be removed from the card cage to double check hardware jumper settings. The Pentek representative was contacted several times to find a number of bugs in the setup. Finally, one of the 4270 boards were removed while the other one was configured, allowing the board to be recognized. The other board was inserted but could not be configured, a hardware problem on the board was assumed.

2.3.3 Research

In parallel with the installation and testing of the system components, research of multiprocessing topics was performed to give a better understanding of the system and the purpose of designing it. The topics included the advantages of a multiprocessor system, the classes of architecture, memory configurations, applications, anticipated difficulties, and process scheduling.

2.3.4 4249 and Communication Port Drivers

After installing and successfully testing the 4270 and 4249 boards, drivers were created from the already proven test programs. The test programs contained information regarding registers and initialization needed in any program using the A/D-D/A converter or communication ports. The 4249 driver consists of a routine which takes data from the input FIFO and a routine which sends data to the output FIFO. The com port driver consists of routines which synchronize the sending and receiving of data over com ports. A program was written to implement the two drivers for testing purposes. The first processor receives data from a function generator through the 4249 board, the data is sent sequentially through each processor, the last of which sends the data out through the 4249 board and into the Gateway PC to be displayed by Hypersignal. Although simple, the drivers form the foundations for data transmission and communication between processors.

2.3.5 Final Projects

There are two projects which are expected to be completed in the final week of the program. One project is to create a custom block function using the Hypersignal Block Wizard software which will represent the 4249 driver program. This will enable the user to select the 4249 block

from the function list of Block Diagram, implement it in a block worksheet, and create C code which can be compiled and downloaded to a 'C40 processor without modification in SwiftTools.

The second project consists of moving an application from the design stage to the execution/analysis stage. After designing the application in Block Diagram and creating the corresponding C code, the application will initially be executed on one processor. By using the Dataflow Design Tool to determine the performance parameters on multiple processors, the C code will be modified to execute on several processors.

3.0 Results

Although no numerical results were obtained from the project, the advantages of constructing the system can be easily seen. After finding all system components to be working properly, example applications can now be created and tested in a very short time. With the 4249 driver program, applications involving the input and output of real signals can be created and executed quickly. The com port driver allows the user to easily synchronize communication between processors, a fundamental aspect of parallel processing. With the completion of the 4249 driver function block in Block Diagram, the user will be able to represent the input and output of the 4249 in graphical form and create C code for applications with the 4249 driver already incorporated.

4.0 Conclusion

The demand for effective mapping procedures for multiprocessor systems was explained with reference to DSP applications and real-time processing. One of these mapping procedures, the dataflow paradigm, has been implemented in the Dataflow Design Tool. The testing of this tool in a dynamic scheduling system was described along with the assembling of a system to test the tool using static scheduling. The individual components comprising this system were listed and their functionality explained. The software/hardware installation was shown to be correct through numerous test programs and the difficulties in integrating the components were recounted. The research of multiprocessing systems performed to gain a better understanding of the system was briefly summarized. Drivers which controlled the communication between processors and signal transmission through the A/D-D/A converter were explained and, finally, the projects still to be completed during the last week of the program were presented.

**NEXT
DOCUMENT**

TECHNOLOGY TRANSFER - MARKETING

TOMORROW'S TECHNOLOGY

ERENE TCHENG

BARRY V. GIBBENS

TECHNOLOGY APPLICATIONS GROUP
AUGUST 8, 1995

ABSTRACT

The globalization of the economy and the end of the Cold War have triggered many changes in the traditional practices of U.S. industry. To effectively apply the resources available to the United States, the federal government has firmly advocated a policy of technology transfer between private industry and government labs, in this case the National Aeronautics and Space Administration (NASA). NASA Administrator Daniel Goldin is a strong proponent of this policy and has organized technology transfer or commercialization programs at each of the NASA field centers. Here at Langley Research Center, the Technology Applications Group (TAG) is responsible for facilitating the transfer of Langley developed research and technology to U.S. industry.

Entering the program, I had many objectives for my summer research with TAG. Certainly, I wanted to gain a more thorough understanding of the concept of technology transfer and Langley's implementation of a system to promote it to both the Langley community and the community at large. Also, I hoped to become more familiar with Langley's research capabilities and technology inventory available to the public. More specifically, I wanted to learn about the technology transfer process at Langley. Because my mentor is a member of Materials and Manufacturing marketing sector of the Technology Transfer Team, another overriding objective for my research was to take advantage of his work and experience in materials research to learn about the Advanced Materials Research agency wide and help market these developments to private industry.

Through the various projects I have been assigned to work on in TAG, I have successfully satisfied the majority of these objectives. Work on the Problem Statement Process for TAG as well as the development of the Advanced Materials Research Brochure have provided me with the opportunity to learn about the technology transfer process from the outside looking in and the inside looking out. Because TAG covers all of the research efforts conducted at Langley, my studies with TAG were able to provide me an excellent overview of Langley's contribution to the aeronautics industry.

INTRODUCTION

The globalization of economic competition coupled with the end of the Cold War necessitated several quick and drastic changes to the international marketplace. To remain competitive, U.S. industry has responded by changing its traditional business practices, and the federal government has followed along. Administrator of the National Aeronautics and Space Administration (NASA) Daniel Goldin writes, "to effectively use the technological, human, financial and other assets of NASA and the U.S. industrial base and to capitalize on the opportunities offered by an ever expanding technology base, we must carefully consider the marketplace and form partnerships with the private sector," (1:1). This new broader role focuses on transferring NASA developed technology to the private industry "to increase US. industrial competitiveness, to create US. jobs, and to improve the balance of trade" (2:3). The national technology transfer policy aims to convert NASA research and development (R&D) efforts into marketable, innovative products.

Currently, there are three forces driving NASA's evolution: President Clinton's technology policy, Vice President Gore's National Performance Review recommendation for NASA, and the growth of the Information Superhighway (1:3). These forces affect the technology push and pull in the United States differently. The President's policy challenges NASA to increase the effectiveness of NASA programs, thereby increasing the industry's economic competitiveness. By emphasizing a cooperative effort between private industry and NASA, the policy views technology as a force of change, an impetus for economic growth. Moreover, the National Performance Review recommends an implementation for technology transfer. The plan makes such suggestions as setting aside 10 to 20% of the research and development budget for partnerships with industry and promoting small business opportunities. Most importantly, the recommendation amends the agency's Vision-Mission-Values statement to include technology transfer as a major mission.

TECHNOLOGY TRANSFER AT LANGLEY RESEARCH CENTER

The Technology Applications Group (TAG) at Langley Research Center was established in February 1994 to "encourage broader utilization of NASA Langley developed technologies in the American industrial community" (3:1). The document "Transferring Langley Research Center Technology" outlines TAG's responsibilities as the following:

- Leading the Center's processes for early identification of technologies of high commercial potential;
- Promoting the expedient transfer of new technologies to the commercial sector;
- Achieving the non-aerospace uses of Langley technology by identifying potential technology applications and creating teams of non-aerospace customers and Langley technologists to accomplish the transfer process;
- Coordinating the Langley program with appropriate NASA Headquarters Offices, other NASA Centers, and other Government Agencies; and
- Supporting the technology transfer processes for aerospace customers.

Furthermore, members of TAG are also charged with leading Langley's Small Business Innovation Research Program and the Small Business Technology Transfer Pilot Program, which

reach out to small businesses for collaborative research and development efforts. The group includes members of the Technology Transfer Team (TTT), who facilitate the transfer of Langley developed technology to private industry, the Patent Counsel Team, as well as Small Business Partnership Team. The TTT is further organized into the following four market sectors: Information Technology, Materials and Manufacturing, Transportation, and Medical, Sensors, Instrumentation, Environment, and Energy (MISEE).

APPROACH

The approach to learning about the Technology Transfer program at Langley was two-fold. While the first project addressed Langley's reach-out to private industry for research ventures, the second project focused on industry's approach to Langley. The first project developed from a Headquarters' initiative to catalog the Advanced Materials research being conducted at the various NASA field centers. With this information, a document was to be created as a marketing tool for NASA's materials developments and distributed to the automobile industry. The second project involved TAG's problem statement process and the elimination of the backlog of Problem Statement Definitions (PSD) collected over the past year.

ADVANCED MATERIALS BROCHURE

The Advanced Materials Inter-Center Initiative involved working with members of the TTT, the Headquarters office, and the Regional Technology Transfer Centers (RTTC), in particular the Rhode Island Technology Transfer Center. Initially the majority of the work involved making contacts at each of the participating centers and determining the format as well as the type of information to be included in the brochure. The field centers which agreed to participate in the effort were Ames Research Center, Jet Propulsion Laboratory, Marshall Space Flight Center, Lewis Research Center, Goddard Space Flight Center, Johnson Space Center, Kennedy Space Center, and Langley Research Center. The next few weeks after making the initial contacts were spent waiting for the centers to collect and send their information. Once a substantial amount of information arrived at Langley, I met with some researchers in the Materials Division for guidance in consolidating and categorizing the research initiatives across the agency. Although the final version of the brochure will not be completed before the ten weeks are completed, all of the preliminary work has been completed. The materials research for each of the centers has been organized and the unique facilities and research have been identified. The first draft has been sent to each center for further review and we are now waiting for the suggested modifications. Once these changes are made, we will send the information to Headquarters for the graphics layout. The facilities and resources which proved to be the most helpful for this project were the NASA Technical Library, the researchers from the Langley Materials Division, and the World Wide Web.

This assignment provided an abundance of information about the extensive amount of research NASA conducts in the Materials research area, especially at Langley. With most of NASA's research conducted in the aeronautical field, it's focus on materials for engines and flight structures is highly marketable to the private sector, specifically the automotive and aeronautics industries. However, the difficulties in coordinating such an effort among the various NASA installations revealed another aspect of technology transfer. While marketing NASA research

increases the U.S. industrial international power base, effective technology transfer also requires a new way of thinking.

PROBLEM STATEMENT PROCESS

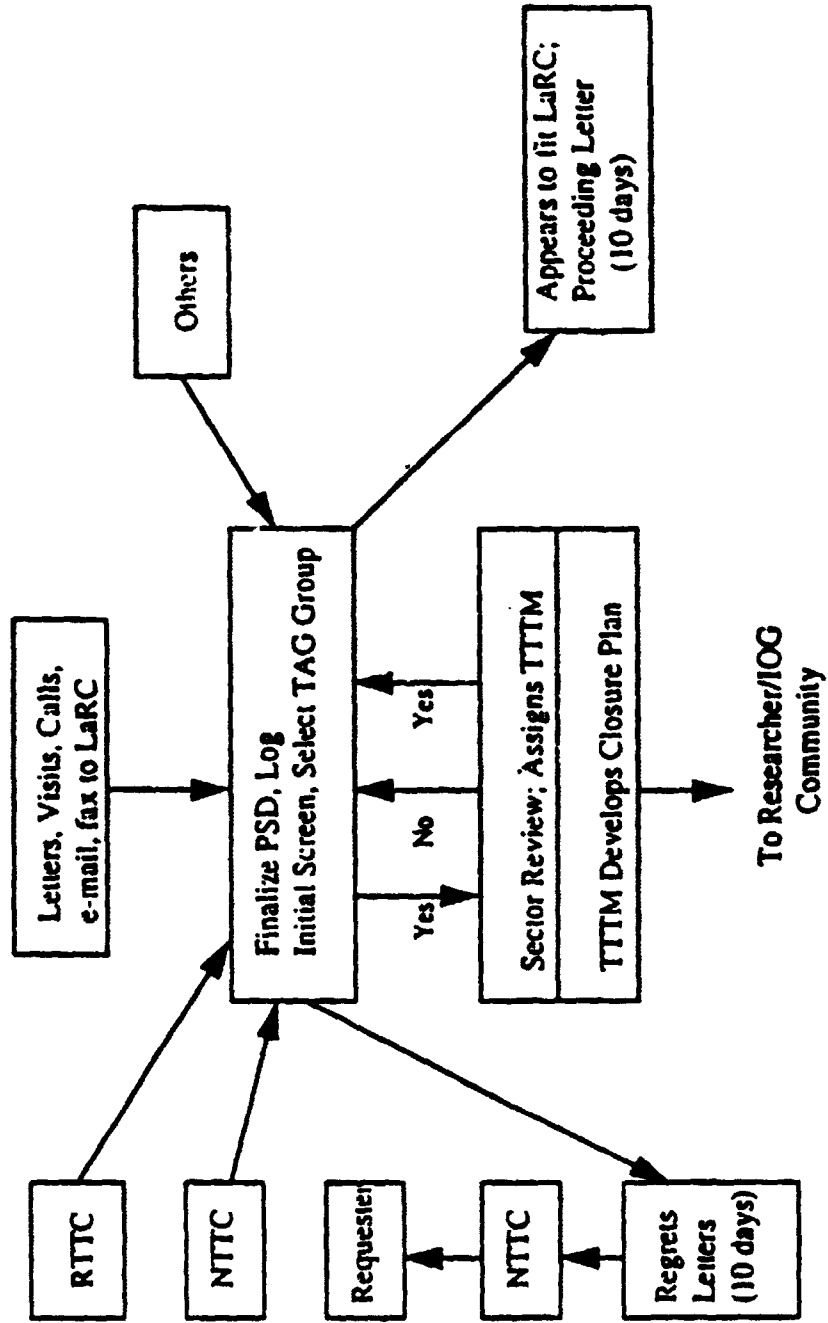
The Problem Statement Process (Appendix A) is the means through which industry approaches Langley with a problem or an inquiry to find a solution using Langley technologies or facilities. The process attempts to identify an optimum match between a customer's needs and Langley's capabilities, providing a mutual benefit to both the private sector and Langley. Within the last few months, TAG has centralized the process and created a position within the group to oversee its implementation and administration. The initial work was focused on eliminating the backlog of problem statements. This first step of this process was to centralize the problem statements into a database. Because this was not done in the past, PSDs were scattered among all of the members of the TTT. Once we were able to collect all of the statements, we entered them into the backlog database and assigned market sectors for each one. At that point, the sectors became responsible for deciding whether they wanted to pursue further action with the companies based on the technological match with Langley's resources. If the sector decided that the PSD was something that Langley should pursue, then we responded to the company notifying them of our decision. Likewise, if the sector decided that it was not in Langley's best interest to work a PSD, then we responded to the company telling them that we were unable to match their needs with Langley's resources. Within a month of beginning work on the process, the Data Systems Team for TAG completed work on the new TAG database Management Analysis of Scientific Knowledge (MASK), which tracks the majority of TAG's activities, including the problem statements. Thus, the incoming problem statements were tracked in MASK while the existing ones were left in the backlog.

Like the Advanced Materials Brochure, working with the Problem Statement Process broadened my knowledge of the technology transfer process. The sheer number of PSDs that are processed by the system indicates that numerous opportunities exist for cooperative efforts between private industry and NASA. However, limited resources such as funding, facilities, and personnel necessitate NASA's selectivity with whom and in what areas NASA pursues technology transfer. While much of my work on the Problem Statement Process was limited to administrative duties, I was given the freedom to make decisions on issues regarding the procedure. For example, I was responsible for working with the RTTCs and some of the companies on certain PSDs. I was also responsible for corresponding with the market sectors and organizing the correspondence. Finally, my work in this area of the Technology Applications Group revealed the significance of new programs, such as the one at Langley, to proceed with a strong sense of direction. As programs develop goals and solidify procedures, it is important that they build credibility to facilitate long lasting business partnerships.

TAG Problem Statement Process

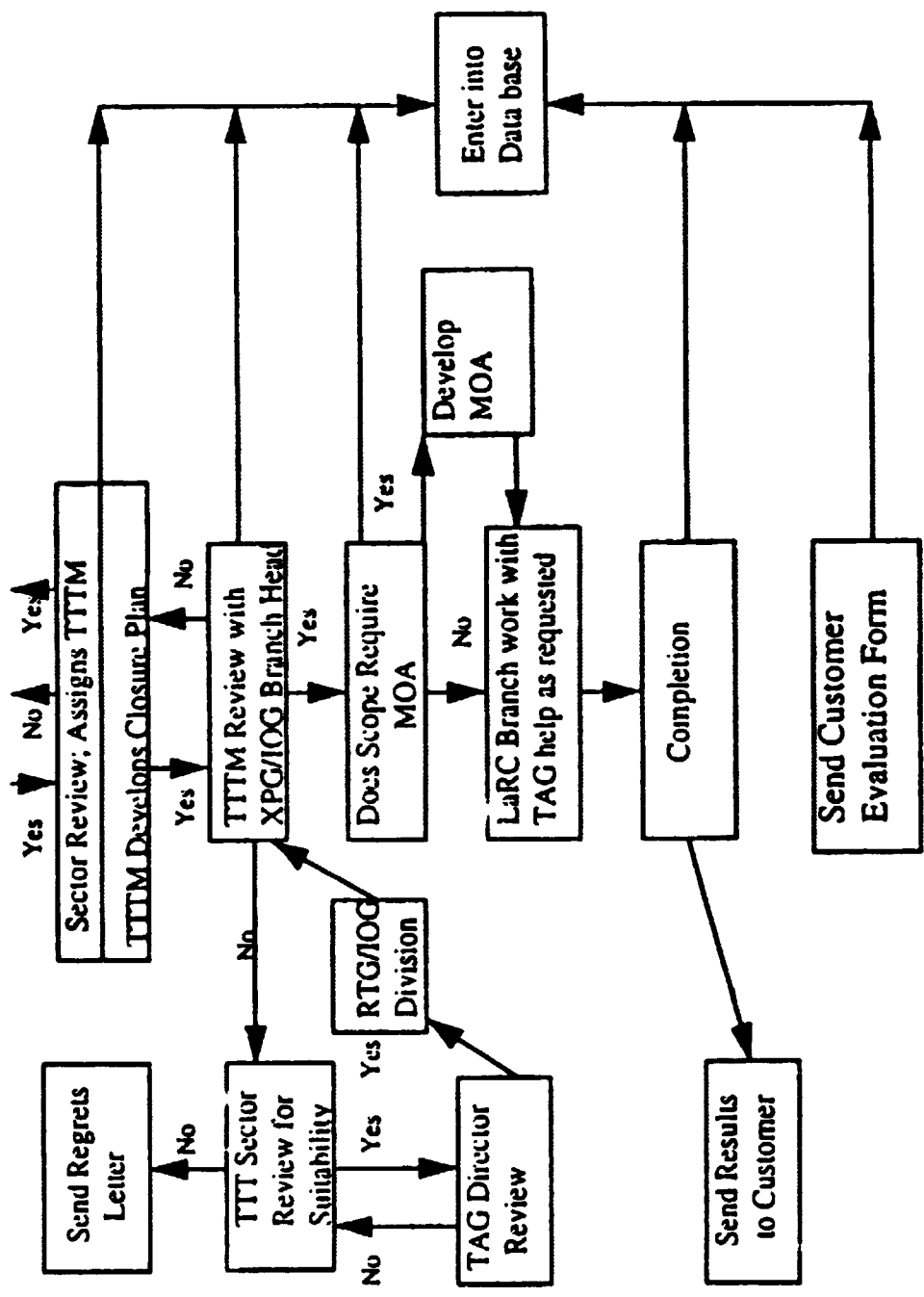
Problem Statement Process Actions

APPENDIX A



TAG Problem Statement Process

Problem Statement Process Actions



REFERENCES

1. "NASA Commercial Technology - Agenda for Change," NASA Commercial Technology Team. July 1994.
2. "The Technology Transfer Process - Working with NASA Langley Research Center," March 3, 1995.
3. "Transferring Langley Research Center Technology."

**NEXT
DOCUMENT**

OPEN LOOP SIMULATION

TAMERA L. THOMAS

VINCENT HOUSTON, BILL LYNN

JOHN WHITE, MONICA HUNTER

FOSD, OEB

ABSTRACT

My project is designing a flight control program utilizing "C" language. It consists of paths made up of fixed radius arcs and straight lines. Arcs will be defined by a center, a radius and turn angle. Straight lines will be defined by an end way point and an inbound course. Way points will be pre-defined such that the location of the end of each leg accurately matches the beginning of the next leg. The simulation paths will closely match paths normally flown by the TSRV, but will not necessarily be defined identically in terms of type and number of way points.

OPEN LOOP AIRCRAFT SIMULATION

My project for this summer was to write software to implement open loop aircraft simulations for onboard testing and troubleshooting purposes. This program, written in C language, calculates way points for an inbound course using a list of given data such as pitch, roll, indicated airspeed, magnetic heading, latitude, longitude, etc. This data is then used to calculate successive points on a three dimensional coordinate plane. These points ultimately result to a flight path. I was also given other tasks working with a High-Speed Research (HSR).

The approach used for this project was an analytical process. I had to break my project into component parts or constituent elements. I also learned to utilize the "C" computer language to complete this project.

NASA's Boeing 737 Transport Systems Research Vehicle (TSRV) was acquired by the Langley Research Center in 1974 to conduct research into advance transport aircraft technologies. TSRV has played a critical role in developing and gaining acceptance for numerous significant transport technologies, including "glass cockpits," airborne windshear detection systems, data link for air traffic control communications, the microwave landing system, and the satellite-based global positioning system.

Thorough preflight testing of Transport Systems Research and Vehicle flight controls requires that the system be exercised through an approach and automatic landing. At present, there is a limited capability to accomplish the usage of Microwave Landing System (MLS) signals simulated onboard. The increasing use of Global Positioning System (GPS) and inevitable demise of MLS require that this capability be provided for GPS as well. The availability of smaller and more sophisticated computers provides an opportunity to improve simulation fidelity.

The hardware equipment used is a VME chassis containing a 68010 processor card with Random Access Memory (RAM), Read Only Memory (ROM), RS 232 serial port, an ARINC 429 interface card and other interface cards as required. The software equipment is pSOS real-time kernel in ROM. This program will eventually be used on the 737 airplane during preflight.

In addition to my project, I was able to work with the High-Speed Research Program (HSR). High-Speed Program is the cornerstone of NASA Aeronautics for the 1990s. It addresses the challenges of emissions effects on the atmosphere, airport noise and sonic boom. If solved it could support and industry decision to build a supersonic transport. A supersonic transport flying through the atmosphere at more than twice the speed of sound is extremely sensitive to aerodynamic "drag" generated by air friction. One way to reduce drag and increase an aircraft's fuel

efficiency is to reduce turbulent airflow over the wings, leaving smooth or "laminar" flow. The most important technology work in HSR program focuses on advanced combustor (combustion chamber) concepts that could significantly cut NOx emissions.

The Flight Deck Systems (FDS) technology area is conducting the first in a series of flight tests designed to develop and flight validate a cockpit display system that will eliminate the necessity of a droop-nose configuration for a High Speed Civil Transport (HSCT). The lack of a nose droop capability on the HSCT will require that the pilot's forward visibility be functionally replaced by an External Visibility System (XVS). Additionally, the XVS will enable all-weather, suitable-site operations.

I enjoyed working with HSR. I was able to attend weekly meetings and write work orders for the hardware pertaining to HSR. This part of my intern gave me an opportunity to interact with the employees in a business manner.

**NEXT
DOCUMENT**

Entrepreneurship Within General Aviation

Brian M. Ullmann
L.A.R.S.S. Student

With the direction of

Mr. Daniel J. DiCarlo
Research and Technology Group
Flight Dynamics and Control Division
Vehicle Performance Branch

August 8, 1995

Abstract

Many modern economic theories place great importance upon entrepreneurship in the economy. Some see the entrepreneur as the individual who bears risk of operating a business in the face of uncertainty about future conditions and who is rewarded through profits and losses. The 20th century economist Joseph Schumpeter saw the entrepreneur as the medium by which advancing technology is incorporated into society as businesses seek competitive advantages through more efficient product development processes.

Due to the importance that capitalistic systems place upon entrepreneurship, it has become a well studied subject with many texts to discuss how entrepreneurs can succeed in modern society. Many entrepreneuring and business management courses go so far as to discuss the characteristic phases and prominent challenges that fledgling companies face in their efforts to bring a new product into a competitive market. However, even with all of these aids, start-up companies fail at an enormous rate. Indeed, the odds of shepherding a new company through the travails of becoming a well-established company (as measured by the ability to reach initial public offering (IPO)) have been estimated to be six in 1,000,000.

Each niche industry has characteristic challenges which act as barriers to entry for new products into that industry. Thus, the applicability of broad generalizations is subject to limitations within niche markets. This paper will discuss entrepreneurship as it relates to general aviation. The goals of this paper will be to:

- Introduce general aviation.**
- Discuss the details of marrying entrepreneurship with general aviation.**
- Present a sample business plan which would characterize a possible entrepreneurial venture.**

Many modern economic theories place great importance upon entrepreneurship in the economy. Some see the entrepreneur as the individual who bears risk of operating a business in the face of uncertainty about future conditions and who is rewarded through profits and losses. The 20th century economist Joseph Schumpeter saw the entrepreneur as the medium by which advancing technology is incorporated into society as businesses seek competitive advantages through more efficient product development processes.¹

Due to the importance that capitalistic systems place upon entrepreneurship, it has become a well studied subject with many texts to discuss how entrepreneurs can succeed in modern society. Many entrepreneuring and business management courses go so far as to discuss the characteristic phases and prominent challenges that fledgling companies face in their efforts to bring a new product to a competitive market. However, even with all of these aids, start-up companies fail at an enormous rate. Indeed, the odds of shepherding a new company through the travails of becoming a well-established company (as measured by the ability to reach initial public offering (IPO)) have been estimated to be six in 1,000,000.² It is important to recognize that this measure of company success is somewhat artificial as many companies are successful start-ups which either:

- Do not participate in an IPO but stay privately owned and operated instead.
- Do not participate in an IPO because they are bought by another company.

Each niche industry has characteristic challenges which act as barriers to entry for new products into that industry. Thus, the applicability of broad generalizations is subject to limitations within niche markets. This paper will discuss entrepreneurship as it relates to general aviation. The goals of this paper will be to:

- Introduce general aviation.
- Discuss the details of marrying entrepreneurship with general aviation.
- Present a sample business plan which would characterize a possible entrepreneurial venture.

General Aviation

General aviation is all air travel save the scheduled air carriers. This definition includes air taxi, recreational flying, agricultural spraying, instructional flying, and business transportation. The general aviation (GA) fleet represents 96 percent of all civil aircraft registered in the United

¹ Encyclopedia Britannica • Macropedia - Knowledge in Depth, 15th Edition, Encyclopedia Britannica, Inc.: Chicago, 1981.

² High Tech Ventures - The Guide for Entrepreneuring Success, C. Gordon Bell, Addison-Wesley Publishing Company, Inc.: Reading, Massachusetts, 1991.

States. These aircraft accumulate approximately 80 percent of all of the total hours flown and carry one in three intercity passengers.³

Despite these impressive statistics, GA is in decline. It operated in a cyclical manner where it closely mirrored the performance of the GNP and slowly built more capacity with each economic upturn until 1978, where it delivered at 17,811 new aircraft deliveries. Since that peak, it has atrophied to a level where a mere 964 units are shipped per year. Export of GA aircraft declined from 3,995 aircraft in 1979 to 336 in 1984 -- which can be seen to closely parallel the decline in domestic sales.

It is a well-established fact that there was a correlation between the rate of new GA aircraft production and the gross national product of the United States of America prior to 1978 - - i.e. as GNP increased so did GA new aircraft shipments. However, two metrics have become uncoupled since 1978 -- i.e. the GA industry failed to recover from the economic slump of the early 1980s and has continued to decline despite overall economic recovery.

Much analysis of the market has been made of the loss of correlation between GNP and new GA aircraft shipments. Possible causes include:

- Increasing costs of owning and operating a GA aircraft.
- Increasing costs and risks of manufacturing GA aircraft due to product liability concerns.
- Increasing value of the dollar caused foreign exports to decline due to higher prices in the foreign currency³.
- Changes in the tax code which made owning GA aircraft less attractive financially.
- Increasing competitiveness of airline transportation due to the Airline Deregulation Act of 1978⁴.

It is the view of the author that the primary reason for the downturn in GA is primarily related to the increases in direct acquisition and operating costs. It can be seen in Figure 1 that the direct acquisition, operating, and maintenance costs increased dramatically in the years 1978-1982 - the precise years which saw a precipitous decline in GA production. From 1978 through 1984, . . . single-engine piston aircraft prices increased at a yearly rate of close to 12 percent . . . [which] adjusted for inflation, grew at approximately five percent per year⁵.

³ **General Aviation Marketing and Management.** Wells, Alexander and Chadbourne, Bruce, Krieger Publishing Company: Malabar Florida, 1994.

⁴ **FAA Statistical Handbook of Aviation,** 1992.

⁵ **General Aviation Marketing,** Chadbourne, Bruce D. and Wells, Alexander, T., Krieger Publishing Company: Florida, 1987.

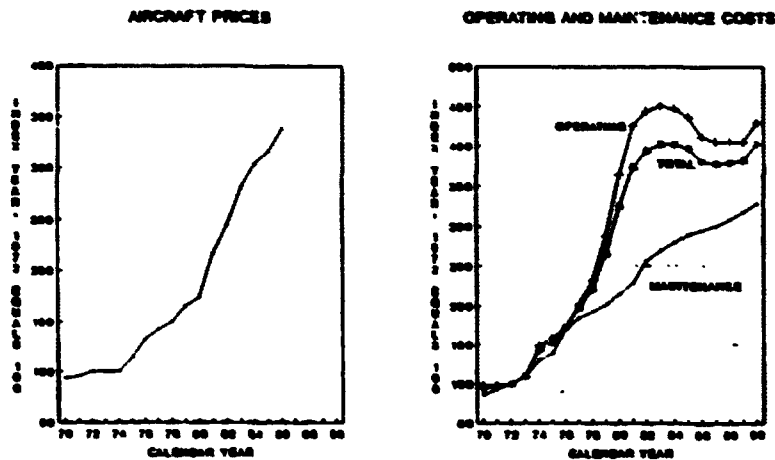
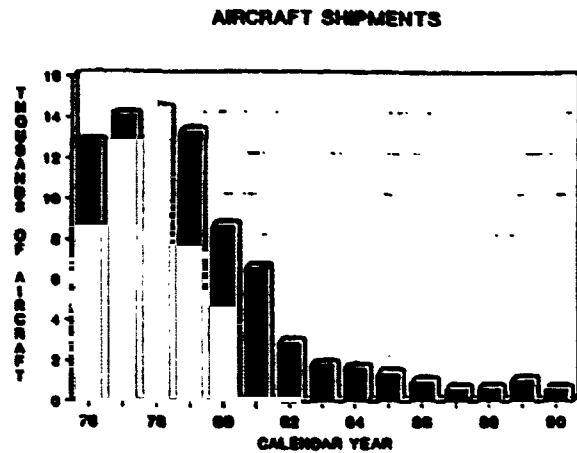


Figure 1: Correlation between Single Engine Piston Prices and Aircraft Shipments (Copied from Reference 6⁵)

Since 1978, much effort has been invested to attempt to revive the GA industry. Companies have downsized, left the market, or gone out of business. However, until recently, there has been a steady decline in the production of GA aircraft since 1978 – reaching five percent of the 1978 levels in 1994.

Entrepreneurship and General Aviation

Currently, it can be seen that GA represents a significant portion of the air transportation system of the U.S. However, the erosion of the GA fleet, ground-based infrastructure, and pilot community (with associated political constituency), all hold dire consequences for GA. If allowed to continue, the market will become antiquated, uncompetitive with other modes of transportation such as the car, and eventually shunted aside from within the airspace system.

⁵ FAA Aviation Forecasts - Fiscal Year 1991-2002, U.S. DOT - FAA, FAA-APO-91-1, February, 1991.

The economically sound application of technology to increase the attractiveness and competitiveness of GA is seen to be the only alternative to make GA more competitive. As discussed in the introduction, the entrepreneur is seen to be the medium for the introduction of this technical innovation. An important caveat must be made. It can be seen that corporations play a large part in the current entrepreneurial model. They innovate and compete on a continual basis and largely assume most of the characteristics of the individual entrepreneur. Thus, it can be seen that the individual and the corporation play a role in introducing new technologies to the marketplace.

However, the entrepreneurial aspects of the start-up GA company will be analyzed in this section as the barriers of entry to the GA marketplace are most formidable to this company instead of the well established company which has considerable resources at hand.

The primary barriers to entry into the GA market are:

- Sufficient capital.
- Management competency to organize teams (often multi-disciplinary) to produce complex new products economically.
- Inadequate time to correctly design and produce a quality product which is certifiable.⁷

There are a variety of initiatives which will overcome these barriers to entry and no unique strategic plan is necessary to navigate the difficulties. However, some primary considerations must be addressed in each issue. These considerations include:

Capital

More than any other aspect, capital determines the corporate structure of the start-up company. Sufficient capital allows for greater flexibility (e.g. by waiting with a mature product until the market becomes mature) and increased performance (e.g. by rapidly developing products by hiring a large team of designers). These additional capabilities can often mean the life and death of a fragile fledgling company.

There are several sources to raise the requisite capital for becoming a successful start-up company. Some of these sources are:

- The founders' savings -- including borrowing on assets.
- Family and friends.
- Formal investment groups, including venture capital concerns and companies that specialize in the private placement of stock.

⁷ "Entrepreneurial Spirit Combines with Hard-Headed Business Sense," Olone, Richard, *Commercial Space*, Fall, 1985.

- **Foundations.**
- **Grants and small-business loans from various government agencies (e.g. SBIR loans (Small Business Innovative Research) from NSF, DoD, or NASA).**
- **Having the company's employees buy equipment and lend it to the firm.**
- **Obtaining the firm's capital equipment through bank loans and leasing companies.**
- **Forming research and development partnerships with investment companies to do incremental development.**
- **University endowments.**
- **Strategic partners that are potential customers and want early access to the start-up's product.**
- **Large companies and pension funds that enter into a venture-investment phase.**
- **Strategic partners that are manufacturers whose products would be enhanced by the start-up's product.**
- **Banking institutions that invest working capital based on firm orders.**
- **Equipment suppliers and vendors that may help a new company get started.**
- **Customers, including other start-ups, that may pay in advance for product or for a development contract (i.e. use someone else's venture capital).**
- **Going public or being acquired by a larger, more cash-rich company.²**

Obtaining adequate capital is a continual challenge of all fledgling companies and is the primary cause of the cessation of business.

Management of Large, Highly Technical Products

Users of aerospace products have high expectations of products. These products are expected to perform at a high level of performance and reliability. Thus, the technical complexity of products is relatively high (when compared to other transportation industries).

Due to the technical complexity of general aviation products, managers must be adept at the management of new technologies, personnel, and personalities. This requirement is a difficult one which may result in the failure of the start-up company or the dismissal of the manager if he or she is not capable of marrying the two diverse requirements into a functioning whole.

Some manufacturers choose to "push the edge of the technological envelope" by moving to exotic materials and technologies while others manufacture components using well-established procedures and materials. The decision between these two production techniques directly influences the challenges that will be encountered in this aspect of the fledgling company.

Inadequate Time

Many start-up companies do not allow enough time to completely develop a product before entry into the market. This complication is generally closely tied with the lack of capital (i.e. an immature product often is rushed to market because there is simply no capital to allow for continued development and/or the capital from sales is needed immediately). Indeed, many business decisions are related to trading capital for time and vice versa. Thus, while it might seem that a fledgling company failed due to a lack of time, it might actually be that the company had too little capital to produce a quality product and so rushed delivery of a new product which simply wasn't complete.

Sample Business Plan

The following business plan is a hypothetical summary of the merits of a proposed new GA airframe company. It is important to note that this plan is preliminary and must be fleshed out with significant quantitative analysis of the market and justification for key decisions within the plan. In the end, although it is important to have a complete plan, it should only be ten pages in length to allow potential investors to read it quickly and to allow important points to be made quickly and efficiently.

This business plan would be used to recruit venture capital to allow for the formation of a fledgling company and is not intended to provide a description of the internal operations of the fledgling. The following additions should be included in the final business plan:

- The market analysis which presents the analysis, justification, and results of a market analysis with the primary purpose of predicting the number of airplanes that will be sold during the initial phases of the company and the return on investment for investors.
- A detailed cost survey of the industry which establishes the cost to which the airplane should be designed and a detailed breakdown of the costs of the company to allow the cost goals to be achieved
- A prediction of the capital that would be required in each phase of the development of the fledgling company.

In all, the business plan is recommended to contain the following broad pieces of information:

- Statement of the proposed company's vision, mission, and business.
- Product concept (what the product is).
- Technological uniqueness that will sustain the firm beyond the initial product.

- **Rationale (why people will buy).**
- **Gross estimates of the target market (who will buy).**
- **Simple “market map” (how the product will be sold).**
- **Plan for reaching the seed stage [the stage of development of a company following conceptual definition], with objectives and milestones.**
- **Outline of a financial plan.**
- **Resources, in terms of dollars and people.**

This business plan will follow the following format:

- **Summary**
- **Market Brief**
- **Product Brief**
- **People**

Summary

The summary concerning the plight of the GA industry is presented in the introduction of this paper. However, all of the misery within the GA industry will likely induce the response of, “Why in this world would I want to get involved in that mess?” from the prospective investor.

It should be emphasized that each problem brings opportunity with it. It is indisputable that GA is currently an anemic industry. However, this lack of size allows an agile manufacturer to dominate the industry quickly with a well-placed product entry and therefore gain the benefits of industry dominance rapidly. Some examples of the benefits from this dominance include:

- **The ability to dictate the type of infrastructure support**
- **The ability to attract significant interest from the media and the market with each product development**
- **The ability to establish significant political attention from sub-contractors - thus enabling a working partnership.**

There is significant evidence of a resurgence of interest in GA airplanes. New aircraft companies are entering the market and established manufacturers are beginning production anew. Approximately 30,000 used GA aircraft are bought and sold annually. In addition, the continual increase of used aircraft prices over the past several years is a strong indicator that there is significant pent-up demand for cost-effective new aircraft.

Market Brief

It can be seen that approximately 60 percent of the current prospective buyers of GA airplanes are receptive to a price of a new aircraft at \$100,000 or below⁸. This product would likely be used for trips of 450-600 statute miles in length. Longer trips are likely to be conducted via airline and shorter trips are likely to be conducted by car. (Please note that this assumption must be validated.)

Product Survey

A preliminary design analysis of this airplane shows that the following characteristics are possible:

- $W_{empty}/W_{gross} = 0.54$
- Baggage: 100#
- Useful Load: 1,140#
- Aspect Ratio: 8
- $C_{D_{parasite}} = 0.0200$
- Wing Efficiency (e): 0.80
- Cruise Speed: 197 MPH
- Brake HP Required: 172 HP
- Range: 824 Miles
- Passengers: 680 #
- Fuel: 360#
- Wing Area: 147 ft²
- Wing Span: 34.3 ft
- $\rho_{7,000 \text{ ft}} = 0.00193 \text{ slug/ft}^3$
- Propeller Efficiency: 0.80
- Thrust HP Required: 138 HP
- Rated HP: 230

It is important to note that these calculations do allow for induced drag⁹. It can be seen that the weight fraction is attainable, but difficult to attain, from the following weight fractions of airplanes in production today:

Airplane	Weight Fraction (W_{empty}/W_{gross})
KIS Cruiser	0.522
GlaStar	0.579
RV-4	0.600

The GlaStar is a metal/ composite hybrid airplane, the RV-4 is a metal airplane, and the KIS Cruiser is a composite airplane. All of these airplanes are fixed gear airplanes.

The other primary constraint on the feasibility of this design is the amount of drag that will be produced by this airplane. It can be seen that the following airplane is feasible from the following data on production airplanes:

⁸ Conversation with Mr. Barry Bond, Utah Department of Transportation, July 6, 1995.

⁹ Study Conducted by Wilmer R. Ullmann, July 27, 1995 Reprinted by permission.

Airplane	Parasite Drag Coefficient (C_{Dp})
1. Piper Arrow	0.027
2. Beech Bonanza	0.019
3. Mooney 201	0.017

It is important to note that all of these airplanes are retractable gear designs. Thus, the primary challenge of this prospective airplane design will be to couple low drag with a low weight fraction.

People

It is important to emphasize just how important people are to a business plan and the viability of a fledgling company. Indeed, veteran venture capitalists have stated that having a sound management team is the key component of start-up companies for which they look when they decide whether to invest in a proposed company².

At the preliminary stage, it is impossible to determine who specifically may be involved in the design and production of this airplane. However, it is possible to describe the title and responsibilities of the key members of the core team:

- **The CEO:** Responsible for managing the company, setting standards, hiring people (although generally not all of them), and keeping and updating the vision of the company.
- **Engineering:** Responsible for technical analysis, design, and fabrication of hardware.
- **Marketing:** Responsible for determining what new performance capabilities, prices, and features should be incorporated into new products.
- **Research and Development:** Responsible for development of technologies to allow for increases in utility of future products.
- **Finances:** Responsible for maintaining the books and providing cost control to the company.
- **Law:** Responsible for insuring that the company remains within the spirit and the letter of the law and defending against product liability suits.
- **Tooling and Manufacture:** Responsible for producing the hardware, quality control, and determining ways to streamline manufacturing (works closely with Engineering).
- **Advanced Design:** Responsible for creating the products of the future (including derivative airplanes) (works closely with Research and Development).
- **Flight Test:** Responsible for testing new prototypes and insuring that airplanes are functioning properly prior to being shipped.

It is important to note that not all of these positions need be filled from within the company. Indeed, it is advisable that a company examine which of these features can best be filled internally and those that can be outsourced. The features of those that can best be filled

internally are that they are essential to the company's vision for the future or incorporate unique, proprietary technologies. Alternatively, outsourcing provides an avenue to tap sub-contractor expertise in areas which are not core to the business plans of the company while allowing for continuing improvement through close communication with the sub-contractor.

Conclusion

In summary, it can be seen that both GA and entrepreneurship contain many exciting aspects for the adventurous individual. By being wary of the pitfalls specific to GA and following the sound principles of entrepreneurship, one may beat the odds, capitalize upon a specific niche which is currently unfilled, and create benefits for both the individual and the general market.

**NEXT
DOCUMENT**

Determination of Stress-Corrosion Cracking in Aluminum-Lithium Alloy ML377

Bryan C. Valek
Georgia Institute of Technology

Mentor
Marcia S. Domack
NASA Langley Research Center

August 17, 1995

Research and Technology Group

Materials Division

Metallic Materials Branch

Abstract

The use of aluminum-lithium alloys for aerospace applications is currently being studied at NASA Langley Research Center's Metallic Materials Branch. The alloys in question will operate under stress in a corrosive environment. These conditions are ideal for the phenomena of stress-corrosion cracking (SCC) to occur. The test procedure for SCC calls for alternate immersion and breaking load tests. These tests were optimized for the lab equipment and materials available in the Light Alloy lab. Al-Li alloy ML377 specimens were then subjected to alternate immersion and breaking load tests to determine residual strength and resistance to SCC. Corrosion morphology and microstructure were examined under magnification. Data shows that ML377 is highly resistant to stress-corrosion cracking.

Background

The High Speed Research program, or HSR, is a joint program between NASA and industry, concerned with developing the next generation of supersonic civil aircraft. Many factors must be studied, including structures, materials, design, commercial feasibility, noise, and pollution. The development of these technologies is necessary to the success of a high speed civil transport. The purposes of this study are to collect corrosion data on candidate alloys for the HSR program and to evaluate the breaking load test method for stress-corrosion cracking. The material tested in this study is aluminum-lithium alloy ML377 in the T8 (near peak aged) condition. This is the most corrosion resistant temper for Al-Li alloys, and is the first of several alloys to be tested.

The phenomena of stress-corrosion cracking (SCC) can lead to catastrophic engineering failures. Many parts in an aircraft frame are subjected to conditions that could lead to SCC. In order for SCC to occur high levels of stress must act in conjunction with a corrosive environment. The breaking load method can be used to determine a threshold stress level for the initiation of SCC. Material below this stress level would be safe from the possibility of SCC.

The breaking load test method determines the residual strength of an alloy after exposure to SCC conditions. Specimens are fixed in stress by static load frames. The specimens are subject to corrosion by alternating immersion and drying cycles in a sodium chloride solution. They are then stressed to failure in tension. By using a test matrix of varying stress levels and exposure times, an alloy's resistance to SCC can be determined. The breaking load method can determine the SCC initiation threshold with fewer specimens and shorter times than traditional pass-fail tests, and can detect differences in highly resistant alloys.

Procedure

Test Procedure

The test procedure involves two major phases. Specimens are exposed to a corrosive environment for a range of stress levels and times in alternate immersion, then they are subject to tensile failure. The specimens are transverse dog bone coupons of Al-Li alloy ML377 in the T8 temper (Figure 1). The gage length has been polished to meet ASTM standards.

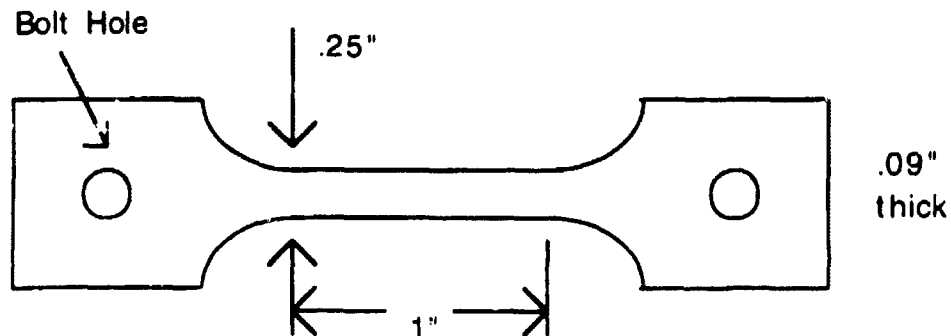
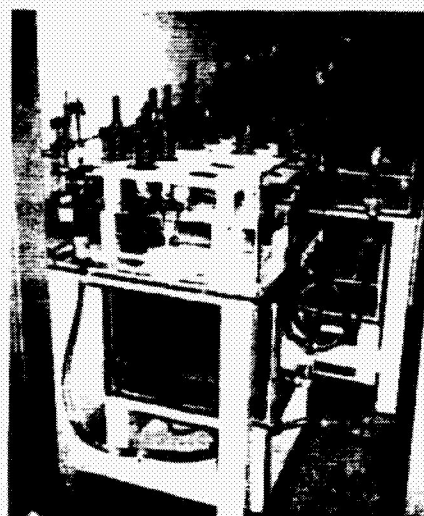


Figure 1 - ML377 Dog Bone Specimen

The static load frame (Figure 2a) is made of steel and protected with a special coating, in order to prevent any rust or galvanic cell formation. The spring has a spring constant of approximately 2200 lbs/in. When loaded, the spring applies pressure to a stainless steel threaded rod, which is connected to the specimen via bolts. A nut on the rod allows adjustment of the stress placed on the alloy. The elongation of the specimen is monitored by an extensometer attached to the specimen. The stress is calculated from the extension and modulus of the specimen. Once the specimen connectors have been protected with wax and the gage length has had all extensometer marks removed, it is placed in the immersion tank.



a)



b)

Figure 2 - a)Static Load Frame b)Specimens in Alternate Immersion Tank

The alternate immersion test (Figure 2b) subjects the specimen to ten minutes of exposure to a corrosive solution and fifty minutes drying time. The solution used was 3.5% by weight sodium chloride in distilled water. The environmental conditions of the test lab are maintained at $80\text{ F} \pm 2$ and 40% humidity $\pm 6\%$. A timer is used to raise and lower the water level in the main test tank. The timer is connected to a pump, which moves water from a reservoir tank to the main tank, and a solenoid, which drains from the main tank to the reservoir. Water levels are monitored to assure a proper solution concentration.

Once alternate immersion exposure is complete, the specimen is removed, unloaded, and examined for any anomalies. It is then subjected to the breaking load test. The specimen is pulled in tension until failure in a hydraulic load machine. The load at failure (ultimate tensile strength) and the load vs. elongation curve are recorded.

In addition, the corrosion morphology and fracture surfaces were examined visually under high magnification. Micrographs were taken of some surfaces to assist examination. Surfaces were then etched to relate corrosion morphology to microstructure.

Test Optimization

Before the testing could begin, it was necessary to study the testing procedure itself. The best ways to protect the frames from corrosion, load the frames, and maintain the test conditions were reevaluated.

Many different coating techniques were studied for their protection and longevity characteristics. The load frame must be protected from exposure to salt water when it is submerged. However, the gage length of the specimen in test must come in contact with the water. Wax, latex, heat shrinkable plastic, and a polymer paint known as Plasti-Dip were examined as coating materials. After extensive testing, a system of coating was chosen that combines wax and Plasti-Dip. The steel frame is coated in Plasti-Dip because it adheres well and has excellent waterproofing properties. The connections between the load bolt and the specimen are coated with wax because it is easily removed and conforms to the contours of the region.

In order for the tests to be as accurate as possible, the load frames must pull the specimen in tension. Any added bending moments or twisting forces can affect test results. Due to the design of the frame, it is easy to induce these forces when loading. Therefore, it was necessary to develop a rig for securing the frame at all points except the point of spring compression. The design of the rig uses gravity to help line the frame vertically. The top and bottom are secured and the spring is loaded by use of a wrench.

The test solution was monitored to maintain conditions. Water evaporated from solution and had to be replenished every two days. The entire tank needed to be emptied and refilled every three weeks to prevent build up of excessive metal ions in solution. A system for changing the solution was developed utilizing an extra tank system in the lab.

Results

Breaking Load Data

The data for this study was collected as the residual ultimate tensile strength of the specimen. The experimental parameters were the time of exposure and the stress level during exposure, given as a percent of the yield strength of the material. Figure 4 shows the number of specimens tested for each combination of exposure and stress.

Exposure	0% stress	50% stress	65% stress	80% stress
0 days	2	0	0	0
10 days	3	0	3	3
15 days	3	3	3	3
30 days	3	3	3	3

Figure 4 - Test Matrix for ML377 SCC specimens

Residual strength is measured as the load at fracture, or the breaking load, divided by the original cross-sectional area of the specimen. As a specimen corrodes, its cross-sectional area is reduced. By using the original area as a standard, the residual strength can be used to gauge the amount of corrosion which has occurred.

Each data point is given as an average of the residual strength of all the specimens subjected to those particular conditions, in most cases three specimens (see Figure 4). Study of the data obtained (Figures 5,6) reveals that ML377 is resistant to stress-corrosion cracking. No specimens failed while in test. Loss of strength appears to be due to general corrosion, aided by stress.

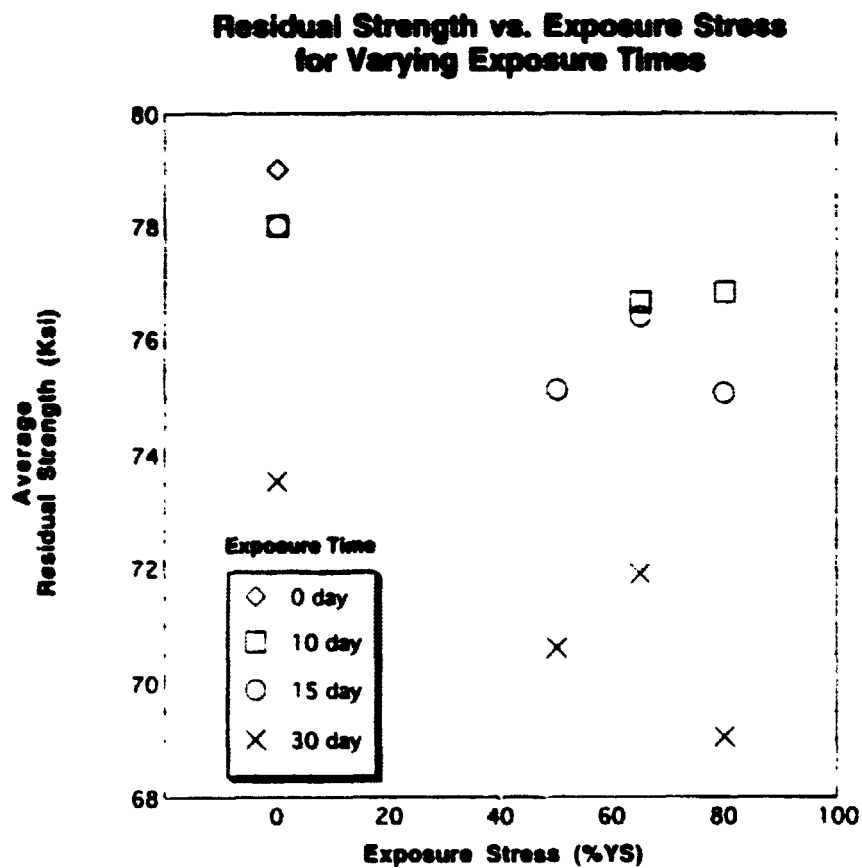


Figure 5 - Residual Strength vs. Exposure Stress

The plot of residual strength versus exposure stress (Figure 5) shows that increasing the exposure stress results in a loss of strength. There is a downward trend in residual strength with increasing exposure stress for each exposure time. The effect of stress is greater for the longer exposure times.

Figure 6 shows the same data plotted as residual strength versus exposure time for varying stress levels. For each exposure stress, residual strength decreases with exposure time.

For example, each point at 15 days is less than or equal to its partner stress level at 10 days.

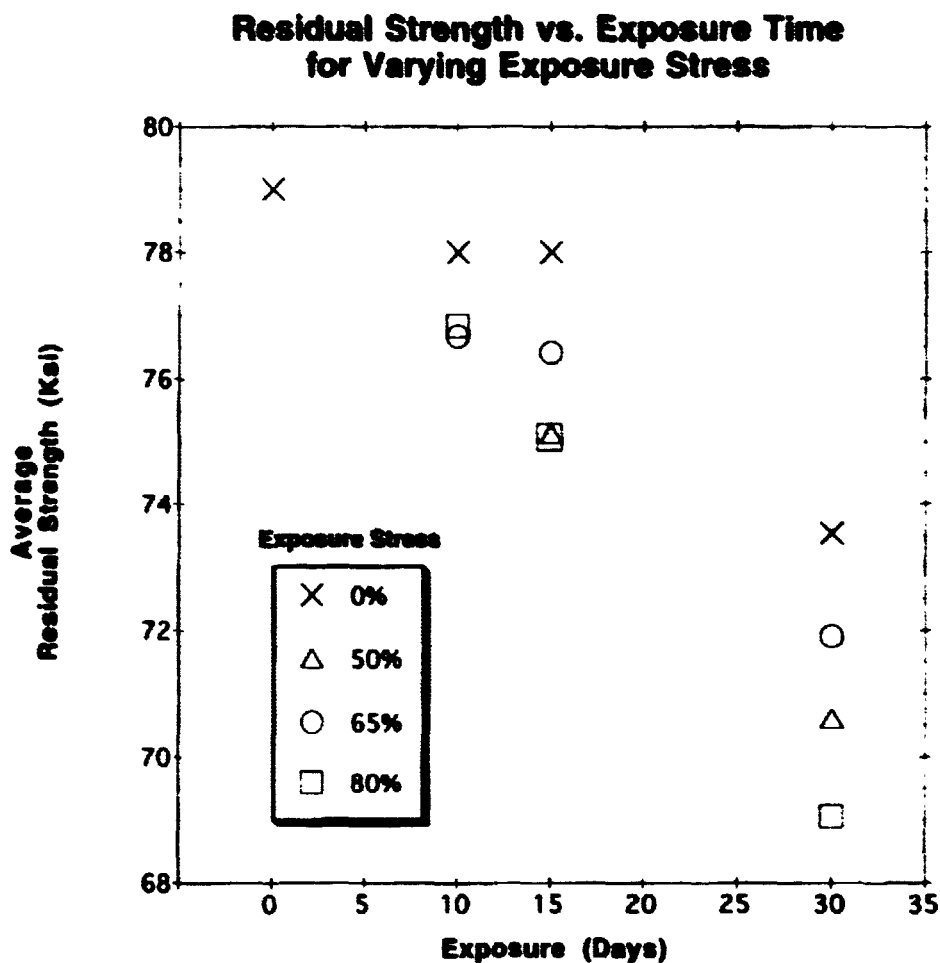


Figure 6 - Residual Strength vs. Exposure Time

For both stressed and unstressed specimens, an additional reduction in residual strength occurs after 30 days exposure. The data indicates a combined effect between stress level and exposure time. The reduction in strength of the unstressed specimen is due to pitting corrosion. The longer the exposure, the more pitting can occur, and thus a greater reduction in area results in a greater loss of strength.

After 30 days, an unstressed specimen has lost 6.7% of its original strength, while an 80% stress specimen has lost 12.7%. The reduction in strength of the highest stressed specimens is approximately double that of the unstressed specimens. This may be due to either stress corrosion cracking or stress assisted pitting.

Corrosion Morphology and Microstructure

Figure 7 shows the grain structure of the alloy, viewed in the T-S plane. Since these are transverse specimens, the rolling direction of the grains goes into the page. The grains are elongated in the rolling direction and flattened to the left and right, as expected for rolled sheet. All micrographs shown are prepared in the T-S orientation.

Figure 8 shows polished sections through corrosion pits. No stress corrosion cracks were present in any of the specimens viewed. Pitting was the only corrosion observed on the specimens. The crack propagating from the base of the pit in Figure 8a was caused by tensile fracture rather than stress corrosion because no stress was present on this specimen. Many different corrosion pits were examined from specimens exposed at the various test conditions. The pit propagation in both stressed and unstressed specimens, in general, follows the transverse direction. However, in the stressed specimens, corrosion propagation seems to be influenced by stress, causing a sharper undercutting of the surface metal, as illustrated in Figure 8b by the narrow pit opening. More material has been dissolved at the surface in the unstressed specimen (Figure 8a). The corrosion mechanism does not seem to prefer a particular grain type and proceeds through grain boundaries, illustrated in the polished and etched cross section shown in Figure 9.

For the exposure stresses and durations conducted, ML377 is resistant to stress-corrosion cracking. Any loss of strength can be contributed to a reduction in area due to pitting corrosion.

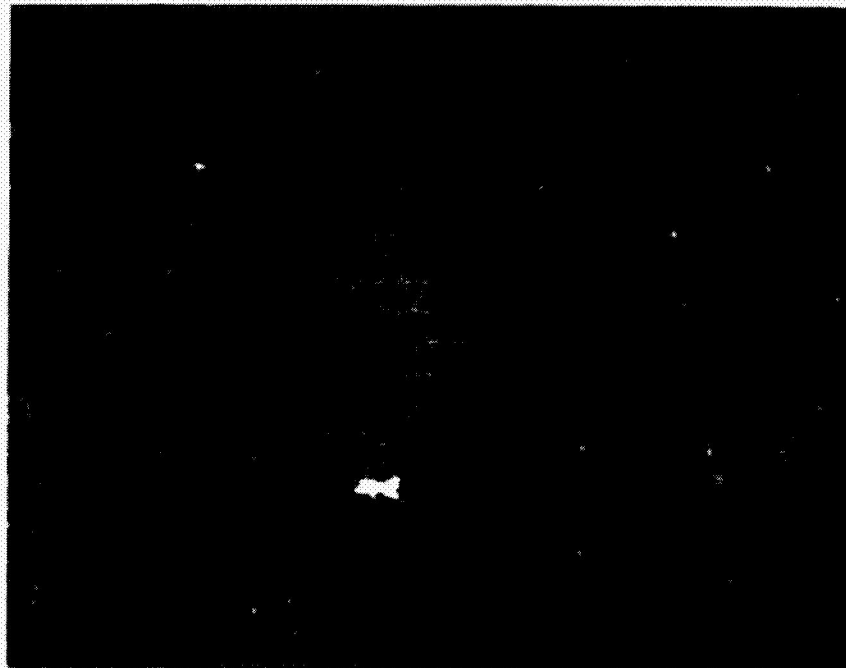
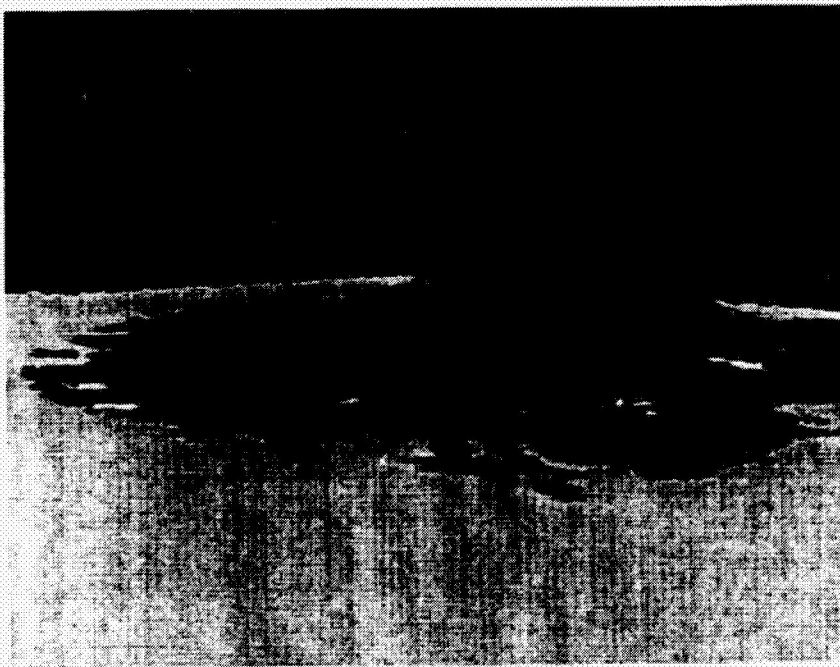


Figure 7 - Grain Structure of ML377-T8 (100X)



a)



b)

Figure 8 - a) 30day, 0% stress specimen pit b) 30day, 65% stress specimen pit (100X)



Figure 9 - Corrosion Pit and Microstructure of 30 day, 65% stress specimen (100X)

Conclusion

Aluminum light alloy ML377 in the T8 temper is resistant to stress-corrosion cracking for the parameters used in this study. A combined effect of exposure stress and exposure time is evident, however corrosion was due to stress assisted pitting rather than stress corrosion cracking. There is a difference in the corrosion morphology between stressed and unstressed specimens.

The breaking load method is showing promise as an effective method for the study of initiation of stress-corrosion cracking in resistant alloys. However, much more testing is needed before this method proves itself.

**NEXT
DOCUMENT**

1995 1/6
1995

**A MATLAB/Simulink based GUI for
The CERES Simulator**

Luis H. Valencia

University of Puerto Rico, Mayaguez Campus

1995 Langley Aerospace Research Summer Scholars Program

Under the Direction of

Calvin Mackey and

John Chapman

Data Management Office

Space and Atmospheric Sciences Program Group

Atmospheric Sciences Division

Abstract

The Clouds and The Earth's Radiant Energy System (CERES) simulator will allow flight operational familiarity with the CERES instrument prior to launch. It will provide a CERES instrument simulation facility for NASA Langley Research Center, NASA Goddard Space Flight Center, and TRW. One of the objectives of building this simulator would be for use as a testbed for functionality checking of atypical memory uploads and for anomaly investigation. For instance, instrument malfunction due to memory damage requires troubleshooting on a simulator to determine the nature of the problem and to find a solution.

Introduction

The purpose of this overview is to provide a brief summary of the Clouds and The Earth's Radiant Energy System (CERES) simulator, objectives, perspective, advantages, and its relationship to other Earth Observing System (EOS) instruments. An important theoretical background concerning the CERES project will be given as a guide for introducing the CERES concepts.

The CERES instrument, as shown in Figure 1, is a key part of NASA's Earth Observing System. It is designed for use in Tropical Rainfall Measurements Mission (TRMM) and EOS satellites that will be measuring radiant energy reflected from Earth's clouds starting in 1997. The CERES data is critical for advancing the understanding of cloud-radiation interactions; in particular, clouds' feedback effects on the Earth's radiation balance. CERES data is fundamental to our ability to understand and detect global climate change. CERES results are also important for studying regional climate changes associated with deforestation, desertification, anthropogenic aerosols, and El Nino events. The CERES simulator is being built at NASA Langley Research Center to be used as a ground testbed for anomaly investigations and to test software uploads, that control the instrument, prior to transmitting them to the satellite.

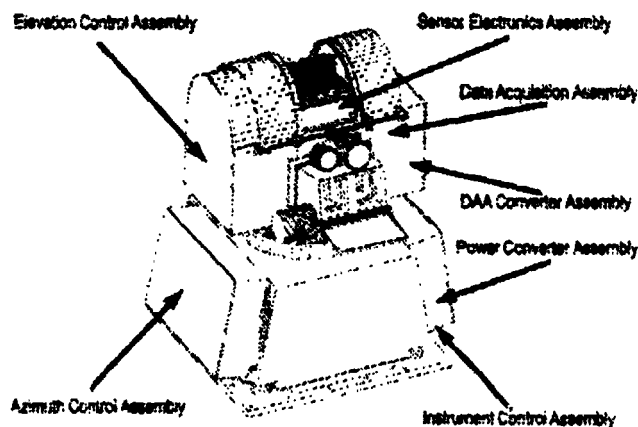


Figure 1. CERES Instrument

CERES Background

The CERES data is intended to substantially improve our understanding of cloud's energy flows. The CERES investigation concentrates on four primary areas: Earth radiation budget and cloud radiative forcing, cloud properties, surface radiation budget, and radiative components of the

atmosphere's energy budget. Therefore, due to the importance of the CERES instrument for TRMM and EOS, the design and implementation of a CERES simulator was proposed.

CERES Simulator Description

The CERES simulator consists of circuit cards functionally identical to the flight items, though fitted with low cost commercial specification microcircuits and components. Two host personal computers (PC's) will support the electronics ensemble. One PC will contain a 1553 interface card which will function as the telemetry path for commands and memory uploads, while the second PC will provide a representation of the mechanical components such as the azimuth and elevation drive components and covers.

DADS/Plant software incorporating a Graphical User Interface (GUI) which will be driven by I/O interface cards via MATLAB/Simulink is currently being developed. The mechanical control system simulation will be accomplished by using the MATLAB/Simulink software package with real-time executable files to call I/O card drivers. The mechanical components of the instrument must be represented by dedicated I/O ports linked with the host PC software to respond to processor commands simulating the physical hardware they represent in a realistic fashion.

The CADSI DADS/Plant software provides for animation of CAD/CAM drawings in real-time, as shown in Figure 2. The DADS/Plant program when linked with Simulink will display interactive visualization of 3D geometry of the controls software.

The MATLAB package is available for SUN, PC-486/Pentium, and SGI platforms, among others etc. The task is to seamlessly integrate PC I/O cards to read the CERES processor control lines, input this signal to the MATLAB/Simulink software, and then output a virtual position back to the CERES processor in a manner that mimics the actual hardware.

The obvious solution would be to use MATLAB on a 120MHz Pentium-based PC and do the I/O on one inexpensive, dedicated platform, with the GUI on the same PC. Likewise, an interesting alternative would be to use the PC to drive command lines to a SUN (or SGI) GUI. MATLAB can do this when linked to DADS/Plant as a recent demonstration has shown (see Figure 2).

The CERES simulator consists of CERES circuit cards (identical to those designed by TRW), populated with socketed DIP and SMT chips. It will use low cost, although identical commercial grade chips, as well as some mil-spec chips. A PC-486 host computer with a 1553 B interface card will be dedicated for TRW developed GSE code and cots. Similarly, a 120MHz Pentium with MATLAB/Simulink software will be used for elevation and azimuth drive simulation. The system will also incorporate multifunction I/O cards: a 16-bit parallel digital I/O card, a time code generator card, a graphics accelerator card, and a DT2811 A/D converter.

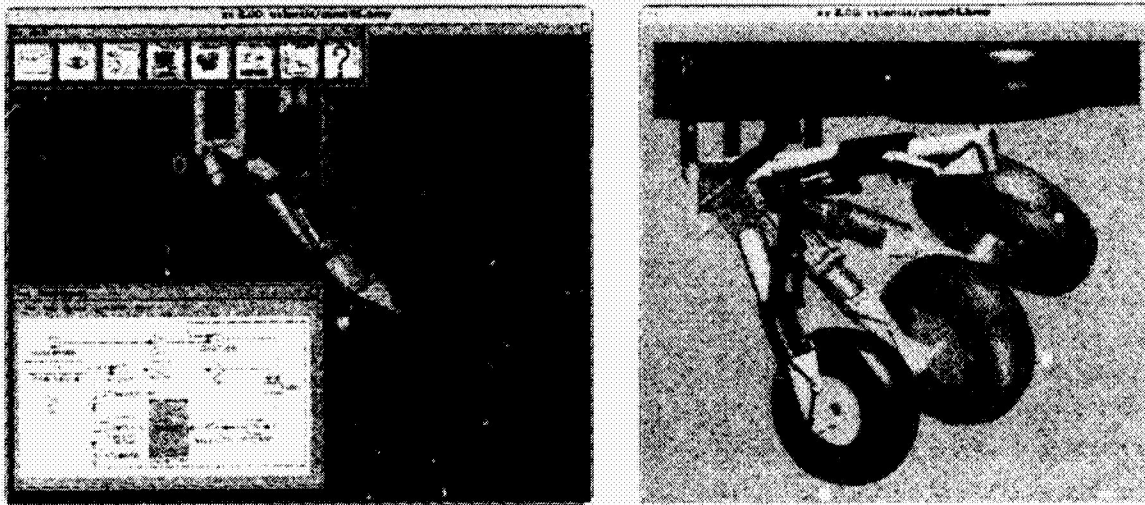


Figure 2. Demo sample of DADS/Plant. Step by step animation of landing gear mechanism.

Method

To accomplish the stated task, Simulink software has been used for simulating the dynamic system. As an extension to MATLAB, which is the controlling platform, Simulink adds many features specific to dynamic systems, while retaining MATLAB's general purpose functionality.

Simulink consists of two phases: model definition and model analysis. A typical session starts by either defining a model or recalling a previously defined model, and then proceeding with an analysis of that model. In practice, these two steps are often performed iteratively as the model designer creates and modifies a model to achieve the desired behavior.

To facilitate model definition, Simulink adds a new class of windows called block diagram windows. In these windows, models are created and edited principally by mouse driven commands. It is imperative that the user becomes familiar with the manipulation of model components within these windows.

After the user defines a model, one can analyze it either by choosing options from the Simulink menus or by entering commands in MATLAB's command window. Built-in analysis tools include various simulation algorithms, such as "linmod", a tool for extracting linear models of systems, and "trim", a tool for finding equilibrium points.

The progress of a simulation can be viewed while the simulation is running, and the final results can be made available in the MATLAB workspace when the simulation is complete.

Simulink uses the metaphor of a block diagram to represent dynamic systems. Defining a system is similar to drawing a block diagram. Instead of drawing the individual blocks, blocks are copied from

libraries of blocks: either the standard block library supplied with Simulink, or block libraries the user creates.

The standard block library is organized into several subsystems, grouping blocks according to their behavior. Blocks can be copied from these or any other libraries or models into a current model. By placing the blocks it most commonly uses into one system and setting your preferences for default values, the software can set up a personal block library.

The CERES elevation and azimuth drive simulation is shown in Figure 3. The equations of motion describing the translation and rotation for each articulation of the CERES instrument, and all associated physical parameters were obtained from TRW, see reference 1. The appropriated equations and parameters were extracted and used in designing the MATLAB/Simulink software program input block diagrams to simulate the control system of the azimuth and elevation drives. Each equation of motion defines a particular parameter such as friction, torque, or scanning mode (see Figures 4 through 7) within the azimuth or elevation drive control system. Each module parameter contains a unique simulation which will be governed and connected by the main module shown in Figure 3. The entire simulation requires a CERES voltage command which, for this particular case, is generated by a signal generator.

A TRW scan head mechanical model would be simulated as the diagram depicted in Figure 7 validated for open loop gains. From the diagram, the $Kdeg$ gain converts any input from radians to degrees. After obtaining the input in degree format, integration will yield the velocity of the motor; while a second integration produces the position and elevation. This approach was used for all of the mechanical parameters within the CERES simulator.

Results

Figure 8 presents the results for a simple open loop control system configuration. The entire simulation has been successfully executed for non real-time data. However, the results obtained should vary with real-time input data driven by I/O cards. To study the system behavior in the presence of noise, gains and amplitudes were varied. A given input corresponds to a certain output, which yields a variation for each input parameter. As mentioned earlier, a typical periodic sinusoidal signal generator was used as an input generator rather than real-time data. However, the CERES simulator will require real-time input driven by I/O cards in order to obtain accurate results.

The simulator was also tested for the azimuth drives. The results were similar to those of the elevation drives. Although the azimuth simulation appeared to be noisier in some cases, the scanning position was accurated. As previously mentioned, Figure 8 shows the preliminary results from the control system of the CERES simulator. The effects visibly changed through time, as computing time increases from 1 to 5 seconds.

At this point, the control system simulations show the behavior of the TRW's CERES scanner sensor model. Applying a computer aided design (CAD) tool such as DADS/Plant software would enable complete visualization of the CERES simulator.

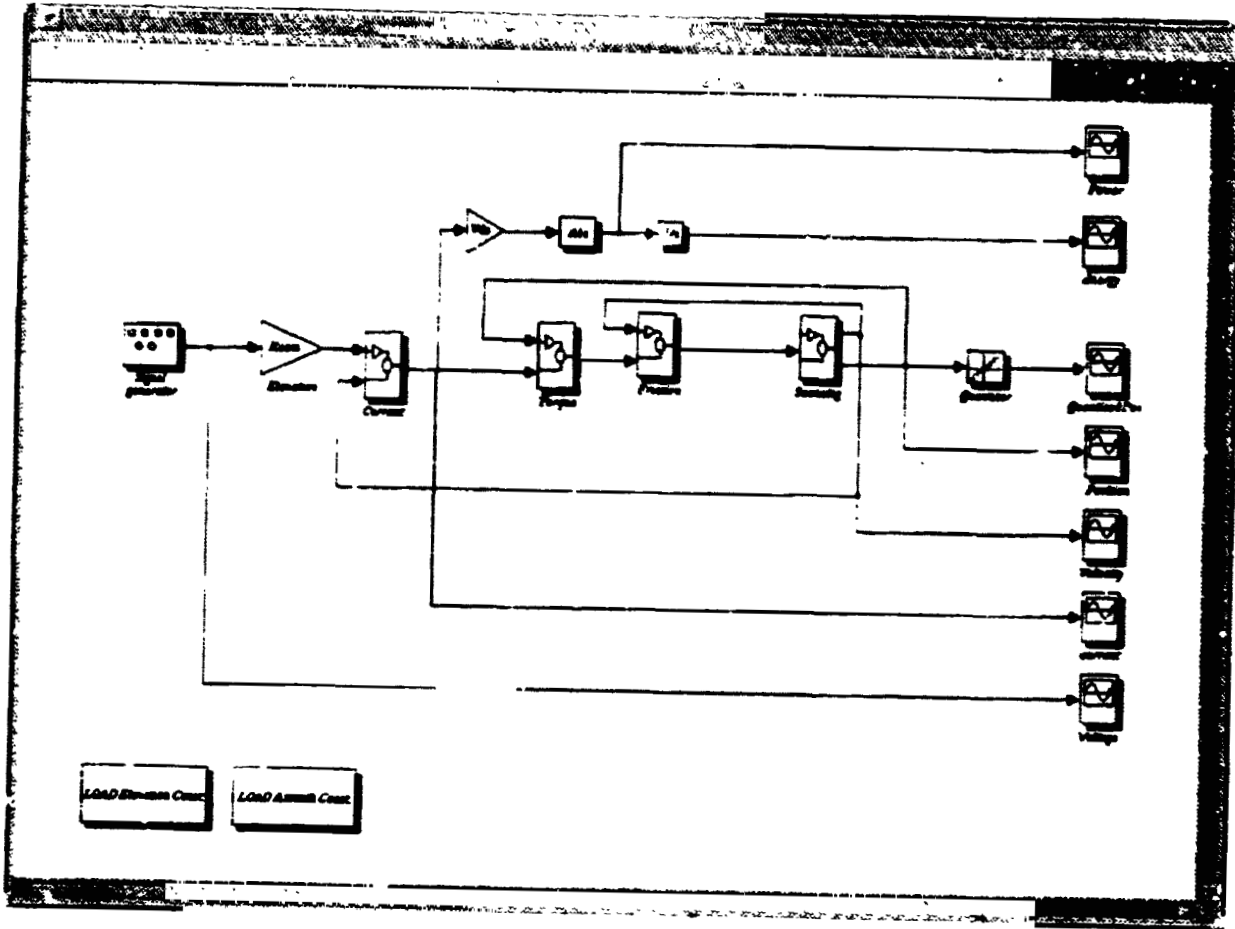


Figure 3. Main Module

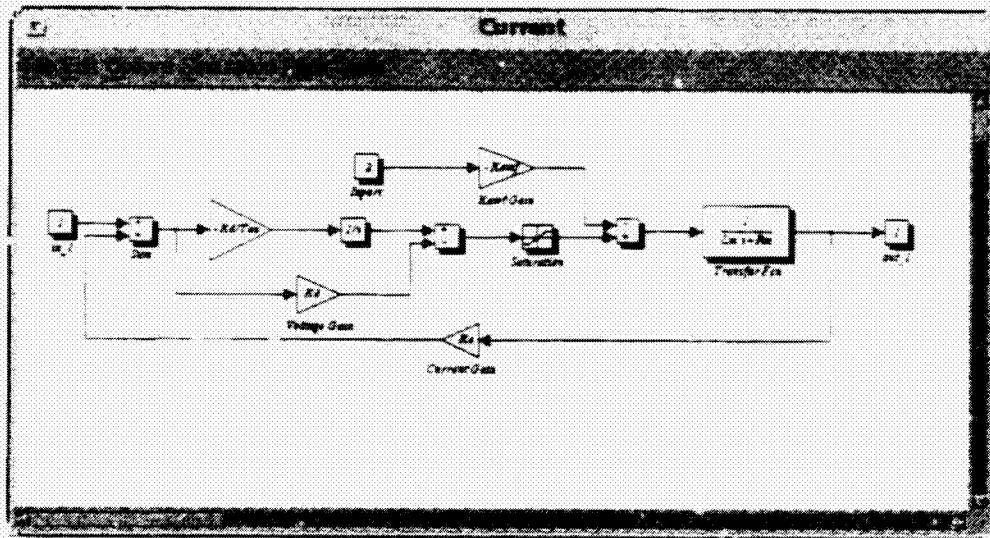


Figure 4. Current Module

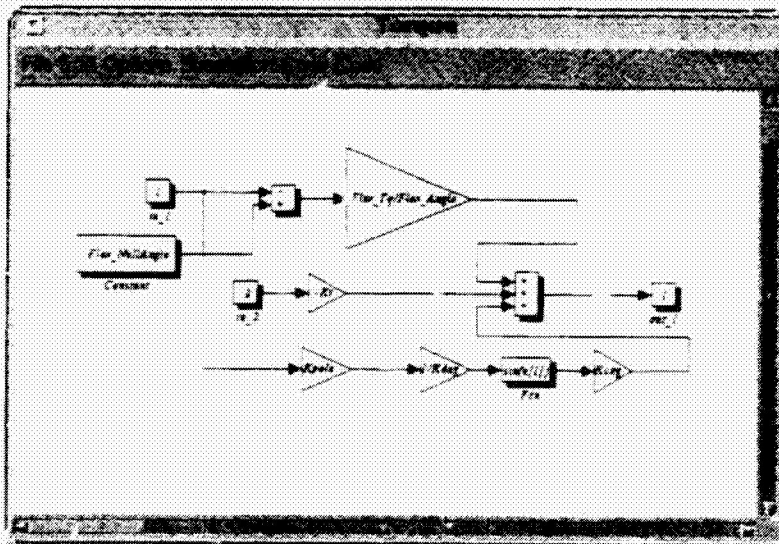


Figure 5. Torque Module

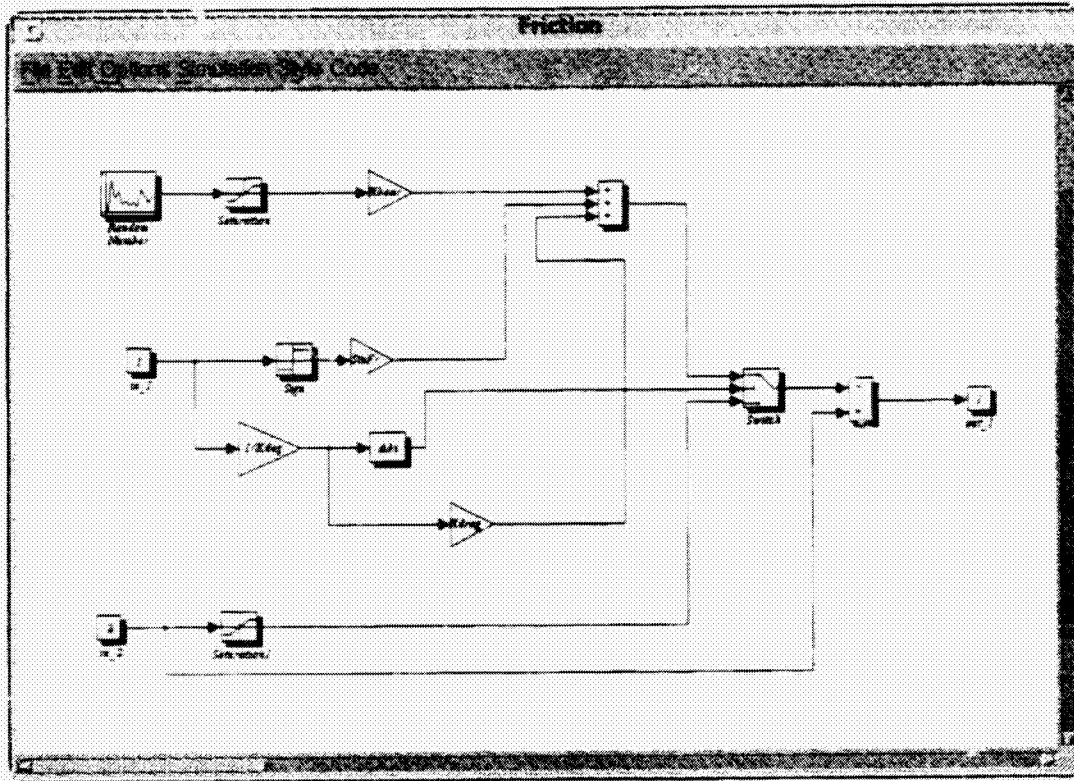


Figure 6. Friction Module

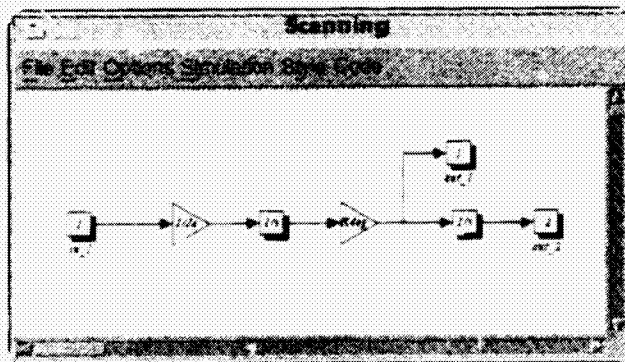


Figure 7. Scanning Module

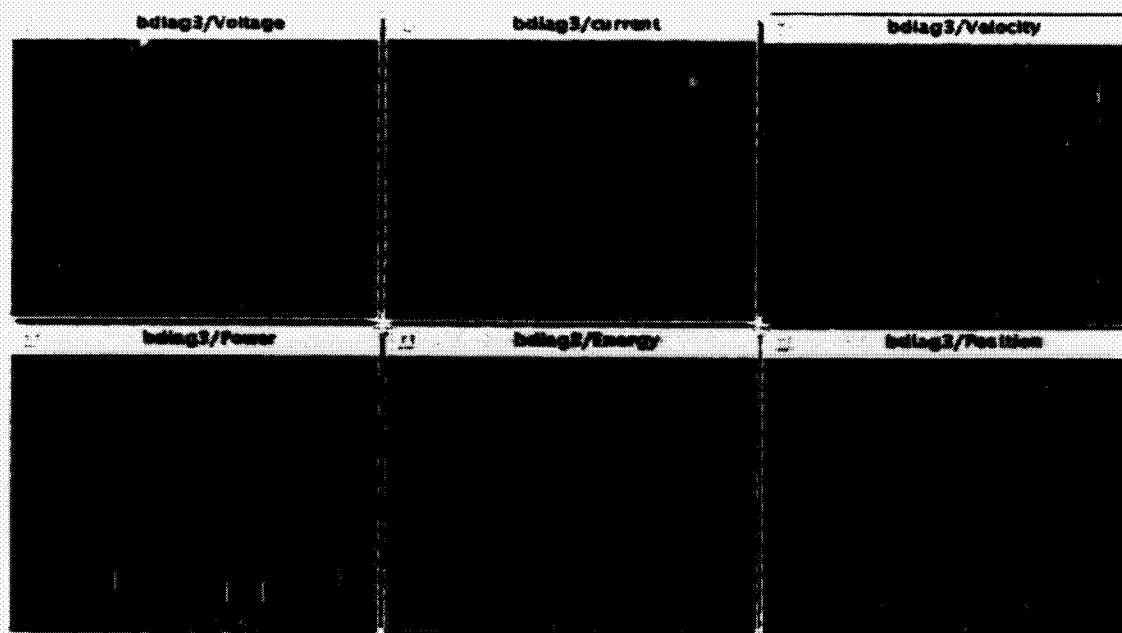


Figure 8. Results

Conclusion

At this point the CERES simulator is still being assembled, and circuit cards are being populated and wired. It is scheduled to be completed well before the launch of the CERES instrument. Recent work has focused upon the completion of the elevation and azimuth drivers in the MATLAB/Simulink simulation. Most of the I/O cards and some other hardware parts are ready for integration into the system. Work will continue under the direction of John Chapman.

The MATLAB input files, describing the coefficients and equations of motion, the block diagrams depicting the mechanical components, and parameters for the elevation and azimuth scanner have been produced for MATLAB on a SUN workstation. MATLAB claims file portability between IBM PC, SUN, and SGI platforms. A functional demonstration of MATLAB/Simulink linked with CADSI DADS/Plant has been performed to verify this claim.

The DADS/Plant software eliminates the time-consuming, error-prone process of deriving and manipulating equations of motion for the plant model in simulation programs. It provides interactive, graphical and visualization construction of the plant mechanism model as well. The system simulation is performed under the control of the simulation program. Data transfer between DADS/Plant and the simulation program is completely automatic and transparent. The goal is to simulate the behavior of the CERES mechanical system in order to validate and improve designs from concepts of testing. Both the MATLAB/Simulink and DADS/Plant software are available for either Unix or SGI platforms.

Langley Research Center Equipment and Facilities Employed

The project involved the use of several different computer platforms at Langley. Code development and control system simulations were performed on a SUN workstation. Simulations were performed using MATLAB/Simulink software. The DADS/Plant software is intended to be used as a visualization tool, which combines its features of mechanism modeling with the systems and control modeling features available in MATLAB/Simulink. This integrated solution provides an accurate, easily manipulated simulation of simple mechanisms and highly complex controlled mechanical systems.

Acknowledgments

The author would like to thank the following people for their help and support during the course of this study: John Chapman, who served as a mentor; Jim Miller, who spent an extraordinary amount of time overseeing the project; Mark Shipham and Calvin Mackey, who provided software support; and the NASA Langley University Affairs staff, who made the whole project possible.

References

- [1] Miller, J.B., "*Program TRW's CERES Scanner Servo Model*". NASA Langley Research Center.
- [2] Wielicki, Bruce A., Barkstrom, Bruce R., "*Instrument Geolocate and Calibrate Earth Radiances*." Technical Report, April 1994.
- [3] Evert, T., "*Pointing Subsystem Analysis*." TRW DRL60 Technical Report, June 21, 1994.
- [4] Wielicki, Bruce A., Barkstrom, Bruce R., "*CERES Algorithm Overview*." Technical Report, April 1994.
- [5] Wielicki, Bruce A., Barkstrom, Bruce R., "*CERES Data Processing System Objectives and Architecture*." Technical Report, March 1994.

**NEXT
DOCUMENT**

Oxidation Behavior of Carbon Fiber Reinforced Silicon Carbide Composites

**Victor M. Valentín
LARSS**

**Wallace Vaughn
Mentor**

Ceramic Based Materials, Materials Research, Environmental Interactions Branch

Abstract

Carbon fiber reinforced Silicon Carbide (C-SiC) composites offer high strength at high temperatures and good oxidation resistance. However, these composites present some matrix microcracks which allow the path of oxygen to the fiber. The aim of this research was to study the effectiveness of a new Silicon Carbide (SiC) coating developed by DUPONT-LANXIDE to enhance the oxidation resistance of C-SiC composites. A thermogravimetric analysis was used to determine the oxidation rate of the samples at different temperatures and pressures.

The Dupont coat proved to be a good protection for the SiC matrix at temperatures lower than 1240°C at low and high pressures. On the other hand, at temperatures above 1340°C the Dupont coat did not seem to give good protection to the composite fiber and matrix. Even though some results of the tests have been discussed, because of time restraints, only a small portion of the desired tests could be completed. Therefore, no major conclusions or results about the effectiveness of the coat are available at this time.

Introduction

Carbon-Carbon (C-C) composites are a generic class of composites similar to the graphic/epoxy family of polymer matrix composites. These materials were originally developed for the space program in 1958 by the NASA administration and the U.S. Air Force.¹ These composites offer many desirable characteristics such as tailorable properties, strength and modulus retention at high temperatures, thermal shock resistance, fatigue resistance, low density, good frictional characteristics, low coefficient of thermal expansion, and immunity to natural space radiation. Nevertheless, C-C composites have also proven to be an excellent material not only for advanced aircraft and aerospace applications, but also for numerous common life applications, such as automotive pistons, clutch assembly and brakes for racing cars and even parabolic RF antennas. As previously mentioned, this material offers high strength and stiffness at high temperatures in an inert atmosphere; however C-C composites are easily oxidized in temperatures over 500°C.

Different coats and techniques have been developed to protect the fiber and matrix of C-C composites from oxidizing environments. The most common coats used today are SiC, and Si₃N₄. The most useful techniques used to apply these coats are chemical vapor deposition (CVD) and chemical vapor infiltration (CVI)¹. Although some material has been published on these techniques many companies are secretive about their manufacturing process. Other published methods that can be found are sputtering, Ion plating, electroplating, and liquid metal transfer which uses TiB, TiC, TiN, Al, Co, and Cu as coats, among others.¹ Even though many reports have been published in this area, it is difficult to compare the results of these investigations due to the difference of their testing environments. In an effort to improve the oxidation resistance of C-C composites Dupont-Lanxide licensed the C-SiC technology from the Société Européenne de Propulsion. This technique combines the high strength of carbon fibers and the good oxidation resistance of the silicon carbide matrix. However, the protection of the matrix is diminished because of the presence of some microcracks in the matrix of the C-SiC composites. These microcracks are a result of the thermomechanical cycles the composites are exposed to during service or manufacturing and they allow the path of oxygen to come into contact with the reinforcement fiber.²

The purpose of this research is to study the effectiveness of a Silicon Carbide coat developed by DUPONT-LANXIDE to protect the C-SiC composite in an oxidizing environment. This material (C-SiC composite with the Dupont coating) might be used to protect the lead wing edge and nose cap of the reusable launch vehicle (RLV) under research by McDonnell Douglas, Boeing and NASA. The lead wing edge and nose cap of this vehicle will encounter temperatures ranging from 840°C to 1540°C and pressures between 1 torr and 40 torr.

In order to prove the effectiveness of the coated C-SiC composite, some samples of the material will be exposed to the same temperatures and pressures that the RLV might encounter during entry to earth. A thermogravimetric analysis machine (TGA) will be used to setup an oxidizing environment at the desired pressures and temperatures. The data acquired by the TGA will be used to determine the oxidation behavior of the composites.

Research Project

The composites were developed and manufactured by DUPONT-LANXIDE industries.

Three panels were manufactured:

1. 041-02-001 : Uncoated, heat treated.
2. 347-02-197 : Dupont-Lanxide Coated (CVIP) , heat treated as fabric
3. 765-02-014 : Dupont-Lanxide Coated (CVIP) , non heat treated

The same panels were cut in small squares with surface areas that ranged between 6 cm^2 and 7 cm^2 , and weighed between 1 gram and 2 grams. The oxidation behavior of the samples were measured by a STA-409 Nezschi TGA/DTA with a computer based data acquisition system.

The flow rate of air was kept constant at 100 sccm. Pressure and temperature were also kept constant during each test. However, different combinations of pressure and temperature were chosen for each test. The combinations were selected to match the entry profile of a future reusable launch vehicle lead wing edge and nose cap (Fig. 1).

A maximum mass loss per surface area of 75 g/m^2 was established for the samples. The C-SiC composites were left to oxidize at the desired pressures and temperatures until they reached a maximum mass loss (target mass loss, TML) or for a maximum time of 22 hours.

$$\text{TML (mg)} = \text{Initial Mass (mg.)} - 75 \text{ (g/m}^2\text{)} * \text{Surface Area (cm}^2\text{)}$$

10

A graph of mass versus time was drawn in order to look at the oxidation behavior of the samples (Fig 2 and 3). The oxidation rate and mass loss per time per surface area ($\text{g/m}^2 \text{ min}$) were calculated. The objective was to verify that the samples would have a maximum oxidation rate of $-0.001 \text{ g/m}^2 \text{ min}$, which would give a service time of 75,000 hrs.

Pressure-Temperature Test Points for DuPont C-SiC

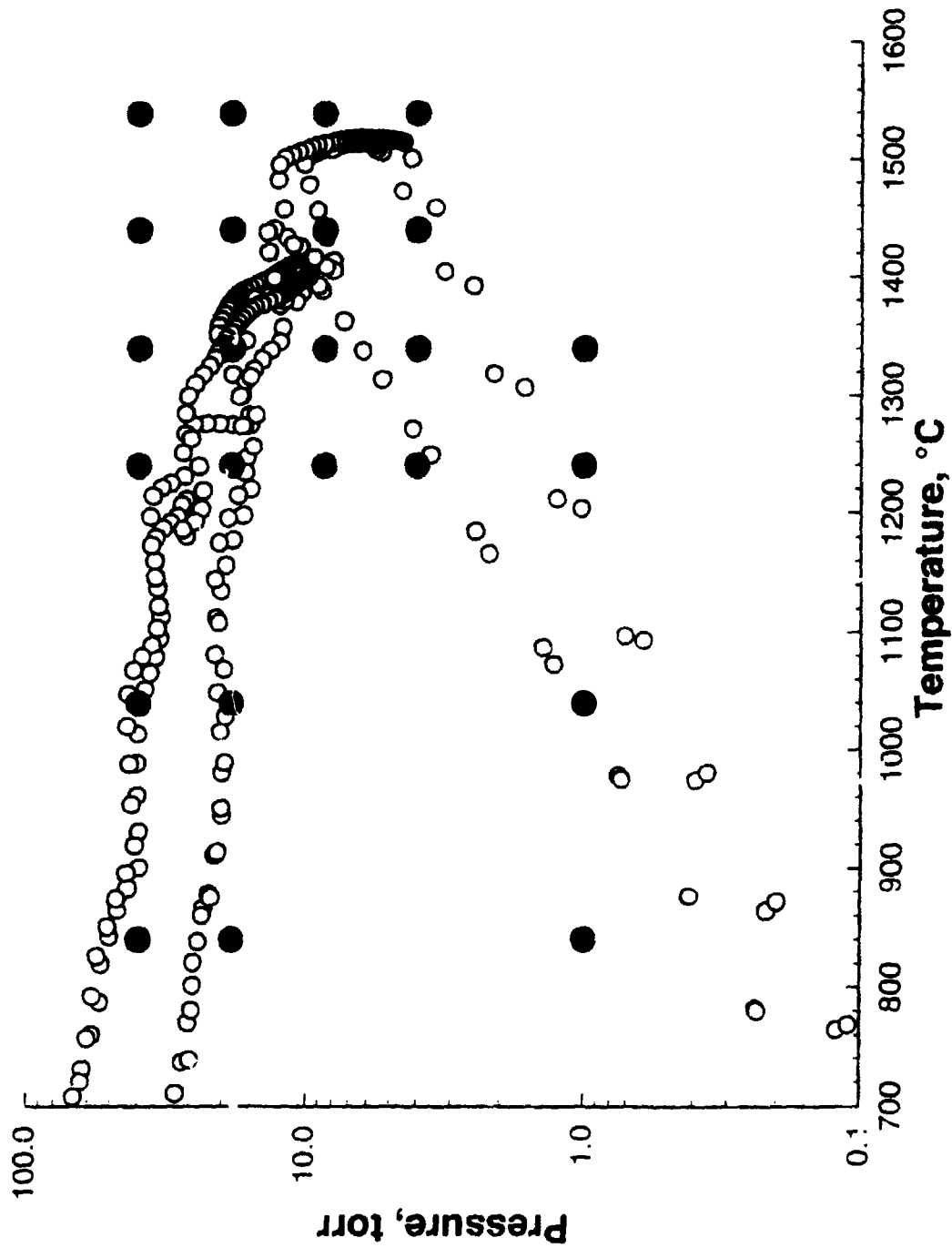


Fig 1

Compared Oxidation Behavior of the Same Panel(765) at Different Temperatures and Pressures

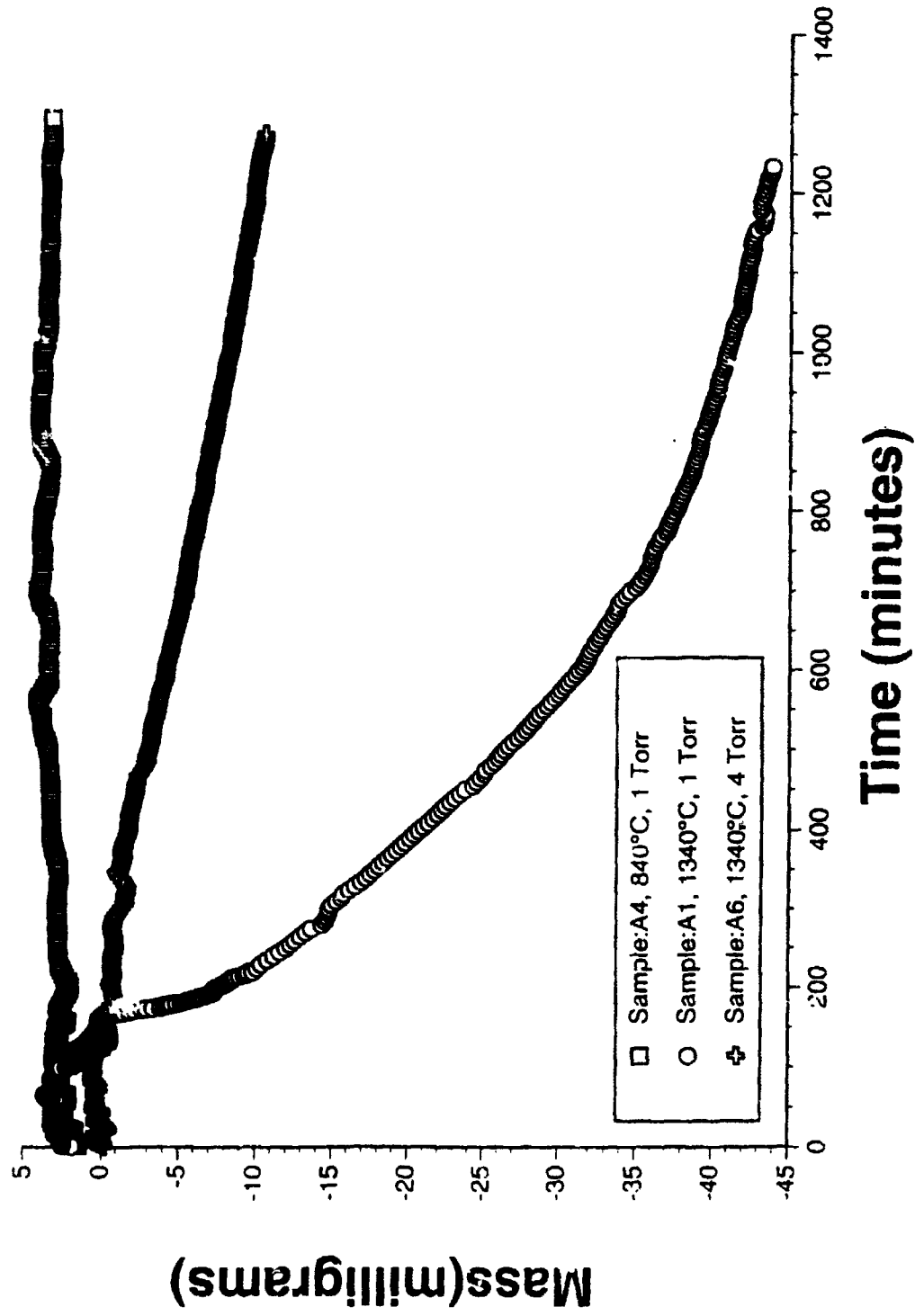


Fig. 2

Compared Plot of the Oxidation Behavior of the Three Panels at the Same Temperature and Pressure

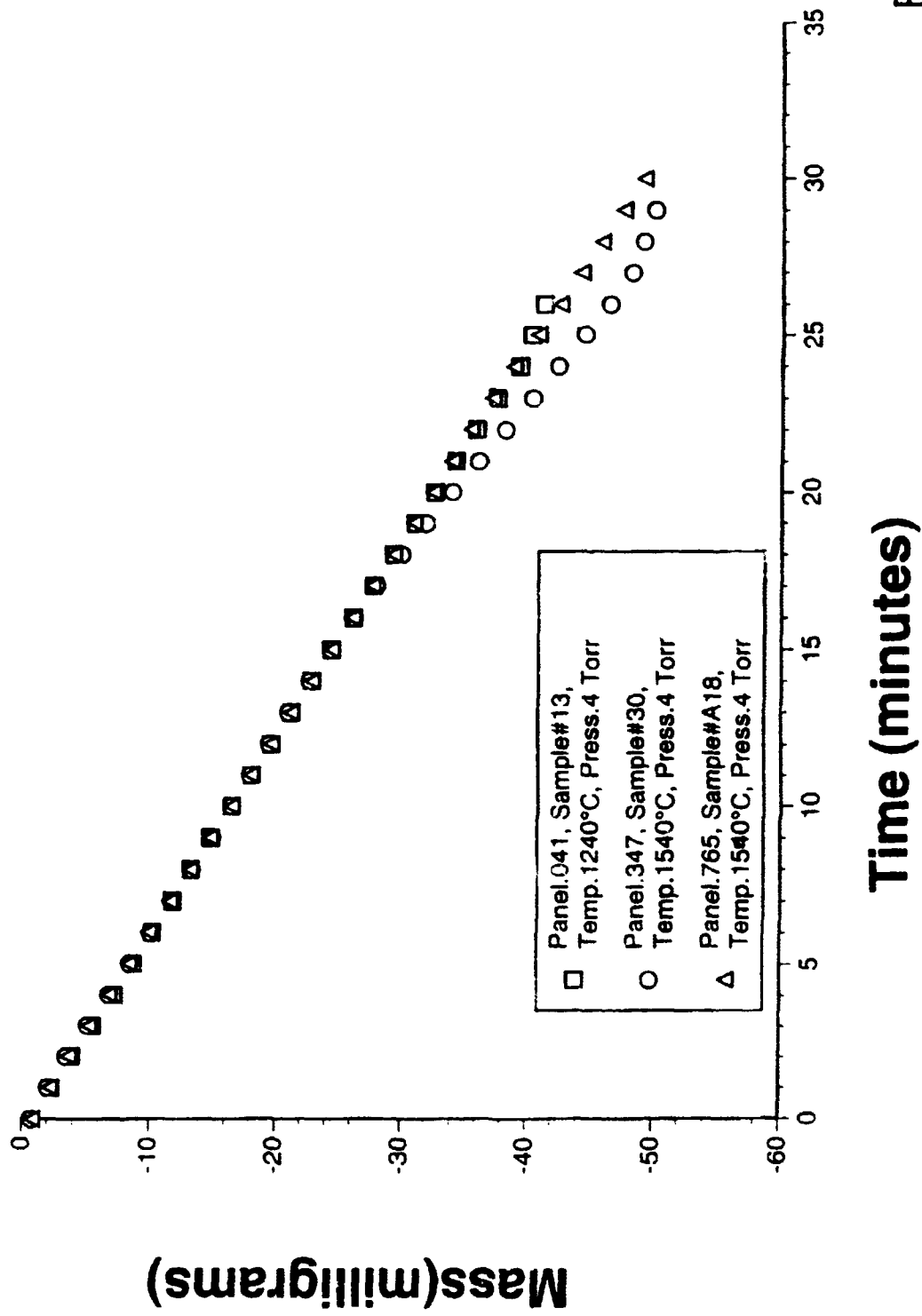


Fig. 3

Results & Conclusion

The Dupont coat proved to be a good protection for the SiC matrix at temperatures lower than 1240°C at low and high pressures (Table 1). On the other hand, at temperatures over 1340°C the Dupont coat did not seem to give good protection to the composite fiber and matrix (Table 1).

Sample	Temperature (°C)	Pressure (Torr)	Areal Mass Change Rate (g/m ² min)
765#A4	840	1	-0.0008
765#A15	840	18.6	-0.0004
765#A21	1040	1	0.0002
765#A23	1240	1	-0.0012
765#A25	1240	4	-0.0007
765#A1	1340	1	-0.0574
765#A6	1340	4	-0.0162
765#A20	1440	4	-0.4267
765#A18	1540	4	-3.5397

Table 1

The thickness of the Silicon Carbide coating might have been reduced during the heat up preparation process of the sample in an inert atmosphere. Because of the low pressures and high temperatures the Silicon Carbide may have encountered its phase change point from solid to gas. The heating process of the sample is not part of the desired environment to test the coat. Because the Silicon Carbide coating may have been lost before starting the test, these results may not be too reliable. It was suggested to repeat the tests at high temperatures by heating up the sample in an oxidizing environment to verify the above mentioned results. Even though some results of the tests have been discussed, because of time restraints, only a small portion of the desired tests could be completed. Therefore, no major conclusions or results about the effectiveness of the coat are available at this time.

References

- [1] John D. Buckley, D.D. Edie, *Carbon-Carbon Materials and Composites*, Langley Research Center Hampton, Virginia ,1992
- [2] F. Lamouroux, X. Bourrat, R. Naslain, J. Thebault, Silicon Carbide Infiltration of Porous CC Composite for Improving Oxidation resistance ,*Carbon*, Vol. 33 No.4 pp.525-535 ,1995
- [3] Wu Tsung-Ming, Wu Yung-Rong, Methodology in exploring the oxidation behavior of coated-carbon/carbon composites, *Journal of Materials Science* Vol.29 pp 1260-1264,1994
- [4] Charles M. Earnest, The Modern Thermogravimetric Approach to the Compositional Analysis of Materials, *American Society for Testing and Materials*, Philadelphia,1988,pp.1-18

**NEXT
DOCUMENT**

1-2/11
2/

Homepage for the Global Tropospheric Experiment
Eugene Ward
Jim Hoell
Atmospheric Sciences Division, Atmospheric Studies Branch

Abstract

The objective of my NASA summer research project was to create a homepage to describe and present results from the NASA Global Tropospheric Experiment (GTE). The GTE is a major component of NASA's Tropospheric Chemistry Program and is managed in the Atmospheric Studies Branch, Atmospheric Sciences Division at the NASA Langley Research Center.

In 1984, the National Academy of Sciences recommended initiation of a Global Tropospheric Chemistry Program (GTCP) in recognition of the central role of tropospheric chemistry in global change. Envisioned as the U.S. national component of an ultimately international research effort, the GTCP calls for the systematic study, supported by numerical modeling, of (1) biological sources of atmospheric chemicals; (2) global distributions and long-range transport of chemical species, and (3) reactions in the troposphere that lead to the conversion, redistribution, and removal of atmospheric chemicals.

These research challenges demand a broadly-based program to address them. The resources required are distributed among several federal agencies, scores of universities, and a variety of scientific disciplines -- including atmospheric science, biology, land processes, and oceanography. It was already clear in 1984 that the National Aeronautics and Space Administration (NASA) would play a leading role in such a program. Some GTCP objectives require large-scale field studies and the most advanced instrumentation. NASA brings together unique research facilities, strength in atmospheric science, and technical expertise needed to achieve those objectives.

NASA's contribution to GTCP is the Global Tropospheric Experiment (GTE), which utilizes large, extensively instrumented aircraft -- ideal platforms for many atmospheric chemistry experiments -- as primary research tools. However, GTE has also drawn heavily upon satellite observations of meteorology, land use, and atmospheric chemical species to aid experiment design and in the scientific analysis of results obtained from aircraft and ground-based measurements.

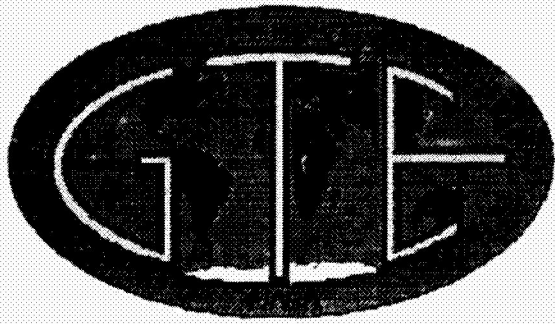
Understanding the chemical processes in the troposphere on a global scale is critical if we are to predict, and potentially ameliorate, harmful man-made changes to the global environment. The GTE was initiated as a series of global airborne measurement campaigns to address these issues. A series of rigorous airborne intercomparisons called the Chemical Instrumentation Test and Evaluation (CITE) experiments have evaluated our ability to measure critical tropospheric species, field studies known as Atmospheric Boundary Layer Experiment (ABLE) have studied major ecosystems that are known to exert a major influence on global chemistry and, in some cases, are undergoing profound changes, and the impact of long range transport of continental emissions, natural and anthropogenic, have been studied through focused missions such as the Transport and Chemistry near the Equator in the Atlantic (TRACE-A) experiments and Pacific Exploratory Missions (PEM) A and B.

The GTE group previously had a homepage located under the Atmospheric Sciences Division (ASD) of the NASA Langley homepage. My project for this summer was to revise the homepage into a more user-friendly homepage that directly addresses the importance of the experiment and perhaps more importantly provides direct access to results from the GTE missions.

The first step in my project was to design a preliminary outline of the homepage. The outline of the homepage consisted of the following: the main page, the three subpages and what each subpage would address, and the graphics that would go on each page. The first subpage on the homepage deals with the most frequently asked questions about GTE: "What is it?", "Why is it important?", "Where is it heading in the future?", etc. The second homepage addresses the origin and direction of the mission, as well as a brief overview of some of the missions, such as TRACE-A and PEM. The last subpage gives a more in-depth description of the GTE, along with a map that not only displays all of the past missions of the experiment, but also allows the user to link to other pages where data about the missions can be found. The user will be able to extract

the date from the files.

The GTE homepage will be online and available worldwide -- It is anticipated that there will be periodic updates to the homepage to include new missions as well as additional data from completed and future missions.



NASA Langley Research Center

Hampton, Virginia

Established in 1984

 [Frequently Asked Questions](#)

 [An Overview of the GTE](#)

 [In-depth Look at the GTE](#)



[NASA Home Page](#)



[LaRC Home Page](#)

Last Updated: Sun Jun 8 13:30:50 EDT 1995

Mail Questions/Comments to Dennis Owen (d.w.owen@larc.nasa.gov)



GTE's Frequently Asked Questions

Here are some of the most frequently asked questions by our users. Hopefully, you will be able to find the answers to all of your questions.

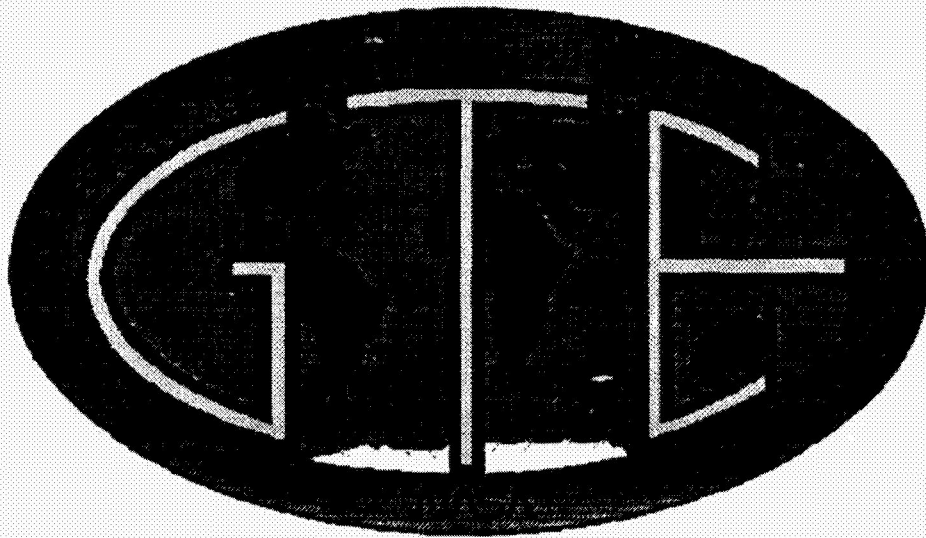
- **What is GTE?**
The Global Tropospheric Experiment (GTE) is a research program initiated by the National Aeronautics and Space Administration (NASA) designed to reveal the causes of atmospheric chemical change and to forecast their effects.
- **Why is GTE important?**
The GTE is critical in that it helps scientists develop an understanding of the chemical cycles that control the composition of the troposphere, mainly, the air we breathe.
- **What effects in the atmosphere are the GTE monitoring?**
There are three main effects that are being monitored by the GTE. They are:
(1) The biological sources of atmospheric chemicals,
(2) The global distribution and long-range transport of chemical species, and,
(3) The reactions in the troposphere that lead to the conversion, redistribution, and removal of atmospheric chemicals.
- **Where is the GTE heading in the future?**
NASA is currently in the process of planning two new missions in the GTE.
- **How can one learn more about the GTE?**
If you want to learn more about the GTE, feel free to click onto the e-mail address below.



Back to

[GTE's Home Page](#)

Mail Questions/Comments to Dennis Owen (dwowen@larc.nasa.gov)



The GTE is a large, multi-disciplinary program which is NASA's contribution to the National Academy of Sciences Global Tropospheric Chemistry Program. It is part of a comprehensive international research effort coordinated through the International Global Atmospheric Chemistry Program, which is a core project of the International Geospheric-Biospheric Program. The GTE program utilizes large, extensively instrumented aircraft as its primary research tools. However, the program also draws heavily upon satellite observations, meteorology, land use, and atmospheric chemical species to aid in experiment design and in the scientific analysis of results obtained from aircraft and ground-based measurements.

The greenhouse effect, acid rain, degradation of global air quality, and the tropospheric ozone depletion have all heightened worldwide awareness of the need for better understanding of the global troposphere. Projects carried out through GTE are responding to that need.

Such programs include CITE, ABLE, PEM, and TRACE.

The Chemical Instrumentation Test and Evaluation (CITE) projects were designed to foster the development of sensitive new instruments and techniques to detect and measure concentrations of tropospheric trace gases in the parts-per-trillion range and below.

The Atmospheric Boundary Layer Experiments (ABLE) employed instrumentation on ground, air and space platforms to more fully understand the chemistry and dynamics of the troposphere, in particular the interactions between the biosphere and the atmosphere.

The Pacific Exploratory Mission (PEM) West projects investigated the atmospheric chemistry of ozone and its precursors (NO_x, CO, methane, NMHC) over the western Pacific and the natural budgets of these species.

The Transport and Atmospheric Chemistry near the Equator - Atlantic (TRACE-A) expedition focused on understanding the seasonal enhancement in tropospheric ozone observed over the tropical south Atlantic Ocean.



Global Tropospheric Experiment

Established in 1984.

Wouldn't it be nice if every day the sky looked like the one in this picture. It looks very trusting, as if nothing were wrong. However, something is wrong with our atmosphere. The Global Tropospheric Experiment (GTE) was established to make sure that the air we breathe is still fit to live in. Read on for more details.

In 1984, the National Academy of Sciences recommended initiation of a Global Tropospheric Chemistry Program (GTCP) in recognition of the central role of tropospheric chemistry in global change. Envisioned as the U.S. national component of an ultimately international research effort, GTCP calls for the systematic study, supported by numerical modeling, of (1) biological sources of atmospheric chemicals; (2) global distributions and long-range transport of chemical species; and (3) reactions in the troposphere that lead to the conversion, redistribution, and removal of atmospheric chemicals. NASA's contribution to the GTCP is the Global Tropospheric Experiment (GTE), which utilizes large, extensively instrumented aircraft-ideal platforms for many atmospheric chemistry experiments-as primary research tools.

-
- **History**
 - **Map of Missions and Mission's Data**
-



Back to

[GTE's Home Page](#)

**NEXT
DOCUMENT**

**System Construction for the Measurement
of
Bragg Grating characteristics
in Optical Fibers**

Douglas P. West* and Dr. Robert S. Rogowski

**Non-Destructive Evaluation Sciences Branch
Fiber Optic Sensors Group
MS 231
NASA Langley Research Center
Hampton, VA 23681**

***Langley Aerospace Research Summer Scholar**

ABSTRACT

Bragg gratings are used to measure strain in optical fibers. To measure strain they are sometimes used as a smart structure. They must be characterized after they are written to determine their spectral response. This paper deals with the test setup to characterize Bragg grating spectral responses.

INTRODUCTION

Bragg gratings are a photo-induced phenomena in optical fibers. The gratings can be used to measure strain by measuring the shift in wavelength. These gratings have real world applications as shown by R. M. Measures et al., 1993. They placed the fibers into a smart structure to measure the stress and strain produced on support columns placed in bridges. As the cable is subjected to strain the grating causes a shift to a longer wavelength if the fiber is stretched and a shift to a shorter wavelength shift if the fiber is compacted. Our applications involve using the fibers to measure stress and strain on airborne systems.

There are many ways to write Bragg gratings into optical fibers. Our focus is on side writing the grating. Our capabilities are limited in the production rate of the gratings. C. G. Askins et al., 1994, was able to side write fibers using an on-line fiber draw, but we have to write the fiber one grating at a time since we do not have drawing capabilities. We are writing Bragg gratings into AT&T's "Accutether" 9% germania-doped optical fiber using the "Phase Mask" Method as described in Morey et al., 1994. When the Bragg grating is written into a fiber it becomes a permanent fixture. We are writing the grating to be centered at 1300 nm because that is the standard phase mask wavelength. The optimum wavelength for writing the fiber is at 240 nm. Since our laser has a wavelength of 266 nm, which is the fourth harmonic of a ND:Yag, we are loading the fiber with hydrogen to produce the effect necessary to write the grating

EXPERIMENTAL

The grating is written by passing an UV beam through a phase mask, which produces an interferometric pattern. Care must be taken to ensure complete stability of the fiber during the writing process. The writing of the grating is energy dependent. The laser we are writing with has an output of 10 mJ/pulse @ 10 Hz. (This correlates to 100 mW.) After the grating is written it must be characterized before use in a smart structure.

I developed software to interface with a Hewlett Packard 70951A Optical Spectrum Analyzer. I wrote programs in the "C" computer language to control the sampling rate and store the data in a user named file for further data presentation. I connected all the equipment together and built a cable for serial port communication from the Apple computers. Qudus Olaniran was my technical advisor for problems I had with program development and Mark Froggatt was my direct research supervisor.

The programs written transferred data back and forth over a serial port, through a National Instruments RS-232 - GPIB converter and to the spectrum analyzer. The serial port communication code was already written by Qudus for another purpose and needed minor changes. The main development of the software was in the controlling of the spectrum analyzer and the storage of the received data.

The first code written was a complete measurement response data collection package. This code was written in "C" language using a development package named "Think C v5.0" by Symantec. These programs were developed using a PowerBook 520c as the controlling device to give the spectrum analyzer complete portability. After that was accomplished I offered the ability of controlling the sampling rate, thereby speeding up the data collection process.

The next batch of programs controlled the output of a National Instruments Digital to Analog converter card to drive a laser thermally. This application also measured the response of a fiber and stored the data in a user named file. This code was also written in "C" language, but the development package was changed to "Code Warrior" and the computer was changed to a PowerMac 8100 AV model.

EQUIPMENT SETUP

National Instruments GPIB - 232CV

The National Instruments GPIB - 232CV is a device that allows connection of a device with a RS-232 port to a GPIB bus. It allows "transparent" conversion of data between the two ports - meaning that control codes aren't necessary to inform the converter to do what it was designed to do. The set up codes for the National Instruments converter are set internally using dip switches. The switches are set up for the following data transfer.

Internal settings of the dip switches

1 = on 0 = off

U22 10110111 - C mode, CR termination, address 23

U20 01001101 - Xon/Xoff protocol disabled, 8 bits/character, 1 stop bit,
parity checking disabled, 9600 baud

In C mode operation the GPIB - 232CV operates as a controller. It asserts an *IFC (interface clear) for 500µsec when the device is powered up. This initializes the bus and makes the converter the controller. It is important that all equipment connected to the bus is on and initialized before the converter is powered up, otherwise it will interfere with the initialization procedures.

The information sent to the GPIB - 232CV from the serial port is buffered until the device on the GPIB is ready to receive data. After the device on the GPIB has completed the instructions it sends a data ready signal back to the converter. The converter receives the data and transmits the data back to the computer, the information isn't buffered before being sent to the device on the serial port.

Our converter is set up to terminate in carriage return. This allows us to send the character "\n", in "C", to tell the converter it needs to change from listen mode to talk mode so information can be transferred from the device on the GPIB to the serial port. The converter will stay in the talk mode until a character is received on the serial port from the computer. At this time the converter changes to listen so instructions can be sent to the receiving device.

The address is set to 23 because that is the address of the Hewlett Packard Optical Spectrum Analyzer.

The converter transmits data in 8 bit words with 1 stop bit, at 9600 baud.

National Instruments NB-MIO-16XH Interface Board
pn 180675-11 Rev. C

The National Instruments NB-MIO-16X Interface Board is a multifunction control board. It can be used to control analog, digital, and timing input/output operations. Analog to digital conversions, control of test equipment, and analysis of incoming signals are also possible. We used it to drive the laser temperature set-point control to +/- 500mV, and to +/- 750mV and to control the timing of the data accumulation.

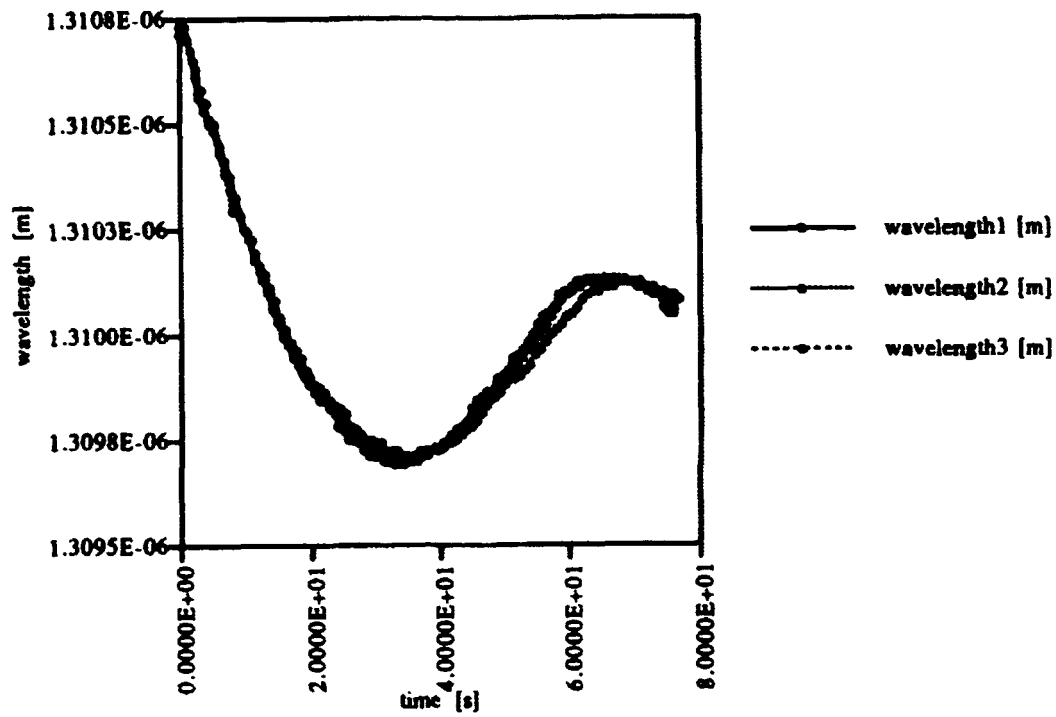
ACKNOWLEDGMENTS

I would like to thank the following people for their contributions. Mark Froggatt for the mentorship and the precise outlay of project goals and direction, Qudus Olinaran for his expertise in programming, Nurul Abedin for the optical theory discussions and technical writing assistance, John Deaton for the diagrams on writing Bragg gratings.

REFERENCES

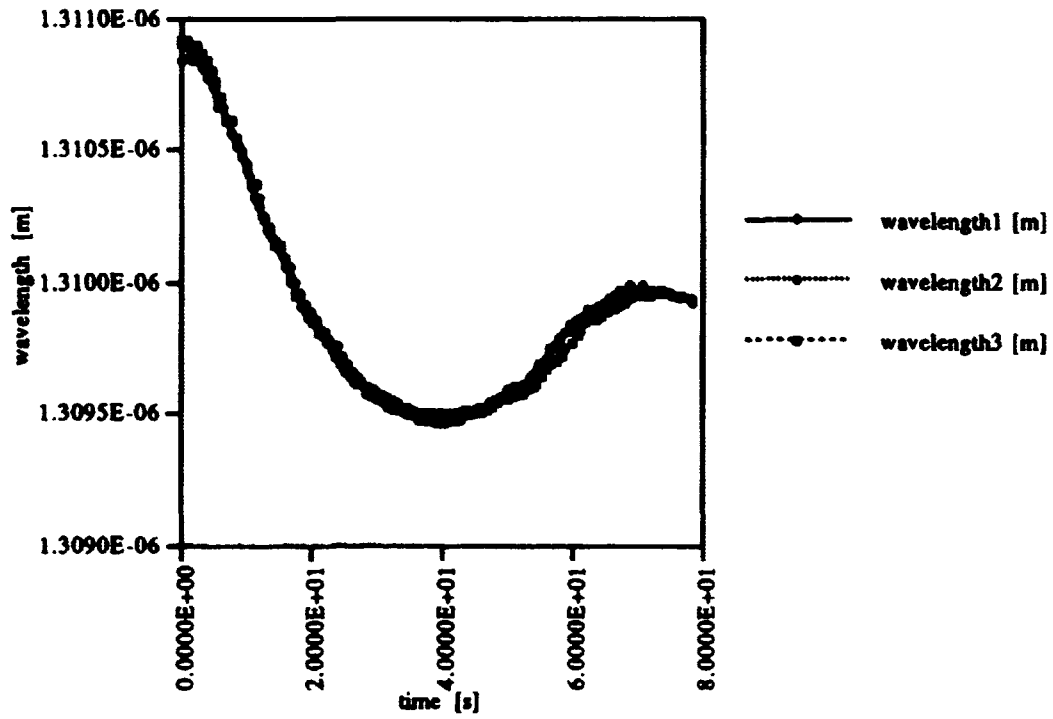
1. C.G. Akins, G.M. Williams, and E.J. Freible, "Contiguous Fiber Bragg Grating Arrays Produced On-Line During Fiber Draw", SPIE Proceedings - Smart Sensing, Processing, and Instrumentation, 14 - 16 Feb. 1994, Orlando Fla.
2. William W. Morey, Gary A. Ball, and Gerald Meltz, "Photoinduced Bragg Gratings in Optical Fibers", Optics and Photonics News, Feb. 1994.

500mV Thermal Set Point



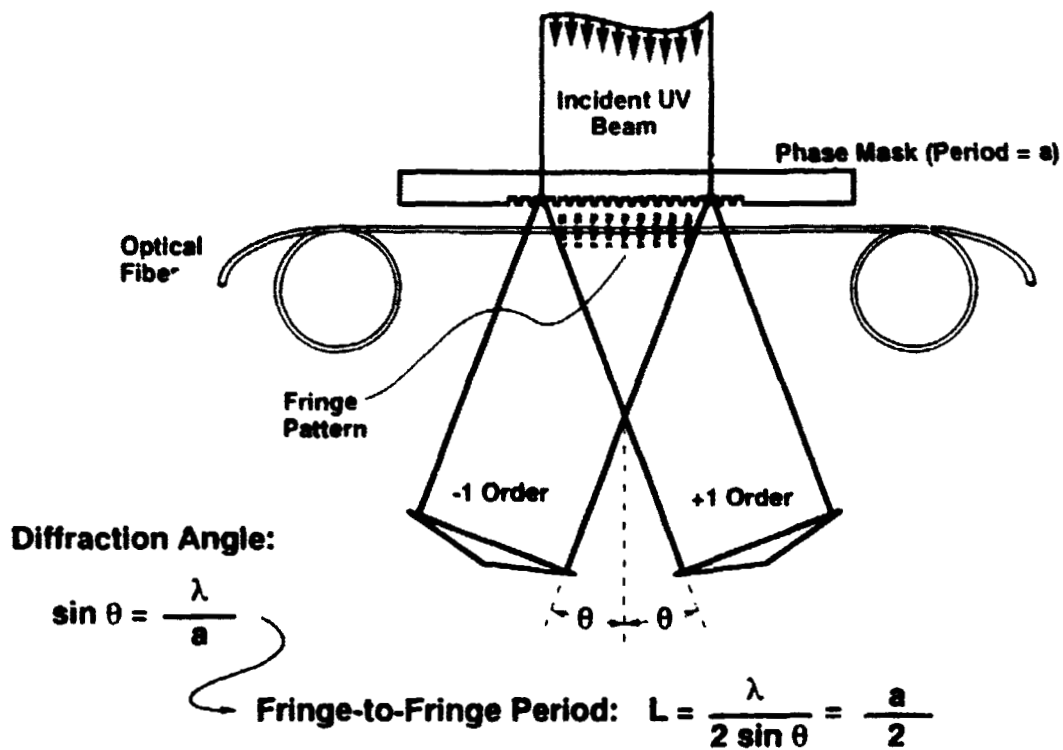
Calibration curve for the determination that a two second data accumulation time will be used using a 500mV thermal set point.

750mV Thermal Set Point

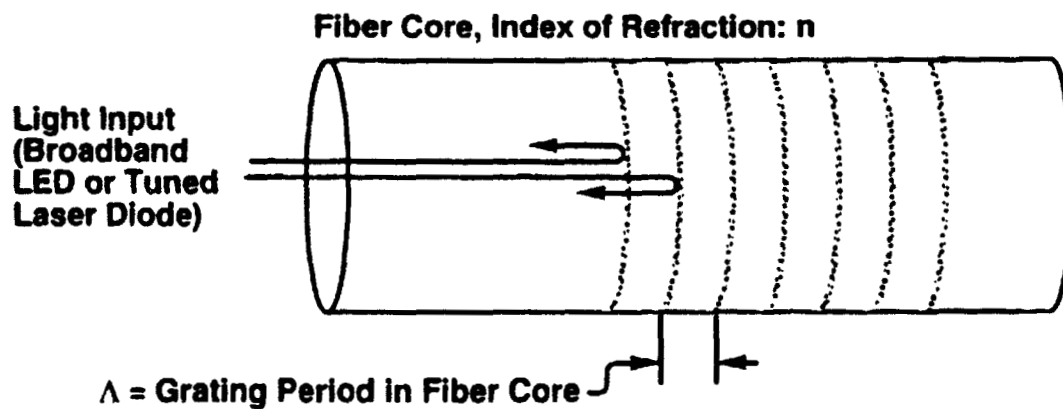


Calibration curve for the determination that a two second data accumulation time will be used using a 750mV thermal set point. Notice the non-linear response at the start of the signal accumulation. The actual linearity will be accumulated after a few milliseconds.

Writing Gratings in Optical Fibers with a Phase Mask



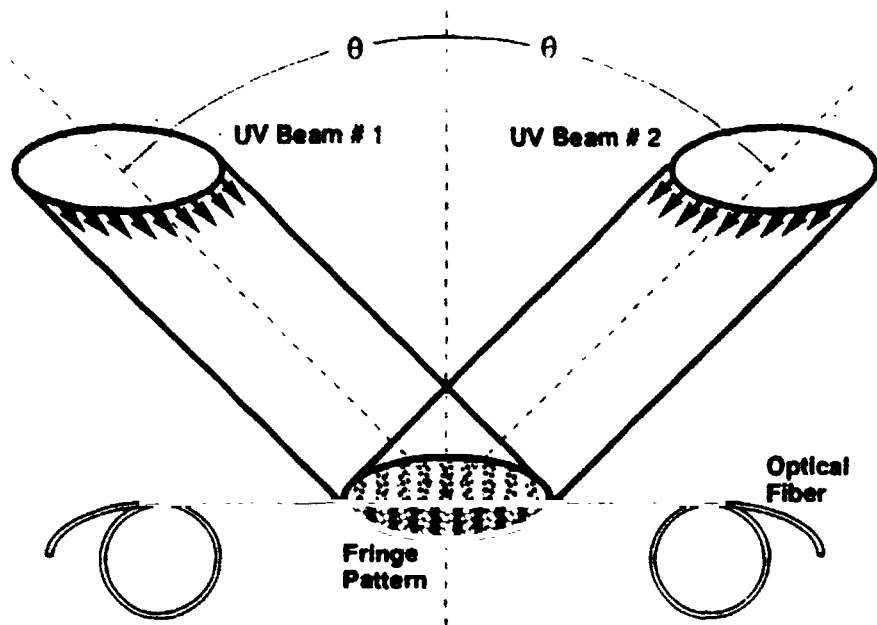
The Bragg Condition for an Intra-Core Fiber Grating



$2n\Lambda$ = Optical path difference between light 'reflected' from adjacent 'lines' in the intra-core grating

The Bragg wavelength of the reflected signal: $\lambda_B = 2n\Lambda$

Bragg Gratings in Optical Fibers: Two Beam Interference



Fringe-to-Fringe Period: $L = \frac{\lambda}{2 \sin \theta} = \Lambda$

To Write a Grating at a Particular Bragg Wavelength

Phase Mask Method

$$a = \frac{\lambda_B}{n}$$

Holographic Method

$$\theta = \text{Sin}^{-1} \left[\frac{n\lambda_W}{\lambda_B} \right]$$

**NEXT
DOCUMENT**

**Analysis of a High-Lift Multi-Element Airfoil
Using a Navier-Stokes Code**

**1995 LARSS Program Participant:
Mark E. Whitlock**

**Mentor:
Kenneth M. Jones**

**NASA Langley Research Center
Research and Technology Group
Aerodynamics Division
Subsonic Aerodynamics Branch**

ABSTRACT

A thin-layer Navier-Stokes code, CFL3D, was utilized to compute the flow over a high-lift multi-element airfoil. This study was conducted to improve the prediction of high-lift flowfields using various turbulence models and improved gridding techniques. An overset Chimera grid system is used to model the three element airfoil geometry. The effects of wind tunnel wall modeling, changes to the grid density and distribution, and embedded grids are discussed. Computed pressure and lift coefficients using Spalart-Allmaras, Baldwin-Barth, and Menter's $\kappa\text{-}\omega$ SST turbulence models are compared with experimental data. The ability of CFL3D to predict the effects on lift coefficient due to changes in Reynolds number changes is also discussed.

INTRODUCTION

Improving the cruise and high-lift efficiency of commercial subsonic transports has received increased attention in recent years. Current wing designs produce higher cruise lift coefficients than those of years past. The higher lift coefficients reduce the wing area required at cruise conditions. At the present time however, takeoff and landing requirements dictate the wing area of a commercial aircraft. This is in part due to inefficiencies in the high-lift systems. More efficient high-lift system designs will allow trade studies to be performed to improve the overall aircraft system. One such tradeoff is to reduce the size of the wing (and possibly reduce the cost of the aircraft).

Researchers are currently investigating ways to use computational fluid dynamics (CFD) to improve the aerodynamic performance of three dimensional (3D) high-lift systems. This task is very complicated, largely due to complex flow physics and grid generation issues. Many of the issues in 3D grid generation also exist in 2D. The time required to create a 2D grid and perform multiple analyses, however, is much less than that for a 3D grid. Many researchers, therefore, are studying 2D geometries to gain insight into the complex fluid physics of high-lift flowfields that will in turn help the understanding of 3D high-lift systems.

The geometry used for this study is a three element airfoil (slat, main element, and flap) that was designed by Douglas Aircraft. The geometry was sent to several universities, aerospace corporations, and NASA centers as part of the NASA High-Lift CFD Challenge Workshop in 1993. The purpose of the CFD Challenge was to define the state-of-the-art in 2D multi-element airfoil prediction codes. This optimized airfoil and its extensive experimental aerodynamic database is currently being used throughout the aerospace industry as a means of calibrating CFD codes. The experimental database includes forces, skin friction distributions, and velocity and total pressure profiles for two geometries at Reynolds numbers of 5 and 9 million. The task assigned for the summer was to investigate methods to improve the correlation between the experimental data and computational results. These methods include wind tunnel wall modeling, selection of turbulence models, and improving the grids which define the airfoil geometry.

APPROACH

Several key issues were investigated in an attempt to more accurately predict the flow over the Douglas airfoil. Building on the work of Ken Jones and others at the CFD Challenge, three key issues were investigated to improve the flow solution for the Douglas airfoil. Research conducted by H.V. Cao¹, et al., of the Boeing Company indicates that the wind tunnel walls have to be modeled in order to make an accurate comparison between the computational results and the experimental data. One task for the summer was improve the wind tunnel wall modeling and to correct the implementation of the tunnel boundary conditions. A second task for the summer was to improve on the existing grid that was used during last summer's analysis. This study investigated improvements in the Chimera grid cutouts, embedded grids, and the effect of grid density on the flow solution. A third task was to investigate the effects of turbulence models on the flow solution. The Spalart-Allmaras, Baldwin-Barth, and Menter's κ - ω SST turbulence models were used for this investigation. Finally, CFL3D's ability to predict changes in lift coefficient due to Reynolds number changes was investigated.

The high-lift geometry was modeled using a gridding technique known as overlapped or Chimera gridding. For the Chimera gridding scheme, the overlapped grids are each created independently. MAGGIE cuts holes in the individual grids along user defined boundaries so that no grids overlap the airfoil surfaces. The final grids used for this analysis are shown in Figure 1 (for clarity only every other grid point is shown). A total of six grids were used: a tunnel grid, main element grid, slat grid, flap grid, flap trailing edge grid, and cove grid. MAGGIE then creates interpolation stencils which the flow solver, CFL3D, uses to pass information between grids. One benefit of the Chimera gridding is that the individual grid blocks are created

independently, so a change in flap location or rotation for example will not effect the design of the individual grid blocks. It will only effect the hole cutout and interpolation stencils. These grids are then analyzed using the Reynolds-averaged Navier-Stokes code, CFL3D. CFL3D solves the 3D, compressible Navier-Stokes equations using thin-layer approximations. To accelerate convergence, the code uses multi-gridding and local time-stepping techniques.

The approach used for this research involved first determining what improvements could be made in the flow solutions in light of work presented at the 13th AIAA Applied Aerodynamics Conference.² The procedure used involved first making modifications to the grids used or flow solver input files, and then running these grids through the flow solver CFL3D. Unless otherwise specified, all runs in this study were computed at the following conditions: $\alpha = 16.02^\circ$, $Re = 9 \times 10^6$, $M_\infty = 0.2$. Also, unless stated otherwise, all solutions were obtained using the Spalart-Allmaras turbulence model. Only one change was made to the grids at a time. This allowed the results to be compared to past solutions and determine what the effect of each change was. This approach allowed a better understanding of the effects of different grids and of the fluid physics around the airfoil.

LANGLEY RESEARCH CENTER EQUIPMENT AND FACILITIES USED

This project required the use of several computer systems at Langley. Grid generation and post-processing was done on a Silicon Graphics IRIS 4D25 workstation. Complex calculations, including running the flow solver and grid adaptation, were performed on Sabre, a Cray YMP located at the NASA Langley Research Center. Storage of the input files and flow solutions were made possible through the Mass Storage Subsystem on Sabre. All experimental results were provided by a wind tunnel test conducted in Langley's Low Turbulence Pressure Tunnel (LTPT).

RESULTS

Wind Tunnel Walls

It is believed that the wind tunnel wall corrections currently used in the LTPT may become inaccurate at high lift coefficients, particularly near maximum lift. Therefore, the best way to calibrate a code with this dataset is to use experimental data which has not been corrected for wall interference or tunnel blockage effects and model the wind tunnel walls. Care must be taken when modeling the wind tunnel, however, to properly set the tunnel boundary conditions to those used in the LTPT. Two changes were made to the tunnel modeling from last summer. First, the tunnel inlet plane was extended further upstream. And second, the tunnel back pressure was adjusted to more accurately match LTPT reference conditions.

The first change made on last summer's tunnel grid was to extend the inlet plane further upstream. The inlet from last summer's grid was approximately four chords upstream of the model leading edge¹. Cao demonstrated that the inlet for the tunnel is best if extended at least five chords upstream of the leading edge. If the inlet is closer to the leading edge, the constant Mach number boundary conditions set on the inlet plane will over-constrain the solution. To correct this problem, two grid changes were made. The first extended the tunnel out to six chords upstream of the leading edge (Figure 1d), and the second to eight chords. It was found that by extending the inlet to six chords dropped the lift coefficient by approximately 0.013. Extending the inlet to eight chords produced only negligible changes in the lift coefficient. This seems to confirm Cao's results and indicates that the tunnel inlet should be at least five chords upstream of the model leading edge for accurate computations. The remainder of this study was completed with the six chord tunnel grid.

The second change made in modeling the wind tunnel was a change in the tunnel exit boundary condition. Last summer the back pressure was computed using the isentropic flow equations and assuming an isentropic expansion through the diffuser. It was found, however, that this is not the method used to set the LTPT reference conditions. The LTPT flow conditions are set using static and total pressures at tunnel station -64.0 (which is approximately 53 inches upstream of the slat). The tunnel conditions are adjusted until the pressures at this tunnel station match those from an empty tunnel calibration. It was found that the back pressure calculated from the isentropic expansion did not yield pressures at station -64.0 which match the calibration curve. Thus, the tunnel back pressure was increased until the static and dynamic pressures matched the reference conditions used for the LTPT data. It is still unclear why the back pressure calculated by the isentropic expansion formula did not match the back pressure required to match the reference conditions at station -64.0. Using the correct back-pressure, however, resulted in a decrease in the lift coefficient of nearly 0.03.

Grid Improvements

The second task was to make improvements to the grids used to model the multi-element airfoil geometry. Five studies were completed in an attempt to more accurately match the experimental data. The first study resulted in an improved flap grid. Second, the main element and cove grids were modified to better resolve the flow over the flap. A grid resolution study was performed on this new grid. Finally, an embedded grid was used in an attempt to better resolve the off-body flowfield above the flap.

The first improvement made to the grid from last summer was on the flap grid. The flap grid used last summer extended approximately one flap chord in all directions from the flap surface.² The grid spacing near the flap grid boundary was very sparse. Not only were the sparse grid points far from the surface of the grid a waste of points, but the grid may have added a form of dissipation to the flap flowfield. To remedy the situation, the flap grid was cut to approximately 0.2 flap chords from the surface of the flap (Figure 1b). Cutting the outer boundary of the flap grid resulted in a negligible change in forces or pressure distributions on the airfoil.

The second major change made to the grid was to add more grid points above the flap on the main element and cove grids. Work by Rogers³ demonstrated how very complex the flowfield above the flap can be, especially at high angles of attack. There was concern that the grid used last summer was too sparse in the streamwise direction on the main element to resolve this complex flowfield. To remedy this situation, approximately twenty points were added in the streamwise direction to the main element grid. Due to temporary problems with the patching routines in CFL3D, the cove grid had to have an equal number of points added in the streamwise direction to maintain a one-to-one matching along the grid boundary. Adding these points to the main element and cove grids increased the time required to obtain a converged solution. More importantly, however, a comparison of surface pressures demonstrated that the new grids improved the ability of the code to capture the flow physics.

In an attempt to decrease the time required to generate a flow solution, a normal direction grid resolution study was performed on the main element and slat. Last summer the main element and slat grids were doubled in points in the normal direction to better resolve the slat wake over the main element. It was believed that after a solution adaptation was done to the main element grid in the slat region this grid doubling became unnecessary. Thus to increase convergence rates the main element was reduced from 161 points in the normal direction to 117 points. The points were removed from near the surface of the airfoil while maintaining y^+ values of less than 1.0. Removing these points resulted in only minimal change to the flow solution. Similarly, every other point in the normal direction of the slat was removed, reducing the size of the slat grid from 145 to 73 normal points with an even smaller change in the flow solution. By reducing the grid sizes in the normal direction about 30,000 grid points were removed resulting in decreased computer resource requirements with minimal changes in the flow solution. A plot of the pressure distributions over the airfoil is shown in Figure 2. Note that there is excellent agreement between

the experimental and computational pressure profiles over the main element and slat. The flap, however, shows a leveling off of the pressure profile indicative of separation which the experimental data does not support. It is not known whether this separation on the flap is due to the grids or turbulence model.

The experimental flowfield data for the Douglas airfoil indicates that near the maximum lift coefficient there is a region of off-body separation above the flap.⁴ The new main element grid greatly improved the ability of CFL3D to resolve this flowfield but as shown in Figure 2, the flap pressures do not closely match the experimental values. An embedded grid was placed above the flap to try and correct the flap pressure distributions. For the 16° and 21° angle of attack cases the embedded grid made very minor changes to the pressure distributions over the airfoils. A successful solution was not obtained with the embedded grid on the airfoil at 8° angle of attack.

Turbulence Models

High-lift, multi-element flowfields are dominated by viscous phenomena. Computational studies have shown that the choice of turbulence model can have a large effect on pressure contours, velocity profiles, and overall forces. Studies completed by Rogers^{3,5} and others have shown the Baldwin-Barth (BB) and Menter's $\kappa\text{-}\omega$ SST (SST) turbulence models often are more accurate at modeling the turbulence found in high-lift flowfields than the Spalart-Allmaras (SA) turbulence model. To determine the effect of turbulence models on lift coefficient a turbulence model study was performed using the SA, BB, and SST turbulence models at Reynolds numbers of 5 and 9 million. Figure 3 shows the lift coefficient versus angle of attack for the three turbulence models at these Reynolds numbers. Note that the Spalart-Allmaras turbulence model yields a lift coefficient which is significantly higher than the experimental values at all angles of attack. The Baldwin-Barth and SST turbulence models produce lift coefficients which agree very well with experimental values at 16° and 21° angle of attack. The BB and SST models, however, do not agree well with experimental values at 8° angle of attack. One possible explanation for this can lie in the fact that the experimental data shows the trailing edge of the flap to be separated at 8° angle of attack. If the grid or the turbulence model do not allow separation to be accurately predicted, then this could result in the overpredicted lift values. This has not yet been looked at and should be investigated further.

Reynolds Number Effects

One goal of the CFD Challenge was to be able to predict changes in lift coefficient due to changes in Reynolds number. The experimental database contained results at Reynolds numbers of 5 and 9 million.⁴ Figure 4 shows the increment in lift coefficient caused by changing from a Reynolds number of 5 million to a Reynolds number of 9 million. Note that CFL3D matches the data fairly well at 8° and 16° angle of attack, but not at 21° angle of attack. At 21° angle of attack, the experimental data suggest that there is off-body separation above the flap. This separation is stronger at a Reynolds number of 5 million. One possible cause of the poor Reynolds number predictive capability at 21° then could be that the grids or solver do not allow the off-body separation to be modeled accurately. This should be investigated further to improve the predictive capability of CFL3D.

CONCLUSIONS

A computational study was performed to improve the predictive capability of a Navier-Stokes code for high-lift flowfields. It was determined that the wind tunnel wall should extend at least

five chords upstream of the model for accurate computations. Furthermore, the exit back pressure must be set to match the tunnel reference conditions at station -64.0, as is done in the LTPT. As shown in this study, for situations where standard wind tunnel wall corrections are inaccurate, it is important to correctly model the wind tunnel walls when analyzing the configuration.

Several improvements were made to the gridding system. The flap grid outer boundary was moved closer to the flap surface. Additional points were added in the streamwise direction to the main element above the flap and improved the ability to capture the complex flow physics. The main element and slat grids were reduced in points in the normal direction. This decreased the required computer resources with little effect on the flow solution. An embedded grid was added above the flap but produced little change in the surface pressures.

The choice of turbulence model was also found to have a large effect on the final flow solution. This study indicated that overall the Baldwin-Barth and Menter's κ - ω SST turbulence models are more accurate than Spalart-Allmaras for the high-lift flowfield investigated. CFL3D was able to closely predict the effect of a change in Reynolds number on lift coefficient at low angles of attack. Near maximum lift, this predictive capability diminished.

REFERENCES

- [1] Cao, H.V., Fujisunose, K., Spalart, P.R., Ishimitsu, K.K., Rogers, S.E., McGhee, R.J., "Study of Wind Tunnel Wall Interference for Multi-Element Airfoils Using a Navier-Stokes Code", AIAA-94-1993, 1994.
- [2] Jones, K.M., Biedron, R.T., Whitlock, M.E., "Application of a Navier-Stokes Solver to the Analysis of Multielement Airfoils and Wings Using Multizonal Grid Techniques", AIAA 95-1855, 1995.
- [3] Rogers, S.E., "Progress in High-Lift Aerodynamic Calculations," *Journal of Aircraft*, Vol. 31, No. 6, P1244-1251, Nov.-Dec. 1994.
- [4] Chin, V., Peters, D., Spaid, F., and McGhee, R., "Flowfield Measurements about a Multi-Element Airfoil at High Reynolds Numbers," AIAA Paper 93-3137, July, 1993.
- [5] Rogers, S.E., Menter, F.R., Durbin, P.A., Mansour, N.N., "A Comparison of Turbulence Models in Computing Multi-Element Airfoil Flows", AIAA-94-0291, 1994.

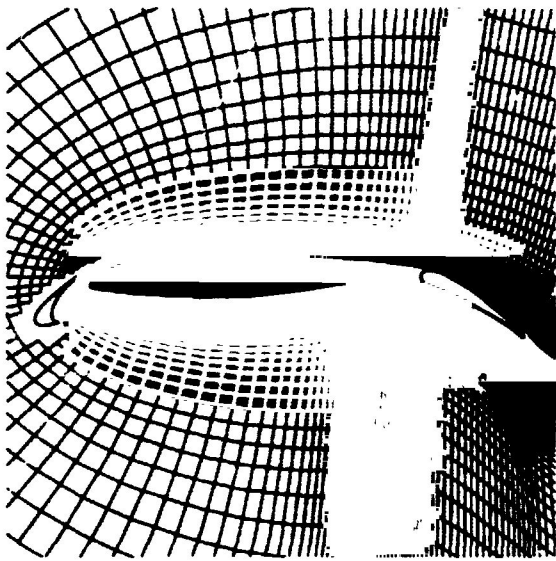


Fig. 1a. 3 element airfoil main element grid

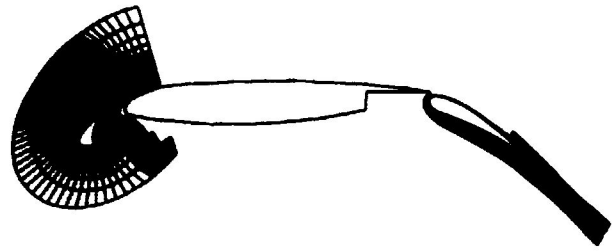


Fig. 1b. 3 element airfoil slat, flap, and flap trailing edge grids



Fig. 1c. 3 element airfoil cove grid

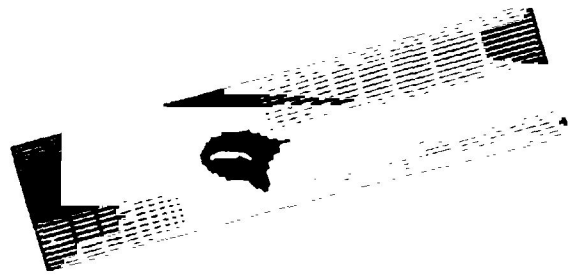


Fig. 1d. Tunnel grid

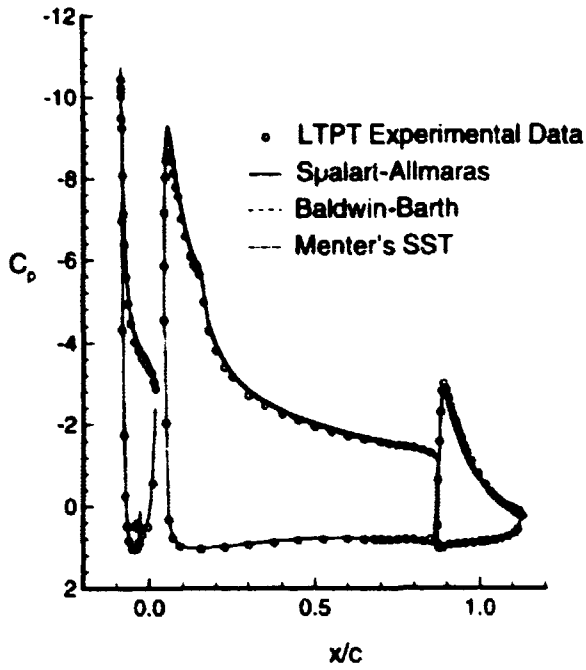


Fig. 2a. Pressure distribution, $\alpha = 16^\circ$,
 $M = 0.2$, $R_e = 9 \times 10^6$

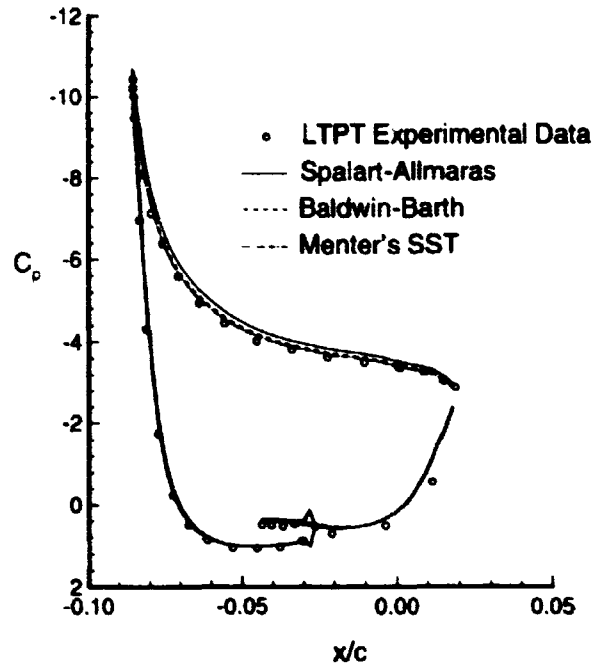


Fig. 2b. Slat pressure distribution, $\alpha = 16^\circ$,
 $M = 0.2$, $R_e = 9 \times 10^6$

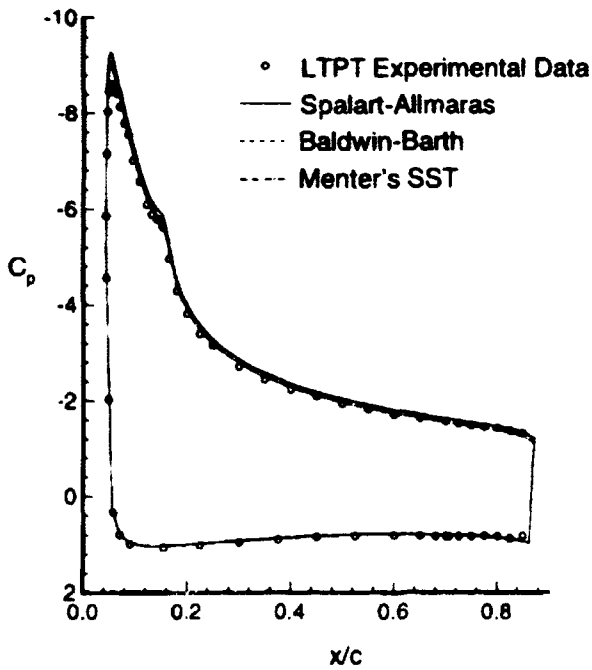


Fig. 2c. Main element pressure distribution,
 $\alpha = 16^\circ$, $M = 0.2$, $R_e = 9 \times 10^6$

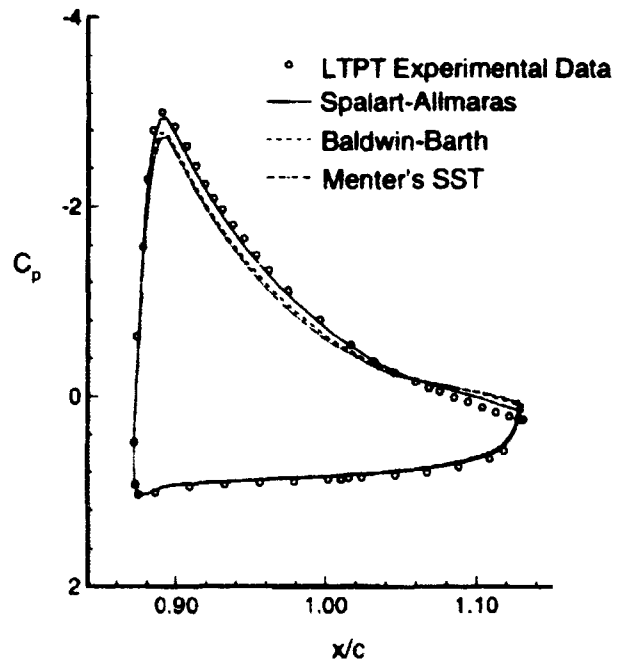


Fig. 2d. Flap pressure distribution, $\alpha = 16^\circ$,
 $M = 0.2$, $R_e = 9 \times 10^6$

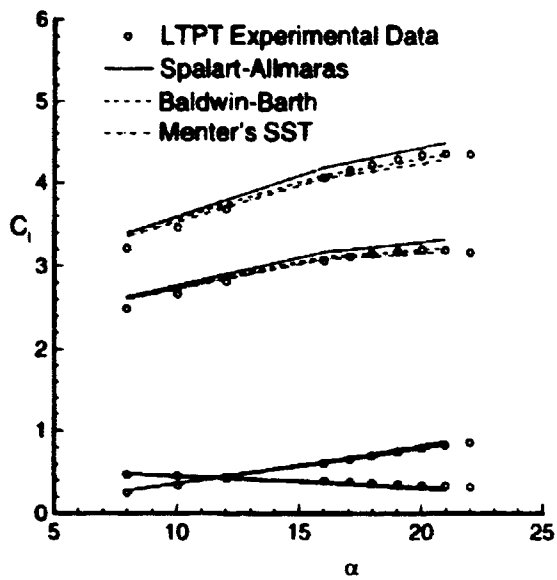


Fig. 3a. Lift curve, $M = 0.2$, $R_e = 9 \times 10^6$

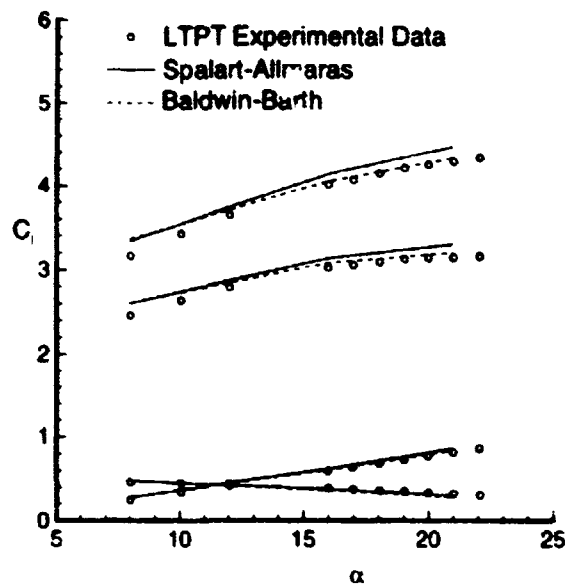


Fig. 3b. Lift curve, $M = 0.2$, $R_e = 5 \times 10^6$

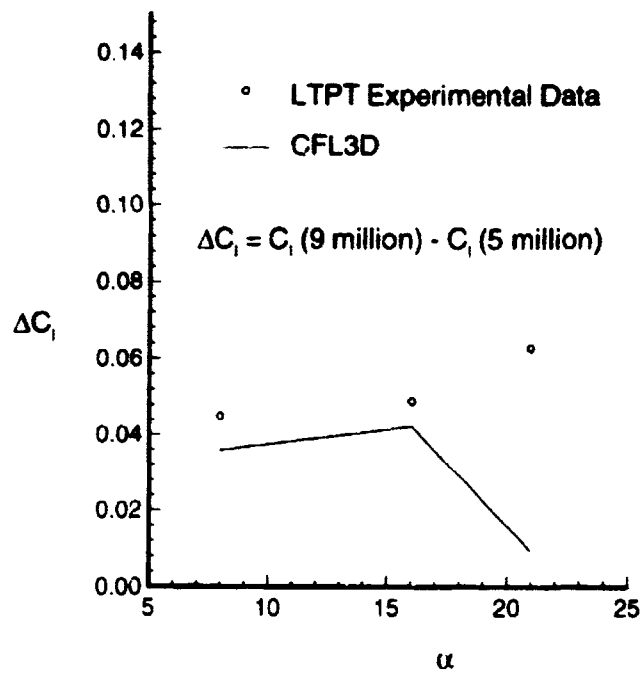


Fig. 4. ΔC_l vs. α for different Reynolds numbers

**NEXT
DOCUMENT**



Wake Vortex Encounter Research

Jeffrey M. Wilson
The University of Kansas
Langley Aerospace Researchers Summer Scholar

Robert A. Stuever
NASA Langley Research Center
Hampton, VA

Research and Technology Group
Flight Dynamics and Control Division
Vehicle Dynamics Branch

Abstract

The National Aeronautics and Space Administration (NASA) is conducting research to improve airport capacity by reducing the separation distance between aircraft. The limiting factor in reducing separation distances and improving airport capacity is the wake vortex hazard. The ability to accurately model wake vortices and predict the outcome of a vortex encounter is critical in developing a system to safely improve airport capacity. This is the focus of the wake vortex research being done at NASA Langley Research Center (LaRC). This paper will concentrate on two topics. The first topic is the control system developed for the Boeing 737 freeflight model in support of vortex encounter tests to be conducted in the 30- by 60- foot tunnel at NASA Langley Research Center later this year. The second topic discussed is the limited degree of freedom (DOF) trajectory generation study that is being conducted to determine the relative severity of a multitude of paths through a wake vortex.

Introduction

While the number of aircraft in the world fleet is projected to more than double by the year 2015, many of the world's major airports are already capacity limited.⁽¹⁾ The National Aeronautics and Space Administration (NASA) is currently conducting research to enable safe improvements in the capacity of the nation's air transportation system. One part of the NASA research program is the Terminal Area Productivity (TAP) Program. This program is responsible for conducting the necessary research to support the Federal Aviation Administration (FAA) and the aviation industry in safely achieving fair weather airport capacity in instrument meteorological conditions. The TAP Program is subdivided into four elements: Air Traffic Management, Aircraft-Air Traffic Control Systems Integration, Low-Visibility Landing, and Reduced Spacing Operations.

The Reduced Spacing Operations element is responsible for conducting research on reducing the in-trail spacing distance between airplanes. Improvements in landing frequency by reducing in-trail spacing distances have the potential to increase system capacity by 10-15%.⁽²⁾ The limiting factor in reducing the spacing distances is the wake turbulence phenomena. The wake of an aircraft is characterized by two counter-rotating vortices that are spaced at a distance of slightly less than the aircraft span. Another aircraft encountering one of these vortices could either be mildly perturbed or catastrophically upset. The degree of upset is dependent on a number of factors including relative sizes of the aircraft.

The current aim of the wake vortex research program at NASA Langley Research Center (LaRC) is to create a methodology that will allow researchers to accurately model wake vortices and characterize the hazard posed by them. The purpose of this hazard characterization research is to relate the potential vortex hazard to sensor observable quantities. A sensor based system designated as Aircraft Vortex Spacing System (AVOSS) will then be developed to predict, detect, track, and quantify wake vortices.⁽³⁾ Hazard analyses will be applied to determine if an aircraft could safely penetrate a vortex that has been detected in the approach corridor. This report will discuss the development of a freeflight model control system and the trajectory generation study conducted at LaRC as part of the wake vortex research program.

Freeflight Model Control System

As part of the wake vortex research program, tests will be conducted to determine the dynamic effects of flying a Boeing 737 within the wake of another aircraft. In one test a scale model of the Boeing 737 aircraft will be flown behind a simulated second aircraft within the test section of the 30- by 60- foot tunnel at LaRC. Control laws were developed for the Boeing 737 freeflight model based on the control system for the Boeing 737-100 at LaRC. The control laws represent the Boeing 737 for eight candidate approach flight conditions in which the flap settings and airspeed vary. Aerodynamic data for each of the eight flight conditions were obtained for the state-space matrices from a Boeing 737 simulation database. Actuator models, maximum control surface deflections, and yaw damper models were obtained from Boeing documentation. A SIMULINK file was then created to analyze the dynamics of the full scale aircraft. The control laws for the full scale aircraft were scaled down to the model size using Froude number scaling as explained by Wolowicz, et al.⁽⁴⁾ The model control system was then analyzed to ensure dynamic similarity existed between the model and the actual aircraft.

Trajectory Generation Study

The purposes of the trajectory generation study were twofold. The first objective was to determine the validity of using simple and approximate planform and mass characteristics to predict the severity of vortex encounters. The primary advantage of using such relatively simple techniques is the ease of which the study could be applied as a means of hazard prediction for the entire commercial fleet. The second objective of the study was to obtain a database about the severity of a vortex-induced upset for a multitude of paths through a wake for several follower-generator aircraft pairs.

For this study, a MATLAB simulation was developed based on simplified math models of aircraft. Generator aircraft were assumed to have elliptic spanwise lift distributions. Using the known characteristics of vortices shed from aircraft with elliptic spanwise lift distributions, the wake vortices of the generator aircraft were then modeled by an accepted vortex velocity-distribution. Strip theory was used to calculate the aerodynamic forces and moments induced on the follower aircraft by the vortices. Explicit solutions for the induced lift and rolling moment coefficients were obtained from Tatnall by integration of the strip theory equations.⁽⁵⁾ Using the induced lift and rolling moment coefficients, Bowles determined the equations of motion of the follower aircraft in the wake of the generator aircraft.⁽⁶⁾ With these equations, the simulation could be altered to allow the follower aircraft either one degree of freedom (DOF), roll, or three DOF, roll and translation along the Y and Z axes.

To simulate the decay of actual vortices with time in the atmosphere, the wake vortices in the vortex encounter simulation were decayed linearly with non-dimensional time. This vortex decay model is based on worst case situation of tower fly-by data in research conducted by Greene.⁽⁷⁾

In the simulation runs completed for this report, the Boeing 737 was used as the follower aircraft. In previous vortex encounter simulations, the follower-generator span ratio was determined to be a key parameter in predicting the severity of a vortex encounter. Accordingly, generator aircraft were selected to represent a range of follower to generator span ratios. The

selected ratios were 0.5 (Boeing 747 as the generator aircraft), 1.0 (Boeing 737), and 2.0 (Learjet 60). An additional aircraft pair with a span ratio of 0.7 was analyzed. This span ratio represents the Lockheed C-130 as the generator aircraft and was selected since the C-130 is a candidate vehicle for flight experiments.

Each simulation run consisted of 99 passes through the generator wake in which each pass differed in the lateral and vertical approach angles. The lateral approach angles selected were -20° to 20° in 5° increments. The vertical approach angles used were -10° to 10° in 2° increments. The Boeing 737 began each pass two generator spans away from the location of maximum induced rolling moment in the wake and aimed for this location. The pass ended when the follower aircraft was once again two generator spans away from the location of maximum rolling moment. Simulation runs will be completed for cases in which the follower aircraft will have no roll control power and full roll control power.

After the data is collected, a sensitivity analysis will be conducted for a nominal approach condition. The objective of the analysis is to evaluate the relative importance of certain parameters in determining the outcome of a vortex encounter. This information will be useful in hazard prediction.

Trajectory Generation Study Results

The trajectory generation study was not completed at the time this report was written. Sample 1 and 3 DOF results of a Boeing 737 encountering the wake of a Boeing 747 are available and will be discussed presently. These results are for the follower aircraft with no roll control inputs.

Figure 1 is a series of plots which contain the results of a 1 DOF penetration of the location of maximum rolling moment. The penetration occurs at the FAA specified separation distance of 5 nautical miles for this aircraft combination. The encounter shown in Figure 1 occurs when the Boeing 737 is on a 4° glideslope in the approach flight condition. The plot in the upper right corner indicates the follower aircraft reaches a maximum bank angle of -243° . The plot on the middle right shows that the maximum induced roll rate is $-58^{\circ}/\text{sec}$. These results are unrealistic but are explained by the fact that since the penetration occurs at such a slow rate, the aircraft is allowed to remain inside the vortex for a considerable period of time. Furthermore, the follower aircraft is constrained to only roll. As will be seen in Figure 2, if the aircraft would have had additional degrees of freedom, the magnitudes of the vortex induced perturbations would have been smaller.

Figure 2 contains the 3 DOF results for the same initial trajectory as in Figure 1. As can be seen in the plot in the upper left corner, the follower aircraft is removed from the intended path and is driven over 200 feet off course. It is apparent from the plot in the lower left that the aircraft is also accelerated downward. If this dangerous situation had occurred, the follower aircraft could have potentially crashed. At the very least, the aircraft would have been forced out of the approach corridor and would have had to execute a 'go-around'. It should also be noted that the bank angle and roll rate perturbations are smaller than the 1 DOF values but nonetheless result in unacceptable passenger comfort levels.

Once the trajectory generation study is completed, the data will be analyzed to determine a criteria for the estimating the potential of a wake vortex upset on a given trajectory. A worst case trajectory for a vortex encounter will then be determined.

Acknowledgments

I would like to thank the personnel at NASA Langley Research Center who have assisted with the research conducted in this paper. I would like to especially thank Robert A. Stuever for his guidance and assistance not only with this project but also with my professional development.

References

1. Mecham, Michael; and McKenna, James T.: "Cost, Not Size, To Drive Success of Superjumbo". *Aviation Week & Space Technology*, November 21, 1994, pp. 45-46.
2. Scott, William B.: "Technology, Economics, Fuel, Public-Private Cooperation". *Aviation Week & Space Technology*, June 7, 1993, pp. 69-76.
3. Vicroy, Dan; et al: "NASA Wake Vortex Research". ICAS-94-6.2.2, September 1994.
4. Wolowicz, Chester H.; Bowman, James S., Jr.; and Gilbert, William P.: "Similitude Requirements and Scaling Relationships as Applied to Model Testing". NASA TP 1435, 1979.
5. Tatnall, Chris R.: Unpublished Notes, 1995.
6. Bowles, Roland: Unpublished Notes, 1995.
7. Greene, George C.: "An Approximate Model of Vortex Decay in the Atmosphere". *Journal of Aircraft*, Vol. 23, No. 7, July 1986, pp. 566-573.

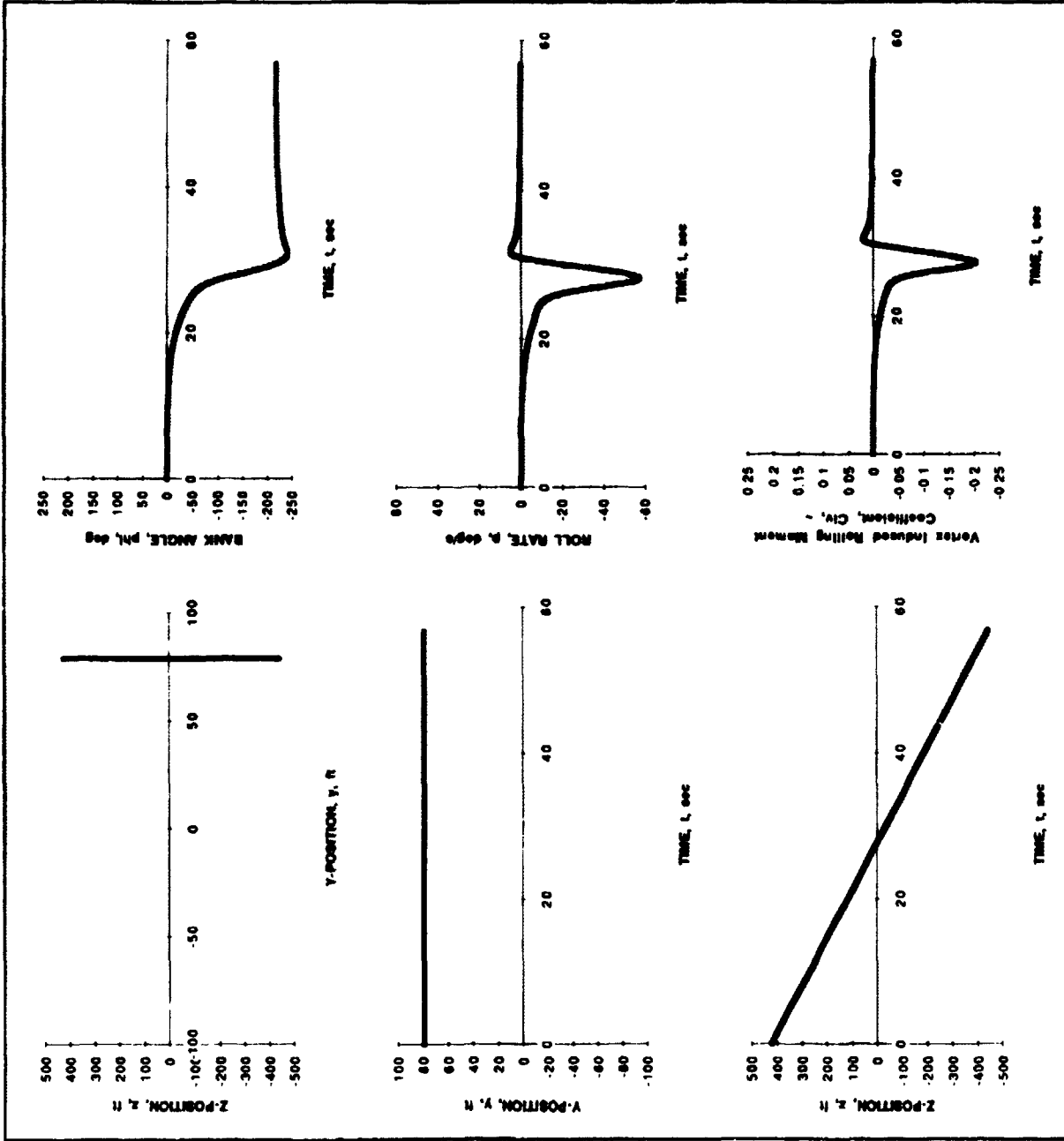


Figure 1. One Degree of Freedom Data of a Boeing 737 Encounter with a Boeing 747 Wake Vortex

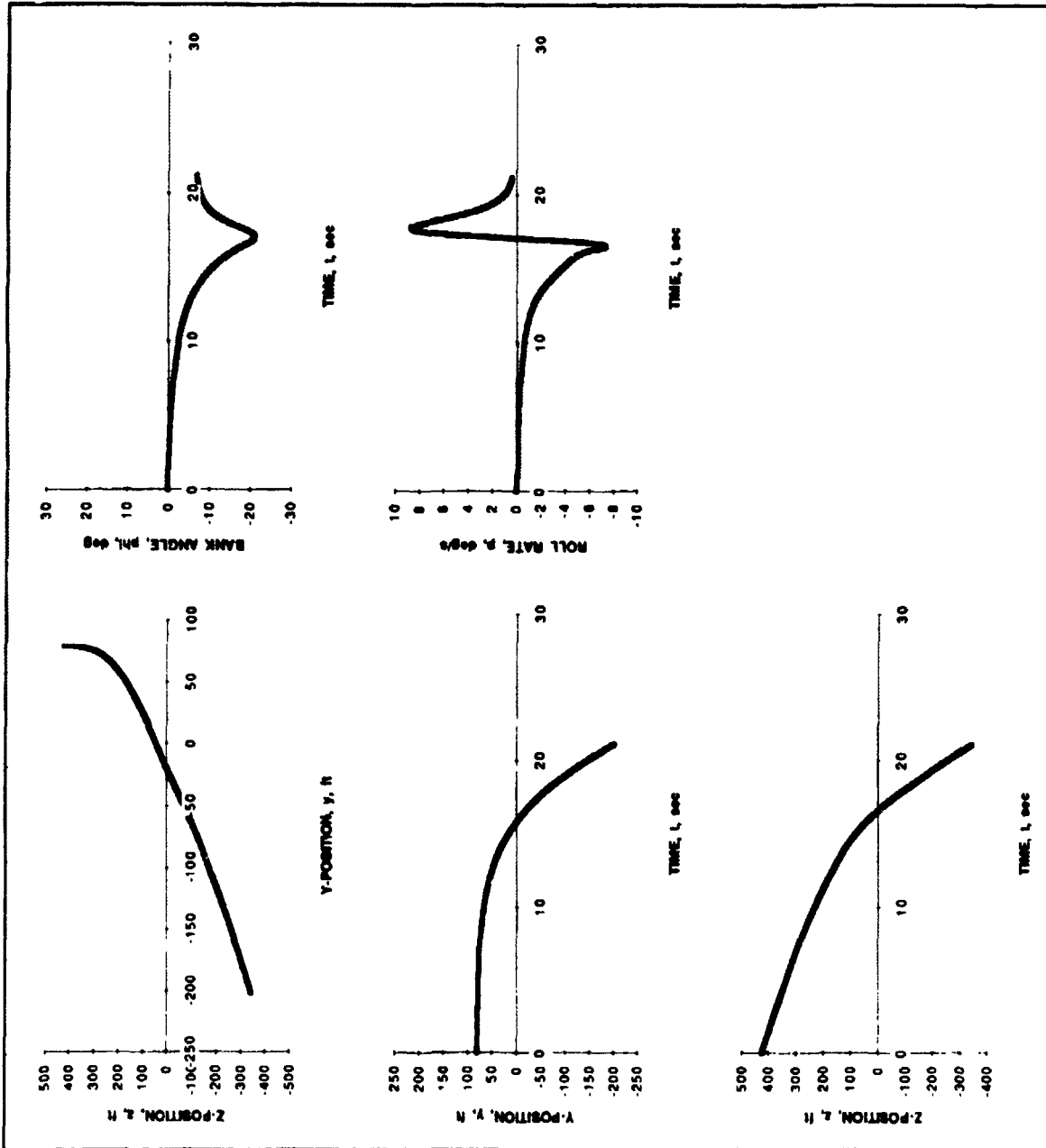


Figure 2. Three Degree of Freedom Data of a Boeing 737 Encounter with a Boeing 747 Wake Vortex

**NEXT
DOCUMENT**

Converting the Active Digital Controller for Use in Two Tests

Robert G. Wright

Mentor : Sheri Hoadley

**Research and Technology Group
Structures Division
Aeroelasticity Branch**

Modifying the Active Digital Controller for Use in Two Tests

The Active Digital Controller (ADC) was modified for use in the Actively Controlled Response of Buffet Affected Tails (ACROBAT) tests and for side-wall pressure data acquisition. The changes included general maintenance and updating of the controller as well setting up special modes of operation. The ACROBAT tests required that two sets of output signals be available. The pressure data acquisition needed a sampling rate of four hundred hertz, twice the standard ADC rate. These modifications were carried out and the ADC was used during the ACROBAT wind tunnel entry.

The Active Digital Controller is a system used to control the various functions of wind tunnel model. It has the capability of digitizing and saving of up to sixty-four channels of analog data. It can output up to 16 channels of analog command signals. In addition to its use a general controller, it can run up to two distinct control laws. All of this is done at a regulated speed of two hundred hertz.

The ADC

Main Computer

The base computer in the Active Digital Controller (ADC) is a SUN 3/160 Workstation using the UNIX operating system. This system provides the user interface for the ADC. It is also used to store and move the data collected. The SUN runs the information display and storage program as well as the user interface program.

Within the base computer there are three additional processor boards. The integer digital signal processor that is used to run the real time data acquisition and control program. Next is a floating point digital signal processor. This board is used to execute the active control laws and calculate the desired commands based upon the current sensor readings. The last board is an array processor. This was previously used as a back-up board but is now used for memory only. These three boards compose the real-time part of the ADC.

Along with the three processor boards within the SUN there are also four interface boards. The first two of these are analog to digital boards. In total this translates up to sixty-four analog input signals into 12 bit digital values. The second set are digital to analog boards, which provide up to sixteen analog outputs to the model.

The hardware rack used with the ADC contained three major components. The filter box provides for analog signal filtering and antialiasing. Along with the filter box was a patch box to allow the raw unfiltered signals to go to the ADC. The second component is the status display panel. It provided a visible confirmation of various control parameters. Lastly the rack contained an oscilloscope for use in diagnostics.

Programs

There are four main programs that run the ADC, the user interface, the information display and data saving program, the real-time controller, and the control law processor. These programs communicate using shared memory space but are generally independent of each other.

The user interface program is one of two programs which run concurrently of the SUN CPU. All interaction with the ADC is from this program. It starts and stops the real time system and the information display program, and allows the user to interact with the operation of the other CPU boards and their programs. The operator uses this program to change the operating modes of the ADC, operating and changing the parameters of the excitations and control laws, and starting and stopping a data save.

This information display and data saving program provides two functions. It allows the ADC user to quickly and easily see the signals being received. Second it saves the data taken to a file on the SUN computer. The information display window is run by the SUN computer and has an update rate of one to three times per second. The information window is used to get a rough view of the data and its speed is not important.

Operating on the primary real time board, the real-time program controls most aspects of the ADC. It controls the analog-to-digital and digital-to-analog boards to provide input from and output to the model. The program sends the excitations out and collects the incoming data to be saved by the information display and saving program. In addition to this, it also controls the status display board mounted in the rack.

The control law processor runs on the two nodes of the floating point digital signal processor. Its task is to execute the control laws given to it. By using both nodes, multiple control laws can be run at the same time.

Together, all of these programs comprise the software element of the ADC. The real time system can perform all of its tasks namely, acquiring the previous control law and excitation outputs, sending these outputs to the model, reading in new sensor signals, computing the control inputs, running the control laws, storing data, and other housekeeping tasks within a five millisecond time frame. This allows the real time components to achieve a two hundred hertz sampling rate that is adequate for most control needs.

Overview of the ACROBAT Tests

The ADC's most recent use has been in the Actively Controlled Response Of Buffet Affected Tails (ACROBAT) test runs. The test deals with the tail buffet problems of the F-18 during high angle of attack maneuvers. During these maneuvers, vortices from the wing-fuselage interface cover the two tails on the plane. By using active controls on the rudder, one of four other smaller control surfaces, or piezoelectric actuators on an internally warped tail, it was hoped that the buffet could be alleviated.

The ACROBAT tests ran using a one sixth scale F-18 drop model. The model was sting mounted to provide an angle of attack range of seven to thirty-seven degrees. An internally mounted hydraulic actuator provided actuation of the rudder and other control surfaces. A servo control rack was used to provide position and hydraulic pressure feedback to the hydraulic servo actuator. After calibration, this control system provided excellent correlation between the commanded and the actual movement of the actuator. The piezo-electric packs were activated from a piezoelectric control box designed for that purpose.

The test was run in NASA Langley's Transonic Dynamics Tunnel from July 10 to July 28. The model was flutter tested up to a maximum dynamic pressure of 18 pounds per square foot and 0.1 mach. Standard test runs were conducted at 14 psf. and 0.1 mach.

Changes in the ADC

There were three major types of changes made in the ADC and its programming. First, some changes were of the general maintenance and upgrading variety. Second, the ADC was configured to run during the ACROBAT tests. Third, a special mode was set up to acquire data for an ongoing project. This project was to take data from eight side-wall pressure transducers in the Transonic Dynamics Tunnel.

General Changes

To upgrade the ADC program a few features were added. First the number of output signals could be changed at will. Outputting signals is a very time consuming process and in order to keep the real time processor at 200 Hertz in all modes, the number of outputs needed to be selectable. The code was changed so that all excitations sent started at the beginning of the excitation. A new information display was set up that would display thirty-two channels of information at one time. There were many more small maintenance changes made. These changes

include better command names, cleaner looking displays and other beautifications. Also the code was cleaned up in places to allow for faster running.

ACROBAT changes

The ACROBAT tests demanded a few changes be made in the ADC. First two sets of output actuators were needed. One set was for the control surfaces. The second was for the piezoelectric tail. This was accomplished by using two data files and an option to switch the two. Many of the changes in the upgrade area were prompted by ACROBAT needs, such as changing the number of actuators. Finally different data scaling files were set up to scale the input and output signals correctly.

Pressure Data Acquisition Changes

The data from the pressure transducers was needed at at least 400 Hertz. This required work to streamline the code for this mode of data acquisition. The number of input signals in one mode was lowered to allow for faster running. In the same mode the output options were disabled. Also for this project a remote triggering mechanism was set up. This required setting up an input trigger signal as well as an output to provide voltage for such a signal. Upon receiving a voltage in the input signal a data save was executed and the ADC readied for another similar data save. An additional new feature was also added for this test. A monitor system was installed that would send an alarm if the tunnel was at the desired conditions to collect pressure data.

Actual Use of the ADC

During the test run the Active Digital Controller worked very well. Few problems were encountered. Most of the errors during the test were caused by human error. This improved as the operator gained experience. There were few other problems and these were quickly fixed.

Overall the test went well in terms of the ADC's involvement. Besides taking general data about the functioning of the model, a few control laws were implemented during the final third of the test. These control laws will provide a basis for which the next ACROBAT entry can be planned.

An initial set of data has been taken for the side-wall pressure data. This data came from the wind tunnel entry prior to the ACROBAT test. This data has gone through basic analysis and more data will be taken in the future.

Future of the ADC

The ADC has at least two more projects left in its operating life. First is the second wind tunnel entry of ACROBAT. This test is scheduled for late November and is to concentrate on more control law testing. Also the pressure data acquisition has not stopped and the ADC will continue to take data for that project.

**NEXT
DOCUMENT**

Very Light Aircraft: Revitalization Through Certification

Michael K. Zyskowski
B.S., Aerospace Engineering, University of Kansas

August 1995

Mentor: Natale Strain
Research and Technology Group
Flight Dynamics and Controls Division
Vehicle Performance Branch

Very Light Aircraft: Revitalization Through Certification

Michael K. Zyskowski

Prepared for the Langley Aerospace Research Summer Scholars' program, in coordination with the Advanced General Aviation Transport Experiments (AGATE) and NASA Langley Research Center

August 1995

Abstract

As the future of the general aviation industry seems to be improving, a cultural paradigm shift may be imminent with the implementation of an advanced, revolutionary transportation system within the United States. By observing the support of government and industry for this idea, near and long term effects must be addressed if this change is going to occur. The high certification costs associated with general aviation aircraft must be reduced without compromising safety if a new transportation system is to be developed in the future. With the advent of new, streamlined rules recently issued for the certification of small aircraft, it seems as though new opportunities are now available to the general aviation industry. Not only will immediate benefits be realized with increased sales of certified small aircraft, but there would now be a way of introducing the advanced concepts of future aircraft at varying degrees of technology and cost as options to the customer.

1. Introduction

General aviation (GA) is usually defined as all of aviation except the military, air freight operators and commercial airlines. With this definition, general aviation industry provides more than 540,000 jobs, \$40 billion in economic contributions, and serves 120 million people every year. There are currently 212,000 general aviation aircraft in domestic service, providing 62 percent of all flight hours, 37 percent of all flight miles, and 78 percent of all flight departures within the United States.¹ This is obviously a large market with many different missions and types of aircraft.

In the mid- to late-seventies, the GA market flourished with an all time record high sales of over 17,000 aircraft in 1978.¹ These airplanes were equipped with relatively unreliable navigation equipment, and the flying of these aircraft was generally considered a "hobby" to aviation enthusiasts. With the steadily increasing number of aircraft sales, the GA industry seemed to have a very bright future.

Unfortunately, this was not the case. Over the past 15 years, GA sales have plummeted to an all time low of just over 800 aircraft delivered last year. *This is a 95% decline in sales over a 15 year period.* This incredible drop in what seemed to be a thriving industry is usually credited to two very important issues.

As aircraft became more and more prevalent in the skies, the accident rate of the general aviation population began to increase as well. Although the Federal Aviation Administration (FAA) imposed numerous safety rules and regulations on the aircraft manufacturers, the victims of aircraft accidents sued the aircraft manufacturers with liability claims. As more court cases were brought against the manufacturers, insurance costs protecting against liability suits became increasingly expensive. Eventually, the insurance costs alone contributed to over 30% of the total airplane cost.

Although liability insurance was a problem, it is only half of the story. In today's faster paced society, the time and cost required to obtain and maintain a private pilot's license contributed even further to the decline in general aviation aircraft sales. As the basic cost of the aircraft became more expensive, so did the operational costs associated with flying the aircraft. General aviation aircraft were no longer affordable to the recreational aviation enthusiast.

To combat these problems, the government has set into motion a new revitalization effort for the general aviation industry. Last year, congress put into law the General Aviation Revitalization Act of 1994, limiting aircraft manufacturer liability to 18 years after the sale of an aircraft.² This was a tremendous achievement for the GA industry, as insurance costs began to drop to a more affordable level.

Although this first step was important, the technologies used in the general aviation field consist of technology dated over 20 years. Not only does the current aircraft fleet utilize old technology, but the Air Traffic Control (ATC) system has not had much improvement over the same number of years.

Today, we have seen a resurgence in the demand for a general aviation transportation system. Although not aimed at the recreational pilot, this new transportation system will enable a multitude of users to operate an aircraft at minimal cost, with improved safety, and at a high level of automation. This in turn will reduce the pilot workload and time required to maintain a current private pilots license. Leading this revolution is the Advanced General Aviation Transport Experiments (AGATE) Consortium, a partnership of government, industry, the FAA, and universities formed to improve and implement the technologies of today into the general aviation marketplace. With the combined effects of the tort reform and the AGATE program, the general aviation industry seems once again to have a very promising future.

2. A Revolutionary Transportation System

The word to emphasize in this title is transportation. As we have already seen, aircraft costs have become too high for the recreational aviator. Unless one is independently wealthy, purchasing an aircraft for fun becomes too large a financial burden for most people. There are then three main goals of this new transportation system:

- Capability
- Reliability
- Affordability

The key concept here is the user-friendly capability of this new aircraft. Much of the redundant burden placed on a pilot can be automated with today's technologies and computer systems. With these advanced systems, the ease of operating an aircraft will mimic as closely as possible the ease of operating an automobile. Although now the vehicle is in three dimensions, the pilot will eventually develop into a "flight systems manager", or some other derivative. This will enable the owner to operate the aircraft with a minimum amount of training and reduce by a great degree the workload during a flight operation.

Although this new automated aircraft would be in great demand if offering the capabilities aforementioned, the aircraft must also be safe to fly. The answer to most safety issues is redundancy. For instance, if one computer goes down, there is a backup to take its place. If the backup goes down, the backup to the backup takes its place. This redundancy ensures that should "any unforeseeable" event occur, there is a minimum safety factor to account for a failure.

However, as more and more back-up systems are placed in the aircraft, the increase in cost associated with the redundant systems reaches a critical level. This is where the affordability issue is encountered. There must be a trade-off between safety and affordability, and this is known as the "accepted failure rate." In commercial and military applications, this number is 1 fatal accident in 1×10^9 flying hours. Although there are not set standards in general aviation, it has been found that this number is around 1×10^5 flying hours.¹ Because of the litigation problems, an effort should be made to increase this number closer to the acceptable rate of commercial and military operations, which would reduce the costs associated with liability insurance. Though more concentrated effort is needed early on in the critical design and testing phase, costs associated with the implementation of redundant systems should also be reduced without compromising safety and capability for this new future aircraft.

3. How Will This Work?

Many studies have been conducted by the human factors discipline on the interaction of the "pilot" and the aircraft cockpit for this new automated system. The envisioned concept is one with complete removal of the analog instruments used in current cockpits, all being replaced by two flat panel displays and possibly a Heads-Up Display (HUD) for navigational aid. The touch screen concept has also been considered, but turbulence effects on pilot interaction create problems that have yet to be resolved.

Another main difference in this new cockpit will be the operation of the controls. In today's aircraft, the yoke, throttle, and rudder pedals must be manipulated together to coordinate a maneuver. This is a difficult process to learn, and is not intuitive to the user. The envisioned new system will automate by computer the control inputs to command rates as opposed to headings, (i.e., a rate of turn as opposed to a bank angle), which will be more like driving a car. With the technology available today, this system would not be difficult to design. However, we once again face the redundancy issue, and must take into account safety and affordability.

To implement this new system, an air and ground infrastructure, termed "free-flight", will enable the aircraft operator to more easily navigate their aircraft and ensure collision avoidance with other aircraft. The Radio Technical Commission for Aeronautics (RTCA), an organization that is working with the FAA and recommends standards for aeronautical electronics and telecommunications, defines the concept as one that would allow pilots "to operate the flight without specific route, speed or altitude clearances."³ Although still in the preliminary stage, the FAA already recognizes the importance of developing this infrastructure, "Even if we don't know where free flight will be in 2010, we know enough to tell which direction to go in 1995."⁴

Specifically, this new system would accept electronically transmitted flight plans, re-route aircraft to avoid collision and/or imposing weather conditions, and submit real-time weather and position data via satellite-based data-links and the Global Positioning System (GPS). Of course, this new infrastructure must also be proven reliable and not require the purchase of unaffordable equipment from the aircraft owner.

4. The Problems

As previously mentioned, one of the main problems with the development of this new transportation system is cost. The aircraft alone can be a major investment for some people, and with the addition of new avionics and hardware requirements, we may be "shooting ourselves in the foot." The main goal of this new renaissance is the revitalization of the general aviation industry. Therefore, the market to be targeted for these aircraft must be defined before a cost standard can be set. One of the most probable markets would be for relatively small corporations (\$1M to \$100M annual income) or traveling businessmen. This type of transportation would save the owner the cost of hiring a pilot and/or reduce the cost and time associated with his/her own training. Thus, the market must be defined to ensure that an achievable cost standard is met.

There must also be a shift in the cultural paradigm for this system to be successful. The general population is either comfortable with travel via commercial airlines or piloting their own aircraft. To implement such a radical change in the way people travel might not be readily accepted by the community. The FAA and ATC systems must also improve current procedures to meet the future needs of this system. Furthermore, experienced pilots are concerned with the ability of the "untrained" pilots to safely manage emergency situations. People's minds must be put to rest that the future GA aircraft will be safe and beneficial to the overall community. Although seemingly an insignificant problem, I believe this will be one of the hardest to overcome.

One final problem would be the issue of certification. The FAA has set strict standards on the design and testing of all types of aircraft. Particularly, the Federal Aviation Regulation's (FAR's) were created as a guideline for aircraft manufacturers to follow for aircraft certification. Although necessary for safety, these guidelines have proven to add the greatest overhead cost to the aircraft sale price. First, the aircraft design must be certified as flight worthy through numerous testing procedures, then the manufacturing facilities must be certified to ensure that the

every aircraft produced will meet the standards achieved by the prototype aircraft. As flight testing is one of the major contributors to the certification cost, Figure 1 shows the increasing trend of flight hours required for certification over the past 30 years.⁵

The fact that only three new airplanes have been certified to FAR 23 rules over the past 10 years shows the tremendous problems with this certification process.⁶ Furthermore, for modified aircraft there is an increase in the total program cost and engineering cost per pound of new weight due to the certification requirements. These cost trends have been rising substantially over the years, and can be seen in Figures 2 & 3.⁷

5. The Solutions

By implementing the "free-flight" mode, it has been found that a 2-3% savings in fuel efficiency can be achieved on an average flight of 500 nm.⁷ Furthermore, domestic airlines could save an average of two minutes on en route flights.⁸ Not only is there a time and workload savings involved with this new system, but it is evident there is a cost savings as well. Concerning the avionics issue, there is a tendency for hardware to remain at a fixed price over time with increased capabilities. The best example of this would be the home computer. Every year new models are introduced to the market, and these computers generally stay the same price as computers introduced the year before. It would therefore seem that avionics costs associated with the implementation of this new system would be relatively insignificant. As long as the target market and net worth of this new aircraft is identified, a fixed allowable cost to the manufacturer could then be set.

The AGATE program is the driving force in developing the technologies for the revitalization of the general aviation industry. As industry continues to become more aware and involved in the AGATE program, the attitude of the aviation industry is also starting to shift. New products are being developed, future problems are being addressed, and public access to useful information is becoming more readily available. This fact in itself will help to achieve public acceptance of the new general aviation transportation system idea simply through education. Once people understand the system, they are more apt to listen to the pros and cons thereof and make an informed decision on the validity of the idea. Through this program, and perhaps by implementing the transportation system in "steps", people will become more encouraged by the advantages than discouraged by the challenges.

As has been seen, the cost issue tends to dominate the problem area of creating the new automated aircraft. Directly related to this problem is the tremendous cost and frustration involved in the certification process. Furthermore, some vehicle for first implementation of these new technologies must be identified. In the past, the certification requirements for any aircraft under 12,500 pounds were the same. This basically means the certification process of a large twin engine aircraft (usually quite extensive and expensive) would be the same for a small homebuilt aircraft. Fortunately, in the last couple of years, the FAA has established new guidelines for certifying smaller aircraft. These new certification rules open the door for a vast number of aircraft companies to certify their aircraft at a greatly reduced cost. Hence, with the certification of new airplanes, there is now an opportunity to implement a new integrated transportation system.

6. The New Certification Rules

On December 31, 1992, the Primary Aircraft rule became effective as Advisory Circular (AC) 21-37.⁹ This rule supplied new certification options to the small aircraft industry. In general, the Primary Category allows a multitude of different certification procedures to be used to certify small aircraft, providing that the procedures are accepted by the FAA. There have already been four different methods observed as adequate by the FAA:

- TP101-41: Transport Canada's ultralight design standards for certification of "sportplane" aircraft.¹⁰
- AC 21.17-3: Type certification of Very Light Airplanes (VLA) under FAR 21.17(b).⁶
- AC 23-11: Type certification of Very Light Airplanes (VLA) with powerplants and propellers certified to FAR parts 33 and 35, respectively.¹¹
- Traditional certification standards under FAR part 23 and FAR part 27 for aircraft and rotorcraft, respectively.¹²

The Primary Category limits aircraft to being a single engine, naturally aspirated, unpressurized, four seat, 2,700 pound, 61 knot stall speed airplane operated only for personal use. These provisions can be deemed a "shell" with which to work. Any aircraft exceeding these limits are not allowed to be certified with the simplified procedures outlined in AC 21-37.

The Sportplane Category is the most streamlined option available, and the limits for certification are the same as above except for the weight being limited to 1,058 pounds and the stall speed to 39 knots. These standards are reduced in complexity, and can greatly reduce the cost of certification if the aircraft limits are met.

AC 21.17-3 allows the use of the Joint Aviation Requirements for Very Light Aeroplanes (JAR-VLA) as issued by the Joint Aviation Authorities (JAA) of Europe as an acceptable means of certifying aircraft under the Primary Aircraft rule. This new category simplifies the certification process and sets new limits on the aircraft to be certified to a single engine, naturally aspirated, two seat, 1654 pound, 45 knot stall speed airplane operated only for personal use. There are four different ways this rule can be applied for certification of VLA:

- May obtain a "Primary" category type certificate, provided the manufacturing of the aircraft is supervised or manufactured by a Production Certificate holder.
- May obtain an experimental kit-built airworthiness certificate provided the kit components were manufactured under an FAA approved quality assurance system.
- May be applied to obtain a "VLA-Special Class" certification, which restricts use to day/VFR operations.
- May be used in conjunction with other FAR part 23 requirements (AC 23-11, which is described below) to certify the aircraft in the "normal" category.

The first two applications basically state that the aircraft may be sold as a kit, without limitation on assembly or fabrication proportion to the builder, or the assembly of the kit by the customer may be supervised to allow the obtainment of a Primary airworthiness certificate. The third application allows the actual certification of the aircraft under this rule, but restricts the use thereof to day or Visual Flight Rules (VFR) operation. Finally, the last application gives the manufacturer an opportunity to certify the aircraft to the FAR part 23 "normal" category when incorporating the use of additional certification rules. The normal category of aircraft allows greater flexibility of operation, including night or Instrument Flight Rules (IFR) when applied. The additional certification requirements to achieve this category are outlined in AC 23-11.

AC 23-11 was formed as a supplement to the JAR-VLA rules outlined above. After examination by the FAA, it was found that 225 of the sections in the FAR part 23 certification procedures (the traditional aircraft standards) were applicable to the new Primary Aircraft rule. Upon further examination of the JAR-VLA rules, it was found that 204 of the sections in the FAR part 23 regulations were addressed in these new rules. Therefore, AC 23-11 was formed to allow aircraft manufacturers to use the JAR-VLA rules along with the AC 23-11 rules to certify an aircraft to the normal category of airplanes. This category differs from the Primary category in that it allows greater flexibility of use of the airplane.

Of course, if an aircraft manufacturer chooses to utilize the original FAR part 23 requirements to certify the aircraft, they would be eligible to obtain the Primary Category flight certification as well.

Although somewhat confusing, these rules basically do two things: reduce the level of FAA involvement and reduce the cost of certification. With the increased number of very light aircraft in the United States, it would seem that we now have a method by which to certify these aircraft and achieve a near term benefit by increasing their marketing potential.

7. Very Light Aircraft (VLA)

As the general aviation industry as a whole has been declining over the past 15 years, the demand for aircraft in this category has not. These aircraft are usually unconventional in design and make wider use of composite materials than either the GA aircraft of the past or the current larger commercial aircraft. To by-pass the high insurance costs associated with the liability issue discussed earlier, these airplanes are not sold as a completed unit. Instead, up to 49% of the aircraft is manufactured by the company selling the kit, and the remaining majority of the manufacturing is left to the purchaser.

When the aircraft owner builds the 51% of the aircraft, he essentially becomes the "aircraft manufacturer". Therefore, if an accident should occur while in operation, the only person liable is the one who is flying the aircraft. Currently, there are around 17,000 homebuilt aircraft in operation, with over twice this amount still in the building stage.¹³ Furthermore, there are around 1,000 homebuilt aircraft sold and around 1,500 aircraft experimentally certified each year.¹⁴ It is interesting to note the adaptation of industry when a demand is present but the supply is not by the success of the homebuilt industry. These aircraft are affordable to the customer, mainly because of the reduction in cost of manufacturing and certification to the designing company. There are many different kinds of homebuilts: monoplane low-wing, high-wing, biplanes, amphibians, acrobatic, etc., which all vary in cost and time required for fabrication.

8. Why Certify Homebuilts?

As society continues to become more time conscious, the hours associated with building these aircraft are becoming more of an issue to the aircraft owner. It is for this reason that a majority of the "homebuilt" aircraft will no longer be built in the home. With the new certification rules available, it could be more cost effective for the manufacturer to build these aircraft. One other possibility is that aircraft could be certified under the new experimental rules, which allows any portion of the kit to be assembled by the purchaser of the aircraft.⁶ This would enable the company to compromise with the customer on what portion he/she is willing to buy already assembled.

As the GA industry is predicted to grow well into the year 2000, the homebuilt market needs to capture a significant percentage of this GA growth. Without certifying these airplanes, the homebuilt market will probably lose a significant share of sales once production of the larger certified GA aircraft begins. Another option the new certification rules make available is the level of certification of the aircraft. For instance, if a customer does not require near all-weather operation, a lower level of certification may be issued, and hence the customer is given the option of a lower cost aircraft. On the other hand, if the customer wants the same airplane, but also wants near-all weather operation, a higher level of certification can be issued at a proportionately higher cost to the customer. This would help the marketing possibility of the smaller companies.

Figures 4 and 5 show the percentage of a sample database of existing aircraft that would be able to achieve certification under the new rules by meeting the weight and stall speed limits. It can be seen that *90% of the current homebuilt aircraft would be certifiable under the new Primary Category rules.* Keep in mind, however, that this graph represents only a small portion of the total

* These aircraft are also required to prominently display the words "experimental" in plain view of anyone who may be operating the vehicle.

homebuilt aircraft types available, but is representative of the overall homebuilt market. It is therefore evident that the certification rules available to the kit aircraft manufacturers are a possible means of increasing market at lower cost to the majority of these companies. Furthermore, the variety of aircraft available to the general aviation customer would increase tremendously, with the addition of 509 different homebuilt manufacturers currently producing kit aircraft.¹³

As was discussed earlier, the technology for a new transportation system requires some testing and vehicle integration before large scale implementation can occur. It would seem, with the certification of a low cost, small aircraft, the new technologies for this arena might be a viable option to the customer. Relating to the cultural paradigm shift problem, a step such as this might be the answer to getting public acceptance of such a system as well. With the available options of day/VFR and night/IFR operations, why not make it an option for "near-all weather, minimal training operations"? Although the near-term issues may make the certification issue important to the homebuilt manufacturers, the long-term benefits, which may prove more beneficial than the short term, must be taken into account as well.

9. Example Applications

As a result of the FAA issuing the new Primary Certification rules and the derivatives thereof, three different homebuilt aircraft have been certified. In July of 1993, the Quicksilver GT-500 became the first aircraft certified under the Sportplane Category. Then, in May of 1995, this same aircraft received the first Production Certificate under the Primary Category regulations.¹⁵ The certification of this aircraft was done at a fraction of the usual \$25 to \$30 million associated with certification costs. Although some changes were necessary to the original design, the final ready-to-fly selling price of these airplanes is \$30,000.¹⁵ This was a great first step for the certification of homebuilt aircraft.

As of July 1995, the CH-2000 of Zenair Aircraft became the second homebuilt aircraft to be certified.¹⁶ This aircraft was certified utilizing the JAR-VLA regulations and the additional AC 23-11, because of the higher aircraft weight and stall speed. Also certified under these rules is the Katana Diamond, which utilized composite structures as opposed to aluminum.

It is evident that with the certification of these aircraft, the majority of homebuilts currently in production could be certified in a similar fashion. Although different aircraft will have specific configuration modifications necessary for certification, the overall process of certification has been shown to work and be cost effective.

10. Other Aspects of VLA Certification Needing Examination

As more and more small aircraft become certified, there will be a need for improved certification processes. For one, the noise constraints associated with any aircraft in the FAR part 23 category are the same, and there have been no reductions or streamlining of the certification process for VLA. Secondly, there should be an analysis done on the cost and time associated with certification of aircraft at various weights, perhaps in a cost per pound versus certification method used. Also, specific VLA certification rules for composite aircraft must be examined in greater detail. Finally, a new certification method must be developed for the implementation of the new transportation system discussed earlier. By examining those needs now, the future distribution of this new automated aircraft may be realized in a more timely fashion.

11. Conclusions

After examining the plight of the general aviation industry and the revitalization attempts thereof, it seems as though a new general aviation transportation system will inevitably be incorporated into the way people travel in the future. Furthermore, the FAA has established new certification rules that make it easier to certify the small aircraft that make up a majority of the United State's homebuilt market today. By implementing these new certification procedures, the Very Light Aircraft of today might not only dramatically increase their market share with the

current aircraft configurations, but might also be the first to implement the new automated aircraft system into the market. This would not only help the small aircraft market, but would also help to revolutionize the entire general aviation industry as well. Although further examination of the noise and cost issues associated with certification are needed, the homebuilt manufacturer's of today should take better advantage of the new rules that have been made available. Possibly, by developing a certification methodology for small aircraft that is relatively inexpensive and time effective more small aircraft companies will attempt to certify their aircraft.

12. References

1. General Aviation Manufacturer's Association, General Aviation Statistical Databook, Washington, D.C., 1994.
2. Phillips, Edward H., "Clinton to sign Product Liability Bill," Aviation Week & Space Technology, August 15, 1994.
3. Hughes, David, "Free Flight Sparks International Debate," Aviation Week & Space Technology, July 31, 1995.
4. Dornheim, Michael A., "Equipment Will Not Prevent Free Flight," Aviation Week & Space Technology, July 31, 1995.
5. Etherington, Richard E., General Aviation Cost Effectiveness, Gates Learjet Corporation, Wichita, KS, 1985.
6. U.S. Department of Transportation, FAA, "Type Certification of Very Light Airplanes Under FAR 21.17(b)," AC 21.17-3, December 1992.
7. Ott, James, "Airlines, General Aviation Weigh Time/Cost Issues," Aviation Week & Space Technology, July 31, 1995.
8. Norwall, Bruce D., "Free Flight: ATC Model for the Next 50 Years," Aviation Week & Space Technology, July 31, 1995.
9. U.S. Department of Transportation, FAA, "Primary Category Aircraft," AC 21-37, June 1994.
10. Transport Canada, Design Standards for Ultra-Light Aeroplanes, TP101-41, February 1988.
11. U.S. Department of Transportation, FAA, "Type Certification of Very Light Airplanes with Powerplants and Propellers Certified to Parts 33 and 35 of the Federal Aviation Regulations," AC 23-11, December 1992.
12. U.S. Department of Transportation, FAA, "Airworthiness Standards: Normal, Utility, Acrobatic, and Commuter Category Airplanes," 14 CFR Ch. 1, Part 23, January 1994.
13. Conversation with Ben Owen, Experimental Aircraft Association, August 7, 1995.
14. Conversation with Tim Smythe, Federal Aviation Administration, August 7, 1995.
15. Jones, Mary, "Quicksilver GT-500-First U.S. Sportplane Production Certificate Awarded to Quicksilver Enterprises, Inc.," Sport Aviation, June 1995.
16. Davisson, Budd, "Zenair CH-2000-First of a Newly Certified Breed?," Sport Aviation, January 1994.

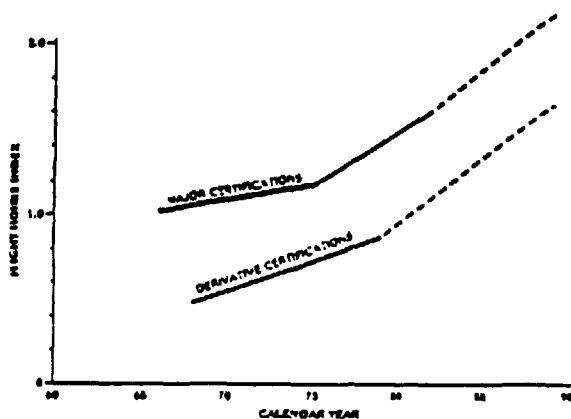


Figure 1. Flight Hours Required for Certification
(Copied From Reference 5)

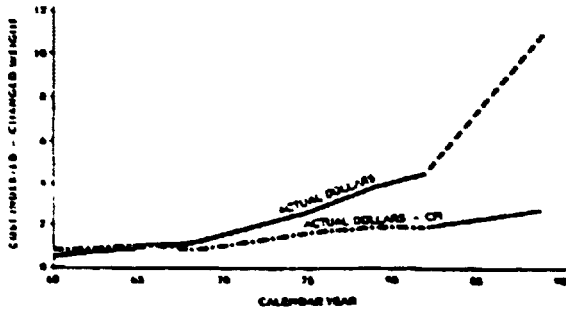


Figure 2. Total Program Cost per Pound for Certification
(Copied from Reference 5)

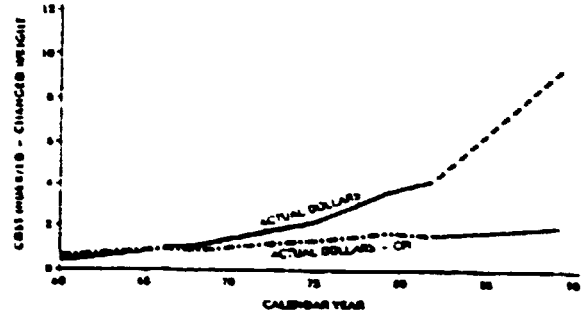


Figure 3. Total Engineering Cost per Pound for Certification
(Copied from Reference 5)

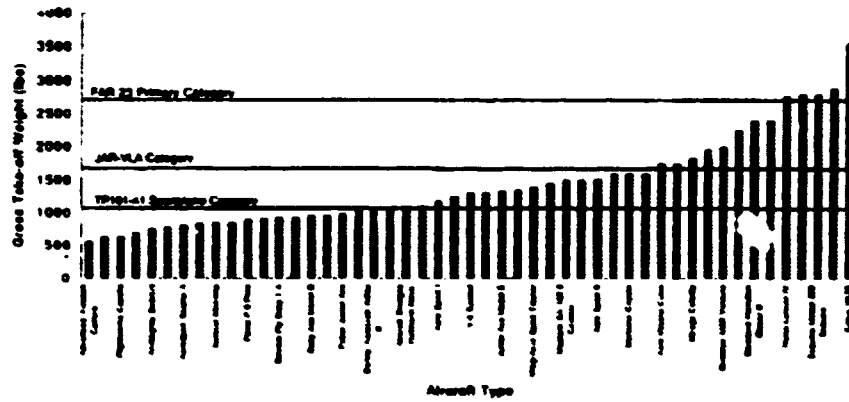


Figure 4. Very Light Aircraft Weights

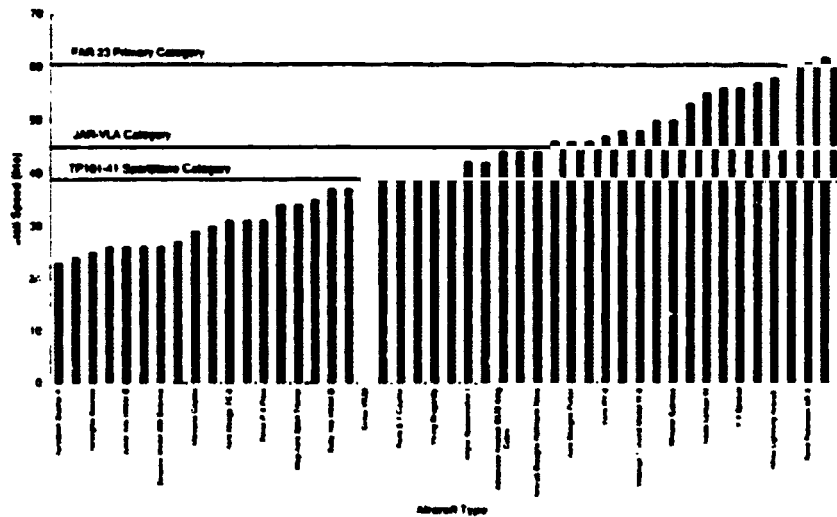


Figure 5. Very Light Aircraft Stall Speeds